

1974

Band Structure of Nickel: Spin-Orbit Coupling, the Fermi Surface and Theoptical Conductivity.

Ching-ping Shih Wang
Louisiana State University and Agricultural & Mechanical College

Follow this and additional works at: https://digitalcommons.lsu.edu/gradschool_disstheses

Recommended Citation

Wang, Ching-ping Shih, "Band Structure of Nickel: Spin-Orbit Coupling, the Fermi Surface and Theoptical Conductivity." (1974). *LSU Historical Dissertations and Theses*. 2700.
https://digitalcommons.lsu.edu/gradschool_disstheses/2700

This Dissertation is brought to you for free and open access by the Graduate School at LSU Digital Commons. It has been accepted for inclusion in LSU Historical Dissertations and Theses by an authorized administrator of LSU Digital Commons. For more information, please contact gradetd@lsu.edu.

INFORMATION TO USERS

This material was produced from a microfilm copy of the original document. While the most advanced technological means to photograph and reproduce this document have been used, the quality is heavily dependent upon the quality of the original submitted.

The following explanation of techniques is provided to help you understand markings or patterns which may appear on this reproduction.

1. The sign or "target" for pages apparently lacking from the document photographed is "Missing Page(s)". If it was possible to obtain the missing page(s) or section, they are spliced into the film along with adjacent pages. This may have necessitated cutting thru an image and duplicating adjacent pages to insure you complete continuity.
2. When an image on the film is obliterated with a large round black mark, it is an indication that the photographer suspected that the copy may have moved during exposure and thus cause a blurred image. You will find a good image of the page in the adjacent frame.
3. When a map, drawing or chart, etc., was part of the material being photographed the photographer followed a definite method in "sectioning" the material. It is customary to begin photoing at the upper left hand corner of a large sheet and to continue photoing from left to right in equal sections with a small overlap. If necessary, sectioning is continued again - beginning below the first row and continuing on until complete.
4. The majority of users indicate that the textual content is of greatest value, however, a somewhat higher quality reproduction could be made from "photographs" if essential to the understanding of the dissertation. Silver prints of "photographs" may be ordered at additional charge by writing the Order Department, giving the catalog number, title, author and specific pages you wish reproduced.
5. PLEASE NOTE: Some pages may have indistinct print. Filmed as received.

Xerox University Microfilms

300 North Zeeb Road
Ann Arbor, Michigan 48106

75-1961

WANG, Ching-ping Shih, 1947-

BAND STRUCTURE OF NICKEL: SPIN ORBIT COUPLING,
THE FERMI SURFACE AND THE OPTICAL CONDUCTIVITY.

The Louisiana State University and Agricultural
and Mechanical College, Ph.D., 1974
Physics, solid state

Xerox University Microfilms, Ann Arbor, Michigan 48106

BAND STRUCTURE OF NICKEL: SPIN ORBIT COUPLING,
THE FERMI SURFACE AND THE OPTICAL CONDUCTIVITY

A DISSERTATION

Submitted to the Graduate Faculty of the
Louisiana State University and
Agricultural and Mechanical College
in partial fulfillment of the
requirements for the degree of
Doctor of Philosophy

in

The Department of Physics and Astronomy

by

Ching-Ping Shih Wang

B.S., Tung-Hai University, Taiwan, 1969

M.S., Louisiana State University, Baton Rouge, La., 1971
August 1974

To My Mother

TABLE OF CONTENTS

	Page
ACKNOWLEDGEMENTS	ii
LIST OF TABLES	vi
LIST OF FIGURES	vii
ABSTRACT	ix
CHAPTER I. INTRODUCTION	1
CHAPTER II. THE TIGHT BINDING METHOD AND SELF- CONSISTENCY PROCEDURES	10
A. The Basic Approximations	10
B. The Tight Binding Method	15
C. Self-Consistent Procedure	33
D. Spin Orbit Coupling	41
CHAPTER III. APPLICATIONS AND RESULTS	49
A. Spin and Charge Density	49
B. Momentum Distribution of Electrons	53
C. The Density of States	61
D. The Fermi Surface	64
E. Optical Conductivity	68
CHAPTER IV. CONCLUSION	80
REFERENCES	84
TABLES	93
FIGURES	117
APPENDICES	136
A. The Fourier Transform of Gaussian Orbitals	136

B. Ferromagnetic Kerr Effect	138
C. Computer Programs	142

LIST OF FIGURES

Figure	Page
I. Coordinates for the Evaluation of Three Center Integrals	117
II. Self-Consistent Energy Bands for Majority Spin States	118
III. Self-Consistent Energy Bands for Minority Spin States	119
IV. Self-Consistent Energy Bands Including Spin Orbit Coupling	120
V. Band Electrons Charge Density in Three Principle Directions	121
VI. Magnetic Scattering Form Factors	122
VII. Spin Density in Three Principle Directions ...	123
VIII. Compton Profile in Three Principle Directions	124
IX. Anisotropy in Compton Profile	125
X. Comparison of the Spherical Average Compton Profile with γ -Ray Compton Scattering Measurements	126
XI. Projected Density of States for Majority Spin	127
XII. Projected Density of States for Minority Spin	128
XIII. Total Density of States	129

XIV.	Fermi Surface Cross Section in the (100) Plane.....	130
XV.	Fermi Surface Cross Section in the (110) Plane	131
XVI.	Joint Density of States.....	132
XVII.	The Real Part of the xx Component of the Conductivity Tensor from 0 to 1.2 eV	133
XVIII.	The Real Part of σ_{xx} from 1.0 eV to 6.0 eV.....	134
XIX.	The Imaginary Part of v_{xy} from 0 to 6 eV	135

calculated using matrix elements computed from wave functions including spin orbit coupling. Results were obtained for both the diagonal and the off diagonal elements of the conductivity tensor.

CHAPTER I

INTRODUCTION

Energy band computations for transition metals have been of continuing interest in solid state physics. These calculations are of fundamental importance in the construction of the band theory of itinerant electron magnetism.¹ It is assumed that the electrons responsible for the magnetism are not localized, but instead occupy Bloch states with wave functions extending throughout the crystal. Four major items of evidence strongly support the applicability of the general picture of itinerant electron ferromagnetism to nickel. First, energy band calculations have reproduced in reasonable detail the Fermi surface determined by measurements of the de Haas-Van Alphen effect and cyclotron resonance. Second, the saturation moment for nickel is found to be 0.616 Bohr magnetons/atom.² The difference from an integral number is too large to be attributed to an orbital component of the magnetic moment. Third, the high field Hall and magnetoresistance measurements of Fawcett and Reed³ indicate that the 3d electrons responsible for the magnetism have a mobility comparable with those of predominant s-p character. Fourth, the electronic specific heat measurement for nickel, $7.028 \text{ mJ}/(\text{mol } ^\circ\text{K}^2)$,³ shows that at least some of the 3d electrons have acquired an

itinerant behavior and contributed to the Fermi surface. A detailed comparison of itinerant versus localized-spin models can be found in Herring's book.⁵

Some of the more important calculation on the band structure of nickel used the LCAO (tight binding) method,⁶⁻¹¹ the APW (Augmented Plane Wave) method,¹²⁻¹⁵ the KKR (Green function) method,^{8,16-17} and the combined interpolation scheme.^{16,18-23} Both APW²⁴⁻²⁶ and KKR^{27,28} methods, in their usual forms, employ the "muffin-tin" approximation in which the crystal potential is assumed to be spherically symmetric in spheres inscribed within a polyhedral atomic cell about each lattice site and constant between these spheres. In the case of a APW calculation, the electronic wave functions are expanded in terms of spherical waves (products of radial wave functions and spherical harmonics) inside each sphere and plane waves between them. The eigenvalue problem is solved by varying the expansion coefficients in such a way that the logarithmic derivatives of wave functions are continuous across the boundary of the spheres. The KKR method employs a variational principle in which the Schrödinger equation is transformed into a homogenous integral equation. The trial wave function is expanded in terms of spherical waves. The variational condition gives a set of linear homogeneous equations and the dispersion relation is obtained by solving the secular equation whose

matrix elements consists of two parts. The first part is a geometrical structure constant arising from the lattice Green function which needs to be calculated only once for each type of lattice. The second part involves the logarithmic derivatives of the trial radial wave functions evaluated on the inscribed sphere.

One essential problem in the energy band calculation is to obtain a self-consistent potential. The effects of different starting atomic configurations on the results of non-self-consistent band calculations have been illustrated in the work of Mattheiss.¹³ Both methods described here have been made self-consistent to the extent of the muffin-tin approximation.^{15,17} For a transition metal, the 3d states are moderately sensitive to the nonspherical part of the potential (the crystal field effects).²⁹ The non-muffin-tin corrections to the band structure of paramagnetic nickel has been studied by Painter.^{30,31} The d bandwidth is narrowed by 0.010 Ry. and the s-d separation is reduced by 0.003 Ry. The $L'_{2\uparrow}$ state which is important in determining the Fermi surface neck at L is shifted by +0.010 Ry. Although the order of the $L'_{2\uparrow}$ and $L_{3\uparrow}$ states remains the same, this shift in energy is sufficiently large to effect detailed comparison with experiments. Two calculations have been reported previously in which some degree of self-consistency was achieved. The first of them, by Wakoh¹⁷ employed the KKR method and used the

Slater average free electron exchange potential.³² The effect of reducing the parameter in the $X\alpha$ exchange potential³⁵ has been illustrated in two self-consistent APW calculations by Connolly.¹⁵ The Kohn-Sham-Gaspar exchange potential^{33,34} ($\alpha = 2/3$) was found to yield more realistic results than the full Slater exchange³² ($\alpha = 1$). Spin orbit interaction was neglected in both calculations.

The combined interpolation scheme is an interpolative calculation which describes the energy bands in terms of a minimal basis set and corresponding disposable parameters.^{18,19} It combines a tight binding treatment for the d bands with a pseudo potential appropriate for the s-p bands. The basis functions consist of linear combination of atomic orbitals for d states and orthogonalized plane waves for the s-p bands. The orthogonality condition between the conduction s-p bands and the core states is simulated by the inclusion of the pseudo potential. There are two major interactions between the d bands and the conduction s-p bands. The first, hybridization, is included through the use of k dependent matrix elements. The second interaction, arising from the requirement of orthogonalization of basis states, can be either described in terms of k dependent form factors¹⁹ or included in the hybridization parameters.¹⁸ The parameters appearing in the Hamiltonian matrix elements are optimized to satisfy most experimental data and first principle calculations. The energies and

wave functions are obtained by diagonalizing the Hamiltonian matrix at a general point of the Brillouin zone. The $\vec{k} \cdot \vec{p}$ perturbation theory has been proved to be very useful to determine the energies in the vicinity of symmetric points.²⁰ In general, the combined interpolation scheme provides a simple and economical way of calculating energy bands, when enough experimental information is available to determine the parameters.

The LCAO method employs the variational principle with trial Bloch functions expanded in terms of localized orbitals suitably formed at each lattice site. In its original form,³⁶ this method is limited by severe problems involving calculation of three center integrals. Lin and co-workers^{37,38} showed that this difficulty can be avoided by expressing the crystal potential as Fourier series over the reciprocal lattice vectors. Furthermore, the Hamiltonian and overlap matrix elements can be expressed in a closed form if the basis set is chosen to consist of Gaussian type orbitals. This method has the advantage that energies and eigenfunctions can be obtained directly at a large number of points in the Brillouin zone without resorting to an interpolation scheme.

The self-consistent procedure within the framework of the tight binding approximation was first introduced by Callaway and Fry.³⁹ The present work is the first self-consistent tight binding calculation ever achieved.⁴¹ The Hamiltonian and overlap matrix elements obtained in the

previous non-self-consistent tight binding calculation for ferromagnetic nickel by Langlinais and Callaway¹⁰ were used as input material for the first iteration of the self-consistent procedure. Eighty-nine points in 1/48th of the Brillouin zone were used to determine the charge density in the final stages of an iterative procedure. Exchange has been included according to the $X\alpha$ method.³⁵ It was found that the Kohn-Sham-Gaspar^{33,34} value of the coefficient $\alpha(2/3)$ appeared to yield the most satisfactory results for the Fermi surface and other properties. Separate exchange potentials are obtained for electrons of majority and minority (\uparrow and \downarrow) spins and energy bands are computed separately for the two spin states. This calculation is a test of the ability of such a procedure (the spin-polarized method) to account for the magnetic and electronic properties of a ferromagnetic metal. The results obtained are in reasonable agreement with a variety of different experiments and other self-consistent calculations. This method was later applied to ferromagnetic iron,⁴⁰ paramagnetic chromium,⁴¹ and potassium.⁴² The results are found to be equally successful.

This calculation was subsequently extended to include the effects of spin orbit coupling. Spin orbit coupling is of major significance in a description of the properties of ferromagnetic transition metals. It leads to the existence of magnetic anisotropy, the anomalous Hall effect,

and magneto-optical effects. Substantial modifications of the Fermi surface result from changes in the connectivity of the energy bands. Attempts have been made to study spin orbit effects in the band structure of nickel for more than 30 years.^{18,22,43-49} Much of this work, however, has been based on oversimplified tight binding models of the d band structure. Other investigations have employed interpolation schemes designed to fit empirical information concerning the band structure, magnetic properties, and Fermi surface.^{18,22} We are not aware of previous attempts to include spin orbit coupling into a first principles band calculation for this metal.

The plan of this dissertation is as follows: In Chapter II we outline the procedure of a self-consistent tight binding calculation including the effects of both exchange and spin-orbit coupling. Some emphasis has been placed on the basic approximations reviewed in Section A. Modifications and improvements have been included in the discussion of the tight binding method and the construction of initial one electron potential in Section B. For an exact description of the procedure to construct the non-self-consistent energy bands for nickel, one is referred to Langlinais's dissertation.¹⁰ Section C contains a detailed discussion of the self-consistent procedure. The method employed to incorporate spin orbit interaction is presented in Section D. The energy bands

obtained before and after including the effects of spin orbit interaction are discussed at the end of Sections C and D respectively.

Chapter III is designated to compare the energies and wave functions obtained with the results of different experiments. In Section A the charge and spin density are compared with the X-ray and neutron diffraction measurements. The momentum distribution of electrons was examined through the calculation of the Compton profile in Section B. The Fermi surface effects on the structure observed in the Compton profile is analyzed. Spin orbit interaction is neglected in the above calculations. Including the effects of spin orbit interaction, energies, wavefunctions, and momentum matrices were obtained at 1357 regularly spaced points in 1/16th of the Brillouin zone. The density of states discussed in Section C was obtained by the Gilat-Raubenheimer method in combination with an interpolation scheme. The Fermi surface properties are shown in Section D and are compared with experiments. Major emphasis has been placed on the calculation of the optical conductivity tensor. The one electron theory of the interband conductivity tensor is discussed in Section E. A possible lifetime broadening effect has been considered through the inclusion of a phenomenological constant relaxation time. Detailed analysis and comparison with the ordinary and magneto-optical measurements are

attempted. Our general conclusions are stated in Chapter IV. A complete set of computer programs is included in Appendix C. The first few programs concerning the construction of the initial one electron potential and the Hamiltonian matrices have been rewritten in order to improve their accuracy and efficiency. They will be used subsequently to calculate the band structure of vanadium.

CHAPTER II

THE TIGHT BINDING METHOD AND SELF-CONSISTENCY PROCEDURES

This chapter is divided into four sections. In Section A, we shall briefly discuss the basic approximations. In Section B, we shall review the tight binding method, the choice of a basis set, and the construction of a one-electron potential. In Section C, we shall outline the self-consistency procedure within the framework of tight binding approximation. In Section D, we shall describe the methods employed to incorporate the spin orbit interaction.

A. The Basic Approximations

To calculate the energy levels of electrons in solids one has to solve the Schrödinger equation for a very large number of nuclei and electrons. Numerous simplifying approximations are necessary in order to solve this many body problem. The basic approximations involved in the framework of energy band theory are: first, the solid is an infinite periodic array of atoms or ions; second, the electronic and nuclear motions are independent, the Born Oppenheimer approximation; and third, the single electron moves in a periodic potential due to the nuclei and other electrons, the Hartree-Fock theory.

It is usually not possible to solve the Hartree-Fock equation directly due to the non-local nature of the exchange potential. Several approximations have been developed to construct an averaged local exchange potential. We shall briefly outline them here:

The first approximation was introduced by Slater³² and is based on the theory of the free electron gas. The exchange potential in a gas of density ρ is given by

$$v_{x \text{ gas}} = -8 F\left(\frac{|\vec{k}|}{k_F}\right) \left(\frac{3}{8\pi} \rho\right)^{1/3} \quad (2.1)$$

where \vec{k} is the wave vector of a plane wave state. Electrons occupy states within a sphere centered on $\vec{k}=0$ and of radius k_F for each spin, with

$$F(y) = \frac{1}{2} + \frac{1-y^2}{4y} \ln \left| \frac{1+y}{1-y} \right| . \quad (2.2)$$

Atomic units are used throughout this paper unless otherwise specified. In the Hartree Fock theory the density of states, which depends inversely on dE/dk , would vanish on the Fermi surface. This is one of the major difficulties of Hartree-Fock theory, which results from the neglect of electron correlation. It can be avoided if one considers an averaged local exchange potential. The simplest approximation is to treat ρ as the local charge density and to replace $F(y)$ by its average value over all

occupied states, $3/4$. Thus we have an exchange potential which we call V_{xS} ,

$$V_{xS} = -6 \left[\frac{3}{8\pi} \rho(\vec{r}) \right]^{1/3} . \quad (2.3)$$

An alternative approximation to the exchange potential was suggested by Kohn and Sham³³ following an earlier treatment by Gaspar.³⁴ They applied the variational method to an inhomogeneous system of interacting electrons. In the limit of slowly varying density this procedure leads to an exchange potential differing from V_{xS} in that the value of $F(y)$ at the Fermi level, namely $1/2$ is used.

$$V_{x,KSG} = -4 \left[\frac{3}{8\pi} \rho(\vec{r}) \right]^{1/3} = \frac{2}{3} V_{xS} . \quad (2.4)$$

Attempts have been made to use an exchange potential

$$V_{x\alpha} = \alpha V_{xS} \quad (2.5)$$

now known as the $X\alpha$ method. The parameter α is allowed to vary between 1 and $2/3$ or even slightly smaller than $2/3$ to get the best result.

It may seem desirable to choose the value of α which minimizes the total energy of the system since the theory is based on the variational approximation. The objection against this procedure is that the Hamiltonian instead of

the wavefunctions is varied in the process. Our calculation employed this $X\alpha$ exchange potential. The parameter α is chosen to yield the best results in comparison with experimental measurements. It will be discussed in more detail in Section C.

A more elaborate suggestion was made by Liberman,⁵⁰ independently of Sham and Kohn,⁵¹ and later modified by Slater, Wilson and Wood³⁵ to retain the dependence of $F(y)$ on y with $y=k/k_F$ determined in the free electron gas approximation as a function of energy and density. The problem can be solved self-consistently but the cost in computer time is very high. For a more detailed discussion and comparison of exchange potentials one is referred to the paper by Slater, Wilson and Wood.³⁵ A generalization of the Kohn-Sham theory of the inhomogeneous electron gas with emphasis on spin effects was later made by Rajagopal and Callaway.⁵² For a ferromagnetic system the exchange potential can be written as:

$$\alpha v_{x\sigma}(\vec{r}) = -6\alpha \left[\frac{3\rho_\sigma(\vec{r})}{4\pi} \right]^{1/3} \quad (2.6)$$

where $\sigma=\uparrow, \downarrow$ and $\rho_\sigma(\vec{r})$ is the density of electron with spin σ .

We consider the following one-electron Hamiltonian

$$H_1 = -\nabla^2 + v_C(\vec{r}) + \alpha v_X(\vec{r}) + v_{SO}(\vec{r}) . \quad (2.7)$$

The first term is the kinetic energy. The second term is the Coulomb potential which can be represented by the superposition of atomic potential at each lattice sites.

$$V_C(\vec{r}) = \sum_{R_\mu} V_a(\vec{r} - \vec{R}_\mu) . \quad (2.8)$$

The atomic potential due to the nuclei and the electron charge distribution $\rho_a(\vec{r})$ can be expressed as

$$V_a(\vec{r}) = -\frac{2Z}{|\vec{r}|} + 2 \int \frac{\rho_a(\vec{r}')}{|\vec{r}-\vec{r}'|} d^3 r' \quad (2.9)$$

where Z is the atomic number which is 28 for nickel. The third term in Eq. (2.7) is the $X\alpha$ exchange potential for a spin polarized system as shown in Eq. (2.6) and the last term is the spin-orbit interaction.

$$V_{SO}(\vec{r}) = \frac{\hbar}{4m_e^2 c^2} [\vec{\sigma} \times \vec{\nabla} V(\vec{r})] \cdot \vec{P} , \quad (2.10)$$

where $\vec{\sigma}$ is the Pauli spin operator, $V(\vec{r})$ is the crystal potential and \vec{P} is the momentum operator. The last term was neglected in this calculation until the self-consistent procedure had been completed. It will be discussed in detail in Section D.

B. The Tight Binding Method

The tight binding or LCAO (Linear Combination of Atomic Orbitals) method was first proposed by Bloch (1928)³⁶ and later modified by Lafon and Lin (1966).³⁷ The three center integrals which are normally encountered in the tight binding calculations can be eliminated by expressing the crystal potential as Fourier series over the reciprocal lattice vectors. If the basis set is chosen to consist of Gaussian type orbitals (GTO) all integrals can be done analytically. The elements of the Hamiltonian and overlap matrices are expressed analytically in terms of the interatomic distance and Gaussian exponent parameters. A drastic reduction in the computation can therefore be effected.

In a LCAO calculation, one begins with a set of localized functions $u_j(\vec{r})$ which for convenience will be assumed to be normalized but need not be orthogonal. Conventionally $u_j(\vec{r})$ are chosen to be the atomic orbitals of the corresponding crystal. However, this is not necessary and may even be too restrictive. In the present calculation we used atomic wave functions (GTO) for all states except 3d (e.g. 1s, 2s, 3s, 4s, 2p, 3p, and 4p). The Gaussian exponent parameters and expansion coefficients were determined by Wachters⁵³ from a self-consistent field calculation of free nickel atom. We believe it is

necessary to give the d wave functions more freedom to distort in the crystalline environment. A set of five separate radial GTO were used for each type of angular dependence. The orbital exponents used in defining these d functions were the same as given by Wachters.⁵³ The basis set thus consisted of 38 functions for each spin: 4 for s-type symmetry (1s, 2s, 3s, and 4s), 9 for p-type symmetry ($2p_x$, $2p_y$, $2p_z$, $3p_x$, $3p_y$, $3p_z$, $4p_x$, $4p_y$, and $4p_z$), and 25 for d-type symmetry (xy , yz , zx , x^2-y^2 , and $3z^2-r^2$).

The use of GTO has been criticized since these functions have zero slope at the origin and decay too fast at large distances. In a crystal the second problem may not be as serious as in the case of a free atom since its long distance behavior is strongly modified by the overlap of wave functions on the neighboring lattice sites. To investigate the first problem we compared the Hartree-Fock atomic wave functions based on GTO⁵³ with those based on STO (Slater-type orbitals).⁵⁴ At the origin they disagree by about 2%. Therefore our charge density at the nuclei sites had an uncertainty of about 4% resulting from the use of GTO.

The basis function $\phi_j(\vec{k}, \vec{r})$ which satisfies Bloch's theorem for wave vector \vec{k} can be written as

$$\phi_j(\vec{k}, \vec{r}) = \frac{1}{\sqrt{N}} \sum_{\vec{R}_\mu} e^{i\vec{k} \cdot \vec{R}_\mu} u_j(\vec{r} - \vec{R}_\mu) \quad (2.11)$$

where N is the total number of atoms in the crystal. The localized orbitals $u_j(\vec{r}-\vec{R}_\mu)$ are centered at lattice site \vec{R}_μ . The crystal structure for nickel is face centered cubic. Its lattice constant is 6.644 a.u. when extrapolated to 0°K using the coefficient of thermal expansion.⁵⁵ The localized orbitals can be separated into radial and angular parts

$$u_j(\vec{r}) = u_{n\ell m}(\vec{r}) = R_{n\ell}(|\vec{r}|) K_{\ell m}(\theta, \phi) \quad (2.12)$$

where $K_{\ell m}(\theta, \phi)$ are the Kubic harmonics and the radial wavefunction can be represented by GTO

$$R_{\ell i}(\vec{r}) = N_{\ell i} r^{\ell-1} e^{-\alpha_{\ell i} r^2} \quad (2.13)$$

with the normalization constant given as

$$N_{\ell i} = \left[\frac{2(2\alpha_{\ell i})^{\ell+1}}{\Gamma(\ell + \frac{1}{2})} \right]^{1/2} . \quad (2.14)$$

In the cases where atomic wavefunctions were required the $R_{n\ell}(\vec{r})$ were linearly expanded in GTO

$$R_{n\ell}(\vec{r}) = \sum_i C_{n\ell i} N_{\ell i} r^{\ell-1} e^{-\alpha_{\ell i} r^2} \quad (2.15)$$

where we have included the principle quantum number n .

The values $C_{n\ell i}$ and $\alpha_{\ell i}$ have been tabulated by Wachters.⁵³

In the modified LCAO calculation the crystal potential is expanded in Fourier series

$$v(\vec{r}) = \sum_{\vec{k}} e^{i\vec{k} \cdot \vec{r}} v(\vec{k}) \quad (2.16)$$

which can be inverted to obtain

$$v(\vec{k}) = \frac{1}{N\Omega} \int e^{-i\vec{k} \cdot \vec{r}} v(\vec{r}) d^3 r \quad (2.17)$$

with Ω being the volume of a primitive cell. For a periodic potential, $v(\vec{k})$ vanishes unless \vec{k} is a reciprocal lattice vector. The Coulomb part of the potential has been discussed in Section A. It was assumed that for the initial iterative stage of the self-consistent calculation the crystal charge density can be represented by the superposition of overlapping neutral atom charge density, the atoms being in $3d^9 4s^1$ configuration. This is somewhat different from the ground state configuration of a free nickel atom ($3d^8 4s^2$) because the effective occupation number is expected to change in forming a crystal as the sharp atomic energy levels broaden into overlapping bands. The starting electronic configuration should in principle be immaterial to a self-consistent calculation.

The magneton number which is the difference of occupation number between up and down spin has been measured to be 0.56 electrons per atom.² We assume in

the first iteration that this is due to d electrons only. The spherically averaged atomic charge density in Eq. (2.9) can be written as

$$\rho_a(r) = \rho_{a\uparrow}(r) + \rho_{a\downarrow}(r) \quad (2.18)$$

with

$$\rho_{a\gamma}(r) = \frac{1}{4\pi} \sum_i n_{i\sigma} |R_i(r)|^2 . \quad (2.19)$$

We use the radial wavefunction obtained by Clementi (1965) in a Hartree-Fock self-consistent field calculation for free nickel atom in $3d^8 4s^2$ configuration⁵⁴ in constructing the initial charge densities. The occupation numbers assumed are as follows

i	1s	2s	2p	3s	3p	4s	3d
$n_{i\uparrow}$	1	1	3	1	3	0.5	4.78
$n_{i\downarrow}$	1	1	3	1	3	0.5	4.22

The Fourier coefficient of the Coulomb potential is

$$\begin{aligned}
 v_c(\vec{k}) &= \frac{1}{NQ} \int e^{-i\vec{k}\cdot\vec{r}} v_c(\vec{r}) d^3r \\
 &= \frac{1}{NQ} \sum_{\mu} \int_{R_\mu} e^{-i\vec{k}\cdot\vec{r}} v_a(\vec{r}-\vec{R}_\mu) d^3r \\
 &= \frac{1}{NQ} \sum_{\mu} e^{-i\vec{k}\cdot\vec{R}_\mu} \int e^{-i\vec{k}\cdot\vec{r}} v_a(\vec{r}) d^3r . \quad (2.20)
 \end{aligned}$$

Using the relation

$$\frac{e^{-i\vec{k} \cdot \vec{R}}}{N} = \sum_{\vec{k}_s} \delta_{\vec{k}, \vec{k}_s} \quad (2.21)$$

where \vec{k}_s is a reciprocal lattice vector. We obtain

$$V_C(\vec{k}_s) = \frac{1}{\Omega} \int v_a(\vec{r}) e^{-i\vec{k}_s \cdot \vec{r}} d^3 r . \quad (2.22)$$

Eq. (2.9) is substituted into Eq. (2.22). One obtains

$$V_C(\vec{k}_s) = -\frac{8\pi Z}{\Omega k_s^2} + \frac{32\pi^2}{\Omega k_s^3} \int_0^\infty \rho_a(r) \sin(k_s r) r dr . \quad (2.23)$$

With $\rho_a(r)$ given in Eq. (2.18) the integral can be easily evaluated.

For the limit $\vec{k}_s = 0$ one has to expand the sine term in the integrand before taking the limit $\vec{k}_s \rightarrow 0$

$$\begin{aligned} V_C(0) &= \lim_{\vec{k}_s \rightarrow 0} \left[-\frac{8\pi Z}{\Omega k_s^2} + \frac{32\pi^2}{\Omega k_s^3} \int_0^\infty \rho_a(r) \right. \\ &\quad \left. (\frac{(k_s r)^3}{3!} + \dots) r dr \right] \\ &= \lim_{\vec{k}_s \rightarrow 0} \left[-\frac{8\pi Z}{\Omega k_s^2} + \frac{8\pi Z}{\Omega k_s^2} - \frac{16\pi^2}{3\Omega} \int_0^\infty \rho_a(r) r^4 dr \right] \\ &= -\frac{16\pi^2}{3\Omega} \int_0^\infty \rho_a(r) r^4 dr \end{aligned} \quad (2.24)$$

which can be readily evaluated analytically. The construction of an averaged local exchange potential has been discussed in Section A. The corresponding Fourier coefficients for spin σ are

$$\begin{aligned}
 v_{x\sigma}(\vec{k}_s) &= \frac{1}{N\Omega} \int e^{-i\vec{k}_s \cdot \vec{r}} v_{x\sigma}(\vec{r}) d^3 r \\
 &= \frac{1}{\Omega} \int_{\text{cell}} e^{-i\vec{k}_s \cdot \vec{r}} v_{x\sigma}(\vec{r}) d^3 r \\
 &= \frac{4\pi}{\Omega k_s} \int_0^{r_o} -6 \left(\frac{3}{4\pi} \rho_\sigma(r) \right)^{1/3} \sin(k_s r) r d r
 \end{aligned} \tag{2.25}$$

where r_o is the radius of the Wigner-Sitz sphere which has a volume equal to that of a primitive cell. The spherical averaged total charge density for electrons of spin σ can be written as

$$\rho_\sigma(r) = \left\langle \sum_{R_\mu} \rho_{a\sigma}(|\vec{r}-\vec{R}_\mu|) \right\rangle_{\text{av.}} \tag{2.26}$$

where the atomic charge density $\rho_{a\sigma}(r)$ is defined in Eq. (2.19). The summation from each lattice site was carried out up to the shell of neighbors where the desired degree of convergence has been reached. Although the individual atomic charge densities were assumed to be spherically symmetric, the superposed density has only cubic

symmetry about any lattice site. The bracket $\langle \dots \rangle_{av.}$ stands for the spherical average evaluated in the following way: The total charge density is expanded in a series of Kubic Harmonics up to the eighth order. The spherical average $\rho_0(r)$ is approximated as the zeroth order term in the expansion, and can be obtained by solving a set of four linear inhomogeneous equations along four inequivalent directions. Finally, the 96 point Gaussian formula was used to perform the numerical integration in the Wigner-Sitz sphere for each given reciprocal lattice vectors.

The one-electron Schrödinger equation to be solved takes the following form

$$\hat{H} \psi_n(\vec{k}, \vec{r}) = E_n(\vec{k}) \psi_n(\vec{k}, \vec{r}) \quad (2.27)$$

where \hat{H} is the Hamiltonian described in Eq. (2.7). The crystal wavefunction $\psi_n(\vec{k}, \vec{r})$ were expanded as a series in the basis function $\phi_i(\vec{k}, \vec{r})$

$$\psi_n(\vec{k}, \vec{r}) = \sum_i a_{ni}(\vec{k}) \phi_i(\vec{k}, \vec{r}) \quad (2.28)$$

in which n is the band index and \vec{k} is the wave vector of the state. The set of basis functions consisting of only atomic states does not form a complete set, so the corresponding eigenfunctions are not the exact solution of the Schrödinger equation. However, inclusion of all the

bound states and some of the excited states can be expected to yield a fair approximation to the actual wavefunctions. The expansion coefficient $a_{ni}(\vec{k})$ and energy $E_n(\vec{k})$ are to be determined by solving the Secular equation

$$\text{Det} | H_{mn}(\vec{k}) - \epsilon S_{mn}(\vec{k}) | = 0 \quad (2.29)$$

where

$$\begin{aligned} H_{mn}(\vec{k}) &= \langle \phi_m(\vec{k}, \vec{r}) | \hat{H} | \phi_n(\vec{k}, \vec{r}) \rangle \\ &= \sum_{\vec{R}_\mu} e^{-i\vec{k} \cdot \vec{R}_\mu} \int u_m^*(\vec{r} - \vec{R}_\mu) \hat{H} u_n(\vec{r}) d^3r \\ &= T_{mn}(\vec{k}) + V_{mn}(\vec{k}) . \end{aligned} \quad (2.30)$$

The kinetic energy matrix is given by

$$T_{mn}(\vec{k}) = \sum_{\vec{R}_\mu} e^{-i\vec{k} \cdot \vec{R}_\mu} \int u_m^*(\vec{r} - \vec{R}_\mu) (-\nabla^2) u_n(\vec{r}) d^3r . \quad (2.31)$$

The matrix element of the crystal potential expanded in Fourier series over the reciprocal lattice vectors can be expressed as follows

$$V_{mn}(\vec{k}) = \sum_{\vec{K}_s} [V_C(\vec{K}_s) + \alpha V_{x\sigma}(\vec{K}_s)] S_{mn}(\vec{k}, \vec{K}_s) . \quad (2.32)$$

The generalized overlap matrix is given by

$$S_{mn}(\vec{k}, \vec{K}_s) = \sum_{\vec{R}_\mu} e^{-i\vec{k}\cdot\vec{R}_\mu} \int u_m^*(\vec{r}-\vec{R}_\mu) e^{i\vec{K}_s\cdot\vec{r}} u_n(\vec{r}) d^3r . \quad (2.33)$$

For a crystal with inversion symmetry the $e^{i\vec{K}_s\cdot\vec{r}}$ term in the above equation can be replaced by $\cos(\vec{K}_s\cdot\vec{r})$. The overlap matrix element in Eq. (2.29) is

$$S_{mn}(\vec{k}) = S_{mn}(\vec{k}, \vec{0}) \quad (2.34)$$

All these matrix elements can be evaluated analytically provided one choose linear combinations of GTO as the basis functions. No method has yet been found to express them in a closed form when the atomic wave functions are expanded in Slater-type orbitals. This was the reason for choosing GTO in the expansion of the basis function. We shall evaluate the integral $\langle u_{\ell,m,n}(\vec{r}_A) | (\cos \vec{K} \cdot \vec{r}_C | u_{q,s,t}(\vec{r}_B))$ following the procedure modified by Chaney and Dorman.⁵⁶ The function $u_{\ell,m,n}(\vec{r})$ are GTO of order (ℓ, m, n)

$$u_{\ell,m,n}(\vec{r}) = x^{\ell} y^m z^n e^{-\alpha r^2}. \quad (2.35)$$

Appropriate normalization constants for both the orbital and the angular parts of the wavefunctions have to be included. The orbital on the left hand side has exponent α_1 and is centered at lattice site \vec{A} and that on the right hand side has exponent α_2 and is centered at \vec{B} . The coordinates for various points are shown in Fig. 1. The integral appearing in Eq. (2.33) can be obtained by putting \vec{B} and \vec{C} at the origin.

$$\begin{aligned} & \cdot u_{\ell,m,n}(\vec{r}_A) |\cos \vec{k} \cdot \vec{r}_C| u_{q,s,t}(\vec{r}_B) \\ &= \int d^3r_A x_A^{\ell} y_A^m z_A^n e^{-\alpha_1 r_A^2} \cos \vec{k} \cdot \vec{r}_C x_B^q y_B^s z_B^t e^{-\alpha_2 r_B^2} \end{aligned} \quad (2.36)$$

where

$$\vec{r}_A = \vec{r} - \vec{A}, \quad \vec{r}_B = \vec{r} - \vec{B} \quad \text{and} \quad \vec{r}_C = \vec{r} - \vec{C}.$$

The product of two Gaussians situated at center \vec{A} and \vec{B} is proportional to a third Gaussian situated at a point \vec{D} along the line \overrightarrow{AB}

$$\exp(-\alpha_1 r_A^2 - \alpha_2 r_B^2) = \exp\left[-\frac{\alpha_1 \alpha_2}{\alpha_1 + \alpha_2} \vec{A} \cdot \vec{B}\right] \exp[-(\alpha_1 + \alpha_2) r_D^2]$$

(2.37)

where

$$\vec{D} = \frac{\alpha_1 \vec{A} + \alpha_2 \vec{B}}{\alpha_1 + \alpha_2} \quad (2.38)$$

and

$$\overrightarrow{AB} = \vec{B} - \vec{A} \quad (2.39)$$

Writing

$$\vec{r}_A = \vec{r}_D + \overrightarrow{AD}, \quad \vec{r}_B = \vec{r}_D + \overrightarrow{BD} \quad \text{and} \quad \vec{r}_C = \vec{r}_C + \overrightarrow{CD}$$

$$(2.40)$$

and taking the binomial expansion, the integral can be written as

$$\begin{aligned} & \sum_{\substack{abc \\ def}} \left(\frac{\ell}{a} \right) \left(\frac{m}{b} \right) \left(\frac{n}{c} \right) \left(\frac{q}{d} \right) \left(\frac{s}{e} \right) \left(\frac{t}{f} \right) (AD)_x^{\ell-a} (AD)_y^{m-b} (AD)_z^{n-c} \\ & (BD)_x^{q-d} (BD)_y^{s-e} (BD)_z^{t-f} \\ & [\cos \vec{k} \cdot \overrightarrow{CD} \cdot u_{a,b,c}(\vec{r}_D) | \cos \vec{k} \cdot \vec{r}_D | u_{d,e,f}(\vec{r}_D)] \\ & - [\sin \vec{k} \cdot \overrightarrow{CD} \cdot u_{a,b,c}(\vec{r}_D) | \sin \vec{k} \cdot \vec{r}_D | u_{d,e,f}(\vec{r}_D)] \end{aligned} \quad (2.41)$$

where

$$\xi = \exp \left[- \frac{\alpha_1 \alpha_2}{\alpha_1 + \alpha_2} \vec{AB}^2 \right] \quad (2.42)$$

and $\binom{\ell}{a}$ are binomial coefficients with $0 \leq a \leq \ell$. The remaining integrals are central cell integrals about lattice site \vec{D} . These can be evaluated analytically in Cartesian coordinates. For a crystal with inversion symmetry only those terms which are even functions of K_x , K_y , and K_z will contribute. The integral can be reduced to

$$\begin{aligned} \xi &= \sum_{\substack{abc \\ def}} \binom{\ell}{a} \binom{m}{b} \binom{n}{c} \binom{q}{d} \binom{s}{e} \binom{t}{f} (AD)_x^{\ell-a} (AD)_y^{m-b} (AD)_z^{n-c} \\ &\quad (BD)_x^{q-d} (BD)_y^{s-e} (BD)_z^{t-f} \\ &\quad (-1)^{a+b+c+d+e+f} G_{a+d}(K_x, CD_x) G_{b+e}(K_y, CD_y) \\ &\quad G_{c+f}(K_z, CD_z) \end{aligned} \quad (2.43)$$

In the case that n is an even number

$$G_n(K, R) = \frac{(-1)^{n/2}}{2^n} (\pi \gamma)^{1/2} \exp\left(-\frac{\gamma K^2}{4}\right) H_n\left(\frac{K}{2}, \gamma\right) \cos(KR) \quad (2.44)$$

where

$$\gamma = \frac{1}{\alpha_1 + \alpha_2} \quad (2.45)$$

$H_n(\frac{K}{2}, \gamma)$ is a Hermite polynomial satisfying the following recurrence relation

$$H_{n+2}(\frac{K}{2}, \gamma) = K\gamma H_{n+1}(\frac{K}{2}, \gamma) - 2(n+1)\gamma H_n(\frac{K}{2}, \gamma) \quad (2.46a)$$

with

$$H_0(\frac{K}{2}, \gamma) = 1 \quad (2.46b)$$

and

$$H_1(\frac{K}{2}, \gamma) = K\gamma \quad (2.46c)$$

In the case in which n is an odd number,

$$G_n(K, R) = K^{\frac{n}{2}} (\frac{n}{2} + 1) \gamma^{\frac{n}{2} + 1} {}_1F_1(\frac{n}{2} + 1, \frac{3}{2}; -\frac{\gamma K^2}{4}) \quad (2.47)$$

where $\Gamma(\frac{n}{2} + 1)$ is the Gamma function and ${}_1F_1(\frac{n}{2} + 1, \frac{3}{2}; -\frac{\gamma K^2}{4})$ is a confluent hypergeometric function satisfying the following relation

$$\begin{aligned} \frac{n}{2} {}_1F_1\left(\frac{n}{2} + 1, \frac{3}{2}; x\right) + \left(\frac{3}{2} - n - x\right) {}_1F_1\left(\frac{n}{2}, \frac{3}{2}; x\right) \\ + \left(\frac{n}{2} - \frac{3}{2}\right) {}_1F_1\left(\frac{n}{2} - 1, \frac{3}{2}; x\right) = 0 \end{aligned} \quad (2.48a)$$

with

$${}_1F_1\left(\frac{3}{2}, \frac{3}{2}; x\right) = e^x \quad (2.48b)$$

and

$${}_1F_1\left(\frac{5}{2}, \frac{3}{2}; x\right) = (1 + \frac{2}{3}x) e^x \quad (2.48c)$$

The overlap matrix element can easily be obtained by setting $\vec{k}=0$. The gradient and kinetic energy matrix elements can be expressed as linear combinations of overlap matrix elements in the following way

$$\begin{aligned} & \langle u_{q,m,n}(\vec{r}_A) | v_x | u_{q,s,t}(\vec{r}_B) \rangle \\ &= q \langle u_{q,m,n}(\vec{r}_A) | u_{q-1,s,t}(\vec{r}_B) \rangle - 2 \alpha_2 \langle u_{q,m,n}(\vec{r}_A) | u_{q+1,s,t}(\vec{r}_B) \rangle \end{aligned} \quad (2.49a)$$

and

$$\begin{aligned}
& \langle u_{\ell, m, n}(\vec{r}_A) | -\nabla_x^2 | u_{q, s, t}(\vec{r}_B) \rangle \\
&= -q(q-1) \langle u_{\ell, m, n}(\vec{r}_A) | u_{q-2, s, t}(\vec{r}_B) \\
&\quad + 2\alpha_2(2q+1) \langle u_{\ell, m, n}(\vec{r}_A) | u_{q, s, t}(\vec{r}_B) \\
&\quad - 4\alpha_2^2 \langle u_{\ell, m, n}(\vec{r}_A) | u_{q+2, s, t}(\vec{r}_B) \rangle \quad (2.50)
\end{aligned}$$

Similar expression can be obtained for the y and z components.

The Hamiltonian and overlap matrix elements are either real or imaginary depending on the parity of the wavefunction. We label them as follows

$$H = \sum_{\vec{R}_{\mu}} \begin{matrix} d & s & p \\ \left| \begin{array}{ccc} I_{dd} \cos(\vec{k} \cdot \vec{R}_{\mu}) & I_{sd} \cos(\vec{k} \cdot \vec{R}_{\mu}) & i I_{pd} \sin(\vec{k} \cdot \vec{R}_{\mu}) \\ I_{sd} \cos(\vec{k} \cdot \vec{R}_{\mu}) & I_{ss} \cos(\vec{k} \cdot \vec{R}_{\mu}) & i I_{ps} \sin(\vec{k} \cdot \vec{R}_{\mu}) \\ -i I_{pd} \sin(\vec{k} \cdot \vec{R}_{\mu}) & -i I_{ps} \sin(\vec{k} \cdot \vec{R}_{\mu}) & I_{pp} \cos(\vec{k} \cdot \vec{R}_{\mu}) \end{array} \right| \end{matrix} \quad (2.51)$$

where

$$I_{mn} = \langle u_m(\vec{r}-\vec{R}_\mu) | \hat{H} | u_n(\vec{r}) \rangle . \quad (2.52)$$

Consider the unitary transformation $H' = UHU^{-1}$ with

$$U = \begin{pmatrix} 1 & 0 & 0 \\ 0 & 1 & 0 \\ 0 & 0 & i \end{pmatrix} \quad (2.53)$$

The result is

$$H' = \sum_{\vec{R}_\mu} \begin{matrix} d & \left| \begin{array}{ccc} I_{dd} \cos(\vec{k} \cdot \vec{R}_\mu) & I_{sd} \cos(\vec{k} \cdot \vec{R}_\mu) & I_{pd} \sin(\vec{k} \cdot \vec{R}_\mu) \\ I_{sd} \cos(\vec{k} \cdot \vec{R}_\mu) & I_{ss} \cos(\vec{k} \cdot \vec{R}_\mu) & I_{ps} \sin(\vec{k} \cdot \vec{R}_\mu) \\ I_{pd} \sin(\vec{k} \cdot \vec{R}_\mu) & I_{ps} \sin(\vec{k} \cdot \vec{R}_\mu) & I_{pp} \cos(\vec{k} \cdot \vec{R}_\mu) \end{array} \right| \\ s & \\ p & \end{matrix} \quad (2.54)$$

Here H' is real and symmetry but the pd and ps block must be evaluated with care to avoid a possible error of negative sign. The eigenvectors of the transformed secular equation are

$$a'_{ni}(\vec{k}) = \sum_m U_{nm} a_{mi}(\vec{k}) \quad (2.55)$$

The momentum matrix elements between the cell periodic part of the wavefunctions $w_n(\vec{k}, \vec{r}) = e^{-i\vec{k} \cdot \vec{r}} \psi_n(\vec{k}, \vec{r})$ (the crystal momentum representation) are defined as

$$\vec{P}_{nm}(\vec{k}) = \vec{M}_{nm}(\vec{k}) + \vec{Mk} \delta_{nm} \quad (2.56)$$

in which the momentum matrix elements between the crystal wavefunctions $\vec{M}_{nm}(\vec{k})$ can be evaluated in a similar way

$$\begin{aligned} \vec{M}_{nm}(\vec{k}) &= \sum_{ij} a_{ni}^*(\vec{k}) \vec{p}_{ij}(\vec{k}) a_{mj}(\vec{k}) \\ &= \sum_{ij} (U^{-1} a'(\vec{k}))_{ni}^* \vec{p}_{ij}(\vec{k}) (U^{-1} a'(\vec{k}))_{mj} \\ &= \sum_{ij} a_{ni}'(\vec{k})^* (U \vec{p}(\vec{k}) U^{-1})_{ij} a_{mj}'(\vec{k}) \quad (2.57) \end{aligned}$$

where

$$\vec{p}_{ij}(\vec{k}) = \sum_{R_\mu} s \begin{vmatrix} d & & & p \\ -\vec{\nabla}_{dd} \sin(\vec{k} \cdot \vec{R}_\mu) & -\vec{\nabla}_{sd} \sin(\vec{k} \cdot \vec{R}_\mu) & i\vec{\nabla}_{pd} \cos(\vec{k} \cdot \vec{R}_\mu) \\ -\vec{\nabla}_{sd} \sin(\vec{k} \cdot \vec{R}_\mu) & -\vec{\nabla}_{ss} \sin(\vec{k} \cdot \vec{R}_\mu) & i\vec{\nabla}_{ps} \cos(\vec{k} \cdot \vec{R}_\mu) \\ -i\vec{\nabla}_{pd} \cos(\vec{k} \cdot \vec{R}_\mu) & -i\vec{\nabla}_{ps} \cos(\vec{k} \cdot \vec{R}_\mu) & -\vec{\nabla}_{pp} \sin(\vec{k} \cdot \vec{R}_\mu) \end{vmatrix} \quad (2.58)$$

The gradient matrix elements

$$\vec{\nabla}_{nm} = \langle u_n(\vec{r} - \vec{R}_\mu) | \vec{\nabla} | u_m(\vec{r}) \rangle \quad (2.49b)$$

are given in Eq. (2.49a).

In the next section we shall discuss the self-consistency procedure and the choice of the exchange parameter α .

C. Self-Consistent Procedure

In this section we shall outline the essential feature of the self-consistency procedure.⁵⁹ This is accomplished by an iterative method. At any given iteration a potential was constructed from the band wavefunctions calculated in the previous iteration. The new potential was again used to calculate a new set of wavefunctions. The procedure was repeated until the desired degree of convergence was achieved.

The fundamental problem is to determine a new (or iterated) potential after a given stage of band structure has been completed. Since the calculation requires only the Fourier coefficients of the potential it suffices to obtain these. It was observed that only the Fourier coefficients of the potential for a few of the shortest reciprocal lattice vectors need to be considered in the iterative procedure to achieve self-consistency. Higher coefficients describe the charge density deep inside the core of an atom and do not change appreciably. For $\vec{k}_S \neq 0$ the Fourier coefficients of the Coulomb potential can be expressed as⁵⁷

$$V(\vec{k}_s) = \frac{-8\pi Z}{\Omega k_s^2} + 8\pi \frac{\rho(\vec{k}_s)}{k_s^2} \quad (2.59)$$

The Fourier coefficients of the electron density are given by

$$\rho(\vec{k}_s) = \frac{1}{N\Omega} \int \rho(\vec{r}) e^{-i\vec{k}_s \cdot \vec{r}} d^3r \quad (2.60)$$

in which the charge density can be written as

$$\rho(\vec{r}) = \sum_{\substack{n\vec{k} \\ \text{occupied}}} |\psi_n(\vec{k}, \vec{r})|^2 . \quad (2.61)$$

The Bloch function $\psi_n(\vec{k}, \vec{r})$ are defined in Eq. (2.28). The summation includes that portion of the Brillouin zone in which band n is occupied. Substituting Eq. (2.61) into Eq. (2.60) and converting the sum on \vec{k} into an integral one obtains

$$\rho(\vec{k}_s) = \frac{1}{(2\pi)^3} \sum_{\substack{n \\ \text{occupied}}} \sum_{ij} \int d^3k a_{ni}^*(\vec{k}) s_{ij}(\vec{k}, \vec{k}_s) a_{nj}(\vec{k}) \quad (2.62)$$

The generalized overlap matrix $s_{ij}(\vec{k}, \vec{k}_s)$ has been defined in Eq. (2.33). In the case $\vec{k}_s = 0$ the Fourier coefficient of the Coulomb potential must be determined by a limiting process

$$V(0) = \lim_{K \rightarrow 0} \left[-\frac{8\pi Z}{\Omega K^2} + \frac{8\pi}{K^2} \frac{1}{N\Omega} \int e^{-i\vec{K} \cdot \vec{r}} \rho(\vec{r}) d^3 r \right] \quad (2.63)$$

This limit exists and can be obtained by expanding the exponential term in powers of $|\vec{K}|$ before taking the limit $\vec{K} \rightarrow 0$. The result is

$$V(0) = \frac{-4\pi}{3\Omega} \int_{\text{cell}} \rho(\vec{r}) r^2 d^3 r . \quad (2.64)$$

The integral is over the volume of a primitive cell. The charge in $V(0)$ at a given stage of iteration can be evaluated analytically if we make the following assumption: first, the integral over a primitive cell can be replaced by that over the Wigner-Sitz sphere, and second, the change in $\rho(\vec{K})$ is spherically symmetric. Thus we can write

$$\Delta\rho(\vec{r}) = \sum_{\vec{K}_S} \Delta\rho(|\vec{K}_S|) e^{i\vec{K}_S \cdot \vec{r}} \quad (2.65)$$

Substituting Eq. (2.65) into Eq. (2.64) and evaluating the integral one obtains

$$\Delta V(0) = \frac{-16\pi^2}{3\Omega} \sum_{\vec{K}_S} \Delta\rho(|\vec{K}_S|) \left[\left(\frac{3r_O^2}{|\vec{K}_S|^3} - \frac{6}{|\vec{K}_S|^5} \right) \sin(|\vec{K}_S|r_O) + \left(\frac{6r_O}{|\vec{K}_S|^4} - \frac{r_O^3}{|\vec{K}_S|^2} \right) \cos(|\vec{K}_S|r_O) \right] \quad (2.66)$$

where r_O is the radius of the Wigner-Sitz sphere.

The exchange potential presents more difficulty because of the cube root dependence on the charge density. It was evaluated in the following way: The change in the Fourier coefficients of charge density was averaged over directions of K_S and the resulting Fourier series was summed to determine the change in charge density in an atomic cell for each spin. This was added to the starting charge density, the cube root was extracted, and a corrected exchange potential was formed. The corresponding Fourier coefficients are obtained by a numerical 96 point Gaussian integration. The procedure just described has the disadvantage that the convergence in $\Delta\rho(\vec{K}_S)$ is slower than that in $\Delta V_C(\vec{K}_S)$ by an extra factor of K_S^2 and more terms in $\Delta V_C(\vec{V}_S)$ have to be considered than necessary. An alternative procedure is to construct the iterated charge density directly from Eq. (2.61) and (2.28). This modification has been included in the self-consistency program listed in Appendix C.

The changes in the Coulomb and exchange potential were added to the Hamiltonian matrix in the following way

$$H_{ij}(\vec{k}) = H_{ij}^O(\vec{k}) + \sum_{\vec{K}_S} (\Delta V_C(\vec{K}_S) + \alpha \Delta V_X(\vec{K}_S)) S_{ij}(\vec{k}, \vec{K}_S) . \quad (2.67)$$

The $H_{ij}(\vec{k})$ was the iterated Hamiltonian while $H_{ij}^O(\vec{k})$ was the original Hamiltonian matrices defined in Eq. (2.30). The new Hamiltonian was again diagonalized to obtain a new set of eigenvalues and eigenfunctions. This procedure was repeated until the desired degree of convergency has been achieved. At first, our calculation employed a value of the exchange parameter α close to unity ($\alpha = 0.972$), which had been found to give the most satisfactory results.¹⁰ The charge density was sampled at 20 points in 1/48th of the Brillouin zone. Reasonably self-consistent results were obtained after about eight iterations. The resulting energy bands appeared to be unsatisfactory, both in regard to the relation of the p and d bands, and in regard to the magneton number. Estimates were made which indicated that the exchange parameter α should be decreased. It appeared that $\alpha = 2/3$ should be employed and the self-consistent calculations were repeated with this value. The results obtained in this case appeared to be in substantially better agreement with experiment.

Our experience with the effect of exchange on the band structure is similar to that reported by Connolly.¹⁵ We found, in agreement with Connolly, that if the full Slater exchange is used, the energy of the state L_2' , for both spin directions, is above the Fermi energy. Hence there would be no Fermi surface neck at L. The reduction of the exchange potential produced by use of the Kohn-Sham-Gaspar value of the parameter α raises the d levels substantially more than those of p symmetry. The L_2' levels are then below the Fermi surface, while the large spin splitting of the L_3 states forces $L_{3\downarrow}$ above the surface.

Another point of practical interest has to do with the number of iterations necessary to achieve convergence. In principle, when self-consistency has been reached, the iterated potential $V_{out}(\vec{k}_s)$ should be equal to the input potential $V_{in}(\vec{k}_s)$ based on which $V_{out}(\vec{k}_s)$ are evaluated. Therefore, one should be free to modify the input potential at the beginning of each iteration by using

$$V'_{in}(\vec{k}_s) = \beta V_{out}(\vec{k}_s) + (1-\beta) V_{in}(\vec{k}_s) \quad (2.68)$$

where the unprimed $V(\vec{k}_s)$ are the iterated and input potentials for the last iteration. The weighting factor β was allowed to vary between 0 and 1. We observed that the change in the Fourier coefficients of the Coulomb potential $\Delta V_C(\vec{k}_s)$ oscillated rapidly about their final

convergent values in the first few iterations. This can be avoided if we choose a value of β which will bring $\Delta V_C(\vec{K}_S)$ closer to their convergent values. A value of β close to 0.3 seemed to work very well for the first few iterations for transition metals. It should be increased when the oscillations settle down, especially the change in $V_C(K)$ becomes monotonic. The changes in the relative position of energy levels L_2' , L_3 and the Fermi energy produced an additional problem. The change in the Fourier coefficients apparently became divergent after a rough degree of convergence seemed to have been achieved. This was caused by oscillations in the position of L_2' with respect to the Fermi energy and could only be solved by introducing a very small value of β . The criterion employed to define an adequate degree of self-consistency was that the Fourier coefficients of Coulomb potential should be stable to 0.002 Ry. For the case $\alpha = 2/3$, eight iterations were made using 20 points in 1/48th of the Brillouin zone, followed by three iterations using 89 points. It was sufficient to consider only Fourier coefficients of potential for the 50 shortest reciprocal-lattice vectors in the iterative procedure to achieve self-consistency. The convergence of the exchange potential is somewhat more rapid than that for the Coulomb potential.

Numerical values are presented for some Fourier coefficients in Table I. The calculated band structure is shown in Figs. II and III for electrons of majority (+) and minority spins (-) along some symmetry directions. The bands have the expected shape, showing hybridization between the relatively narrow d band complex and a broad s-p band. Certain characteristic energy differences are listed in Table II. There is a substantial degree of agreement between our values for some of these separations and the corresponding results obtained by Connolly.¹⁵ These energy differences are also in fair agreement with the results of Wakoh,¹⁷ however, this author uses the full Slater exchange ($\alpha = 1$).

Exchange splittings of certain states are given in Table III. Results from the non-self-consistent calculation ($\alpha = 0.972$), together with other self-consistent calculations,^{15,17} are shown for comparison. It is seen that the splitting of states of predominately d symmetry has decreased slightly but not by as much as would have been expected in view of the decrease in α . There is significant variation in the amount of splitting from band to band. A striking result is that the splitting of states of predominately s-p symmetry is nearly zero. These results can be qualitatively explained in terms of the redistribution of spin density which will be discussed in Section A of Chapter III. The spin polarization

becomes negative (minority spin predominates) in the outer portions of the atomic cell. Highly extended states (s-p) experience cancellation of positive and negative exchange potentials. The more extended d states near the bottom of the band are also located on the average in a region of weaker exchange potential.

The self-consistent energy bands and wave functions were used to calculate the spin density, X-ray form factor and Compton profile. In the next section we discuss the inclusion of the spin orbit interaction to the self-consistent potential.

D. Spin Orbit Coupling

The calculation previously described was extended by the inclusion of spin orbit coupling. Other relativistic effects were neglected. Introduction of spin orbit coupling into a band calculation for a ferromagnet causes substantial complications. First, since spin orbit coupling connects states of \uparrow and \downarrow spin, the size of the Hamiltonian matrix is increased (in our case 76x76), and the elements become complex. This causes a considerable increase in computing time. Second, the symmetry group is reduced. The appropriate group theory has been presented by Falicov and Ruvalds⁵⁸ and Cracknell.⁶⁰ In addition the band structure depends on the direction of spin alignment. Separate band structures must be computed for each

direction spin alignment investigated. However, because of limitations of computer time, we have restricted our calculations to a single direction of spin alignment: the [001] axis.

Falicov and Ruvalds⁵⁸ considered for inclusion in the space group: (1) the ordinary lattice translation, (2) rotation about the direction of spin alignment, \hat{n} , (3) the product of these rotations with the inversion, and (4) combinations of these rotation and rotation-inversion with translation. Wigner pointed out that there may be an additional symmetry to be considered.⁵⁹ Although time reversal, by itself, is not a symmetry operation, the product of time reversal and either a two-fold rotation about an axis perpendicular to the field direction \hat{n} or a reflection in a plane containing the \hat{n} axis is a candidate for a symmetry operation of the crystal. A detailed discussion of the additional symmetry operations has been presented by Cracknell.⁶⁰

The computation of the matrix elements of the spin orbit interaction was performed as follows. The additional term in the Hamiltonian has the form

$$H_{S.O.} = \frac{\hbar^2}{4m_e c^2} \vec{s} \cdot (\vec{V}_C \vec{x}) \quad (2.69)$$

The potential V_C used in (2.69) was that obtained from the self-consistent band calculation, expressed as a Fourier

series

$$V_C = \sum_{\vec{K}_S} V_C(\vec{K}_S) e^{i\vec{K}_S \cdot \vec{r}} \quad (2.70)$$

Use of Gaussian orbitals is advantageous, as all matrix elements of the $H_{S.O.}$ can be reduced to sums of simple analytic functions of the reciprocal lattice vectors. We found in several tests that the only non-negligible matrix elements of $H_{S.O.}$ are those in the p-p and d-d blocks, with orbitals centered on the same atomic site ("central cell"). The central cell matrix elements of $H_{S.O.}$ have the following form

$$H_{S.O.} = \begin{array}{|cc|} \hline & \uparrow & \downarrow \\ \uparrow & v_1 & v_2 \\ \hline & \downarrow & -v_2^* & v_1^* \\ \downarrow & & & \\ \hline \end{array} \quad (2.71)$$

in which the spin states considered are indicated by arrows. The forms of the sub-matrices v_1 and v_2 are as follows for the p-p block:

$$\langle p | v_1 | p \rangle = \begin{array}{|ccc|} \hline & x\uparrow & y\uparrow & z\uparrow \\ \hline x\uparrow & 0 & iA & 0 \\ y\uparrow & -iA & 0 & 0 \\ z\uparrow & 0 & 0 & 0 \\ \hline \end{array}, \quad (2.72)$$

The symmetries of the basis states are indicated above and to the left of the matrix.

$$\langle p | v_2 | p \rangle = \begin{array}{|ccc|} & x \uparrow & y \uparrow & z \downarrow \\ x \uparrow & \left| \begin{array}{ccc} 0 & 0 & -A \\ 0 & 0 & iA \\ A & -iA & 0 \end{array} \right| \\ y \uparrow & & & \\ z \uparrow & & & \end{array} \quad (2.73)$$

In these equations,

$$A = \left(\frac{3}{4\pi} \right) N \sum_{\mathbf{k}} V(\mathbf{k}) k^2 F(\mathbf{k}) \quad (2.74)$$

in which

$$F(\mathbf{k}) = \frac{\hbar^2}{24m_c^2} \pi^{3/2} \gamma^{5/2} \exp\left(-\frac{\gamma k^2}{4}\right) \quad (2.75)$$

and

$$\gamma = \frac{1}{\alpha_1 + \alpha_2} . \quad (2.76)$$

The sums include all reciprocal lattice vectors; α_1 and α_2 are the exponents of the Gaussian orbitals, and N is the product of the appropriate normalization constants. The corresponding formulas for the d-d block are⁶¹

	xy^\dagger	yz^\dagger	zx^\dagger	$x^2-y^2^\dagger$	$3z^2-r^2^\dagger$
xy^\dagger	0	0	0	iB	0
yz^\dagger	0	0	iC	0	0
zx^\dagger	0	$-iC$	0	0	0
$x^2-y^2^\dagger$	$-iB$	0	0	0	0
$3z^2-r^2^\dagger$	0	0	0	0	0

(2.77)

	xy^\dagger	yz^\dagger	zx^\dagger	$x^2-y^2^\dagger$	$3z^2-r^2^\dagger$
xy^\dagger	0	C	$-iC$	0	0
yz^\dagger	$-C$	0	0	$-\frac{iB}{2}$	$-\frac{i\sqrt{3}}{2}B$
zx^\dagger	iC	0	0	$-\frac{B}{2}$	$\frac{\sqrt{3}}{2}B$
$x^2-y^2^\dagger$	0	$\frac{iB}{2}$	$\frac{B}{2}$	0	0
$3z^2-r^2^\dagger$	0	$\frac{i\sqrt{3}}{2}B$	$-\frac{\sqrt{3}}{2}B$	0	0

(2.78)

where

$$\begin{aligned}
 B = & \frac{15}{4\pi} \frac{N_Y}{4} \sum_K V(K) F(K) [\alpha_2^2 Y^2 (K_x^4 + K_y^4 + K_z^4) \\
 & + (2\alpha_1 - \alpha_2)^2 (K_x^2 K_y^2 + K_y^2 K_z^2 + K_z^2 K_x^2) - 4K^2] \quad (2.79)
 \end{aligned}$$

$$C = \frac{15}{4\pi} \frac{N_Y}{4} \sum_K V(K) F(K) [\gamma (K_x^2 K_y^2 + K_y^2 K_z^2 + K_z^2 K_x^2) - 2K^2]$$

(2.80)

All of the basis functions are assumed to be normalized with respect to the angular integrations so that N depends on the orbital exponents only. Spherical symmetry of the potential has not been assumed in writing these formulas. There are in this case, two independent constants involved in the d-d spin orbit Hamiltonian. In fact, spherical symmetry is a good approximation, since it is the potential close to a nucleus which is important. For a spherically symmetric potential, we have simply

$$B = 2C = \xi$$

(2.81)

where ξ is the usual spin orbit coupling parameter if atomic wave functions are employed in the usual form,

$$H_{S.O.} = \xi L \cdot S.$$

In our calculation, the spin orbit parameters, A, B, C, depend on the indices of the pair of orbital functions used in calculating the matrix elements. In order to compare calculations of properties of nickel which are dependent on spin orbit coupling, it is useful to compute an equivalent atomic spin orbit coupling parameter. This calculation was performed with the wavefunctions of

Wachters⁵³ and our self-consistent potential. We found $\zeta=0.0067$ Ry. This result is somewhat larger than the atomic value $\zeta=0.0055$ Ry.⁶² The difference between B and 2C was found to be zero within the accuracy of our calculation.

The Hamiltonian including exchange and spin orbit coupling was diagonalized at 1357 points in 1/16'th of the Brillouin zone. The calculated band structure is shown along certain symmetry lines in Fig. IV. Some calculated energy levels at symmetry points are listed in Table IV. Since the actual symmetry group for this problem does not permit a particularly informative classification of states, we have labelled states at symmetry points in Fig. IV in terms of the predominant component; that is, neglecting the mixing of states of majority and minority spin components. This labelling is possible since spin orbit coupling is small compared to the exchange splitting.

It will be noticed that the band structure shown in Fig. IV is quite similar to that formed by superposing the majority and minority spin bands shown in Fig. II and III. However, spin orbit coupling removes many of the accidental degeneracies present in such a picture. The interplay of spin orbit and exchange effects can be illustrated by considering the points X. In the present case, there are two inequivalent points of this type which are not connected by an operation of the symmetry group: these

are denoted $X(001)$ and $X(100)$. Since the exchange splitting is large compared to spin orbit coupling, we can qualitatively consider the latter as a perturbation. Specifically, let us consider the states $X_{5\downarrow}$ near the top of the d band. For $X(100)$, the basis functions are of the symmetry xy^\dagger, xz^\dagger . Spin orbit coupling does not connect these states, instead there is coupling between these and other majority and minority spin states. Since these states are separated from $X_{5\downarrow}$, the splitting of $X_{5\downarrow}$ is small (0.0012 Ry). On the other hand, for $X(001)$, the basis function are zy, zx . There is a non-zero spin orbit matrix element between these states, leading to a considerably larger splitting (0.0078 Ry.).

In the following chapter, results are presented for the charge density, the spin density, the Compton Profile, the density of states, the Fermi surface, and the optical conductivity tensor. A detailed comparison of theory and experiment is attempted.

CHAPTER III

APPLICATIONS AND RESULTS

In this chapter the energy and wavefunctions obtained in our calculation are compared with experiment. We present in Section A the spin and charge density. Section B contains a discussion of the method employed to calculate the momentum distribution of electrons in solids. The procedure used to calculate the density of states is described in Section C. Our results for Fermi surface properties are presented in Section D and are compared with experiment. Finally, the calculation of the optical conductivity is summarized in Section E.

Section A. Spin and Charge Density

The Kohn-Sham-Gaspar exchange prescription is based on a variational calculation of the total energy, regarded as a functional of the charge density. It is therefore particularly interesting to examine the results of our calculation with respect to the charge density. Some calculated charge densities along three main crystallographic directions are listed in Table V. Contribution from the band electrons has been separated in the table. Figure V shows the band electron charge densities $\rho_b(\vec{r})$ along [100], [110], and [111] directions. The spherical average Hartree-Fock atomic charge densities based on

GTO⁵³ are also included for comparison. The ground state atomic configuration ($3d^8, 4s^2$) was employed. There is considerable asymmetry in the charge distribution as $\rho_b(\vec{r})$ is spread out along the [100] direction relative to the [110] and [111] directions.

The contact charge density $\rho_b(0)$ in the solid differs from that in the atom as a result of two principal effects.⁶³ First, the s wave functions are normalized within an atomic cell. This tends to increase $\rho_b(0)$ relative to a free atom. Second, hybridization mixes d and p components into a s band. This tends to reduce $\rho_b(0)$. There is some partially compensating increase due to inclusion of s character into primarily d-like bands. The final result for $\rho_b(0)$ is not greatly different from the free atom value.

The theoretical results for the Fourier coefficients of the charge density can be compared with experimental observations of the X-ray atomic scattering factor by Diana, Mazzone, and De Marco.⁶⁴ The results are presented in Table VI. The small differences between the theoretical values for $\vec{k}_{[333]}$ and $\vec{k}_{[511]}$ and between $\vec{k}_{[600]}$ and $\vec{k}_{[442]}$ indicate slight departures of the charge distribution from spherical symmetry. Although there are deviations between theory and experiment which are outside the quoted experimental error, we feel that the agreement is fairly good. In the case of the [111], [200] vectors, our

results are significantly closer to experiment than are values calculated from free atom Hartree-Fock charge densities for either d^8s^2 or d^{10} configurations and reported by Diana et al.

The distribution of spin density in nickel has been investigated by Mook through neutron diffraction.⁶⁵ This experiment determines a magnetic form factor, $f(\vec{K})$, which is the ratio of the magnetic scattering amplitude for a scattering vector \vec{K} , to that for $\vec{K}=0$. This function has been computed by Hodges, Ehrenreich, and Lang using their combined tight-binding and pseudopotential interpolation method.¹⁸ It is customary to express $f(\vec{K})$ as the sum of three terms

$$f(\vec{K}) = \frac{2}{g} f_{\text{spin}}(\vec{K}) + \frac{(g-2)}{g} f_{\text{orb}}(\vec{K}) + f_{\text{core}}(\vec{K}) ,$$

(3.1)

in which g is the spectroscopic splitting factor and has been determined to be 2.18 for Ni.⁶⁶ The quantity f_{spin} is the form factor for the unpaired (mainly d) electrons, and is normalized so that $f_{\text{spin}}(0) = 1$:

$$f_{\text{spin}}(\vec{K}) = (Nv)^{-1} \int e^{i\vec{K}\cdot\vec{r}} [\rho_{\uparrow}(\vec{r}) - \rho_{\downarrow}(\vec{r})] d^3r ,$$

(3.2)

in which v is the magneton number. Although the core has a net spin of zero, exchange effects produce a slight difference in the radial distributions of \uparrow and \downarrow spin core electrons, and so, lead to a small contribution f_{core} . Finally, there is a contribution, f_{orb} from the possible unquenched orbital angular momentum of the d electrons. This term has been studied by Blume.⁶⁷ However, the assumptions of this calculation are not in accord with the band picture described here.

We have calculated the spin and core contributions to $f(\vec{k})$, using the wavefunctions obtained from our band calculation. The formulas are obtained immediately from Eq. (2.62) and the results are tabulated in Table VII. The magnetic form factors are shown in Fig. VI where they are compared with the experimental values of Mook. A satisfactory, although not perfect degree of agreement is obtained. It will be noted that there can be considerable departures from spherical symmetry: $f(\vec{k})$ is not simply a function of $|\vec{k}|$, in agreement with experiment.

It is also of interest to examine the position dependence of the spin density $\rho_{\uparrow}(\vec{r}) - \rho_{\downarrow}(\vec{r})$. Results are shown in Fig. VII and Table VIII. Contribution from the core and band electrons are separated in the table. In contrary to the results of the charge distribution, the magnetic moment densities in [111] and [110] directions

are larger than that in [100] direction. This result is in agreement with Mook's analysis. The contribution to the contact charge density from electrons of minority spin is slightly larger than that from electrons of majority spin.

It will be noted that the spin density is negative at large values of \vec{r} , indicating that there is a net negative spin polarization in the outer portion of the atomic cell. This result is also in agreement with the measurement of positron annihilation.⁶⁸

B. Momentum Distribution of Electrons

Recently, there has been a renewed interest in the Compton scattering experiments in solids. Unlike X-ray scattering factors, which are insensitive to the outer electron charge density, the Compton measurements are sensitive to the momentum distribution of outer electrons. Thus the Compton scattering experiments can provide a critical test for the wavefunctions from energy band calculation.

Platzman and Tzoar, by considering time dependent scattering theory, justified the use of the impulse approximation in the theory of Compton line shape.⁶⁹ The result can be summarized as follows: The impulse approximation is valid if (1) the wavelength of the incident photon is so short that it interacts with only

a single electron and ejects it instantaneously from the Fermi sea, (2) the energy transferred to the electron is large enough that the collision time is much shorter than the time required for any rearrangement of the remaining electrons. The net effect is that the photon exchanges energy and momentum with a single electron in a constant potential field. The differential scattering cross section of photons from a system of electrons in solid can be shown to be

$$\frac{d\sigma}{d\omega d\Omega} = \left(\frac{e^2}{mc^2}\right)^2 (\vec{\epsilon}_1 \cdot \vec{\epsilon}_2)^2 \left(\frac{\omega_2}{\omega_1}\right) \frac{m}{|\vec{k}|} \frac{1}{\Omega} J_{\vec{k}}(q) . \quad (3.3)$$

The Compton profile is given by

$$J_{\vec{k}}(q) = \frac{\Omega}{(2\pi)^3} \int d^3\vec{p} \rho(\vec{p}) \delta(q - \vec{p} \cdot \hat{\vec{k}}) \quad (3.4)$$

with

$$\hat{\vec{k}} = \frac{\vec{k}}{|\vec{k}|} \quad (3.5)$$

and

$$q = \frac{m\omega}{|\vec{k}|} - \frac{|\vec{k}|}{2} . \quad (3.6)$$

Here $\hat{\vec{\epsilon}}_1$, $\hat{\vec{\epsilon}}_2$, \vec{k}_1 , \vec{k}_2 , and ω_1 , ω_2 are the polarization, momentum and frequency of the incident and the scattered

photons respectively, $\vec{k} = \vec{k}_1 - \vec{k}_2$ and $\omega = \omega_1 - \omega_2$ are the momentum and energy transferred to the electrons, and Ω is the volume of a primitive cell. The delta function appearing in Eq. (3.4) is deduced from the energy conservation

$$\omega = \frac{|\vec{k}|^2}{2m} - \frac{\vec{k} \cdot \vec{p}}{m} . \quad (3.7)$$

The scattered photon is shifted in energy both by the momentum transfer $k^2/2m$ and the doppler shift component $(\vec{k} \cdot \vec{p}/m)$. The momentum distribution function which also appears in Eq. (3.4) gives the probability of finding the initial electron with a given momentum \vec{p} .

$$\rho(\vec{p}) = \sum_{nq} |\psi_n(\vec{q}, \vec{p})|^2 . \quad (3.8)$$

The summation in Eq. (3.8) includes occupied states specified by band index n and wavevector \vec{q} and $\psi_n(\vec{q}, \vec{p})$ is the Fourier transform of the Bloch wavefunction $\psi_n(\vec{q}, \vec{r})$

$$\begin{aligned} \psi_n(\vec{q}, \vec{p}) &= \frac{1}{\sqrt{N\Omega}} \int e^{-i\vec{p} \cdot \vec{r}} \psi_n(\vec{q}, \vec{r}) d^3 r \\ &= \sum_i a_{ni}(\vec{q}) \sum_s \delta_{\vec{q}, \vec{p} - \vec{K}_s} \chi_i(\vec{p}) \end{aligned} \quad (3.9)$$

where the second summation runs over all reciprocal lattice vectors \vec{K}_s , $a_{ni}(\vec{q})$ is the expansion coefficients of the crystal wavefunctions, and $\chi_i(\vec{p})$ is the Fourier

transform of the atomic wavefunctions $u_i(\vec{r})$

$$\chi_i(\vec{p}) = \frac{1}{\sqrt{\Omega}} \int e^{-i\vec{p} \cdot \vec{r}} u_i(\vec{r}) d^3r . \quad (3.10)$$

The expressions for $\chi_i(\vec{p})$ are given in Appendix A. The integral in Eq. (3.4) implies that the Compton profile measures the number of electrons having a fixed value of momentum in the direction of the photon's scattering vector \hat{k} .

Neglecting spin-orbit interaction, the expansion coefficients $a_{ni}(\vec{g})$ have been tabulated for 89 independent points in 1/48th of the Brillouin zone. The summation over all \vec{g} in the Brillouin zone may be expressed in terms of a sum over \vec{g} in the primitive 1/48th of the zone and a sum over group operations which generate the star of \vec{g} . The symmetry properties of the Bloch function can then be used to transform the variables of integration. The final form of the expression for the Compton profile is

$$J_{\vec{k}}^*(q) = \frac{n}{(2\pi)^3} \sum_n \int_{\vec{g} \in \text{occ}} \frac{1}{48} d^3g \sum_{\vec{K}_S} \left| \sum_i a_{ni}(\vec{g}) \chi_i(\vec{g} + \vec{K}_S) \right|^2 \sum_{\beta} \delta[q - (\vec{g} + \vec{K}_S) \cdot \beta \hat{k}] . \quad (3.11)$$

The sum over β includes all operators in the cubic point group.

If a GTO involves the factor $e^{-\alpha r^2}$ its Fourier transform will be proportional to $e^{-p^2/4\alpha}$. These factors govern the convergence of the sum over reciprocal lattice vectors in Eq. (3.11). For band states, the effective α 's are not large and good convergence is obtained. However, convergence is much slower for core functions where large α 's are encountered. A check on convergence can be obtained from the normalization condition on $J_k(q)$:

$$\int_{-\infty}^{\infty} J_k(q) dq = n_e \quad (3.12)$$

in which n_e is the number of electrons per atom. In our calculation, the sums over \vec{k}_s were carried out over approximately 3000 permuted reciprocal lattice vectors. No contribution was included from the 1s wavefunctions (the impulse approximation is probably not valid for 1s electrons in X-ray Compton scattering measurements). The convergence of the reciprocal lattice sum for the band (3d and 4s) electrons is quite good; however, it is not complete for the core electrons. There remain small contributions, mostly from the 2s and 2p electrons, that have been neglected. Consequently, the theoretical curves are probably slightly too low. This effect will be important mainly for larger values of q than are studied here. The contribution from the 1s electrons was determined using atomic wavefunctions. This was included in

our calculation in order to compare with the experimental results using high energy γ rays.

The Compton profile in [100], [110], and [111] directions are shown in Fig. VIII. The contribution from core electrons (2s, 2p, 3s, 3p) has been separated from the total in the figures. The difference in Compton profiles along different directions is illustrated in Fig. IX. The experimental measurements of Eisbergen and Reed⁷¹ are also included for comparison. Considerable structure is evident in the curves. Much of this structure can be attributed to Fermi surface effects.⁷⁰ The momentum density $\rho(\vec{p})$ suffers some discontinuity whenever \vec{p} touches a piece of Fermi surface. For a fixed direction of momentum transfer \hat{k} , the Compton profile $J_{\hat{k}}^{\wedge}(q)$ measures the amount of the momentum density, contained in a plane perpendicular to \hat{k} , sweeping through the momentum space. The profile will have a cusplike behavior when the plane perpendicular to \hat{k} happens to be tangent to a piece of flat Fermi surface. A thorough measurement on the Compton line shape can, therefore, provide information on the shape of the Fermi surface. Similar structures corresponding to Fermi surfaces in the higher order of the Brillouin zone should exist for larger values of q . The sharpness of the breaks in $J_{\hat{k}}^{\wedge}(q)$ indicates the amount of discontinuity presented in $\rho(\vec{p})$. The periodicities in the anisotropy of the Compton profile along different directions reflect

the position of the reciprocal lattice vectors and hence the size and structure of the primitive cell. Of course, many body effects would be expected to reduce the visibility of these structures through the introduction of additional high momentum components into the band wavefunctions.

The Compton profile along the $[1,0,0]$ direction is relatively smooth since most of the Fermi surfaces parallel to this direction are moderately spherical. (See Figs. XIV and XV). The structures presented in $J_{[1,1,0]}(q)$ - $J_{[1,0,0]}(q)$ can be understood based on the Fermi surface effects along the $[1,1,0]$ direction. The fine structure near the origin reflects the anisotropy in the dimensions of the X hole pockets. The structures near 0.45 and 0.58 a.u. correspond to the two square pieces of the Fermi surface centered at $\Gamma(0,0,0)$. Similarly, structures near 0.76, 0.89, 1.79, and 1.92 a.u. correspond to those centered at $2\pi/a(1,1,1)$ and $2\pi/a(2,0,0)$. Fine structures near the Γ points displaced by a reciprocal lattice vector to locations of magnitude 1.34, and 2.68 a.u. when projected onto the $[1,1,0]$ direction, can be attributed to the effects of X hole pockets. The rapid raise near the origin in $J_{[1,1,1]}(q) - J_{[1,0,0]}(q)$ reflects the difference in the cross sectional area of the Γ centered electron Fermi surfaces. The contributions from the $L'_{2\uparrow}$ necks are resolved in this picture into two small bumps near 0.27

a.u.. Fine structures near 0.82 and 1.36 a.u. correspond to $L_{2\uparrow}^1$ centered at $2\pi/a(2,0,0)$. The minima near 0.55 and 1.64 a.u. can be attributed to the cross sections of the X hole pockets in the plane perpendicular to the [1,1,1] direction. Finally, the structures in $J_{[1,1,0]}(q)$ - $J_{[1,1,1]}(q)$ can be interpreted as the combination of the Fermi surface effects described above.

The spherical average Compton profile was obtained using a sixth order Cubic harmonics expansion. The spherical average $J_{av}(q)$ was approximated as the zeroth order term in the expansion. The results are compared with γ ray Compton scattering measurements^{71,72} in Fig. X. The contributions from occupied band states are also included for detailed comparison. The contribution from the atomic core states that we used to subtract from the experimental measurements has been tabulated in Ref. 71. The agreement is reasonably good except for large values of q in the total $J_{av}(q)$. This discrepancy may be attributed to many body effects. Numerical values for the Compton profile and the contribution from band electrons can be found in Tables IX and X respectively.

C. The Density of States

Gilat has reviewed different methods of calculating the density of states.⁷³ We employ here the Gilat-Raubenheimer⁷⁴ method in combination with an interpolation scheme. The method is similar to that used by Cooke and Wood,⁷⁵ except that our interpolation procedure is based on second order $\vec{k} \cdot \vec{p}$ perturbation theory. The band calculation with spin orbit coupling included 1357 points in $1/16$ 'th of the Brillouin zone. Energies, wave functions, and momentum matrix elements were obtained at these points. A finer mesh was constructed by dividing the original step size by three -- this represents 26 additional points around each previous general point. The $\vec{k} \cdot \vec{p}$ calculation was performed as follows. If a given band at the "original" point (\vec{k}_o) was separated by 0.005 Ry or more from all other bands ordinary perturbation theory was employed to determine the energy at the additional points (\vec{k}). Thus

$$\begin{aligned}
 E_n(\vec{k}) = & E_n(\vec{k}_o) + \frac{\hbar}{m} (\vec{k} - \vec{k}_o) \cdot \vec{\pi}_{nn} + \frac{\hbar^2}{2m} (\vec{k}^2 - \vec{k}_o^2) \\
 & + \frac{\hbar^2}{m^2} \sum_{j(j \neq n)} \frac{[(\vec{k} - \vec{k}_o) \cdot \vec{\pi}_{nj}] [(\vec{k} - \vec{k}_o) \cdot \vec{\pi}_{jn}]}{E_n(\vec{k}_o) - E_j(\vec{k}_o)}
 \end{aligned}$$

(3.13)

The matrix element is

$$\vec{\pi}_{nj} = \frac{(2\pi)^3}{\Omega} \int w_n^*(\vec{k}_o, \vec{r}) (\vec{p} + \frac{\hbar}{4mc^2} \vec{\sigma} \times \vec{\nabla} V(\vec{r})) w_j(\vec{k}_o, \vec{r}) d^3 r \quad (3.14)$$

in which Ω is the volume of the cell and w is the cell periodic part of the Bloch function.

$$w_n(\vec{k}, \vec{r}) = e^{-i\vec{k} \cdot \vec{r}} \psi_n(\vec{k}, \vec{r}). \quad (3.15)$$

Numerical tests showed that the spin orbit contribution to the matrix element (the term in (3.14) proportional to $(\vec{\sigma} \times \vec{V}V)$) was negligible; hence in practice $\vec{\pi}_{nj}$ was always replaced by \vec{p}_{nj} . Only 12 bands were included in the sum in (3.13). Thus, the second order term is not computed exactly, but since the other energy denominators are much larger, the accuracy should be sufficient. When two or more bands at \vec{k}_o were separated by less than 0.005 Ry, an effective Hamiltonian was diagonalized. The elements of this Hamiltonian are

$$\begin{aligned} H_{nn}(\vec{k}) &= [E_g(\vec{k}_o) + \frac{\hbar^2}{2m} (\vec{k}-\vec{k}_o)^2] \vec{\pi}_{nn} + \frac{\hbar}{m} (\vec{k}-\vec{k}_o) \cdot \vec{\pi}_{nn} \\ &+ \frac{\hbar^2}{m^2} \sum_j \frac{[(\vec{k}-\vec{k}_o) \cdot \vec{\pi}_{nj}] [(k-\vec{k}_o) \cdot \vec{\pi}_{jn}]}{E_A - E_j(\vec{k}_o)} \quad (3.16) \end{aligned}$$

in which E_A is the average energy of the nearly degenerate levels at \vec{k}_o . The prime on the sum indicates that the nearly degenerate levels are excluded. As before, only twelve bands were included in the sum in Eq. (3.16), so that second order term is not exact.

The linear analytic integration scheme was then applied to each minicell constructed around each mesh point.⁷⁴ Projection operators were used to separate the contributions from majority and minority spins to the density of states. Our results for the majority and minority spin state densities and for the total are shown in Figs. XI-XIII. The total density of states at the Fermi energy was found to be 23.56 electrons/atom-Ry. The electronic specific heat coefficient $\gamma = \pi^2/3 N(E_F)k^2$, where k is the Boltzman's constant, was found to be 4.08 mJ/(mol °K²). Measurements of the low temperature specific heat yield a value of 7.028 mJ/(mol °K²).⁷⁶ Part of the discrepancy may be attributed to neglect of the electron-phonon interaction. The magneton number was found to be 0.62, somewhat higher than the experimental value of 0.56.² Our calculation predicts that a minority spin hole pocket associated with the $X_{2\downarrow}$ level should exist. This has not been observed experimentally, although it has also been predicted by other self-consistent calculations.¹⁵ This hole pocket is probably responsible for the disagreement between theoretical and experimental values of the

magneton number.

D. The Fermi Surface

The Fermi surface of nickel has been carefully studied through measurements of the de Haas-van Alphen effect⁷⁷⁻⁸¹ and cyclotron resonance.⁸² These observations are of great importance in that they confirm the general picture of itinerant electron ferromagnetism in nickel, in which the electrons responsible for magnetic order are not localized, but instead have wave functions extending throughout the crystal and contribute to the formation of a Fermi surface.

The major features of the Fermi surface of nickel can be understood on the basis of a calculation in which spin orbit coupling is neglected, but this interaction must be included in a detailed comparison of theory and experiment.²⁰ As was noted above, the spin orbit splitting of the states X_{5+} (001) and X_{5+} (100) is quite different. This leads to a significant difference in the sizes of the hole pockets around these points and to large anisotropy of de Haas-van Alphen frequencies.⁷⁹ A rapid variation of the de Haas-van Alphen amplitude when the applied magnetic field is tilted a few degrees from the [110] direction in a (1 $\bar{1}$ 0) plane has been interpreted as resulting from magnetic breakdown across a small gap resulting from the removal of an accidental degeneracy between spin

orbit split bands.²⁰

In our calculation, spins are quantized along the [001] axis. We are therefore limited in principle to an investigation of the Fermi surface in the k_z =constant planes. However, the dependence of the band structure on the field direction is probably not large except for the small hole pockets at X, and we will discuss cross sections in a (110) plane as well. Our Fermi surface cross sections shown in Figs. XIV and XV, where they are compared with recent results of Stark⁸¹ for the large portions of the surface and of Tsui⁸⁰ concerning the hole pocket at X. Stark has derived Fermi surface radii from his measurements using the Kubic Harmonic expansion method of Mueller and Priestly.⁸³ His inversion program included seven Kubic Harmonics. We have plotted the Fermi surface radii obtained in this manner on the figures. An empirical formula given by Tsui has been used to outline an experimentally determined cross section for the small hole pocket at X. Some numerical results for dimensions of the $X_{5\downarrow}$ hole pocket are given in Table XI and extremal areas are listed in Table XII. Comparisons are made with experiment^{79,80,81} and with the calculations of Zornberg.²²

There is a substantial degree of agreement between the theoretical and experimental results. It is apparent that the band calculation is able to describe the major pieces of Fermi surface correctly. The most significant

disagreement concerns the $X_{2\uparrow}$ hole pocket, which is not observed experimentally, but is predicted by our calculations. Since this pocket is predicted by other band calculations using a local exchange potential, it is possible that this prediction indicates a basic inadequacy of the local exchange approximation.

The majority-spin portion of the Fermi surface lies entirely in the upper s-p band. The surface is in contact with the Brillouin zone near the points L. A neck of roughly circular cross section is formed at each such point. We obtained a value of 0.0035 a.u. for the cross sectional area of this neck in the hexagonal face of the zone. This is smaller than the experimental measurement of 0.0072 a.u. obtained by Tsui.⁸⁰ It is probable that the $L'_{2\uparrow}$ level is too close below the Fermi level due to insufficient variational freedom in the s-p type basis functions which are expanded in atomic orbitals. The wave function associated with the $L'_{2\uparrow}$ state has pure p-type symmetry. Only the p-p block needs to be considered to investigate this problem. The $L'_{2\uparrow}$ level calculated by expanding the basis functions in ten individual GTO for each type of p symmetry (x, y, and z) lies 0.008 Ry. below that of atomic GTO. The Gaussian exponents used were the same as the one for atomic GTO. But the smallest exponent was not included because it gave rise to a negative eigenvalue in the overlap matrix. A rough

estimate of the new cross sectional area was made after raising the Fermi energy with respect to the $\Delta_{1\uparrow}$ level by 0.008 Ry.. The result is 0.0068 a.u., in good agreement with the measurements of Tsui.

Goy and Grimes⁸² have observed cyclotron resonance associated with the majority spin Fermi surface neck at L, the hole pocket $X_{5\downarrow}$ and, according to our interpretation, the two large pieces of Fermi surface around Γ . The wave functions associated with the smaller piece have predominately $e_{g\downarrow}$ symmetry near the Γ -X line, but mixed components of s-p \downarrow and $t_{2g\downarrow}$ near Γ -K. The states associated with the larger, nearly square section, are of predominately majority spin but have the same spatial symmetry as those on the smaller square, except near the [100] axis where there is a strong, spin orbit induced mixing with minority spin d band states.

The experimentally observed cyclotron effective mass has been compared with the effective mass m_c^* obtained from the band structure according to the formula

$$\frac{m_c^*}{m} = \frac{\mu^2}{\pi} \left(\frac{dA}{dE} \right)_{E_F} \quad (3.17)$$

in which m is the free electron mass, and A is the area of the cyclotron orbit. Our results and the experimental findings are presented in Table XIII. The results of the semi-empirical calculation of Zornberg²² are also

shown. It will be seen that the agreement is fairly good for the X_5 pocket, with the deviation between theory and experiment being of the amount and direction expected to allow for a reasonable enhancement through the electron-phonon and the electron-magnon interactions. However, our result for the minority spin square is larger than the experimental value, while that for the majority spin square is much smaller than that observed.

E. Optical Conductivity

The optical properties of nickel have been the subject of intensive studies for a long time. As a result of difficulties in sample preparation, accuracy of the measurements, and data analyses the agreement among different experiments has frequently been poor. Therefore, a first principles calculation of optical conductivity is desired to settle some of the controversies as well as to improve our understanding of the electronic structure.

We have calculated the interband optical conductivity of nickel. We will present results in two cases: (1) including a phenomenological constant relaxation time τ , and (2) in the limit $\tau \rightarrow 0$ so that the band states are sharp. The general expression can be obtained from the Kubo formula⁸⁴:

$$\hat{e}_{\alpha\beta}(\vec{q}, \omega) = -\frac{Ne^2}{im\omega} \delta_{\alpha\beta} + \frac{1}{N\omega} \int_{-\infty}^{\infty} dt e^{-i\omega t} [J_\alpha(\vec{q}, 0) J_\beta(\vec{q}, t)]_0 e^{-i\omega t} \quad (3.18)$$

where \vec{q} , ω , and N are the wave vector, frequency and the electron density respectively. $J_\alpha(\vec{q}, t)$ are the Cartesian components of the Fourier transform of the current operator of the system in the interaction picture.

$$\hat{j}(\vec{q}, t) = e^{i\hat{H}_0 t} j(\vec{q}) e^{-i\hat{H}_0 t} \quad (3.19)$$

in which \hat{H}_0 is the Hamiltonian of the system in the absence of the external field. The ensemble average $\langle \dots \rangle_0$ is to be computed with the equivalent density matrix $\rho_0 = 1/Z e^{-\beta\hat{H}_0}$ where $Z = \text{Tr}(e^{-\beta\hat{H}_0})$ is the usual partition function. We are concerned with energy in the optical and infrared region. The corresponding photon wavelength is large compared to the lattice constant. Consequently, the spatial variation of the electric field over the unit cell can be neglected and it is sufficient to consider the limit $\vec{q} \neq 0$ only. Denoting $j(t) = j(\vec{0}, t)$, it can easily be verified that

$$\begin{aligned} [J_\alpha(0), J_\beta(t)]_0 &= \frac{1}{Z} \sum_i e^{-\beta E_i} [(-i)[J_\alpha(i) - i[J_\beta(i)]] e^{i\omega_i t}] \\ &= (-i[J_\alpha(i) - i[J_\beta(i)]] e^{-i\omega_i t}) \end{aligned} \quad (3.21)$$

in which $|i\rangle, |j\rangle$ are eigenstates of H_0 with eigenvalue $\epsilon_i \epsilon_j$ and $\hbar\omega_{ij} = \epsilon_i - \epsilon_j$. At zero temperature, further simplification is possible within the Hartree Fock approximation. In this case the wave function of the system is considered to be Slater determinant of single particle Bloch functions $\psi_n(\vec{k}, \vec{r})$. Since the current operator \hat{j} for the system is the sum of one particle operators \hat{j}_s , the possible matrix elements $\langle j | \hat{j} | i \rangle$ involve the excitation of a single particle from a state $\psi_q(\vec{q}, \vec{r})$ which is occupied in the ground state of the system to some unoccupied state $\psi_n(\vec{k}, \vec{r})$

$$\langle \vec{q} | \hat{j}_s | \vec{n} \vec{k} \rangle = -\frac{e}{m} \langle \vec{q} | \vec{\pi} | \vec{n} \vec{k} \rangle = -\frac{e}{m} \pi_{qn}(\vec{k}) \delta_{\vec{k}, \vec{q}} \quad (3.22)$$

where $\pi_{qn}(\vec{k})$ is the matrix element defined in Eq. (3.4).

We can rewrite Eq. (3.21) in the following form:

$$\langle [J_\alpha(0), J_\beta(t)] \rangle_0 = \frac{e^2}{m^2} \sum_{\vec{k}} \sum_{\substack{n \vec{k} \\ o}} (\pi_{qn}^\alpha(\vec{k}) \pi_{n^o}^\beta(\vec{k}) e^{i\omega_{n^o}(\vec{k})t} - \pi_{qn}^\beta(\vec{k}) \pi_{n^o}^\alpha(\vec{k}) e^{-i\omega_{n^o}(\vec{k})t}) \quad (3.23)$$

For convenience we employ discrete normalization.

$\pi_{n^o}(\vec{k})$ is the energy difference between band n and l

$$\omega_{n\ell}(\vec{k}) = \frac{1}{V} (E_n(\vec{k}) - E_\ell(\vec{k})) \quad (3.24)$$

The sum over ℓ, \vec{k} include occupied states (o) only while that over n, \vec{k} include unoccupied states (u) only. Eq. (3.23) is inserted into Eq. (3.18). We considered the frequency ω to have a positive imaginary part i/τ so that the integral in Eq. (3.18) will converge at the lower limit. The result is

$$\begin{aligned} \sigma_{\alpha\beta}(\omega) &= \frac{-Ne^2}{im(\omega + \frac{i}{\tau})} \delta_{\alpha\beta} + \frac{ie^2}{Vm^2(\omega + \frac{i}{\tau})} \sum_{\ell\vec{k}} \sum_{n\vec{k}} \\ &\left[\frac{\pi_{\ell n}^\alpha(\vec{k}) \pi_{n\ell}^\beta(\vec{k})}{\omega + \frac{i}{\tau} - \omega_{n\ell}(\vec{k})} - \frac{\pi_{\ell n}^\beta(\vec{k}) \pi_{n\ell}^\alpha(\vec{k})}{\omega + \frac{i}{\tau} + \omega_{n\ell}(\vec{k})} \right]. \end{aligned} \quad (3.25)$$

Further simplification is possible if one introduces the optical effective mass:

$$\left(\frac{N}{m} \right)_{\alpha\beta} = \sum_{\ell\vec{k}} \left(\frac{1}{m_\ell^*(\vec{k})} \right)_{\alpha\beta} \quad (3.26)$$

where

$$\left(\frac{m}{m_\ell^*(\vec{k})} \right)_{\alpha\beta} = \delta_{\alpha\beta} + \frac{2}{Vm} \sum_n \operatorname{Re} \frac{(\pi_{\ell n}^\alpha \pi_{n\ell}^\beta)}{\omega_{n\ell}} \quad (3.27)$$

and the sum in (3.26) includes all $n\neq\ell$. The final expression for the conductivity tensor is

$$\sigma_{\alpha\beta}(\omega) = \frac{i Ne^2}{(\omega + \frac{i}{\tau})} (\frac{1}{m})_{\alpha\beta} - \frac{2ie^2}{m^2 \hbar} \sum_{\ell k} \sum_{nk} \frac{1}{\omega_{nk}^2(k) - (\omega + \frac{i}{\tau})^2}$$

$$[\frac{\omega + \frac{i}{\tau}}{\omega_{nk}^2} \operatorname{Re}(\pi_{\ell n}^{\alpha} \pi_{n\ell}^{\beta}) + i \operatorname{Im}(\pi_{\ell n}^{\alpha} \pi_{n\ell}^{\beta})] \quad (3.28)$$

The ordinary optical properties of ferromagnetic nickel are determined by the diagonal components of σ (we have $\sigma_{xx} = \sigma_{yy} \neq \sigma_{zz}$, z being the direction of spin alignment). The result of setting $\alpha = \beta$ in (3.28) is

$$\sigma_{\alpha\alpha}(\omega) = \frac{i Ne^2}{(\omega + \frac{i}{\tau})} (\frac{1}{m})_{\alpha\alpha} - \frac{2ie^2}{m^2 \hbar} (\omega + \frac{i}{\tau}) \sum_{\ell k} \sum_{nk} \frac{|\pi_{\ell n}^{\alpha}|^2}{\omega_{nk}^2 - (\omega + \frac{i}{\tau})^2} \quad (3.29a)$$

It can be directly verified that this expression satisfies the sum rule

$$\int_0^\infty \operatorname{Re}(\sigma_{\alpha\alpha}) d\omega = \frac{\pi Ne^2}{2m} \quad (3.30)$$

where m is the free electron mass. The first term in Eq. (3.29a) is the usual Drude formula with relaxation time τ . In the limit in which the band states are sharp ($\tau \rightarrow \infty$), we obtain the familiar expression for the real part of the conductivity for positive frequencies

$$\operatorname{Re} [\sigma_{xy}(\omega)] = \frac{\pi Ne^2}{2(m)_\alpha} \delta(\omega) + \frac{\pi e^2}{m^2 \hbar \omega} \sum_{\ell k} \sum_{n u} |\pi_{\ell n}^\alpha|^2 \delta(\omega - \omega_{n\ell}) \quad (3.29b)$$

The off diagonal components of the conductivity vanish except for $\sigma_{xy} = -\sigma_{yx}$. In this case, we have

$$\sigma_{xy} = \frac{2e^2}{m^2 \hbar} \sum_{\ell k} \sum_{n u} \frac{\operatorname{Im}(\pi_{\ell n}^\alpha \pi_{n\ell}^\beta)}{\omega_{n\ell}^2 - (\omega + \frac{i}{\tau})^2} \quad (3.31a)$$

The sharp limit of this formula is, for positive frequencies,

$$\operatorname{Im}[\sigma_{xy}(\omega)] = \frac{\pi e^2}{m^2 \hbar \omega} \sum_{\ell k} \sum_{n u} \operatorname{Im}(\pi_{\ell n}^\alpha \pi_{n\ell}^\beta) \delta(\omega - \omega_{n\ell}) \quad (3.31b)$$

If the matrix elements in these expressions are treated as constants, the conductivity is proportional to the joint density of states. We have computed this quantity by the same method described in Section C in connection with the ordinary density of states. The joint density of states shown in Fig. XVI is dominated by an enormous spike, resulting from the nearly parallel upper d bands, especially in the region X-W-L. However, the approximation in which the matrix elements are treated as

constant is a bad one since in particular the transition associated with this spike has a very weak matrix element. (The states involved in the spike are predominately of opposite spin, and the matrix element would vanish except for the mixing of opposite spin components in the wave function).

We have calculated the optical conductivity including the \vec{k} dependence of all matrix elements both in the sharp limit, Eqs. (3.29b) and (3.31b) and with the inclusion of a relaxation time. The integration was performed by the method described in Section C in which the $\vec{k} \cdot \vec{p}$ method was used to calculate the energy for \vec{k} corresponding to a subdivided mesh in the Brillouin zone. The momentum matrix elements at the additional mesh points were found by linear interpolation between the values calculated at the basic 1357 point grid. Numerical tests showed that the contribution of the spin orbit coupling term to the matrix element $\pi_{n\ell}$ [Eq. (3.14)] was negligible for the determination of both the diagonal and off diagonal elements of the conductivity. We therefore replaced $\pi_{n\ell}$ by $p_{n\ell}$ throughout the calculation. This implies that the off diagonal conductivity should be regarded as being produced by the modification of the band wave functions produced by the spin-orbit interaction.

Our results for the real part of ϵ_{xx} between 0 and 1.2 eV are shown in Fig. XVII. The solid line represents

the contribution from the interband conductivity in the sharp limit ($\tau \rightarrow \infty$) to which has been added an empirical Drude term,

$$\sigma_D(\omega) = \frac{\sigma_0}{\omega^2 \tau} , \quad (3.32)$$

in which the constants have been taken to be $\sigma_0 = 18.6 \times 10^{15}$ sec⁻¹ and $\tau = 11.3 \times 10^{-15}$ sec. as determined by Lenham and Treherne.⁸⁵ The dashed curve is the sum of the same empirical Drude term plus an interband contribution computed assuming essentially the same τ . We have also computed $\text{Re}(\sigma_{zz})$, which is not the same as $\text{Re}(\sigma_{xx})$ in the present case. However, the differences are quite small and are not significant on the scale of this graph. The conductivity in the energy region 1.0-6.0 eV is shown in Fig. XVIII. The experimental results of several authors⁸⁶⁻⁹¹ are also shown in these figures. Although there is a large amount of scatter in the experimental data, there is a reasonable degree of general agreement between many of the measurements, particularly in regard to the magnitude and the general trend. There is less agreement in regard to detailed structure. We believe that it is significant that our calculations are in good agreement with the general magnitude of the observed conductivity in the low energy region. In particular, the departure from the Drude term seems to be given

satisfactorily. There is little agreement between theory and experiment in regard to specific structures at low energies except, possibly in the 0.2-0.5 eV region where structure in our calculated conductivity appears in some of the observations and is confirmed by thermoreflectance measurements.⁹²

A most important feature of our calculated results is the peak at 0.80 eV which results from transitions between the nearly parallel upper d bands near the zone face. This transition is a direct measure of the exchange splitting responsible for ferromagnetism. This peak is quite pronounced when the band states are considered to be sharp; however, it is much reduced if reasonable allowance is made for finite lifetimes of the states. We do not notice any comparable structure in the experimental data in this energy region, and we infer from this discrepancy that our calculation has probably overestimated the exchange splitting. It is not obvious from the data available to us whether or not this transition has actually been observed; however, we tentatively suggest that the broad rise beginning at 0.5 eV in the results of Lynch et al.⁸⁷ may be associated with this transition. If this interpretation is correct, the d band exchange splitting is about 0.5 eV, in fair agreement with other estimates,²² and significantly smaller than our calculated value.

Some structure is present in our calculated conductivity in the 2-3 eV range, but this is much reduced when lifetime broadening is included. Failure to observe structure in this energy range⁹³ suggests that lifetime effects are indeed appreciable. At higher energies, the experimental conductivity shows a large increase, beginning near 4 eV. A corresponding feature is present in our results, but it is displaced to higher energies by about 1 eV. In our calculations, this peak results from transitions between the lower s-d bands and the s-p bands above the Fermi energy. The bands involved are in the outer part of the Brillouin zone, along the Z axis, and in the vicinity of the symmetry points X and L. The discrepancy in energy between theory and experiment is probably an indication of the inadequacy of our use of atomic wave functions rather than separated orbitals to represent s- and p-like states.

The absorptive part of the off diagonal elements of the conductivity tensor can be determined from measurements of the ferromagnetic Kerr effect⁹⁴: plane-polarized light reflected from a magnetized ferromagnetic metal becomes elliptically polarized with its major axis rotated from the original direction of polarization. Macroscopically, the rotation angle can be related to the absorptive part of the off diagonal elements of the conductivity tensor through Maxwell's field equations.^{94, 95} The detailed

derivation is presented in Appendix B. This effect involves spin orbit coupling in an essential way. Previous calculations have been based on perturbation theory and simple models of the band structure.⁹⁶ A major conflict developed between the results of different measurements.^{97,98} However, more recent work⁹⁹⁻¹⁰³ has tended to confirm, in a general way, the results of Krinchik and collaborators.

We have calculated the off diagonal element σ_{xy} of the conductivity tensor. Our results for $\omega \text{Im}(\sigma_{xy})$ are shown in Fig. XIX, where they are compared with results of Yoshino and Tanaka,⁹⁹ Krinchik and Artemjev¹⁰¹ and Erskine and Stern.¹⁰³ Our calculated results do not include any intraband contribution¹⁰⁴ since the experimental data do not extend to low enough energies to permit determination of this quantity. Such a term would simply shift the calculated curves by a constant. The theoretical curves have the same general shape and order of magnitude as the experimental ones. However, the agreement in detail is not particularly good. The negative portion of σ_{xy} at low energy can be interpreted as indicating the dominance of transitions of minority spin electrons.¹⁰³ The experimental curves become positive at a lower energy than the theoretical results. This is presumably a consequence of our overestimation of the exchange splitting. The negative peak at high energies is found, in our calculation to be displaced by about 1 eV with respect to the corresponding

experimental feature. A similar result was found for the diagonal elements of the conductivity and the explanation is probably the same. The smooth behavior of the experimental curves probably indicates the presence of substantial lifetime broadening.

CHAPTER IV

CONCLUSION

A self-consistent band structure for ferromagnetic nickel has been investigated using the tight binding method. The effects of exchange and spin-orbit interaction have been included. We believe that the comparison of the results of this calculation with experiment indicates that simple energy band theory employing a local exchange potential can successfully predict the essential features of the charge and magnetic moment distributions, momentum density, the Fermi surface, and of the optical properties of nickel. Although numerous discrepancies in detail exist, there is a large degree of general agreement between theory and experiment. There is no evidence for unexpectedly large many body effects, although some of the disagreement between theory and experiment may be due to our use of a simple, single particle approach. In view of the success of these calculations,^{11,105,106} and of our recent application to ferromagnetic iron,¹⁰⁷ it seems that band theory should provide a basically satisfactory account of the properties of ferromagnetic nickel. The principal obstacles to such a conclusion concerns observations of tunneling,¹⁰⁸ and of spin polarized photo-emission^{109,110} which revealed that the spin polarization of electrons at energy 10^{-3} and 0.4-0.8 eV. below the

Fermi level is +11% and +15% respectively. The direction of the electron magnetic moments was found to be parallel to the magnetization. Based on oversimplified theories, it was interpreted as a measure of the spin polarization of the density of states. This indicated a contradiction with the results of band theory. It is possible, however, that detailed calculations of such phenomena based on band theory may remove much of the apparent disagreement.^{111,112} We hope to undertake this investigation.

This calculation can be improved in several ways. First, the variational freedom in the trial wave functions would be increased and the accuracy of the results improved if all the basis functions were chosen to be individual GTO. Some discrepancies in the Fermi surface and the optical properties have been shown in Chapter III as an indication of the inadequacy of our use of atomic wave functions rather than independent Gaussian orbitals to represent s and p-like states. Recently, the band structures of Li,¹¹³ Na,¹¹⁴ and Al¹¹⁵ have been investigated using basis functions consisting of individual GTO. Successful results were obtained after repeating the whole calculation several times with different sets of GTO. In principle, a basis set consists of individual Gaussian orbitals with large exponents that are capable of reproducing the atomic core states and one or two small exponents to allow sufficient variational freedom in the

conduction s and p-like states is more likely to give a satisfactory result. Of course those small exponents are subject to the restriction that the eigenvalues of the corresponding overlap matrices cannot be negative or unreasonably small.

A second modification which would be helpful is to include more conduction states, such as 4f for transition metals. The eigenfunctions are expected to be a better approximation to the exact solutions of the Schrödinger equation. The hybridization between the 4f and band states will undoubtedly improve our results of energy bands and conductivity tensor. In the conventional LCAO calculation,³⁸ where the expressions for integrals between higher states are obtained by successive differentiations, the problem may seem to be too complicated to be considered. The modification, made by Chaney and Dorman,⁵⁶ to separate the variables in Cartesian coordinate and to take binomial expansions in the integrand drastically reduce the complexity of the problem. As a matter of fact, the integral program included in Appendix C is written in general that it can be used to calculate integrals between any pair of Gaussian orbitals.

Another possible improvement is to retain the angular dependence of the charge distribution when calculating the Xα exchange potential. This may effect the relative positions between the Fermi level and the X_{2+} state of e_g

symmetry as well as the unobserved x_{2+} hole pocket. The procedure involves three dimensional numerical integrations over rapidly oscillating functions which must be calculated with care. The cost in computer time, in this case, will be fairly high.

REFERENCES

1. For a review of the band theory of ferromagnetism, see A. J. Freeman and R. E. Watson, in "Magnetism", Vol. IIa, edited by G. T. Rado and H. Suhl (Academic Press, New York, 1965), p. 83.
2. H. Dannan, R. Heer, and A. J. P. Meyer, *J. Appl. Phys.* 39, 669 (1968).
3. E. Fawcett and W. A. Reed, *Phys. Rev. Letters* 9, 336 (1962); *Phys. Rev.* 131, 2463 (1963).
4. M. Dison, F. E. Hoare, T. M. Holden, and D. E. Moody, *Proc. Roy. Soc. (London)* A285, 561 (1965).
5. C. Herring, in "Magnetism", Vol. IV, edited by G. T. Rado and H. Suhl (Academic Press, New York, 1966), p. 120.
6. G. C. Fletcher and E. P. Wohlfarth, *Phil. Mag.* 42, 106 (1951).
7. G. C. Fletcher, *Proc. Phys. Soc. (London)* A65, 192 (1952).
8. J. Yamashita, M. Fukuchi, and S. Wakoh, *J. Phys. Soc. Japan*, 18, 999 (1963).
9. J. Callaway, H. M. Zhang, T. E. Norwood, and J. Langlinais, *Int. J. Quant. Chem.* 4, 425 (1971).
10. J. Langlinais and J. Callaway, *Phys. Rev.* B5, 124 (1972); J. Langlinais, Ph.D. Thesis, Louisiana State University (1971) (unpublished).

11. J. Callaway and C. S. Wang, Phys. Rev. B7, 1096 (1973).
12. J. G. Hanus, M. I. T. Solid State and Molecular Theory Group Quarterly Progree Report No. 44, p. 29 (1962) (unpublished).
13. L. F. Mattheiss, Phys. Rev. 134, A970 (1964).
14. E. C. Snow, J. T. Waber, and A. C. Switendick, J. Appl. Phys. 37, 1342 (1966).
15. J. W. D. Connolly, Phys. Rev. 159, 415 (1967).
16. S. Wakoh and J. Yamashita, J. Phys. Soc. Japan 19, 1342 (1964).
17. S. Wakoh, J. Phys. Soc. Japan 20, 1894 (1965).
18. L. Hodges, H. Zhrenreich, and N. D. Lang, Phys. Rev. 152, 505 (1966).
19. F. M. Mueller, Phys. Rev. 153, 659 (1967).
20. J. Ruvalds and L. M. Falicov, Phys. Rev. 172, 508 (1968).
21. H. Zhrenreich and L. Hodges, Meth. Comp. Phys. 8, 149 (1968).
22. E. I. Zornberg, Phys. Rev. B1, 244 (1970).
23. J. Callaway and H. M. Zhang, Phys. Rev. B1, 305 (1970).
24. J. C. Slater, Phys. Rev. 51, 846 (1937).
25. J. C. Slater, Phys. Rev. 92, 603 (1953).
26. M. M. Saffern and J. C. Slater, Phys. Rev. 92, 1126 (1953).
27. J. Korringen, Physica 13, 392 (1947).

28. W. Kohn and N. Rostoker, Phys. Rev. 94, 111 (1954).
29. J. Callaway and D. M. Edwards, Phys. Rev. 118, 923 (1960).
30. G. S. Painter, Phys. Rev. B1, 3520 (1973).
31. G. S. Painter, J. S. Faulkner and G. M. Stocks, Phys. Rev. B9, 2448 (1974).
32. J. C. Slater, Phys. Rev. 81, 385 (1951).
33. W. Kohn and L. J. Sham, Phys. Rev. 140, A1133 (1965).
34. R. Gaspar, Acta Phys. Hung. 3, 263 (1954).
35. J. C. Slater, T. M. Wilson, and J. H. Wood, Phys. Rev. 179, 28 (1969).
36. F. Bloch, Z. Physik 52, 555 (1928).
37. E. E. Lafon and C. C. Lin, Phys. Rev. 152, 579 (1966).
38. R. C. Chaney, T. K. Tung, C. C. Lin and E. E. Lafon, J. Chem. Phys. 52, 361 (1970).
39. J. Callaway and J. L. Fry in "Computational Methods in Band Theory" edited by P. M. Marcus, J. F. Janak, and A. R. Williams (Plenum, New York, 1972), p. 512.
40. R. A. Tawil and J. Callaway, Phys. Rev. B7, 4242 (1973).
41. J. Rath and J. Callaway, Phys. Rev. B8, 5398 (1973).
42. Y. M. Ching and J. Callaway, Phys. Rev. Letters 30, 441 (1973).
43. H. Brooks, Phys. Rev. 58, 909 (1940).
44. G. C. Fletcher, Proc. Phys. Soc. (London) 67, 505 (1954).
45. K. Merkle, Z. Naturforsch 14a, 938 (1959).

46. J. C. Slonczewski, J. Phys. Soc. Japan 17, S-34 (1962).
47. J. Friedel, P. Lenglart, and G. Leman, J. Phys. Chem. Solids 25, 781 (1964).
48. G. Allan, G. Leman, and P. Lenglart, J. de Phys. 29, 885 (1968).
49. N. Mori, J. Phys. Soc. Japan 27, 307 (1969).
50. D. Liberman, Phys. Rev. 171, 1 (1968).
51. L. J. Sham and W. Kohn, Phys. Rev. 145, 561 (1966).
52. A. K. Rajagopal and J. Callaway, Phys. Rev. B7, 1912 (1973).
53. A. J. H. Wachters, J. Chem. Phys. 52, 1033 (1970).
54. E. Clementi, "Tables of Atomic Functions" (IBM Corp., San Jose, California, 1965).
55. D. E. Gray, American Institute of Physics Handbook, 3rd Edition (McGraw-Hill Book Co., New York, 1972), pps. 9.6, 4.126.
56. R. C. Chaney and F. Norman, Int. J. Quantum Chem. (1974), to be published, and the references cited therein.
57. J. Callaway, Energy Band Theory (Academic Press, New York, 1964) p. 64.
58. L. M. Falicov and J. Ruvalds, Phys. Rev. 172, 498 (1968).
59. E. Wigner, Group Theory and Its Application to the Quantum Mechanics of Atomic Spectra (translated by J. J. Griffin) (Academic Press, New York, 1959) p. 347.

60. A. P. Cracknell, Phys. Rev. B1, 1261 (1970).
61. The d-d portion of the spin orbit coupling matrix in a cubic crystal, with allowance for cubic symmetry of the crystal potential has been given by J. A. Ricodeau, Phys. Rev. B7, 4950 (1973).
62. E. V. Condon and B. H. Shortley, Theory of Atomic Spectra (Cambridge, Eng. Univ. Press, 1951), p. 210.
63. R. E. Watson, A. A. Misetich and L. Hodges, J. Phys. Chem. Solids 32, 709 (1973).
64. M. Diana, G. Mazzone and J. J. DeMarco, Phys. Rev. 187, 973 (1969).
65. H. A. Mook, Phys. Rev. 148, 495 (1966).
66. A. J. P. Meyer and G. Asch, J. Appl. Phys. Suppl. 32, 3305 (1961).
67. M. Blume, Phys. Rev. 124, 96 (1961).
68. V. L. Sedov, Zh. Eksperim. Teor. Fiz. 48, 1200 (1964) [English transl: Soviet Phys. - JETP 21, 800 (1965)].
69. P. M. Platzman and N. Tjoar, Phys. Rev. 139, A410 (1965).
70. P. Eisenberger, L. Lam, P. M. Platzman and P. Schmidt, Phys. Rev. B6, 3671 (1972).
71. P. Eisenberger and W. A. Reed, Phys. Rev. B9, 3242 (1974).

72. S. Manninen and T. Paakkari (to be published).
73. G. Gilat, J. Comp. Phys. 10, 432 (1972).
74. G. Gilat and L. J. Raubenheimer, Phys. Rev. 144, 390 (1966).
75. J. F. Cooke and R. F. Wood, Phys. Rev. B5, 1276 (1972).
76. M. Dixon, F. E. Hoare, T. M. Holden and D. Z. Moody, Proc. Roy. Soc. (London) A285, 561 (1965).
77. A. S. Joseph and A. C. Thorsen, Phys. Rev. Letts. 11, 554 (1963).
78. D. C. Tsui and R. W. Stark, Phys. Rev. Letts. 17, 871 (1966).
79. L. Hodges, D. R. Stone, and A. V. Gold, Phys. Rev. Letts. 19, 655 (1967).
80. D. C. Tsui, Phys. Rev. 164, 669 (1967).
81. R. W. Stark, private communication.
82. P. Goy and C. C. Grimes, Phys. Rev. B7, 299 (1973).
83. F. M. Mueller, Phys. Rev. 148, 636 (1966); F. M. Mueller and M. G. Priestly, Phys. Rev. 148, 638 (1966).
84. R. Kubo, J. Phys. Soc. Japan 12, 570 (1957).
85. A. P. Lenham and D. M. Treherne in "Optical Properties and Electronic Structure of Metals and Alloys", F. Abeles, Ed. (North-Holland, Amsterdam, 1966), p. 196.
86. M. Ph. Stoll, Sol. St. Comm. 8, 1207 (1970); J. Appl. Phys. 42, 1717 (1971).
87. D. N. Lynch, R. Rosei, and J. H. Weaver, Sol. St. Comm. 9, 2195 (1971). We wish to thank Prof. Weaver

- for furnishing corrected values of the conductivity.
88. M. Shiga and G. P. Pells, J. Phys. C₂, 1847 (1969).
 89. M. M. Kirillova, Zh. Eksp. Teor. Fiz. 61, 336 (1971). [Soviet Phys. JETP 34, 178 (1972)].
 90. I. I. Sasovskaya and M. M. Naskov, Fiz. Metal Metaloved 32, 723 (1971); 33, 86 (1972).
 91. P. B. Johnson and R. W. Christy, Phys. Rev. B9, 5056 (1974).
 92. J. Hanus, J. Feinleib, and W. J. Scouler, Phys. Rev. Letts. 19, 16 (1967).
 93. B. W. Veal and A. P. Paulikas, Intern. J. Magnetism 4, 57 (1973).
 94. P. N. Argyres, Phys. Rev. 97, 334 (1955).
 95. H. S. Bennett and E. A. Stern, Phys. Rev. 137, A448 (1965).
 96. B. R. Cooper, Phys. Rev. 139, A1504 (1965).
 97. D. H. Martin, S. Doniach, and K. J. Neal, Phys. Letts. 9, 224 (1964); D. H. Martin, K. J. Neal, and T. J. Dean, Proc. Phys. Soc. (London) 86, 605 (1965).
 98. G. S. Krinchik and G. M. Nurmukhamedov, Zh. Eksp. Teor. Fiz. 48, 34 (1965). [Soviet Phys. JETP 21, 22 (1965)].
 99. T. Yoshino and S. Tanaka, Optics Comm. 1, 149 (1969).
 100. G. S. Krinchik and V. A. Artemjev, Zh. Eksp. Teor. Fiz. 53, 1901 (1967). [Soviet Phys. JETP 26, 1080 (1968)].

101. G. S. Krinchik and V. A. Artemjev, J. Appl. Phys. 39, 1276 (1969).
102. G. S. Krinchik and V. S. Gushchin, Zh. Eksp. Teor. Fiz. 56, 1833 (1969). [Soviet Phys. JETP 24, 984 (1969)].
103. J. L. Erskine and E. A. Stern, Phys. Rev. Letts. 30, 1329 (1973).
104. J. L. Erskine and E. A. Stern, Phys. Rev. B8, 1239 (1973).
105. J. Rath, C. S. Wang, R. A. Tawil and J. Callaway, Phys. Rev. B8, 5139 (1973).
106. C. S. Wang and J. Callaway, Phys. Rev. B9, 4897 (1974).
107. M. Singh, C. S. Wang and J. Callaway, Phys. Rev., to be published.
108. P. M. Tedrow and R. M. Meservey, Phys. Rev. Letts. 26, 192 (1971), Phys. Rev. B7, 318 (1973).
109. U. Banninger, G. Busch, M. Campagna, and H. C. Siegman, Phys. Rev. Letts. 25, 585 (1970).
110. G. Busch, M. Campagna and H. C. Siegman, Phys. Rev. B4, 746 (1971).
111. N. V. Smith and M. M. Traum, Phys. Rev. Letts. 27, 1388 (1971).
112. B. A. Politzer and P. H. Cutler, Phys. Rev. Letts. 28, 1330 (1972).
113. Y. M. Ching and J. Callaway, Phys. Rev. B9, 5115 (1974).

114. Y. M. Ching and J. Callaway, to be published.
115. R. A. Tawil and S. P. Singhal, to be published.

TABLE I

Fourier Coefficients of the Coulomb and Exchange Potential and the
Corresponding Corrections Resulting From Self-Consistency (in a.u.)

$\vec{k}(\frac{2\pi}{a})$	$V_C(\vec{k})$	$\Delta V_C(\vec{k})$	$V_{X^\dagger}(\vec{k})$	$\Delta V_{X^\dagger}(\vec{k})$	$V_{X^\dagger}(\vec{k})$	$\Delta V_{X^\dagger}(\vec{k})$
(0,0,0)	-1.6870	-0.0796	-1.4091	-0.0917	-1.3998	-0.1092
(1,1,1)	-0.9690	-0.0955	-0.2630	0.0150	-0.2532	0.0189
(2,0,0)	-0.8560	-0.0687	-0.1328	0.0210	-0.1246	0.0261
(2,2,0)	-0.6043	-0.0205	-0.0350	0.0062	-0.0334	0.0082
(3,1,1)	-0.5033	-0.0095	-0.0626	-0.0052	-0.0634	-0.0058
(2,2,2)	-0.4775	-0.0076	-0.0666	-0.0068	-0.0677	-0.0079
(4,0,0)	-0.3964	-0.0027	-0.0501	-0.0055	-0.0510	-0.0067
(3,3,1)	-0.3528	-0.0020	-0.0228	-0.0013	-0.0231	-0.0017
(4,2,0)	-0.3399	-0.0015	-0.0145	0.0000	-0.0146	-0.0001
(4,2,2)	-0.2972	-0.0008	0.0062	0.0030	0.0065	0.0035
(3,3,3)	-0.2715	-0.0006	0.0076	0.0029	0.0079	0.0034
(5,1,1)	-0.2710	-0.0001	0.0076	0.0029	0.0079	0.0034
(4,4,0)	-0.2368	-0.0001	-0.0048	0.0004	-0.0048	0.0005
(5,3,1)	-0.2199	0.0001	-0.0130	-0.0011	-0.0132	-0.0013
(6,0,0)	-0.2144	0.0004	-0.0150	-0.0015	-0.0152	-0.0017
(4,4,2)	-0.2149	-0.0000	-0.0150	-0.0015	-0.0152	-0.0017
(6,2,0)	-0.1963	0.0003	-0.0185	-0.0022	-0.0189	-0.0025
(5,3,3)	-0.1847	0.0000	-0.0166	-0.0019	-0.0169	-0.0022
(6,2,2)	-0.1809	0.0002	-0.0153	-0.0017	-0.0156	-0.0020
(4,4,4)	-0.1679	0.0000	-0.0084	-0.0005	-0.0086	-0.0006
(5,5,1)	-0.1591	0.0001	-0.0032	0.0003	-0.0033	0.0004
(7,1,1)	-0.1589	0.0003	-0.0032	0.0003	-0.0033	0.0004
(6,4,0)	-0.1563	0.0001	-0.0017	0.0006	-0.0018	0.0007

Table I (cont'd)

\vec{K}	$V_C(\vec{K})$	$\Delta V_C(\vec{K})$	$V_{x\uparrow}(\vec{K})$	$\Delta V_{x\uparrow}(\vec{K})$	$V_{x\downarrow}(\vec{K})$	$\Delta V_{x\downarrow}(\vec{K})$
(6, 4, 2)	-0.1464	c.ccc1	0.0022	0.0012	0.0023	0.0015
(7, 3, 1)	-0.1397	0.0002	0.0028	0.0013	0.0029	0.0016
(5, 5, 3)	-0.1398	0.0000	0.0028	0.0013	0.0029	0.0016
(8, 0, 0)	-0.1298	c.0002	c.0001	0.0009	0.0001	0.0010
(7, 3, 3)	-0.1247	0.c001	-0.0028	0.0004	-0.0029	0.0004
(8, 2, 0)	-0.1229	0.0002	-0.0038	0.0002	-0.0039	0.0002
(6, 4, 4)	-0.1231	c.0000	-0.0038	0.0002	-0.0039	0.0002
(8, 2, 2)	-0.1168	c.0001	-0.0076	-0.0004	-0.0078	-0.0006
(6, 6, 0)	-0.1169	0.0000	-0.0076	-0.0004	-0.0078	-0.0006
(7, 5, 1)	-0.1126	c.c001	-0.0096	-0.0008	-0.0099	-0.0010
(5, 5, 5)	-0.1127	-c.0000	-0.0096	-0.0008	-0.0099	-0.0010
(6, 6, 2)	-0.1113	0.0000	-0.0101	-0.0009	-0.0104	-0.0011
(8, 4, 0)	-0.1062	0.0001	-0.0106	-0.0010	-0.0111	-0.0013
(7, 5, 3)	-0.1028	c.0000	-0.0101	-0.0009	-0.0104	-0.0012
(9, 1, 1)	-0.1027	c.0002	-0.0101	-0.0009	-0.0104	-0.0012
(8, 4, 2)	-0.1017	c.0001	-0.0097	-0.0009	-0.0100	-0.0011
(6, 6, 4)	-0.0975	c.0000	-0.0074	-0.0005	-0.0076	-0.0007
(9, 3, 1)	-0.0945	0.0001	-0.0053	-0.0002	-0.0055	-0.0004
(8, 4, 4)	-0.0902	c.0000	-0.0021	0.0002	-0.0022	0.0002
(9, 3, 3)	-0.0877	0.0001	-0.0007	0.0005	-0.0007	0.0005
(7, 7, 1)	-0.0877	c.0000	-0.0007	0.0005	-0.0007	0.0005
(7, 5, 5)	-0.0877	0.0000	-0.0007	0.0005	-0.0007	0.0005
(8, 6, 0)	-0.0869	c.0000	-0.0003	0.0005	-0.0004	0.0005
(10, 0, 0)	-0.0868	0.0001	-0.0003	0.0005	-0.0004	0.0005
(10, 2, 0)	-0.0838	c.c001	0.0004	0.0006	0.0004	0.0007
(8, 6, 2)	-0.0839	0.ccc0	0.0004	0.0006	0.0004	0.0007
(7, 7, 3)	-0.0818	c.0000	0.0003	0.0006	0.0003	0.0007
(9, 5, 1)	-0.0818	c.c000	c.0003	0.0006	0.0003	0.0007

TABLE II
Energy Difference for Selected States

	<u>Majority Spin</u>			
Connolly ¹⁵ ($\alpha=2/3$)	Present ($\alpha=2/3$)	Langlinais ¹⁰ and Callaway ($\alpha=0.972$)		Wakoh ¹⁷ ($\alpha=1$)
$\Gamma_{25}^+ - \Gamma_1^-$	0.478	0.483	0.506	0.488
$\Gamma_{12}^- - \Gamma_{25}^+$		0.091	0.084	0.079
$X_5^- - X_1^+$	0.330	0.300	0.324	0.347
$X_5^- - X_2^+$		0.009	0.016	0.019
$X_4^+ - X_5^-$		0.177	0.144	0.226
$X_5^- - \Gamma_1^-$	0.625	0.639	0.663	0.639
$X_4^+ - \Gamma_1^-$	0.841	0.816	0.807	0.865
$L_2^+ - L_{32}^-$		0.036	0.016	-0.011

TABLE II
Energy Difference for Selected States

	<u>Minority Spin</u>			
	Connolly ¹⁵ ($\alpha=2/3$)	Present ($\alpha=2/3$)	Langlinais ¹⁰ and Callaway ($\alpha=0.972$)	Wakoh ¹⁷ ($\alpha=1$)
$\Gamma_{25}' - \Gamma_1'$	0.542	0.534	0.544	0.535
$\Gamma_{12} - \Gamma_{25}'$		0.095	0.087	0.083
$x_5 - x_1$	0.362	0.323	0.324	0.372
$x_5 - x_2$		0.010	0.017	0.020
$x_4' - x_5$		0.118	0.101	0.171
$x_5 - \Gamma_1$	0.698	0.698	0.707	0.695
$x_4' - \Gamma_1$	0.842	0.816	0.808	0.866
$L_2' - L_{32}$		-0.024	-0.029	-0.047

TABLE III
 Exchange Splitting of Certain States
 at Symmetry Points (in Ry)

Present ($\alpha=2/3$)	Langlinais ¹⁰ and Callaway ($\alpha=0.972$)	Wakoh ¹⁷ ($\alpha=1$)	Connolly ¹⁵ ($\alpha=2/3$)
Γ_1	0.001	0.022	0.018
Γ_{25}'	0.052	0.060	0.067
Γ_{12}	0.057	0.063	0.071
X_1	0.038	0.049	0.049
X_3	0.044	0.054	0.058
X_2	0.060	0.065	0.073
X_5	0.060	0.066	0.074
X_4'	0.001	0.023	0.019
L_1	0.030	0.044	0.048
L_{31}	0.052	0.060	0.066
L_{32}	0.060	0.065	0.074
L_2'	0.000	0.020	0.016

TABLE IV
Energy Levels at Symmetry Points (Ry)

$\Gamma(000)$	$X(100)$	$X(001)$	$L(\frac{1}{2}\frac{1}{2}\frac{1}{2})$
-0.2850 (Γ_{12}^{\downarrow})	-0.0983 (X_4^{\downarrow})	-0.0983 (X_4^{\downarrow})	-0.2264 (L_3^{\downarrow})
-0.2851 (Γ_{12}^{\downarrow})	-0.0993 (X_4^{\downarrow})	-0.0993 (X_4^{\downarrow})	-0.2300 (L_3^{\downarrow})
-0.3408 (Γ_{12}^{\uparrow})	-0.2149 (X_5^{\downarrow})	-0.2124 (X_5^{\downarrow})	-0.2520 (L_2^{\downarrow})
-0.3413 (Γ_{12}^{\uparrow})	-0.2160 (X_5^{\downarrow})	-0.2203 (X_5^{\downarrow})	-0.2521 (L_2^{\downarrow})
-0.3778 (Γ_{25}^{\downarrow})	-0.2272 (X_2^{\downarrow})	-0.2255 (X_2^{\downarrow})	-0.2860 (L_3^{\uparrow})
-0.3808 (Γ_{25}^{\downarrow})	-0.2758 (X_5^{\uparrow})	-0.2736 (X_5^{\uparrow})	-0.2898 (L_3^{\uparrow})
-0.3854 (Γ_{25}^{\downarrow})	-0.2773 (X_5^{\uparrow})	-0.2805 (X_5^{\uparrow})	-0.3736 (L_3^{\downarrow})
-0.4304 (Γ_{25}^{\downarrow})	-0.2869 (X_2^{\uparrow})	-0.2859 (X_2^{\uparrow})	-0.3803 (L_3^{\downarrow})
-0.4338 (Γ_{25}^{\downarrow})	-0.5179 (X_3^{\downarrow})	-0.5178 (X_3^{\downarrow})	-0.4263 (L_3^{\uparrow})
-0.4365 (Γ_{25}^{\downarrow})	-0.5398 (X_1^{\uparrow})	-0.5398 (X_1^{\uparrow})	-0.4330 (L_3^{\uparrow})
-0.9144 (Γ_1^{\downarrow})	-0.5619 (X_3^{\uparrow})	-0.5619 (X_3^{\uparrow})	-0.5873 (L_1^{\downarrow})
-0.9155 (Γ_1^{\downarrow})	-0.5775 (X_1^{\uparrow})	-0.5774 (X_1^{\uparrow})	-0.6178 (L_1^{\uparrow})

Table IV (cont'd)

Energy Levels at Symmetry Points (Ry)

$W(1, \frac{1}{2}, 0)$	$W(1, 0, \frac{1}{2})$	$K(\frac{3}{4}, \frac{3}{4}, 0)$	$K(\frac{3}{4}, 0, \frac{3}{4})$
0.2978 (W_3^\uparrow)	0.3057 (W_3^\uparrow)	0.1709 (K_3^\uparrow)	0.1709 (K_3^\uparrow)
0.2978 (W_3^\uparrow)	0.2937 (W_3^\uparrow)	0.1519 (K_3^\uparrow)	0.1519 (K_3^\uparrow)
-0.2164 (W_1^\uparrow)	-0.2164 (W_1^\uparrow)	-0.2368 (K_2^\uparrow)	-0.2367 (K_2^\uparrow)
-0.2766 (W_1^\uparrow)	-0.2766 (W_1^\uparrow)	-0.2703 (K_4^\uparrow)	-0.2707 (K_4^\uparrow)
-0.2881 (W_1^\uparrow)	-0.2881 (W_1^\uparrow)	-0.2967 (K_2^\uparrow)	-0.2962 (K_2^\uparrow)
-0.3429 (W_1^\uparrow)	-0.4328 (W_1^\uparrow)	-0.3272 (K_4^\uparrow)	-0.3273 (K_4^\uparrow)
-0.4387 (W_3^\uparrow)	-0.4357 (W_3^\uparrow)	-0.3670 (K_3^\uparrow)	-0.3669 (K_3^\uparrow)
-0.4389 (W_3^\uparrow)	-0.4428 (W_3^\uparrow)	-0.4090 (K_3^\uparrow)	-0.4091 (K_3^\uparrow)
-0.4766 (W_2^\uparrow)	-0.4736 (W_2^\uparrow)	-0.4837 (K_1^\uparrow)	-0.4836 (K_1^\uparrow)
-0.4815 (W_3^\uparrow)	-0.4823 (W_3^\uparrow)	-0.4929 (K_1^\uparrow)	-0.4929 (K_1^\uparrow)
-0.4833 (W_3^\uparrow)	-0.4848 (W_3^\uparrow)	-0.5219 (K_1^\uparrow)	-0.5219 (K_1^\uparrow)
-0.5183 (W_2^\uparrow)	-0.5182 (W_2^\uparrow)	-0.5359 (K_1^\uparrow)	-0.5359 (K_1^\uparrow)

TABLE V
Charge Density in Three Principle Directions (in a.u.)

r	Total			Occupied Band States			
	[1,0,0]	[1,1,0]	[1,1,1]	[1,0,0]	[1,1,0]	[1,1,1]	Atomic
0.0	13618.5000	13618.5000	13618.5000	7.1773	7.1773	7.1773	7.3732
0.042	1551.1533	1551.1521	1551.1516	0.8591	0.8577	0.8572	0.4326
0.083	306.4941	306.4775	306.4719	0.6035	0.5868	0.5813	0.2974
0.125	167.8367	167.7840	167.7663	1.1779	1.1251	1.1075	1.0040
0.166	109.8645	109.7699	109.7383	1.8276	1.7330	1.7014	1.6909
0.249	37.8764	37.7264	37.6764	2.7304	2.5804	2.5304	2.5369
0.332	13.4470	13.2772	13.2206	3.1473	2.9775	2.9209	2.8997
0.415	7.6750	7.5167	7.4639	3.0128	2.8544	2.8016	2.7698
0.498	6.0684	5.9375	5.8938	2.5477	2.4168	2.3731	2.3408
0.664	3.9026	3.8225	3.7958	1.6061	1.5260	1.4993	1.4679
0.831	2.1085	2.0637	2.0487	0.9272	0.8824	0.8674	0.8287
0.997	1.0764	1.0521	1.0438	0.5367	0.5125	0.5041	0.4566
1.163	0.5794	0.5659	0.5609	0.3376	0.3241	0.3191	0.2647
1.329	0.3404	0.3331	0.3300	0.2281	0.2208	0.2176	0.1582
1.495	0.2211	0.2179	0.2157	0.1638	0.1605	0.1583	0.0961
1.661	0.1611	0.1605	0.1587	0.1269	0.1263	0.1244	0.0610
1.827	0.1304	0.1320	0.1299	0.1061	0.1075	0.1055	0.0414
1.993	0.1141	0.1177	0.1149	0.0940	0.0974	0.0947	0.0299
2.159	0.1047	0.1108	0.1065	0.0866	0.0923	0.0882	0.0224
2.325	0.0990	0.1084	0.1017	0.0817	0.0905	0.0842	0.0171
2.491	0.0954	0.1097	0.0989	0.0786	0.0915	0.0818	0.0131
2.658	0.0932	0.1152	0.0975	0.0766	0.0956	0.0806	0.0102
2.824	0.0920	0.1269	0.0970	0.0754	0.1040	0.0801	0.0080
2.990	0.0913	0.1503	0.0971	0.0748	0.1198	0.0802	0.0064
3.156	0.0910	0.1973	0.0974	0.0745	0.1487	0.0805	0.0051
3.322	0.0909	0.2918	0.0979	0.0744	0.2002	0.0810	0.0042

100

TABLE VI

Atomic Scattering Form Factors (in a.u.)

$\vec{k} \left(\frac{2\pi}{a} \right)$	$\frac{\sin \theta}{\lambda} (\text{Å}^{-1})$	$\rho_{\text{band}} (\vec{k})$	$\rho_{\text{core}} (\vec{k})$	$\rho_{\text{total}} (\vec{k})$	$\rho_{\text{exp}} (\vec{k})$
(1,1,1)	0.2463	4.7865	15.5905	20.3769	20.10 ± 0.16
(2,0,0)	0.2844	4.0977	14.9348	19.0325	18.55 ± 0.16
(2,2,0)	0.4022	2.5201	12.8435	15.3636	15.34 ± 0.12
(3,1,1)	0.4717	1.8478	11.6908	13.5386	
(2,2,2)	0.4926	1.6683	11.3655	13.0338	
(4,0,0)	0.5689	1.1514	10.2906	11.4420	11.18 ± 0.11
(3,3,1)	0.6199	0.8324	9.6686	10.5010	
(4,2,0)	0.6360	0.7690	9.4885	10.2575	
(4,2,2)	0.6967	0.5123	8.8753	9.3875	
(3,3,3)	0.7390	0.3659	8.5054	8.8713	8.74 ± 0.09
(5,1,1)	0.7390	0.4030	8.5055	8.9084	8.73 ± 0.09
(4,4,0)	0.8045	0.2143	8.0121	8.2264	
(5,3,1)	0.8414	0.1497	7.7713	7.9210	
(6,0,0)	0.8533	0.1616	7.6982	7.8598	
(4,4,2)	0.8533	0.1173	7.6982	7.8155	
(6,2,0)	0.8994	0.0807	7.4355	7.5161	
(5,3,3)	0.9326	0.0129	7.2640	7.2769	
(6,2,2)	0.9433	0.0207	7.2108	7.2315	
(4,4,4)	0.9853	-0.0417	7.0146	6.9730	
(5,5,1)	1.0156	-0.0527	6.8821	6.8294	
(7,1,1)	1.0156	-0.0211	6.8822	6.8610	.
(6,4,0)	1.0255	-0.0522	6.8403	6.7881	
(6,4,2)	1.0642	-0.0770	6.6824	6.6054	
(7,3,1)	1.0924	-0.0735	6.5727	6.4992	
(5,5,3)	1.0924	-0.0958	6.5727	6.4769	
(8,0,0)	1.1377	-0.0675	6.4026	6.3351	
(7,3,3)	1.1641	-0.1003	6.3068	6.2065	
(8,2,0)	1.1727	-0.0812	6.2757	6.1945	
(6,4,4)	1.1727	-0.1129	6.2757	6.1629	
(8,2,2)	1.2067	-0.0907	6.1553	6.0646	
(6,6,0)	1.2067	-0.1091	6.1553	6.0461	
(7,5,1)	1.2316	-0.1077	6.0685	5.9608	
(5,5,5)	1.2316	-0.1200	6.0684	5.9484	
(6,6,2)	1.2398	-0.1130	6.0401	5.9272	

TABLE VII
Magnetic Scattering Form Factors

$\frac{a}{2\pi} \vec{k}$	$\frac{\sin \theta}{\lambda} (\text{\AA}^{-1})$	$\rho_{\text{spin}}(\vec{k})$	$\rho_{\text{core}}(\vec{k})$	$f(\vec{k})$
(1,1,1)	0.2463	0.4779	0.0023	0.7598
(2,0,0)	0.2844	0.4241	0.0025	0.6752
(2,2,0)	0.4022	0.2644	0.0026	0.4226
(3,1,1)	0.4717	0.1871	0.0022	0.2998
(2,2,2)	0.4926	0.1724	0.0021	0.2763
(4,0,0)	0.5689	0.1038	0.0015	0.1668
(3,3,1)	0.6199	0.0882	0.0011	0.1414
(4,2,0)	0.6360	0.0750	0.0010	0.1204
(4,2,2)	0.6967	0.0543	0.0006	0.0869
(3,3,3)	0.7390	0.0448	0.0004	0.0716
(5,1,1)	0.7390	0.0313	0.0004	0.0502
(4,4,0)	0.8045	0.0248	0.0002	0.0395
(5,3,1)	0.8414	0.0158	0.0001	0.0250
(6,0,0)	0.8533	0.0024	0.0000	0.0039
(4,4,2)	0.8533	0.0182	0.0000	0.0288
(6,2,0)	0.8994	0.0008	-0.0001	0.0011
(5,3,3)	0.9326	0.0073	-0.0001	0.0113
(6,2,2)	0.9433	-0.0005	-0.0001	-0.0011
(4,4,4)	0.9853	0.0047	-0.0001	0.0072
(5,5,1)	1.0156	-0.0011	-0.0002	-0.0020
(7,1,1)	1.0156	-0.0122	-0.0002	-0.0195
(6,4,0)	1.0255	-0.0040	-0.0002	-0.0066
(6,4,2)	1.0642	-0.0043	-0.0001	-0.0070
(7,3,1)	1.0924	-0.0105	-0.0002	-0.0169
(5,5,3)	1.0924	-0.0027	-0.0002	-0.0045
(8,0,0)	1.1377	-0.0183	-0.0001	-0.0291
(7,3,3)	1.1641	-0.0090	-0.0001	-0.0145
(8,2,0)	1.1727	-0.0162	-0.0001	-0.0259
(6,4,4)	1.1727	-0.0052	-0.0001	-0.0084
(8,2,2)	1.2067	-0.0144	-0.0001	-0.0230
(6,6,0)	1.2067	-0.0081	-0.0001	-0.0129
(7,5,1)	1.2316	-0.0091	-0.0001	-0.0145
(5,5,5)	1.2316	-0.0048	-0.0001	-0.0077
(6,6,2)	1.2398	-0.0073	-0.0001	-0.0117

TABLE VIII
Spin Density in Three Principle Direction

r	Total			Occupied Band States		
	[1,0,0]	[1,1,0]	[1,1,1]	[1,0,0]	[1,1,0]	[1,1,1]
0.0	-0.0455	-0.0455	-0.0455	-0.1041	-0.1041	-0.1041
0.042	-0.0045	-0.0040	-0.0038	-0.0174	-0.0169	-0.0167
0.083	0.0225	0.0282	0.0301	0.0074	0.0130	0.0149
0.125	0.0760	0.0940	0.1000	0.0639	0.0819	0.0879
0.166	0.1378	0.1700	0.1807	0.1312	0.1633	0.1741
0.249	0.2197	0.2706	0.2876	0.2192	0.2701	0.2871
0.332	0.2489	0.3066	0.3258	0.2488	0.3065	0.3257
0.415	0.2318	0.2857	0.3037	0.2310	0.2849	0.3029
0.498	0.1910	0.2356	0.2505	0.1900	0.2347	0.2496
0.664	0.1150	0.1424	0.1516	0.1149	0.1422	0.1514
0.831	0.0620	0.0772	0.0824	0.0625	0.0778	0.0829
0.997	0.0314	0.0396	0.0425	0.0322	0.0404	0.0432
1.163	0.0157	0.0202	0.0219	0.0164	0.0209	0.0226
1.329	0.0070	0.0094	0.0105	0.0076	0.0100	0.0111
1.495	0.0021	0.0032	0.0040	0.0026	0.0036	0.0044
1.661	-0.0006	-0.0002	0.0004	-0.0002	0.0001	0.0007
1.827	-0.0019	-0.0021	-0.0015	-0.0016	-0.0018	-0.0012
1.993	-0.0026	-0.0030	-0.0025	-0.0024	-0.0027	-0.0023
2.159	-0.0030	-0.0035	-0.0031	-0.0028	-0.0032	-0.0028
2.325	-0.0032	-0.0036	-0.0034	-0.0030	-0.0034	-0.0031
2.491	-0.0033	-0.0035	-0.0035	-0.0031	-0.0033	-0.0033
2.658	-0.0033	-0.0032	-0.0036	-0.0032	-0.0029	-0.0034
2.824	-0.0034	-0.0024	-0.0036	-0.0032	-0.0021	-0.0034
2.990	-0.0034	-0.0009	-0.0036	-0.0032	-0.0005	-0.0034
3.156	-0.0034	0.0020	-0.0036	-0.0032	0.0024	-0.0034
3.322	-0.0034	0.0073	-0.0036	-0.0032	0.0078	-0.0034

103

TABLE IX
Compton Profiles

q	$J_{[1,0,0]}(q)$	$J_{[1,1,0]}(q)$	$J_{[1,1,1]}(q)$	$J_{av}(q)$
0.0	5.136	5.169	5.075	5.135
0.084	5.117	5.151	5.097	5.128
0.167	5.089	5.094	5.061	5.084
0.251	5.043	5.017	5.017	5.025
0.334	4.974	4.935	4.952	4.950
0.418	4.877	4.833	4.834	4.846
0.502	4.738	4.685	4.683	4.699
0.585	4.553	4.444	4.527	4.496
0.669	4.379	4.283	4.366	4.332
0.752	4.211	4.119	4.207	4.168
0.836	4.053	4.028	4.036	4.037
0.919	3.905	3.892	3.895	3.896
1.003	3.742	3.751	3.749	3.748
1.087	3.572	3.631	3.579	3.601
1.170	3.414	3.510	3.435	3.464
1.254	3.269	3.382	3.306	3.330
1.337	3.132	3.231	3.164	3.185
1.505	2.870	2.946	2.896	2.912
1.672	2.641	2.664	2.618	2.646
1.839	2.425	2.389	2.468	2.420
1.923	2.320	2.191	2.289	2.253
2.006	2.207	2.061	2.156	2.127
2.090	2.077	1.956	2.049	2.015
2.340	1.765	1.762	1.769	1.765
2.675	1.436	1.487	1.434	1.459
3.009	1.178	1.209	1.185	1.194
3.344	0.975	0.927	0.967	0.951
3.678	0.823	0.812	0.818	0.817
4.012	0.696	0.710	0.696	0.702
4.514	0.550	0.556	0.553	0.554
5.015	0.449	0.441	0.445	0.444
5.517	0.375	0.374	0.374	0.375
6.018	0.298	0.298	0.298	0.298

TABLE X
Occupied Band States Compton Profiles

q	$J_{[1,0,0]}(q)$	$J_{[1,1,0]}(q)$	$J_{[1,1,1]}(q)$	$J_{av}(q)$
0.0	2.739	2.770	2.679	2.738
0.084	2.722	2.755	2.705	2.732
0.167	2.700	2.705	2.675	2.695
0.251	2.665	2.640	2.640	2.647
0.334	2.612	2.574	2.589	2.589
0.418	2.538	2.494	2.491	2.506
0.502	2.428	2.372	2.367	2.387
0.585	2.275	2.165	2.244	2.217
0.669	2.138	2.043	2.121	2.090
0.752	2.011	1.922	2.004	1.969
0.836	1.898	1.879	1.883	1.885
0.919	1.803	1.793	1.795	1.796
1.003	1.695	1.706	1.705	1.703
1.087	1.582	1.642	1.596	1.613
1.170	1.486	1.582	1.515	1.537
1.254	1.405	1.519	1.449	1.468
1.337	1.336	1.437	1.372	1.391
1.505	1.209	1.290	1.238	1.253
1.672	1.114	1.144	1.098	1.124
1.839	1.033	1.001	1.081	1.031
1.923	0.993	0.867	0.966	0.928
2.006	0.941	0.798	0.909	0.867
2.090	0.872	0.752	0.847	0.810
2.340	0.725	0.722	0.721	0.722
2.675	0.581	0.631	0.577	0.603
3.004	0.465	0.494	0.473	0.480
3.344	0.373	0.325	0.366	0.349
3.678	0.308	0.295	0.301	0.300
4.012	0.244	0.256	0.242	0.249
4.514	0.172	0.174	0.170	0.172
5.015	0.123	0.120	0.118	0.120
5.517	0.089	0.093	0.093	0.091
6.018	0.054	0.054	0.054	0.054

TABLE XI

	Location of Pocket	$k_{X\Gamma}$	k_{XW}	k_{XU}
Present Calculation	(00 <u>+1</u>)	0.179	<u>0.077</u>	<u>0.076</u>
	(+100)	<u>0.195</u>	W(10½) 0.080	0.076
			W(1½0) <u>0.077</u>	
Zornberg ¹⁰	(00 <u>+1</u>)	0.201	<u>0.092</u>	<u>0.095</u>
(Parameter set IV)	(<u>+1</u> , 0, 0)	<u>0.218</u>	W(10½) 0.096	0.104
			W(1½0) <u>0.104</u>	
Hodges et al ⁷⁹	(00 <u>+1</u>)	0.184	<u>0.095</u>	<u>0.089</u>
	(<u>+1</u> 00)	<u>0.208</u>	<u>0.106</u>	0.102
Tsui ⁸⁰		0.207	0.099	0.087

Table XI. Comparison of $X_{5\downarrow}$ hole pocket dimensions in atomic units. Numbers underlined are dimensions in the plane normal to the applied magnetic field. These dimensions contribute to the observed dHvA areas.

TABLE XII

Band	Present	Zornberg ¹⁰	Hodges et al ⁷⁹	Tsui ⁸⁰	Stark ⁸¹
Small square (sp.)	0.84	0.86	1.12		0.90
Large square (sp [†])	1.24	1.18	1.33		1.15
Centered d. sheet	2.20	2.05	2.25		
X ₅ (d [*]) pocket (100)	0.038	0.0665		0.0665	
(001)	0.018	0.0270		0.0270	
X ₂ (d [*]) pocket (100)	0.144			Not observed	
(001)	0.089				

Table XII. Extremal areas of Fermi surface cross sections in atomic units.

Refer to Fig. XIV for designations.

TABLE XIII

Band	Goy and Grimes ⁸²	Present Results	Zornberg ¹⁰ Parameter Set IV
Γ Centered $d\downarrow$ sheet		8.84	8.
Large square ($sp\uparrow$)	5.09	2.22	2.9
Small square ($sp\uparrow$)	4.33	4.75	3.7
X_5 pocket ($d\downarrow$)	0.75	0.66	0.89
X_2 pocket ($d\downarrow$)	Not Observed	1.97	

Table XIII. Effective mass associated with Fermi surface portions. Refer to Fig. XIV for designations.

TABLE XIV
 Interband Optical Conductivity Tensor ($\tau = \infty$)
 and the Joint Density of States

$\hbar\omega$ (eV)	σ_{xx} (10^{15} sec^{-1})	σ_{zz} (10^{15} sec^{-1})	σ_{xy} (10^{14} sec^{-1})	$J(\omega)$ <small>electrons atom-Ry</small>
0.0408	2.2537	1.9899	-2.3711	0.3414
0.0816	4.7354	5.1174	-11.1349	1.2429
0.1224	3.9798	4.7546	-9.6446	1.7012
0.1633	4.6289	4.8414	-8.5351	2.6104
0.2041	4.2559	4.4975	-6.3714	3.0738
0.2449	4.0836	4.1380	-7.3101	4.0153
0.2857	4.5829	4.6463	-7.3332	6.0053
0.3265	3.9790	3.9935	-8.4532	6.8389
0.3673	3.5278	3.5156	-6.4196	7.2788
0.4081	3.3142	3.2513	-5.8522	7.8564
0.4490	3.1276	3.1673	-4.9153	8.5088
0.4898	3.3000	3.2881	-4.5063	9.3547
0.5306	3.1265	3.1415	-3.2335	10.1667
0.5714	3.2011	3.1181	-3.4648	11.2430
0.6122	3.4887	3.3870	-3.7514	14.1012
0.6530	3.7059	3.6539	-3.4448	17.9035
0.6938	3.8296	3.8454	-2.8521	22.2797
0.7347	4.2822	4.3175	-2.2969	32.5283
0.7755	5.3013	5.3783	0.6616	36.7087
0.8163	7.6532	7.7952	1.9108	181.4664
0.8571	4.3829	4.4612	0.0539	21.4999
0.8979	3.5683	3.5660	-0.4021	16.5715
0.9387	3.4647	3.4196	-0.1400	16.0072
0.9796	3.4643	3.4322	-0.0041	16.2677
1.0204	3.5312	3.5528	0.1203	17.4664
1.0612	3.8740	3.8372	-0.0625	17.9405
1.1020	4.1484	4.1131	-0.1571	18.4901
1.1428	4.2504	4.2150	0.3799	19.3762
1.1836	4.1631	4.1280	0.5193	20.0248
1.2244	4.0752	4.1056	0.5948	21.1490
1.2653	4.1265	4.0986	0.0886	21.7379
1.3061	4.0708	4.0771	0.5278	22.4225
1.3469	3.9955	3.9815	0.3871	22.8702
1.3877	4.0162	4.0175	0.2342	24.1174
1.4285	4.0641	4.0428	0.0907	25.0759
1.4693	4.0633	4.0259	-0.1182	26.4830
1.5101	4.3316	4.2770	0.1363	28.4940
1.5510	4.1438	4.1066	-0.0739	28.4150
1.5918	4.2070	4.1614	-0.2074	29.9438
1.6326	4.0669	4.1345	0.2721	27.8842
1.6734	4.0662	4.2404	0.5568	27.4582

Table XIV (cont'd)

$\hbar\omega$ (eV)	$\sigma_{xx} (10^{15} \text{ sec}^{-1})$	$\sigma_{zz} (10^{15} \text{ sec}^{-1})$	$\sigma_{xy} (10^{14} \text{ sec}^{-1})$	$J(\omega) \frac{\text{electrons}}{\text{atom-Ry}}$
1.7142	4.3716	4.3720	0.9243	27.2723
1.7550	4.2671	4.2802	0.7948	27.7195
1.7958	4.2589	4.2394	0.9393	28.9409
1.8367	4.4599	4.4263	0.6959	30.7563
1.8775	4.5780	4.5947	0.6151	31.7540
1.9183	4.6536	4.6571	0.6177	33.0074
1.9591	4.7252	4.8259	0.5865	33.4380
1.9999	4.7430	4.6773	0.6460	33.9664
2.0407	4.3871	4.2097	0.3761	32.8843
2.0815	4.4274	4.2739	0.5209	34.9897
2.1224	4.9052	4.9245	0.7135	36.1732
2.1632	4.8603	4.8450	0.9064	37.5786
2.2040	4.7364	4.8265	1.0126	38.4460
2.2448	4.2935	4.3039	0.6593	34.7219
2.2856	4.1560	4.1778	0.6456	33.8604
2.3264	3.8819	3.9011	0.3808	32.1304
2.3673	3.8071	3.8180	0.3738	32.7620
2.4081	3.8241	3.7689	0.2038	34.3767
2.4489	3.7167	3.7243	0.3939	35.4507
2.4897	3.7892	3.7862	0.5515	36.7933
2.5305	3.6329	3.6449	0.4935	36.6607
2.5713	3.6539	3.6535	0.4566	38.3892
2.6121	3.7284	3.7166	0.6078	40.1800
2.6530	3.7383	3.7476	0.7072	41.5117
2.6938	3.6769	3.6813	0.6340	41.8614
2.7346	3.6140	3.6094	0.6092	41.9760
2.7754	3.5857	3.5917	0.6008	43.2199
2.8162	3.4096	3.4063	0.5960	40.1607
2.8570	3.3197	3.2999	0.5480	38.8336
2.8978	3.2505	3.2251	0.5724	37.6377
2.9387	3.2441	3.2970	0.3463	37.4590
2.9795	3.2860	3.2892	0.4203	37.5396
3.0203	3.2150	3.2425	0.0470	37.4480
3.0611	3.2139	3.2178	-0.1060	37.1560
3.1019	3.1868	3.1586	0.0035	37.5572
3.1427	3.2137	3.1990	0.0478	38.7696
3.1835	3.1511	3.0957	0.3136	38.4639
3.2244	3.1206	3.0705	0.3797	38.8837
3.2652	3.1185	3.0907	0.2971	40.0209
3.3060	3.0679	3.0792	0.4024	40.0965
3.3468	3.0218	3.0149	0.3709	40.7901

Table XIV (cont'd)

$\hbar\omega$ (eV)	$\sigma_{xx} (10^{15} \text{ sec}^{-1})$	$\sigma_{zz} (10^{15} \text{ sec}^{-1})$	$\sigma_{xy} (10^{14} \text{ sec}^{-1})$	$J(\omega) \frac{\text{electrons}}{\text{atom-Ry}}$
3.3876	2.9113	2.9180	0.3937	40.5959
3.4284	2.8614	2.8650	0.4114	40.8686
3.4692	2.7936	2.7931	0.3971	40.5713
3.5101	2.7559	2.7610	0.4289	41.7064
3.5509	2.7085	2.7045	0.4407	42.2081
3.5917	2.6355	2.6355	0.4483	41.7068
3.6325	2.6152	2.6126	0.4430	42.5698
3.6733	2.5958	2.5962	0.4369	44.0135
3.7141	2.5301	2.5281	0.4286	43.1315
3.7550	2.4593	2.4621	0.4308	43.3902
3.7958	2.4327	2.4350	0.4263	43.6496
3.8366	2.3722	2.3711	0.4201	43.0997
3.8774	2.3250	2.3271	0.4316	42.3829
3.9182	2.3122	2.3123	0.4493	43.5909
3.9590	2.2692	2.2681	0.4503	42.5486
3.9998	2.2506	2.2506	0.4588	42.6453
4.0407	2.2311	2.2299	0.4782	43.1461
4.0815	2.1933	2.1916	0.4789	42.6006
4.1223	2.1584	2.1568	0.4885	41.3906
4.1631	2.1266	2.1297	0.4876	40.4671
4.2039	2.1142	2.1169	0.5182	41.5194
4.2447	2.0830	2.0886	0.5350	41.5038
4.2855	2.0252	2.0351	0.5055	39.9411
4.3264	1.9856	1.9992	0.5122	39.1976
4.3672	1.9384	1.9427	0.4552	39.0465
4.4080	1.9154	1.9120	0.4417	38.4534
4.4488	1.8764	1.8754	0.4329	36.6313
4.4896	1.8833	1.8722	0.4070	37.2382
4.5304	1.8818	1.8770	0.3909	37.2621
4.5712	1.8530	1.8575	0.3682	35.8148
4.6121	1.9026	1.9058	0.3336	35.3211
4.6529	1.9340	1.9264	0.3366	35.5382
4.6937	2.0211	2.0652	0.3080	34.6421
4.7345	2.1293	2.1480	0.2882	34.0283
4.7753	2.1940	2.1399	0.2751	33.8213
4.8161	2.2768	2.3095	0.3035	34.2403
4.8569	2.4612	2.4485	0.3240	33.7910
4.8978	2.6167	2.6337	0.2697	34.2334
4.9386	2.6572	2.6747	0.2653	33.3648
4.9794	3.0350	3.0562	0.2605	34.5350
5.0202	3.1548	3.1505	0.2006	33.2610

Table XIV (cont'd)

$\hbar\omega$ (eV)	$\sigma_{xx}(10^{15} \text{ sec}^{-1})$	$\sigma_{zz}(10^{15} \text{ sec}^{-1})$	$\sigma_{xy}(10^{14} \text{ sec}^{-1})$	$J(\omega) \frac{\text{electrons}}{\text{atom-Ry}}$
5.0610	3.3770	3.3605	0.1460	32.5243
5.1018	4.0941	4.0864	0.1825	33.4321
5.1427	4.6287	4.5910	0.1345	34.3460
5.1835	4.7559	4.7905	-0.0794	34.3935
5.2243	4.2909	4.3012	-0.2217	33.7726
5.2651	4.6827	4.6745	-0.7261	34.4385
5.3059	4.5734	4.5838	-0.6189	33.9670
5.3467	4.5101	4.5151	-0.5517	33.4005
5.3875	4.6082	4.5948	-0.6026	33.3439
5.4284	4.7765	4.7782	-0.6014	33.8064
5.4692	4.8602	4.8496	-0.6127	34.6154
5.5100	4.9812	4.9776	-0.5968	35.3434
5.5508	5.1815	5.1828	-0.6189	35.7380
5.5916	5.5112	5.5119	-0.6544	36.5002
5.6324	5.7101	5.7182	-0.6424	36.9517
5.6732	6.4058	6.4050	-0.7145	38.3271
5.7141	5.1021	5.1020	-0.4581	36.2511
5.7549	4.6284	4.6270	-0.3532	35.8680
5.7957	4.2889	4.2885	-0.2839	35.9324
5.8365	4.0348	4.0341	-0.2362	36.1857
5.8773	3.8348	3.8348	-0.1966	35.3147
5.9181	3.6534	3.6533	-0.1638	33.2858
5.9589	3.5053	3.5055	-0.1329	32.2855
5.9988	3.3589	3.3593	-0.1039	31.5007
6.0406	3.2486	3.2487	-0.0823	30.7950
6.0814	3.1255	3.1260	-0.0682	30.0848
6.1222	3.0222	3.0228	-0.0556	29.5603
6.1630	2.9224	2.9217	-0.0476	28.9820
6.2038	2.8265	2.8165	-0.0401	28.4784
6.2446	2.7269	2.7181	-0.0273	27.8997
6.2855	2.6453	2.6438	-0.0149	27.4429
6.3263	2.5589	2.5642	-0.0049	27.0529
6.3671	2.4611	2.4611	0.0062	26.4964
6.4079	2.3926	2.3937	0.0095	26.0890
6.4487	2.3223	2.3205	0.0148	25.6627
6.4895	2.2515	2.2489	0.0201	25.2986

FIGURE CAPTIONS

- Figure I Coordinates for the evaluation of three-center integrals.
- Figure II Band structure for majority-spin states along certain symmetry directions.
- Figure III Band structure for minority-spin states along certain symmetric directions.
- Figure IV Band structure of nickel along some symmetry lines in the Brillouin zone. The effects of spin orbit coupling are included. States are labelled according to the symmetry of the largest spin component. The solid lines indicate states of minority spin, the dashed lines of majority spin. The horizontal line at -0.239 Ry. indicates the position of the Fermi energy.
- Figure V Band electrons (3d, 4s-p) charge density along three principle directions. Solid lines indicates the [100] direction, long dashes, the [110] direction, and dotted line, the [111] direction. The spherical average atomic charge density in $3d^8 4s^2$ configuration is shown as short dashes.
- Figure VI Comparison of calculated and observed magnetic scattering form factors.

- Figure VII Spin density in three principle directions.
Notation is the same as in Figure V.
- Figure VIII Compton profile $\hat{J}_k(q)$ for nickel. The
(----) line is the core ($2s^2, 3s^2, 2p^6, 3p^6$)
contribution. The other curves include the
occupied band electrons and pertain to the
following directions: long dashes, [100];
short dashes [111]; and solid curve, [110].
- Figure IX Comparison of calculated and observed aniso-
tropy in Compton profile. The solid curves
are the present results and the long dashes
are the experimental measurements of
Eisenberger and Reed.⁷¹
- Figure X Comparison of the spherical averaged Compton
profile with γ -rays Compton scattering
measurements. The solid curves are the
present results. The contribution from
atomic 1s wave function has been included.
Experimental results of Eisenberger and
Reed⁷¹ and Manninen and Paakkari⁷² are
shown as closed and open circles respect-
ively. The dashed curve is the contribution
from occupied (3d, 4s-p) band states.
Corresponding experimental results are
shown as ▲, Ref. 71 and △ Ref. 72. Typical

⁷²
experimental uncertainties are indicated by
the error bars.

Figure XI Projected density of states for majority spin.

Figure XII Projected density of states for minority spin.

Figure XIII Total density of states.

Figure XIV Fermi surface cross sections in the (100) plane. The solid and short dashed curves are our results. A solid line indicates that states are predominately (\downarrow) minority spin, the short dashed line indicates majority (\uparrow) spin. The open circles, triangles, and squares are the experimental results of R. W. Stark.⁸¹ The long dashed lines are obtained from an empirical formula given by Tsui.⁸⁰ The sheet (a) is the $x_{5\downarrow}$ pocket, (b) is the $x_{2\downarrow}$ pocket, (c) is the Γ -centered $d\downarrow$ sheet, (d) is the large (spt) square, (e) is the small (sp \downarrow) square.

Figure XV Fermi surface cross sections in the (1 $\bar{1}0$) plane. The notation is the same as in Figure XIV. Note that the s-pt neck at L merges in to the large $d\downarrow$ sheet.

Figure XVI Joint density of states.

Figure XVII The real part of the xx component of the

conductivity tensor from 0 to 1.2 eV. Long dashes indicate the empirical Drude term (Eq. (3.32); solid curve, the interband contribution in "sharp" limit, plus the Drude contribution, dashed curve, the interband contribution with ($\hbar/\tau=0.06$ eV) plus the Drude contribution. Experimental results are shown as follows: \square , Stoll⁸⁶; \diamond , Shiga and Pells⁸⁸; Δ , Lynch et al.⁸⁷; \blacktriangle , Johnson and Christy⁹¹; \circ , Sasovskaya and Naskov⁹⁰; \bullet , Kirillora.⁸⁹

Figure XVIII The real part of σ_{xx} from 1.0 to 6.0 eV.
Notation is the same as in Figure VII.

Figure XIX The imaginary part of σ_{xy} from 0 to 6 eV.
The solid curve is the interband conductivity in the "sharp" limit; the short dashed curve is the conductivity calculated with $\hbar/\tau=0.06$ eV. Experimental results are shown as follows: long dashed line, Erskine and Stern¹⁰³; \bullet , Yoshino and Tanaka⁹⁹; \circ , Krinchik and Artemjev.¹⁰¹

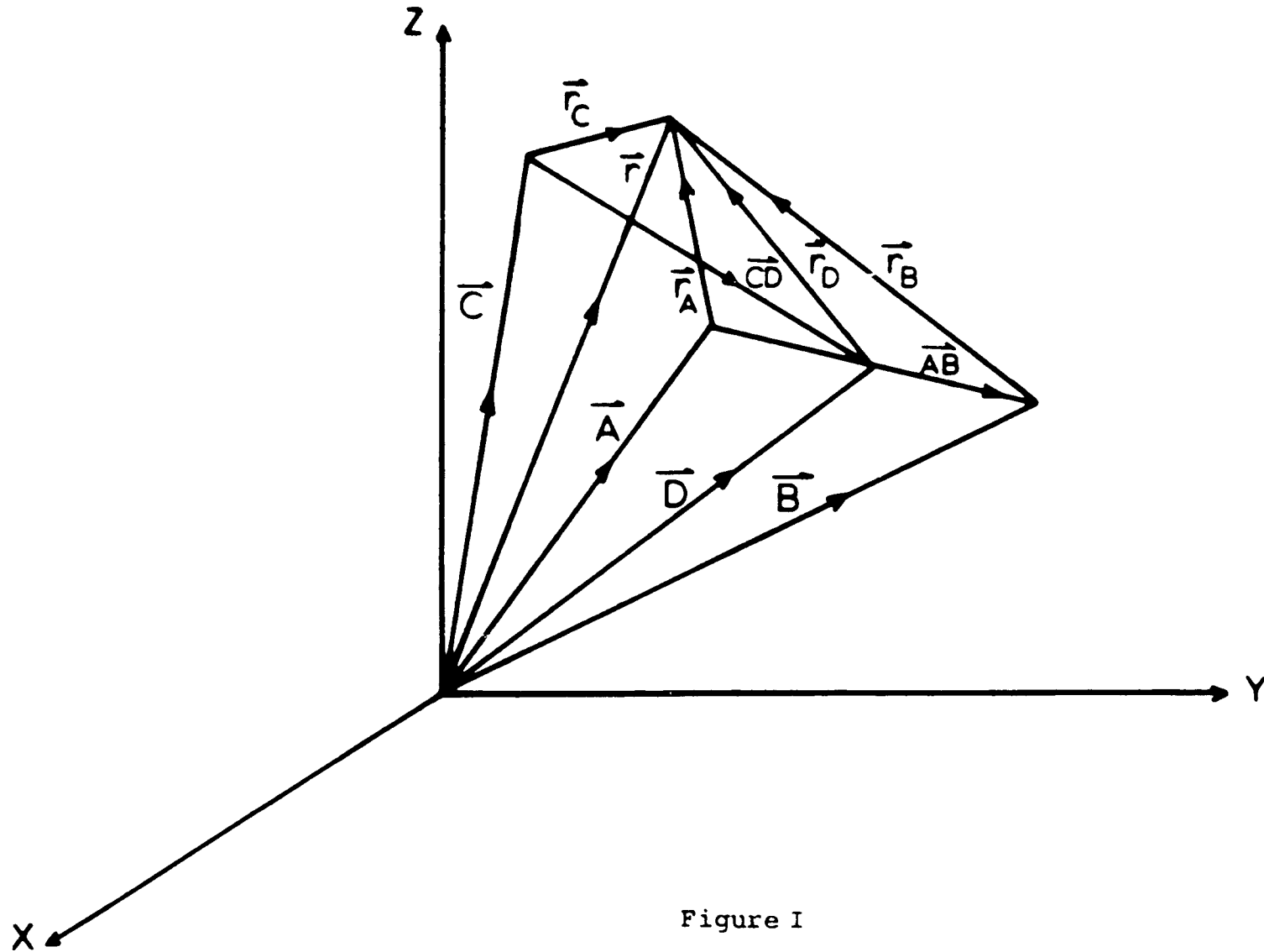


Figure I

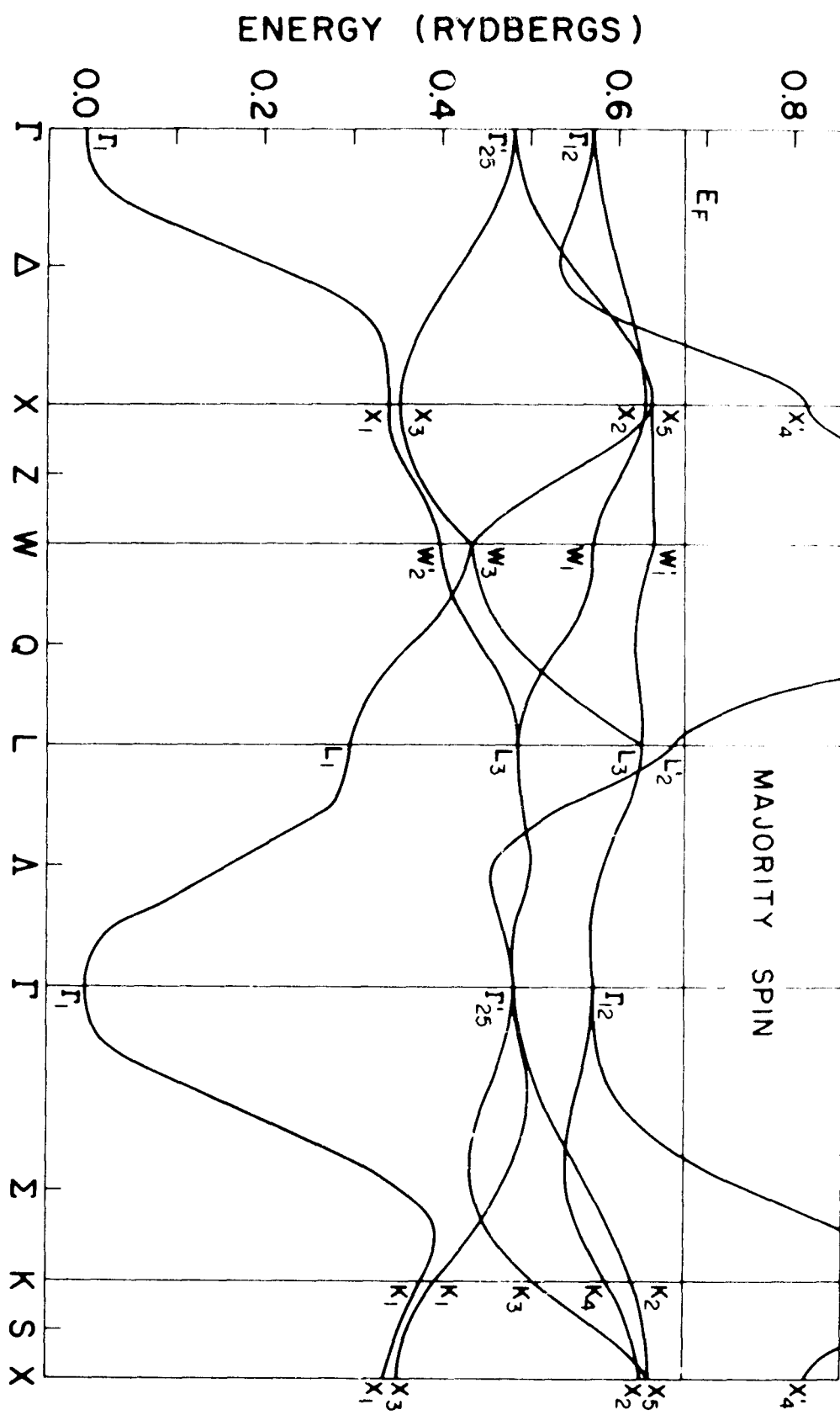


Figure II

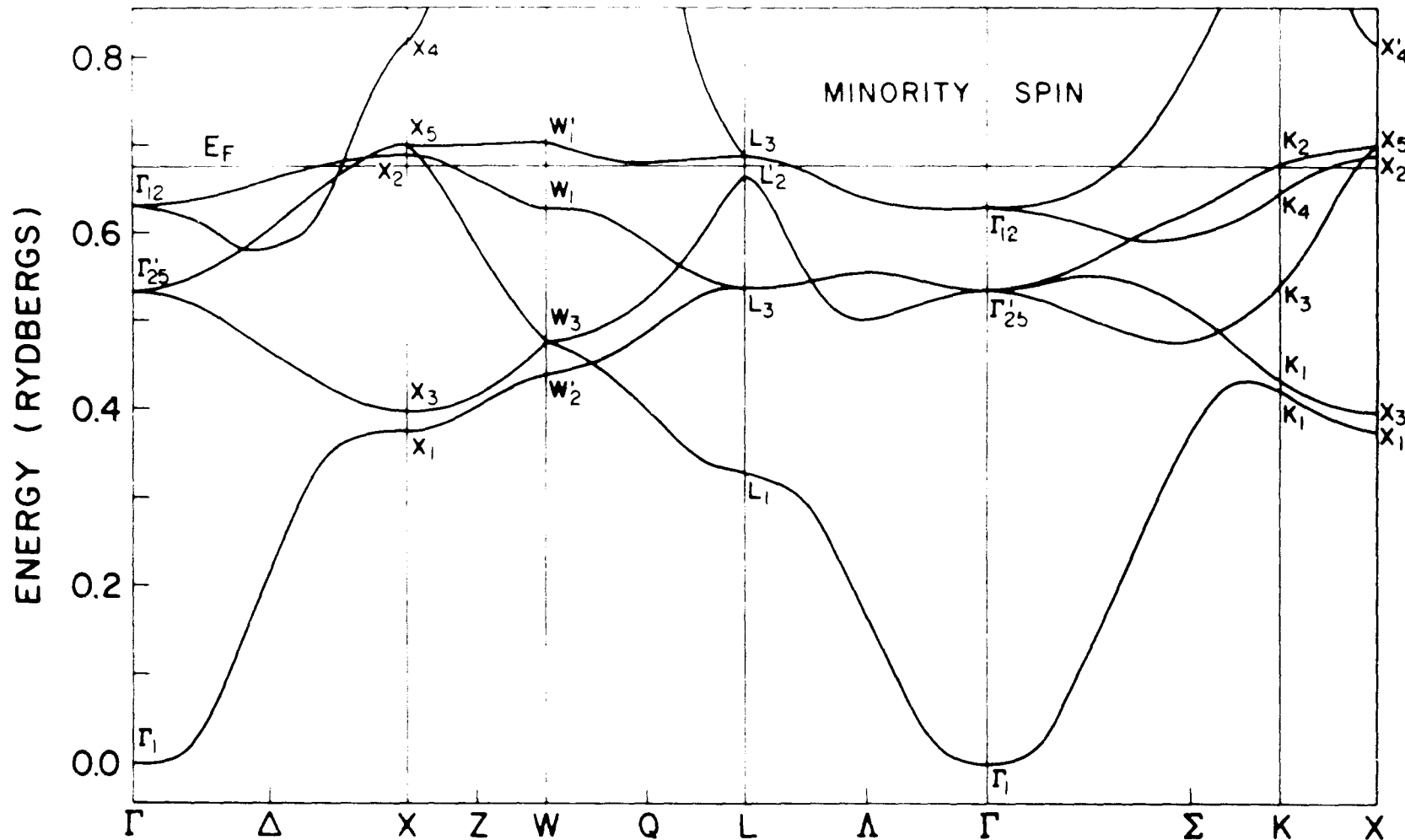
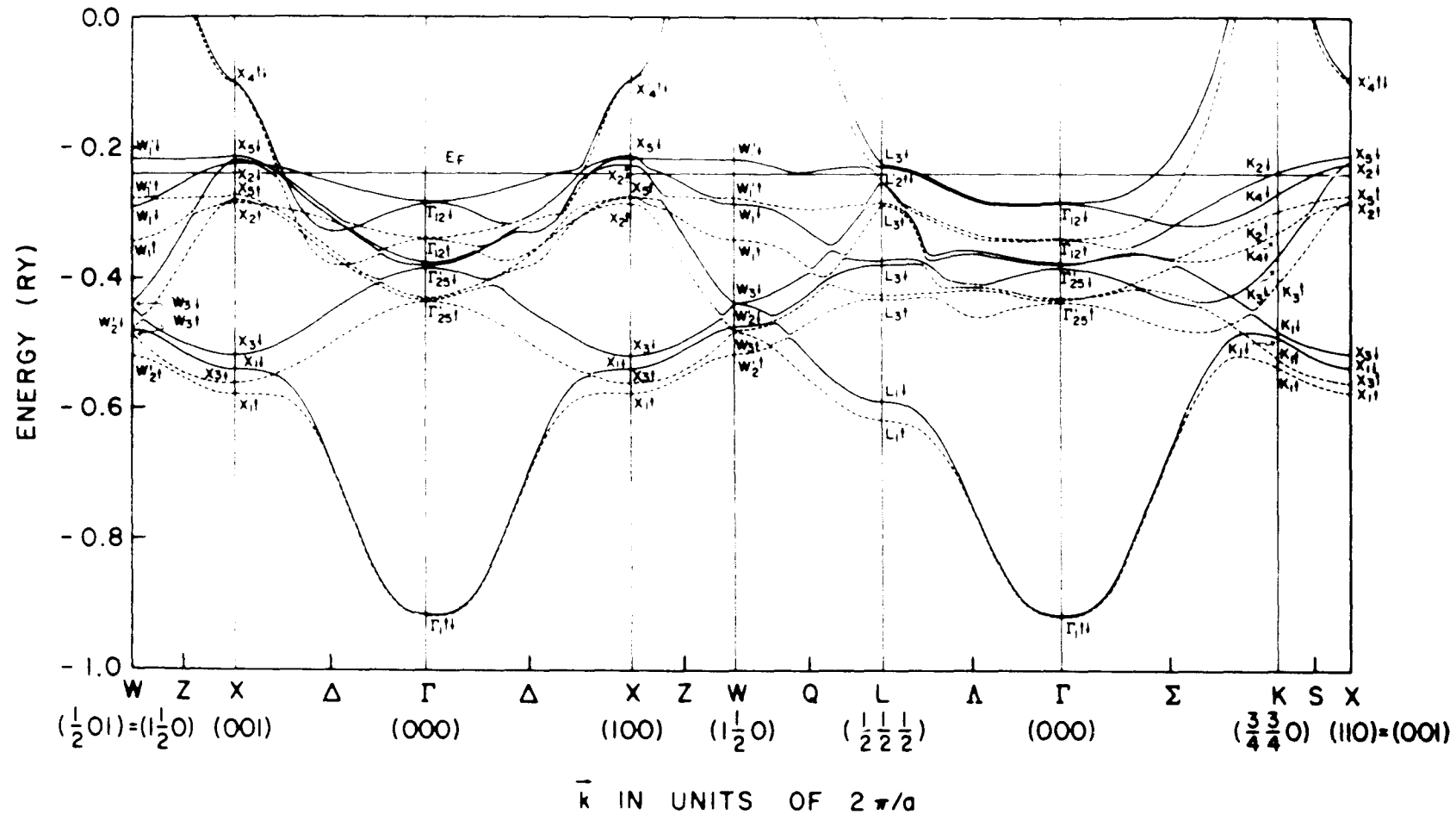


Figure III



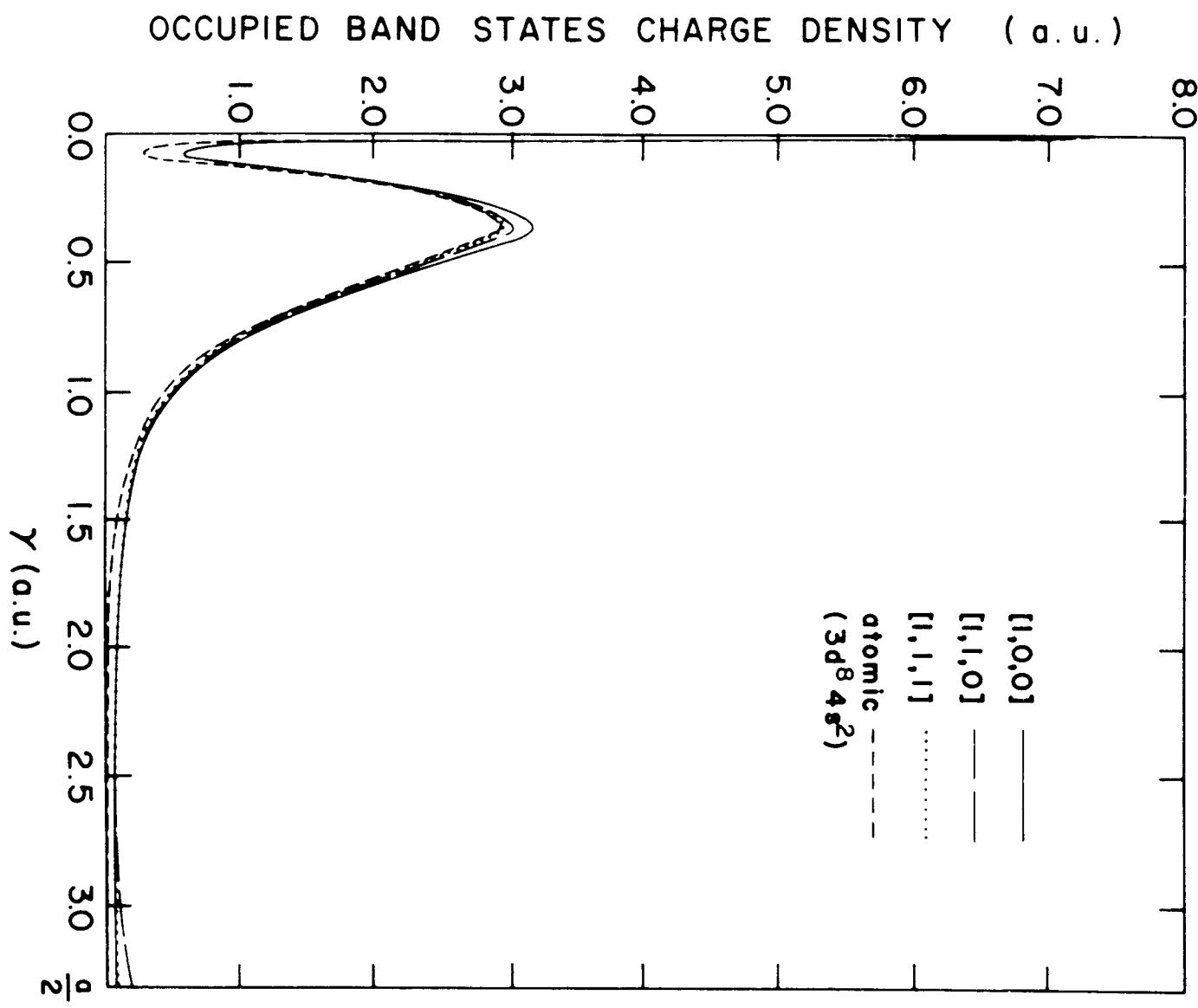


Figure V

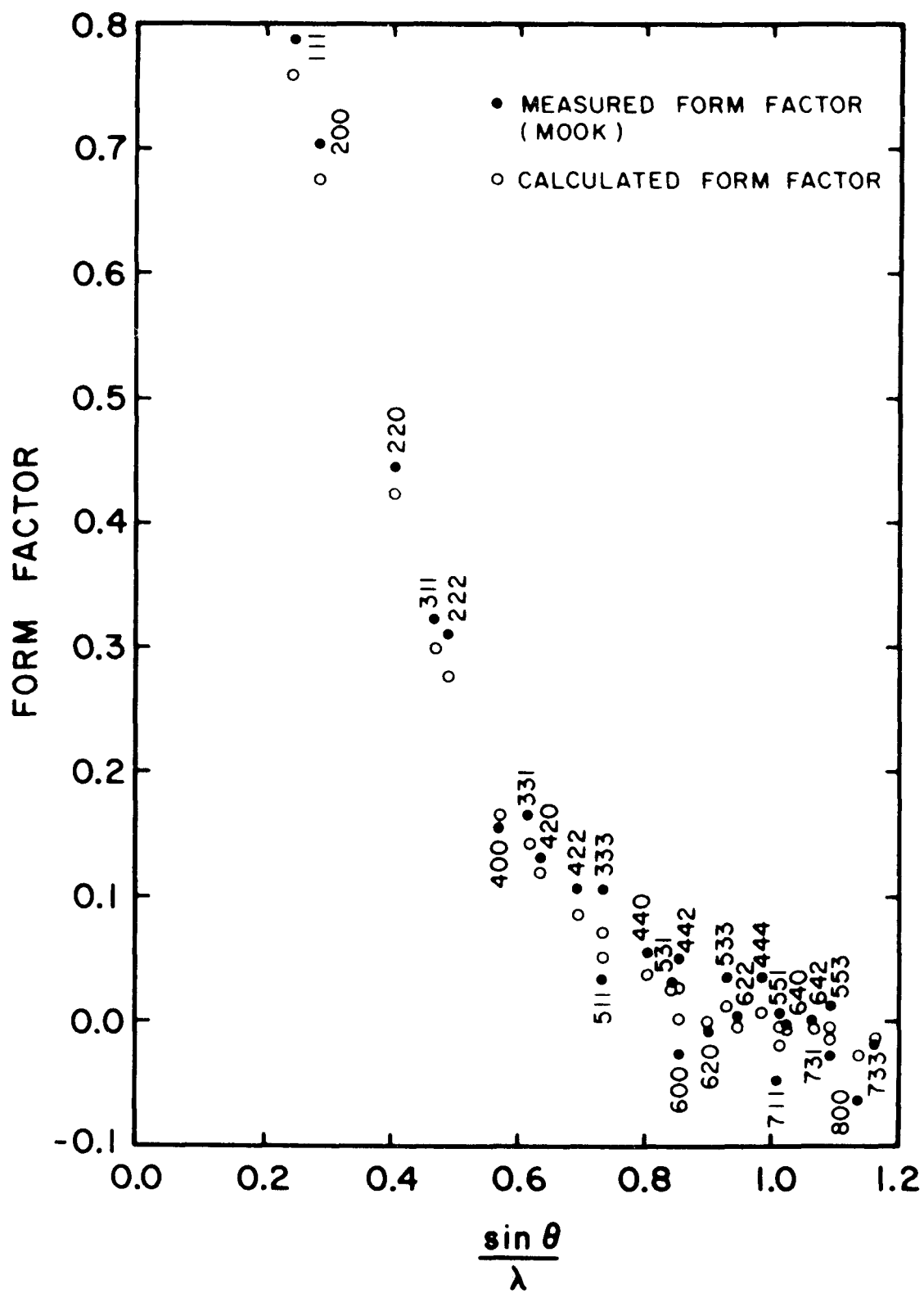


Figure VI

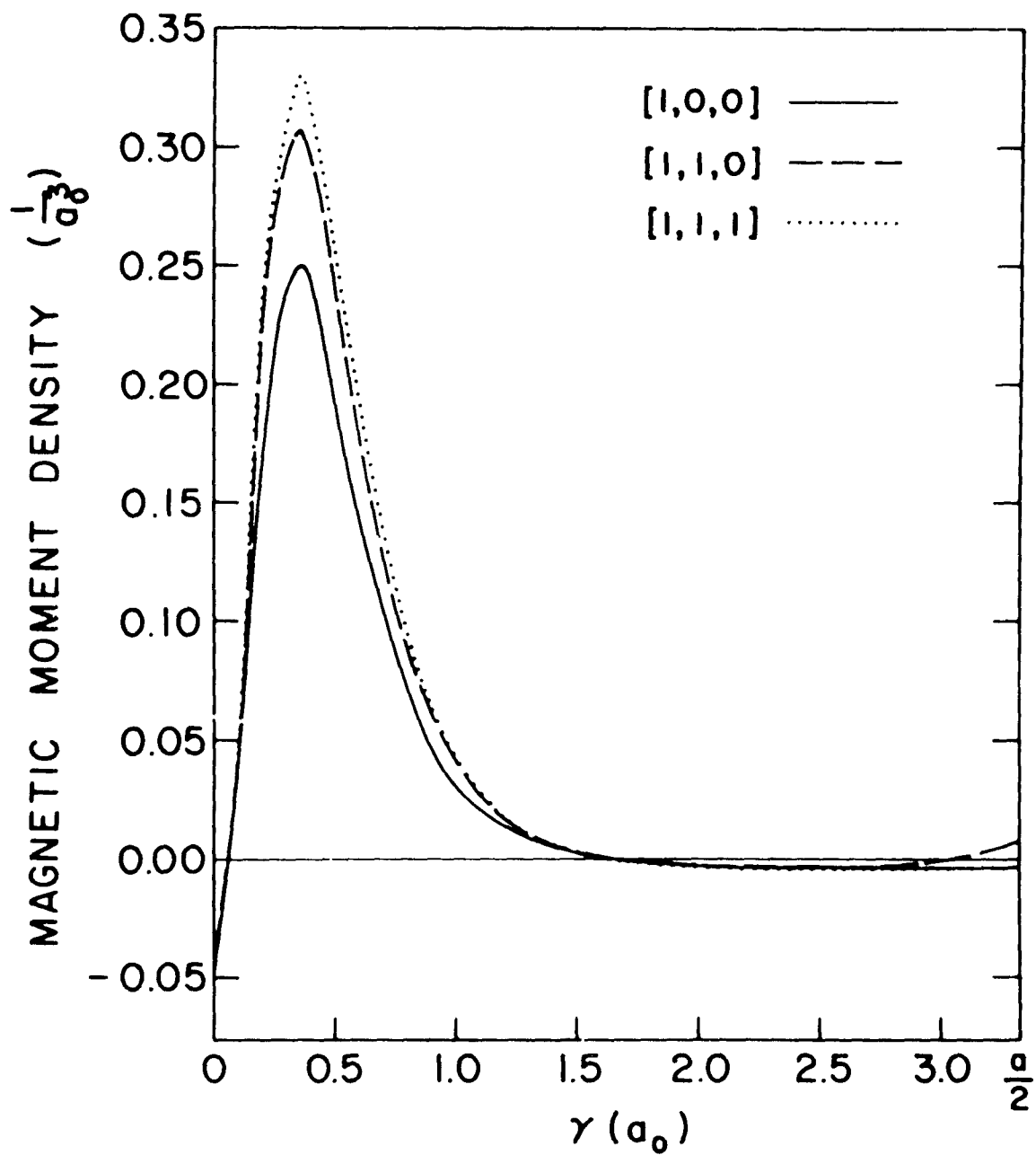


Figure VII

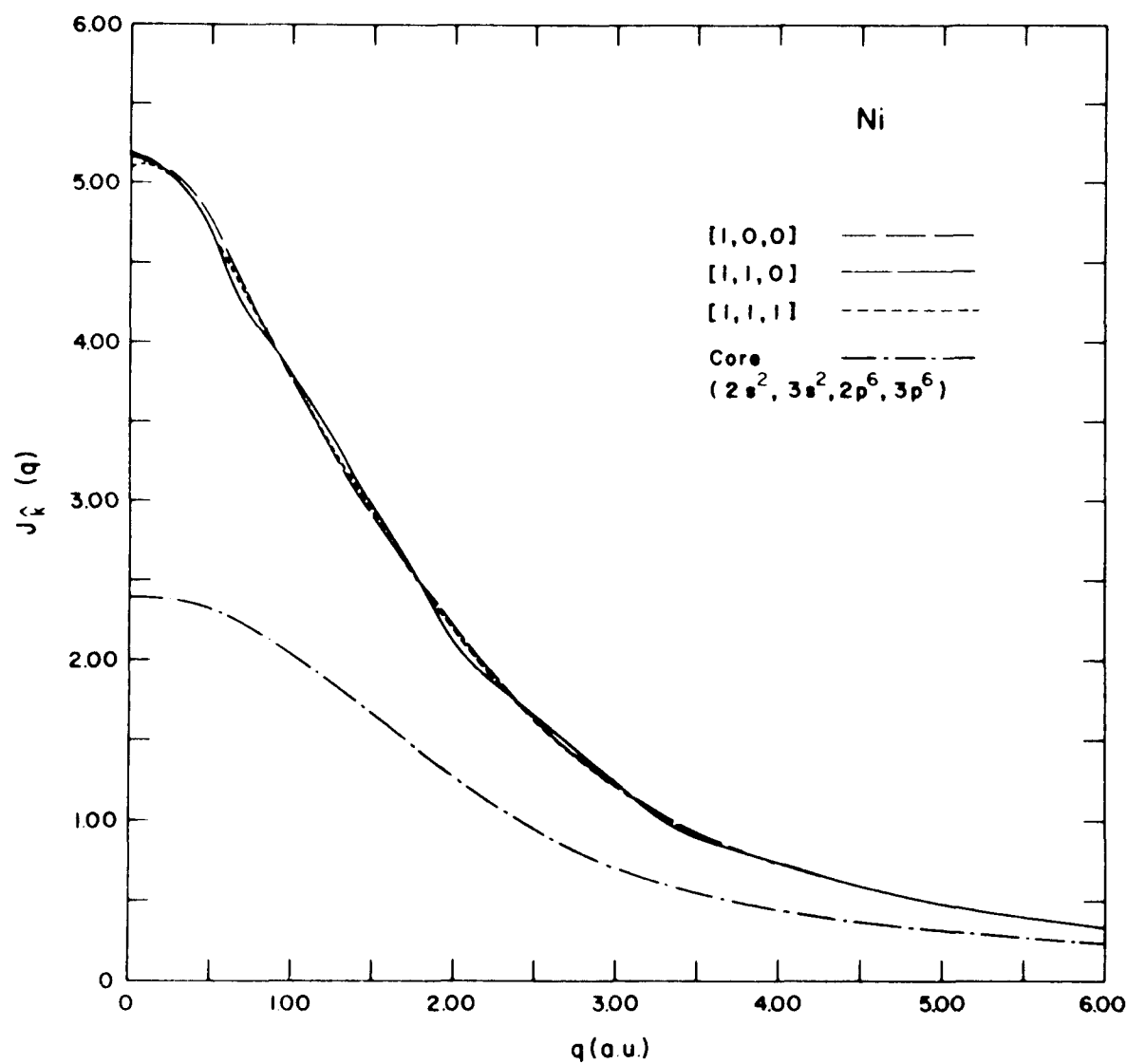


Figure VIII

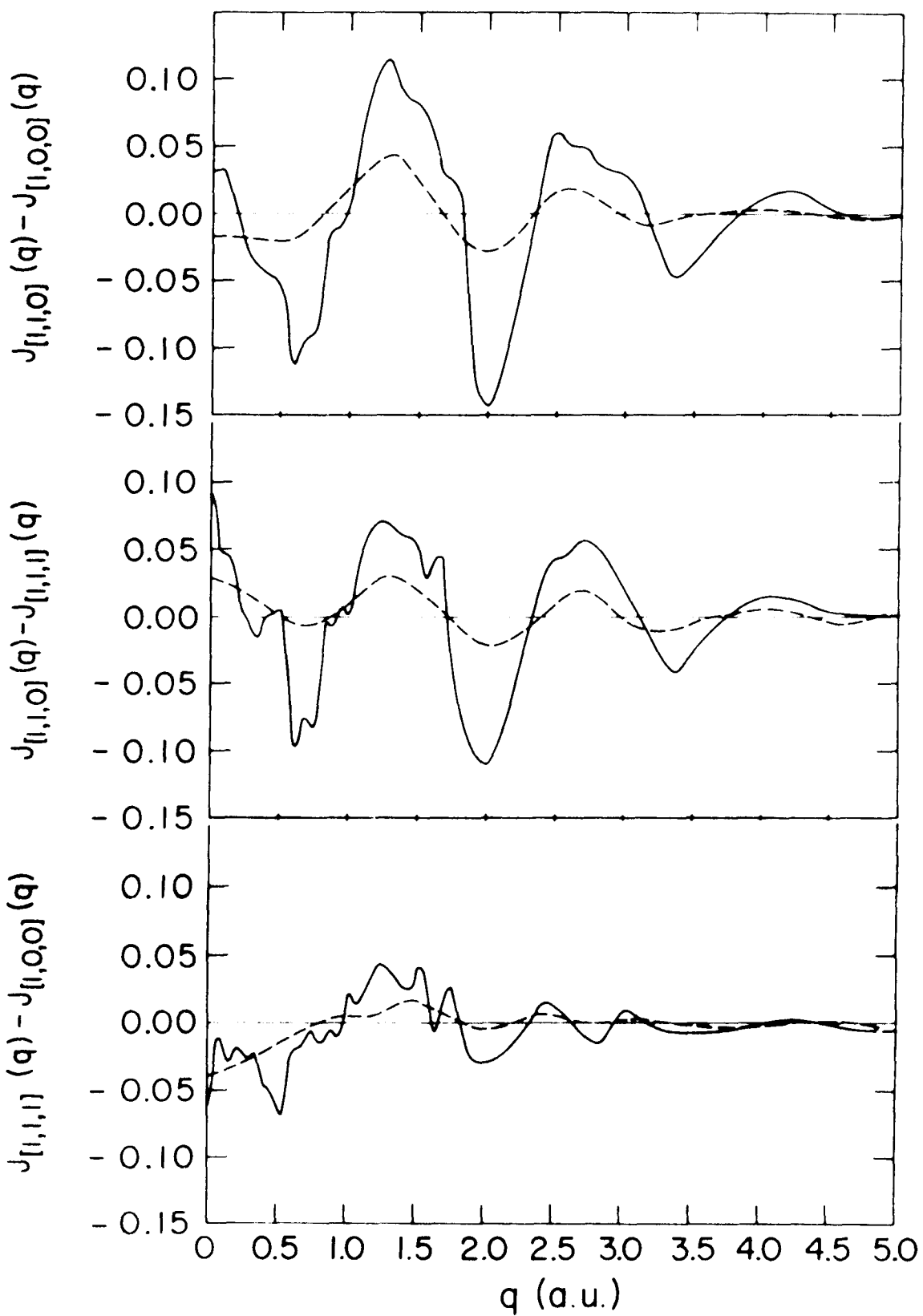


Figure IX

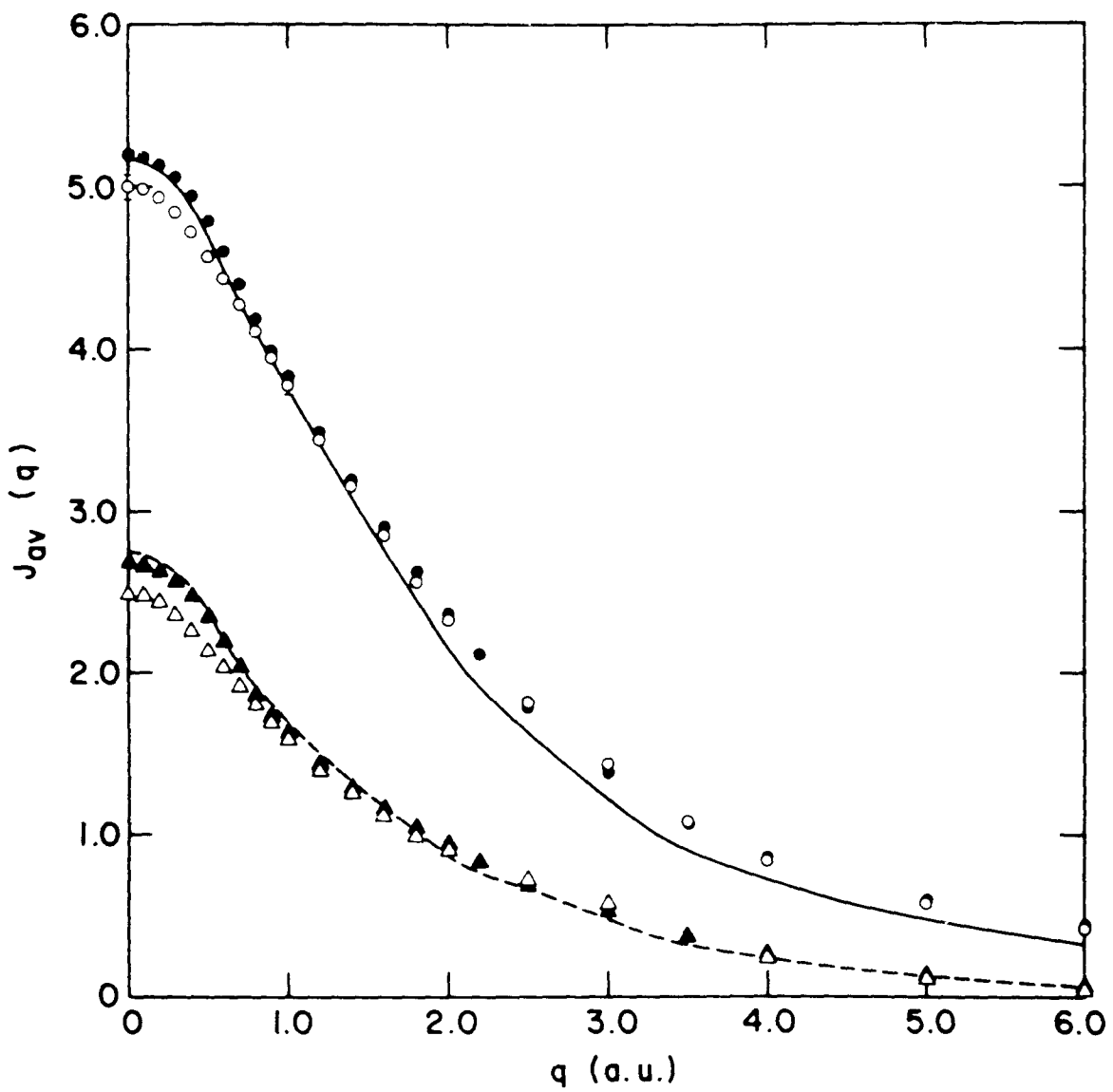


Figure X

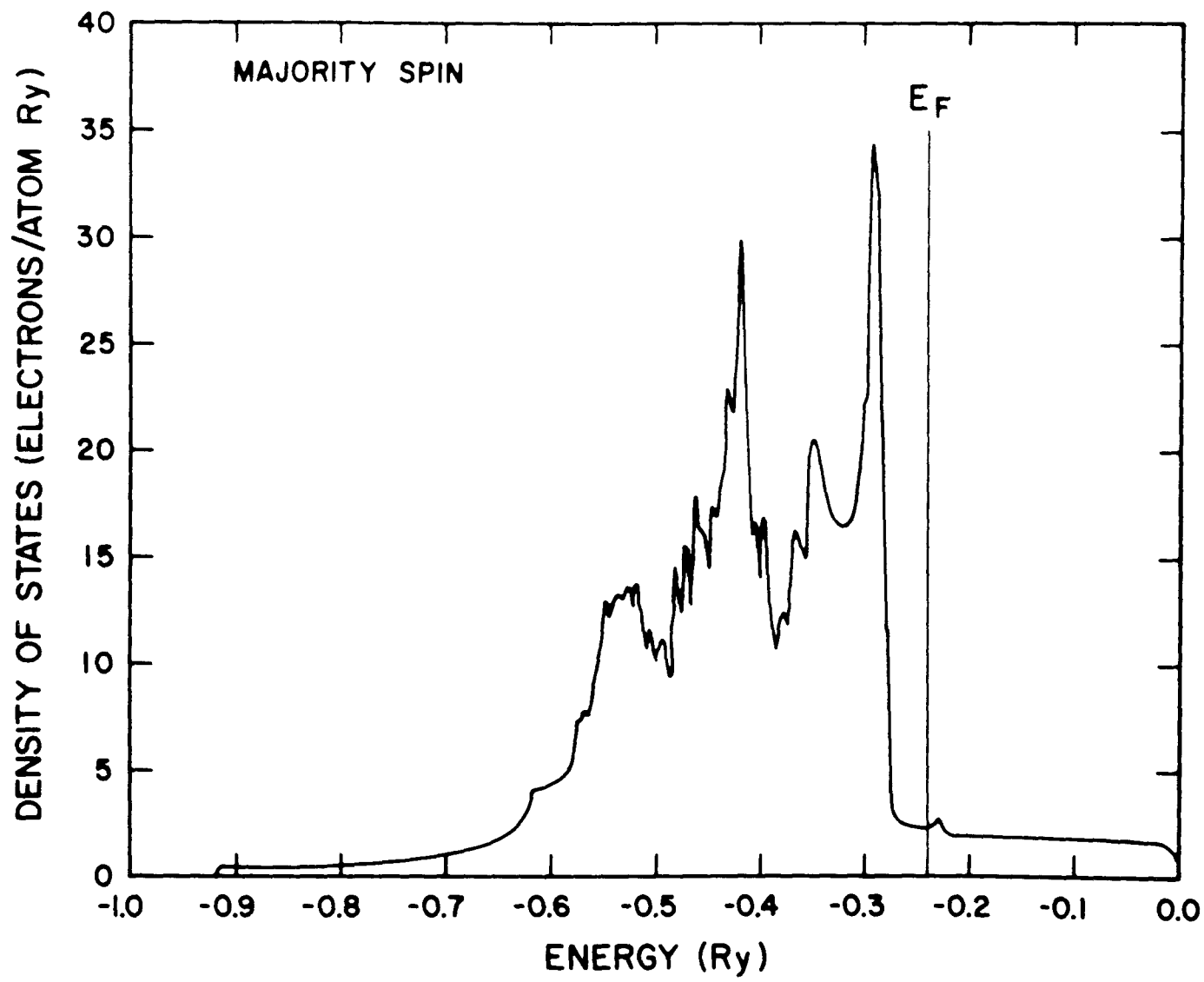


Figure XI

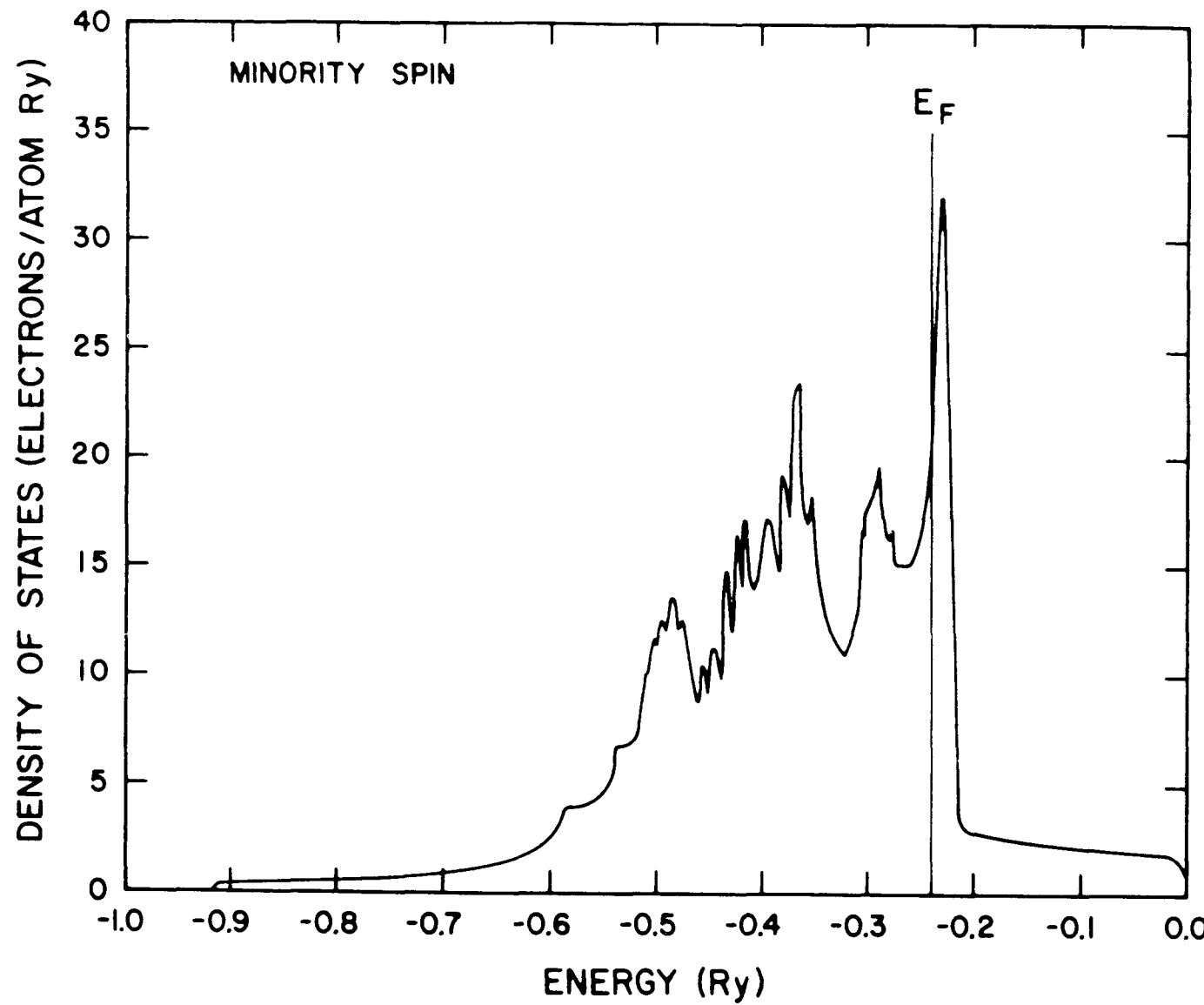


Figure XII

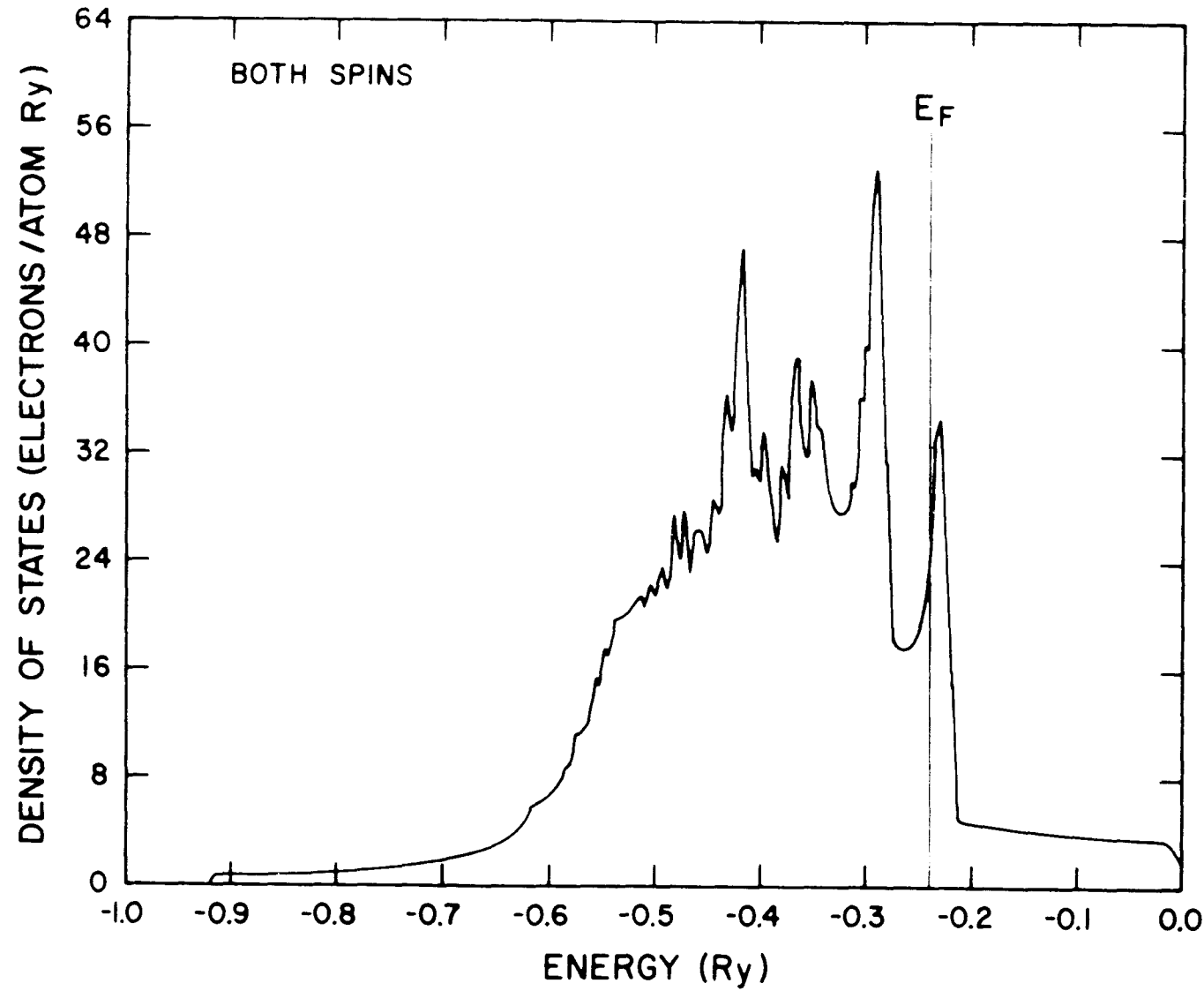


Figure XIII

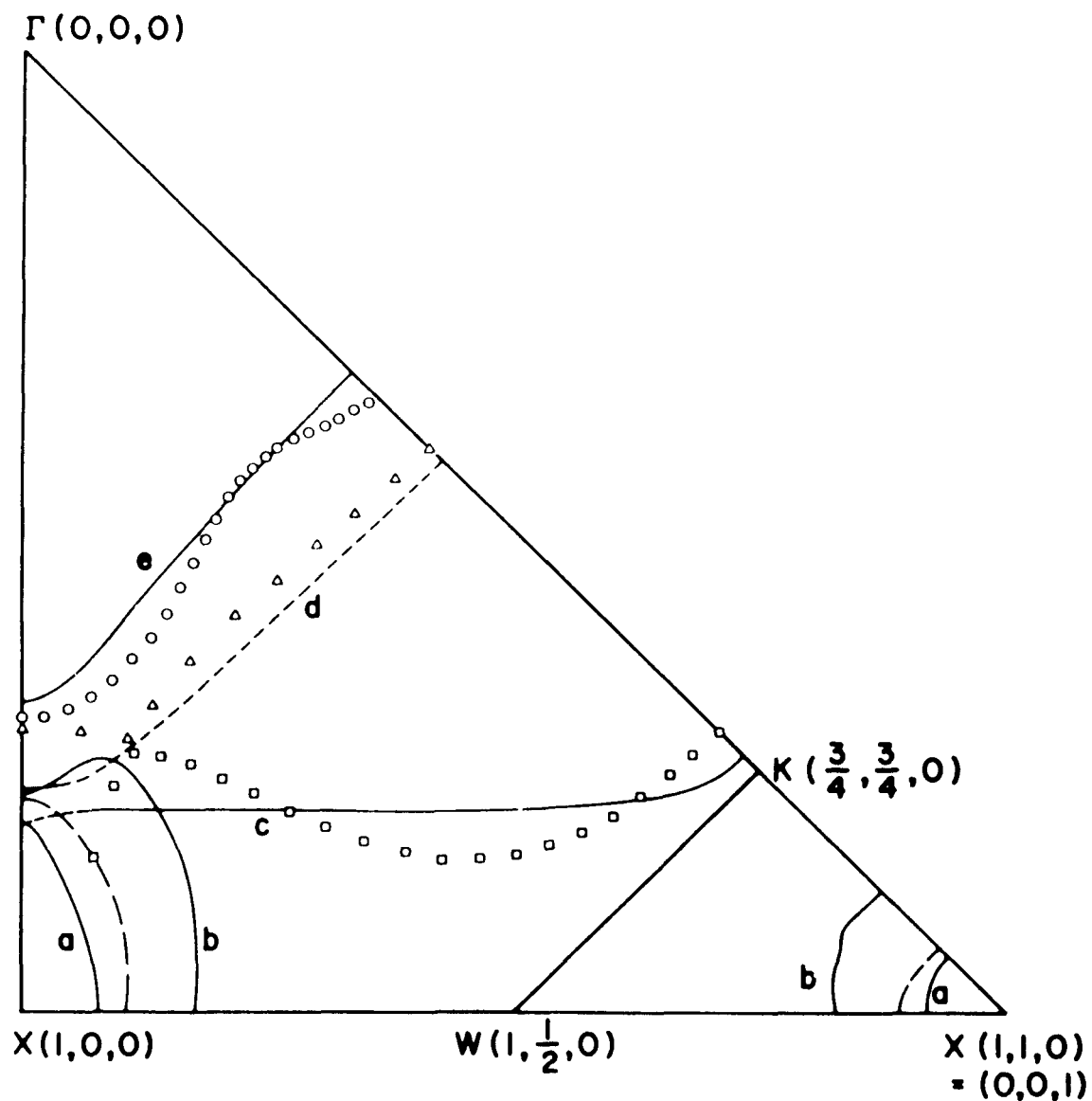


Figure XIV

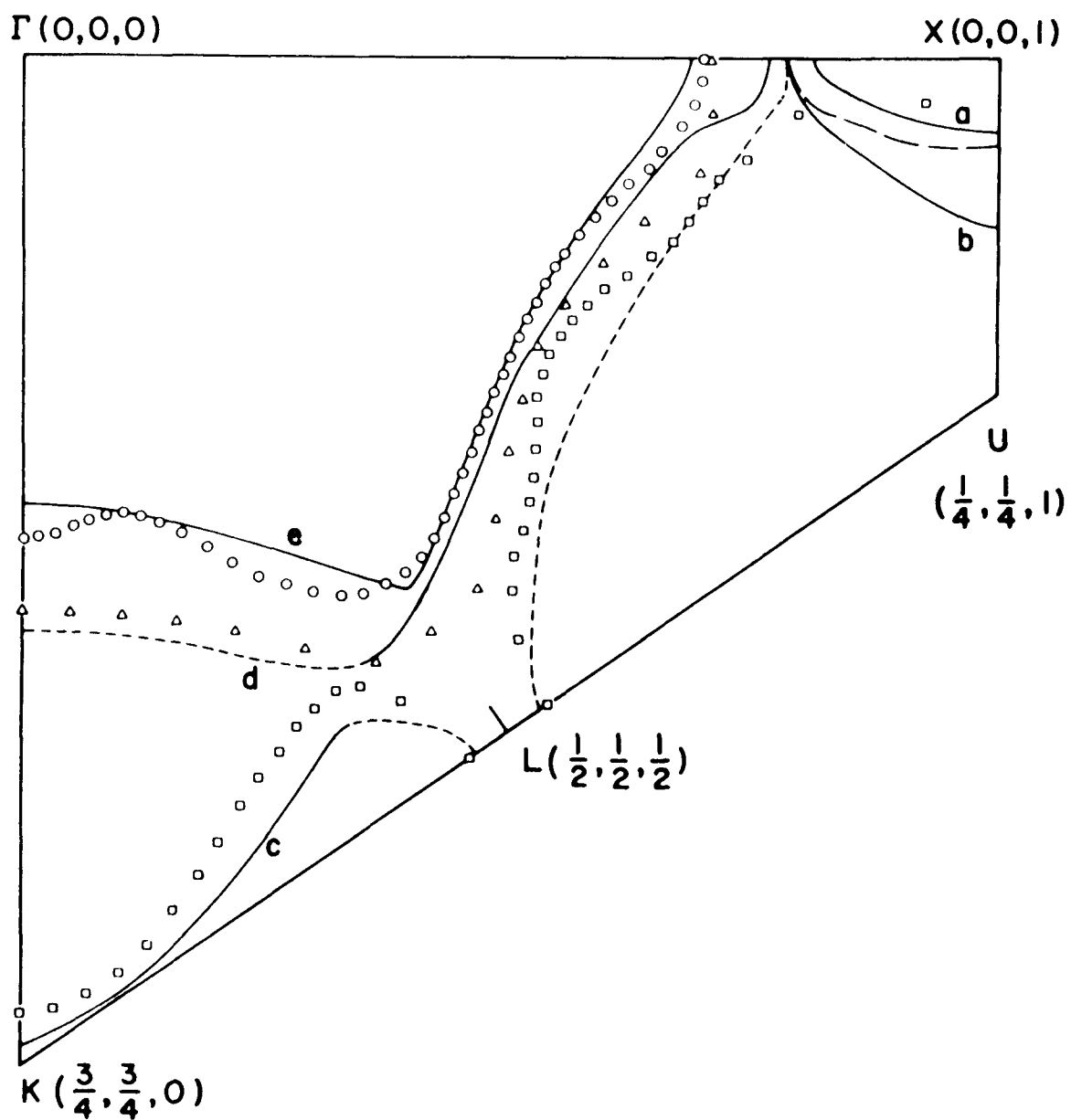


Figure XV

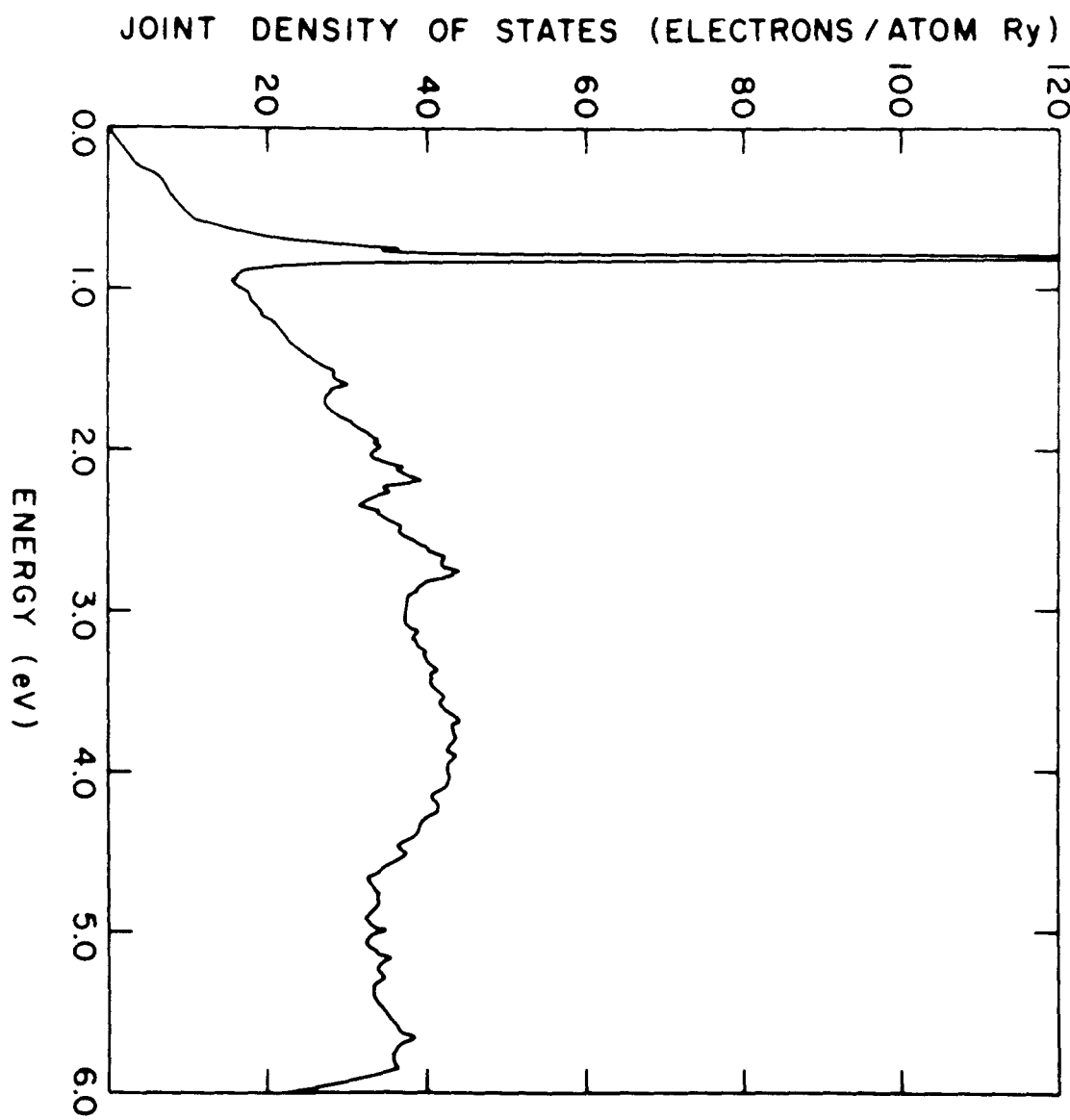


Figure XVI

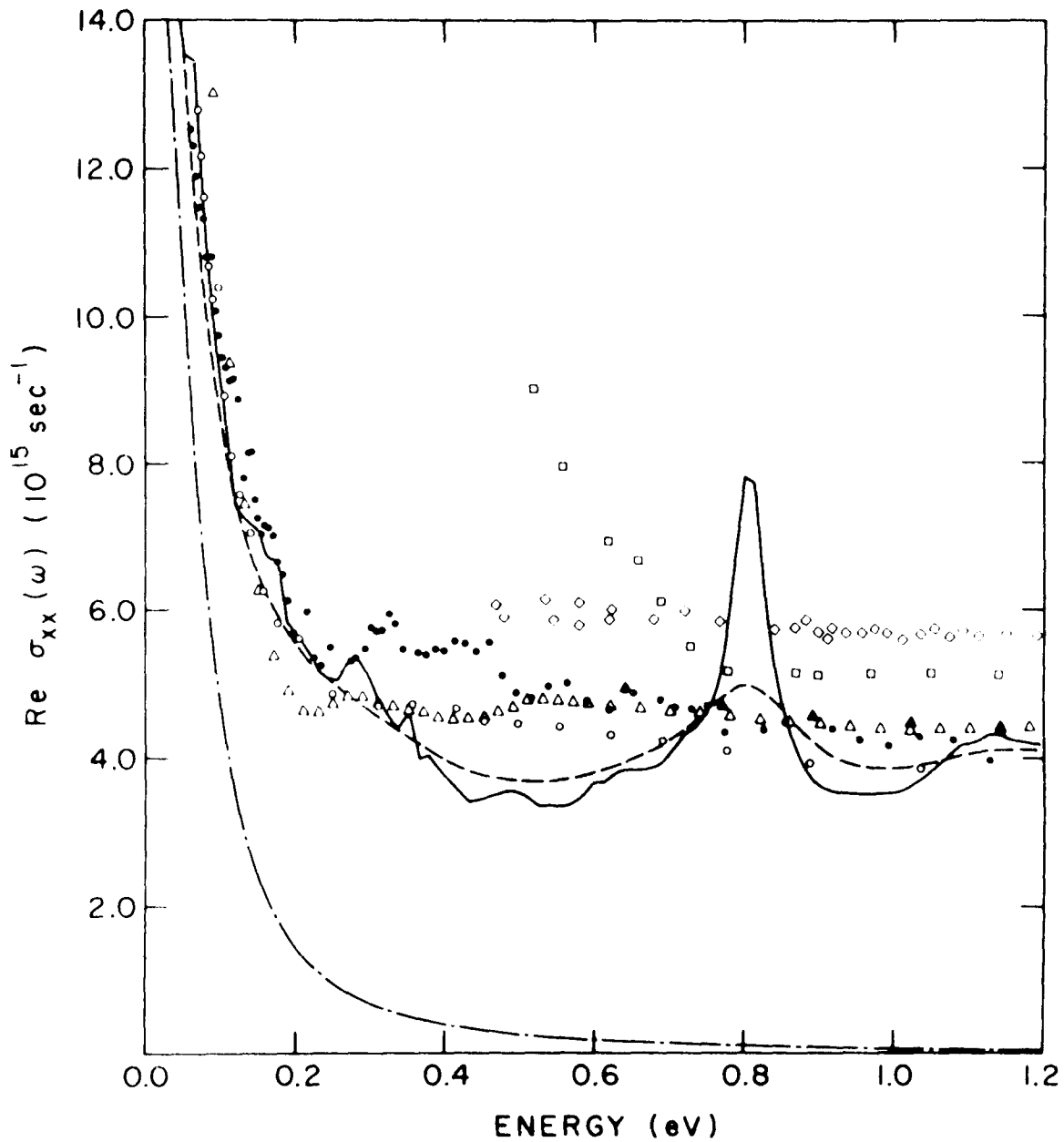


Figure XVII

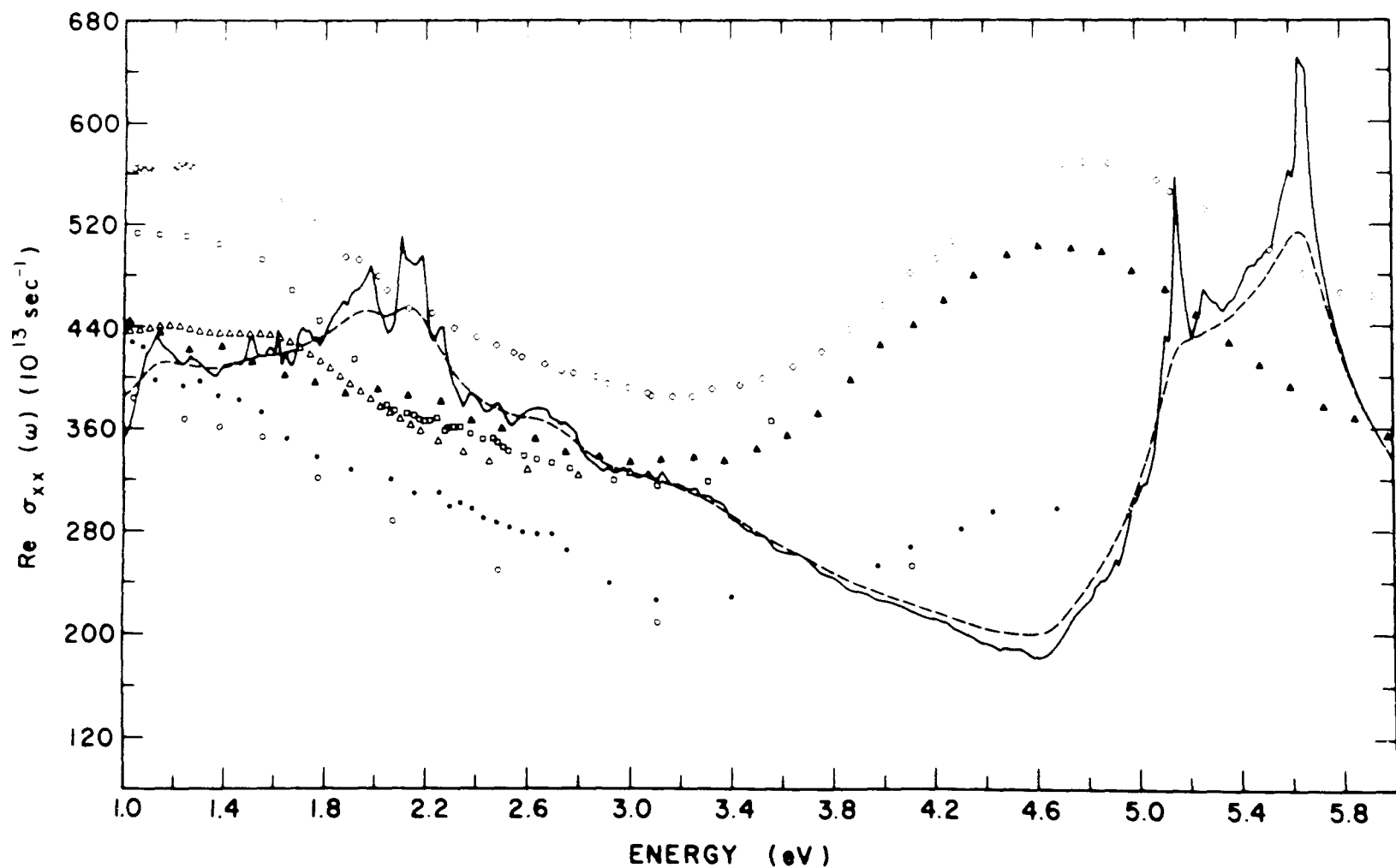


Figure XVIII

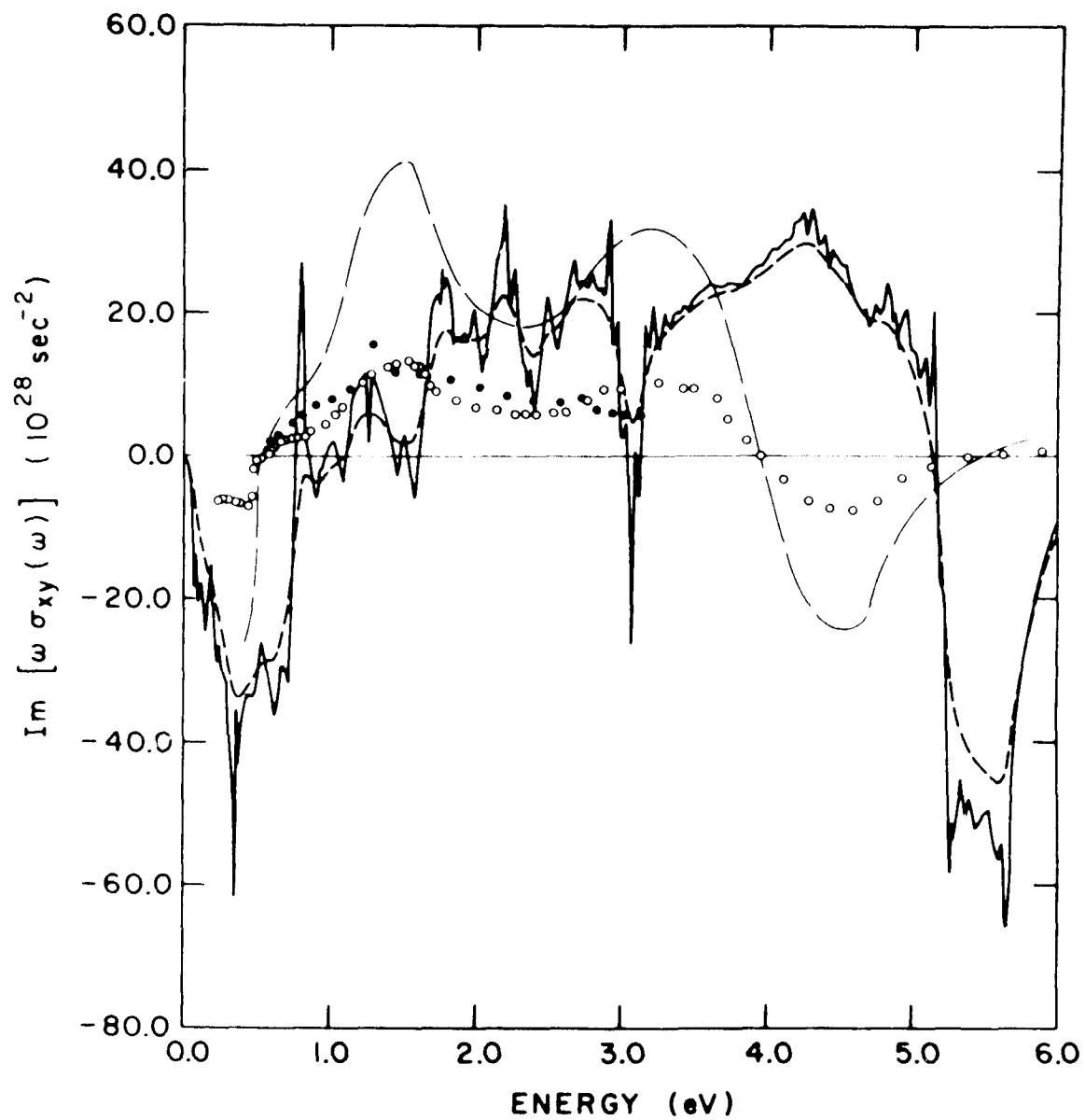


Figure XIX

APPENDIX A

The Fourier Transform of Gaussian Orbitals

In the calculation of Compton profile, it is necessary to evaluate the Fourier transforms of atomic functions

$$x_i(\vec{p}) = \frac{1}{\sqrt{\Omega}} \int e^{-i\vec{p} \cdot \vec{r}} u_i(\vec{r}) d^3 r \quad (3.10)$$

where Ω is the volume of a unit cell and the atomic functions are expanded in terms of Gaussian orbitals of the type

$$\frac{1}{\sqrt{4\pi}} e^{-\alpha r^2}; \sqrt{\frac{3}{4\pi}} x e^{-\alpha r^2}; \sqrt{\frac{15}{4\pi}} xy e^{-\alpha r^2}, \text{ etc.}$$

according to different atomic symmetry, s, p, d. Additional normalization constants from the radial part of the wave functions must be included (see Eqs. (2.13) and (2.15)). The Fourier transforms of these functions are tabulated below

S-functions

$$x_s(\vec{p}) = \frac{1}{\sqrt{4\pi\Omega}} \left(\frac{\pi}{\alpha}\right)^{3/2} e^{-\frac{p^2}{4\alpha}} \quad (A.1a)$$

P-functions

$$\begin{vmatrix} x_x(\vec{p}) \\ x_y(\vec{p}) \\ x_z(\vec{p}) \end{vmatrix} = \frac{-i}{2} \sqrt{\frac{3}{4\pi\Omega}} \frac{1}{\alpha} \left(\frac{\pi}{\alpha}\right)^{3/2} e^{-\frac{p^2}{4\alpha}} \begin{vmatrix} p_x \\ p_y \\ p_z \end{vmatrix}$$

(A.1b)

D-functions

$$\begin{vmatrix} x_{xy}(\vec{p}) \\ x_{yz}(\vec{p}) \\ x_{zx}(\vec{p}) \\ x_{x^2-y^2}(\vec{p}) \\ x_{z^2-r^2}(\vec{p}) \end{vmatrix} = \frac{-1}{4} \sqrt{\frac{15}{4\pi\Omega}} \frac{1}{\alpha^2} \left(\frac{\pi}{\alpha}\right)^{3/2} e^{-\frac{p^2}{4\alpha}} \begin{vmatrix} p_x p_y \\ p_y p_z \\ p_z p_x \\ \frac{1}{2}(p_x^2 - p_y^2) \\ \frac{1}{2\sqrt{3}}(3p_z^2 - p_r^2) \end{vmatrix}$$

(A.1c)

APPENDIX B

Ferromagnetic Kerr Effect

In Chapter III, Section E we compared the absorptive part of the off-diagonal elements of the conductivity tensor $\text{Im}[\sigma_{xy}(\omega)]$ with the results obtained from the magneto-optical measurements. In this appendix we shall examine the formal relationship between $\hat{\sigma}(\omega)$ and the Kerr rotation angle.^{94,95} Consider a time dependent electric field

$$\vec{E}(t) = \frac{1}{\sqrt{2\pi}} \int \vec{E}(\omega) e^{-i\omega t} d\omega \quad (\text{A.2})$$

In the optical and infrared region the wave vector is effectively zero. The induced current takes the following form

$$\vec{j}(t) = \frac{1}{\sqrt{2\pi}} \int \hat{\Sigma}(t, t') \vec{E}(t') dt' \quad (\text{A.3})$$

For a homogenous medium the conductivity is invariant under displacement of time, $\hat{\Sigma}(t, t') = \hat{\Sigma}(t-t')$. The Fourier transform of Eq. (A.3) can be written as

$$\vec{j}(\omega) = \hat{\sigma}(\omega) \vec{E}(\omega) \quad (\text{A.4})$$

in the case of a cubic crystal with electron spin

quantized along the z-axis the conductivity tensor can be shown to be

$$\hat{\sigma}(\omega) = \begin{vmatrix} \sigma_{xx} & \sigma_{xy} & 0 \\ -\sigma_{xy} & \sigma_{xx} & 0 \\ 0 & 0 & \sigma_{zz} \end{vmatrix} \quad (\text{A.5})$$

As a result of broken symmetry by the spin orbit interaction the off diagonal elements σ_{xy} are nonzero. For convenience we shall consider the incident plane wave as superposition of equal amplitude right and left circularly polarized light.

$$E_r = E(\omega) \frac{(\hat{x} + i\hat{y})}{\sqrt{2}} e^{-i\omega t} \quad (\text{A.6})$$

where \hat{x} and \hat{y} are unit vectors along x and y directions respectively. In a similar manner, we define the RCP and LCP currents as

$$J_r = J(\omega) \frac{(\hat{x} + i\hat{y})}{\sqrt{2}} e^{-i\omega t} \quad (\text{A.7})$$

The corresponding conductivity which satisfies the relation

$$\frac{J_r}{v} = \frac{i}{\omega} \frac{E_r}{\epsilon} \quad (\text{A.8})$$

is a simple scalar

$$\frac{\sigma_r}{\epsilon_r} = \sigma_{xx} + i \sigma_{xy} . \quad (A.9)$$

Maxwell's field equations then relate the complex index of refraction ($n+ik$) for RCP and LCP electric fields to the complex conductivity

$$(n_r + ik_r)^2 = 1 + i \frac{4\pi \sigma_r}{\omega} \quad (A.10)$$

In the case of light normally incident from vacuum

$$\frac{E_{\text{reflected}}}{E_{\text{incident}}} = \zeta e^{i\phi} = \frac{(n+ik)-1}{(n+ik)+1} \quad (A.11)$$

where ϕ is the phase change of the reflected light and the sign convention is that for polarization along the plane of incidence. Denoting

$$\Delta\theta = \theta_r - \theta_\ell , \quad \Delta n = n_r - n_\ell \quad \Delta k = k_r - k_\ell \quad (A.12)$$

it can be shown that to the first order in these changes

$$\phi = \frac{2i(\Delta n + i\Delta k)}{[(n+ik)^2 - 1]} \quad (A.13)$$

Similarly from Eqs. (A.10) and (A.9) one obtains

$$n+ik = \frac{i - 2\pi \Delta\theta}{(n+ik)_0} = \frac{-4\pi \sigma_{xy}}{(n+ik)_0} \quad (A.14)$$

Eq. (A.14) was substituted into Eq. (A.13)

$$\Delta\theta = \frac{-i 8\pi \sigma_{xy}}{\omega(n+i\kappa)((n+i\kappa)^2-1)} \quad (\text{A.15})$$

The major axis of the elliptically polarized reflected light is rotated from the plane of polarization by an angle

$$\frac{\Delta\theta}{2} = \text{Re} \left[\frac{-i 4\pi \sigma_{xy}}{\omega(n+i\kappa)((n+i\kappa)^2-1)} \right] \quad (\text{A.16})$$

Eq. (A.16) is the constant for the Magneto Kerr effect which is positive for rotation from x- to y-axis but it must be kept in mind that the reflected beam is traveling along the -z direction and Eq. (A.16) is valid for small values of ω , Δn , and $\Delta\kappa$ only.

APPENDIX C
LIST OF PROGRAMS

	Page
1. Fourier coefficients of the Coulomb and exchange potential.....	144
2. The Coulomb, exchange, kinetic, overlap, and momentum integrals.....	150
3. The integrals of $\sum \cos(\alpha \vec{k} \cdot \vec{R})$ where α generates the star of \vec{k}	158
4. Sum over direct lattice vectors for Hamiltonian overlap and momentum matrices.	164
5. Bloch basis functions along three principle directions.....	174
6. Self-consistency.....	179
7. The central cell integrals of the spin-orbit coupling (p-p and d-d blocks).....	190
8. Energy bands including the effects of spin orbit coupling.....	197
9. The momentum matrices between band states.	201
10. The density of states.....	204
11. The interband optical conductivity tensor.....	211
12. The Compton profile.....	216

LIST OF SUBROUTINES

	Page
1. CONDUC.....	222
2. COULOM.....	224
3. DENSIT.....	225
4. FOURFC.....	227
5. FUNCT.....	229
6. GBZPT.....	230
7. GINDPK.....	233
8. GINTFC.....	236
9. GNBDE.....	238
10. GNBPT.....	242
11. GNDPUM.....	246
12. GPERMK.....	248
13. GWTGAS.....	250
14. GSICO.....	252
15. GSIJFC.....	254
16. HRIN.....	256
17. READ.....	257
18. RDGTO.....	262
19. RTINH.....	264
20. SEXCH.....	265
21. SPLOTE.....	268
22. SVK0.....	270
23. WFCC16.....	271

```

C PROGRAM 1. FOURIER COEFFICIENTS OF THE COULOMB AND EXCHANGE POTENTIAL
C ****
C CALCULATION OF THE FOURIER COEFFICIENT OF POTENTIALS
C SLATER TYPE WAVE FUNCTIONS ARE USED IN THIS PROGRAM
C SC IDCUB=1, BCC IDCUB=2, FCC IDCUB=4
C A=LATTICE CONSTANT (IN A. U. )
C IGRLV=0, V(K) IS GENERATED IN ORDER OF INCREASING K**2
C IGRLV=1, FOURIER COEFFICIENTS OF THE CHARGE DENSITY FOR BOTH SPINS ARE
C GENERATED IN ORDER OF K VECTORS
C IF(I SORT.NF.0) K IS SORTED IN ORDER OF INCREASING MAGNITUDE
C NKPT IS THE DIMENSION OF THE RECIPROCAL LATTICE VECTORS KXX(I) ECT.
C MAXK2=THE SQUARE OF THE MAXIMUM MAGNITUDE OF THE RECIPROCAL LATTICE
C VECTORS GENERATED
C IDIM IS THE DIMENSION OF THE DIRECT LATTICE VECTORS
C MAXR2=THE SQUARE OF THE MAXIMUM MAGNITUDE OF THE DIRECT LATTICE VECTORS
C KPTPRT IS THE NO OF LINES OF RESULTS TO BE PRINTED
C NSTA IS THE NUMBER OF ATOMIC STATES CONSIDERED. MAXIMUN=7
C C(I,J) IS THE J'S COEFFICIENT OF THE I'S WAVE FUNCTION
C EX(I,J) IS THE J'S EXPONENTS OF THE I'S WAVE FUNCTION
C NORB(I) IS THE NUMBER OF ORBITALS IN THE I'S WAVE FUNCTION
C IB(I,J) IS THE ORBITAL IDENTIFICATION OF THE I'S WAVE FUNCTION
C CHARGE(I) IS THE NUMBER OF ELECTRONS IN THE I'S STATE
C EXCH(I) IS DENSITY**0.333 AT POINT R(I)
C ****
C IMPLICIT REAL*8(A-F,H,O-Z)
C INTEGER*2 KXX,KKY,KKZ,NB,KX,KY,KZ,NNB
C DIMENSION AX(400),AY(400),AZ(400),Y(100)
C DIMENSION KSQ(500)
C COMMON/CHARGE/CHARGE(7),CHARUP(7),CHARDN(7)
C COMMON/VKO/C(7,11),EX(7,11),FACTO(10),IB(7,11),NORB(7),NSTA
C COMMON/EXCH/R(96),W(96),EXCH(96),EXUP(96),EXDN(96)
C COMMON/CONST/A,RO,PI,ONETHD
C COMMON/LCS/KKX(500),KKY(500),KKZ(500),NB(500)
C PI=3.141592653589793D0
C ONETHD=1.D0/3.D0
C FACTO(1)=1.D0
C DO 11 I=2,10
11 FACTO(I)=FACTO(I-1)*DFLOAT(I)
C READ(5,3) A, IDCUB, NKPT, MAXK2, IDIM, MAXR2, KPTPRT, NSTA, IGRLV, ISORT,
C & IPUN
3 FORMAT(F10.5,10I5)
AAA=A*A*A
AKR=2.D0*PI/A
OMEGA=AAA/DFLOAT(IDCUB)
AHALF=A/2.D0

```

```

C IF(IDCUB.EQ.1) AHALF=A
C
C DEFINE R AND WEIGHT FACTOR FOR 96 POINTS GAUSSIAN INTEGRATION IN THE
C WIGNER SEITZ CELL
C
C R03=3.D0/(4.D0*PI)*OMEGA
C R0=R03**ONETHD
C CALL GWTGAS(96,Y,R,W)
C DO 54 I=1,96
C 54 R(I)=R0*(R(I)+1.D0)/2.D0
C
C RENORMALIZATION OF THE WAVE FUNCTION
C
C 2 FORMAT(15.2F10.5)
C 1 FORMAT(3A4,BX,15.2F10.5)
C ELECT=0.D0
C FMAG=0.D0
C 12 FORMAT(1X,//,1X,3A4.5X,'NO OF ORBITALS=',I4,5X,'ELECTRONS UP=',
C &F8.3,5X,'ELECTRONS DOWN=',F8.3,5X,'TOTAL ELECTRONS=',F8.3,/)
C ELEUP=0.D0
C ELEDN=0.D0
C DO 10 I=1,NSTA
C READ(5,1) Z1,Z2,Z3,NORB(I),CHARUP(I),CHARDN(I)
C ELEUP=ELEUP+CHARUP(I)
C ELEDN=ELEDN+CHARDN(I)
C CHARGE(I)=CHARUP(I)+CHARDN(I)
C WRITE(6,12) Z1,Z2,Z3,NORB(I),CHARUP(I),CHARDN(I),CHARGE(I)
C NN=NORB(I)
C DO 15 J=1,NN
C READ(5,2)IB(I,J),EX(I,J),C(I,J)
C 4 FORMAT(1X,'L=',I5.5X,'EXPONENTS=',F10.5,5X,'COEFFICIENT=',F10.5)
C WRITE(6,4)IB(I,J),EX(I,J),C(I,J)
C AJ=IB(I,J)
C II=2*IB(I,J)
C TWOZ=(2.D0*EX(I,J))**AJ
C 15 C(I,J)=C(I,J)*TWOZ/DSQRT(FACTO(II))
C 10 CONTINUE
C ELECT=ELEUP+ELEDN
C FMAG=ELEUP-ELEDN
C
C GENERATE PERMUTED DIRECT LATTICE VECTORS
C
C IDC=8/IDCUB
C IF(IDCUB.EQ.1) IDC=1
C CALL GPERMK(KKX,KKY,KKZ,KSQ,1DIM,1DC,MAXR2,0)
C DO 31 II=1,1DIM

```

```

      AX(I)=AHALF*KKX(I)
      AY(I)=AHALF*KKY(I)
31   AZ(I)=AHALF*KKZ(I)
      CALL SVKO(VKO)
      CO1=ELECT*PI*8.D0
      CEXCH=-9.D0/R03*(3.D0/PI)**ONETHD*R0/2.D0
      CEXFE=-9.D0/R03*(6.D0/PI)**ONETHD*R0/2.D0
      WRITE(6,501) A,R0,ELECT,EMAG, IDCUB,NKPT,MAXK2, IDIM, MAXR2, NSTA, IGRLV
      & .ISORT
      PRINT 51

C      INDIPENDENT DIRECTIONS USED TO CALCULATE THE SPHERICALLY AVERAGED CHARGE
C      DENSITY ARE READ IN SUBROUTINE SEXCH
C
C      CALL SEXCH(AX,AY,AZ, IDIM)
C
C      PUNCH THE DENSITY AS INPUT TO THE SELF-CONSISTECE PROGRAM
C
34   FORMAT(5D15.8)
      DO 33 KR=1,96
      IF(IPUN.NE.0) WRITE(7,34) R(KR),W(KR),EXCH(KR),EXUP(KR),EXDN(KR)
      EXCH(KR)=EXCH(KR)**ONETHD
      EXUP(KR)=EXUP(KR)**ONETHD
      EXDN(KR)=EXDN(KR)**ONETHD
33   CONTINUE
      PRINT 51
51   FORMAT(1H1)
      IF(IGRLV.EQ.0) PRINT 55
55   FORMAT(3X,'K2',5X,'COULOUMB(K)',7X,'EXCHANGE(K)',7X,'EXCH UP(K)',7X,
      'EXCH DOWN(K)',/)
      IF(IGRLV.NE.0) PRINT 56
56   FORMAT(3X,'K2',5X,'COULOUMB(K)',7X,'EXCHANGE(K)',7X,'EXCH UP(K)',7X,
      'EXCH DOWN(K)',8X,'DEN UP(K)',8X,'DEN DOWN(K)',6X,'KX',3X,'KY',
      23X,'KZ',2X,'NO',/)

C      GENERATE INDEPENDENT RECIPROCAL LATTICE VECTORS.
C
      IF(IGRLV.NE.0) CALL GINDPK(KKX,KKY,KKZ,KSQ,NKPT, IDCUB,MAXK2,NB,1,
      & .ISORT)
      KINCM=1
      IF(IGRLV.EQ.0.AND.IDCUB.EQ.2) KINCM=2
      K2=1
      DO 999 NPT=1,NKPT,KINCM
      IF(IGRLV.EQ.0) GO TO 21
      KX=KKX(NPT)
      KY=KKY(NPT)

```

```

KZ=KKZ(NPT)
NNB=NB(NPT)
IF(K2.EQ.KSQ(NPT)) GO TO 99
K2=KSQ(NPT)
GO TO 22
21 K2=NPT-1
22 CONTINUE
RK2=DFLOAT(K2)
RS=RK2*AKR*AKR
RK=DSQRT(RS)
IF(K2.NE.0) GO TO 69
C
C      CALCULATE THE FOURIER COEFFICIENT V(K=0)
C
VKX=0.D0
VKUP=0.D0
VKDN=0.D0
DO 42 I=1,96
VKUP=VKUP+EXUP(I)*W(I)*R(I)**2
VKDN=VKDN+EXDN(I)*W(I)*R(I)**2
42 VKX=VKX+EXCH(I)*W(I)*R(I)**2
VEXCH=CEXCH*VKX
VEXUP=CEXFE*VKUP
VEXDN=CEXFE*VKDN
GEXCH=VEXCH
GEXUP=VEXUP
GEXDN=VEXDN
VCOUL=-4.D0*PI*VK0/3.D0/OMEGA
GCOUL=VCOUL
IF(IGRLV.EQ.0) GO TO 25
GUMUP=ELEUP/OMEGA
GUMDN=ELEDN/OMEGA
IF(NPT.LE.KPTPRT)WRITE(6,7)K2,GCOUL,GEXCH,GEXUP,GEXDN,GUMUP,GUMDN,
&KX,KY,KZ,NNB
WRITE(1) K2,GCOUL,GEXCH,GEXUP,GEXDN,GUMUP,GUMDN,KX,KY,KZ,NNB
GO TO 999
25 CONTINUE
IF(NPT.LE.KPTPRT)WRITE(6,7)K2,GCOUL,GEXCH,GEXUP,GEXDN
WRITE(1) GCOUL,GEXCH,GEXUP,GEXDN,K2
GO TO 999
C
C      CALCULATE THE FOURIER COEFFICIENTS OF THE EXCHANGE POTENTIAL BY 96 POINTS
C      GAUSSIAN INTEGRATION
C
69 CONTINUE
VKX=0.D0

```

```

VKUP=0.00
VKDN=0.00
41 DO 44 I=1,96
VKUP=VKUP+EXUP(I)*R(I)*W(I)*DSIN(RK*R(I))
VKDN=VKDN+EXDN(I)*R(I)*W(I)*DSIN(RK*R(I))
44 VKX=VKX+EXCH(I)*R(I)*W(I)*DSIN(RK*R(I))
VEXCH=CEXCH*VKX/RK
VEXUP=CEXF*VKUP/RK
VEXDN=CEXF*VKDN/RK
GEXCH=VEXCH
GEXUP=VEXUP
GEXDN=VEXDN
IF(IGRLV.NE.0) GO TO 101
C
C CALCULATE THE FOURIER COEFFICIENTS OF THE COULOMR POTENTIAL
C
FACT=8.00*PI/RS/OMEGA
SUM=-C01/RS
CALL COULOM(CHARGE,SUM,RS,FACT)
GCOUL=SUM
23 IF(NPT.LE.KPTPRT) WRITE(6,7) K2,GCOUL,GEXCH,GEXUP,GEXDN
WRITE(1) GCOUL,GEXCH,GEXUP,GEXDN,K2
GO TO 999
101 CONTINUE
C
C CALCULATE THE FOURIER COEFFICIENTS OF THE CHARGE DENSITIES FOR BOTH SPINS
C AS INPUT TO THE SELF-CONSISTENCY PROGRAM
C
FACT=1.00/OMEGA
SUMUP=0.00
SUMDN=0.00
CALL COULOM(CHARUP,SUMUP,RS,FACT)
CALL COULOM(CHARDN,SUMDN,RS,FACT)
GUMUP=SUMUP
GUMDN=SUMDN
GCOUL=(SUMUP+SUMDN)*8.0*PI/RS
99 CONTINUE
IF(NPT.LE.KPTPRT) WRITE(6,7) K2,GCOUL,GEXCH,GEXUP,GEXDN,GUMUP,GUMDN,
&KX,KY,KZ,NNB
WRITE(1) K2,GCOUL,GEXCH,GEXUP,GEXDN,GUMUP,GUMDN,KX,KY,KZ,NNB
999 CONTINUE
7 FORMAT(15.6E18.8,5I5)
WRITE(6,50) A,R0,ELECT,EMAG,1DCUB,NKPT,MAXK2,1DIM,MAXR2,NSTA,IGRLV
6,ISORT
50 FORMAT(1X,//,1X,'LATTICE CONST=',F10.5,3X,'R=',F10.5,3X,'ELECT NO='
1',F7.2,3X,'MAG NO=',F7.4,3X,'NO ATOMS/LATTICE=',15,//,1X,

```

```
2*K NO=*,18.3X,*K2 MAX=*,15.3X,*R NO=*,18.3X,*R2 MAX=*,15.3X,*ORBIT  
3ALS NO=*,15.3X,*GEN RLV=*,12.3X,*SORT=*,12)  
STOP  
END
```

```

C PROGRAM 2. THE COULOMB, EXCHANGE, KINETIC, OVERLAP, & MOMENTUM INTEGRALS
C ****
C CALCULATE INTEGRALS <G(I,R-A) | V(R) | G(J,R)>
C GAUSSIAN TYPE WAVE FUNCTIONS ARE USED
C A=ATTICE CONSTANT (IN A. U.)
C SCO IDCUB=1, BCC0 IDCUB=2, FCC0 IDCUB=4
C EXPCVG= CONVERGENT CRITERIAL DEXP(-EXPCVG)=0.00
C MXDBND=NO OF SYMMETRIES CONSIDERED =3 FOR S,P, AND D FUNCTIONS
C K2MAX=THE SQUARE OF THE MAXIMUM MAGNITUDE OF THE RECIPROCAL LATTICE
C VECTORS USED
C MAXA2=THE SQUARE OF THE MAXIMUM MAGNITUDE OF THE DIRECT LATTICE VECTORS
C NKPT=MAXIMUM NO OF RECIPROCAL LATTICE VECTORS.DIMENSION KXX(NKPT)
C KREAD=NO OF FOURIER COEFFICIENTS READ IN (1)
C DIMENSION FCS(NORDIM,NKDIM,NRDIM),FCS1(NORDIM,NKDIM)
C IOBNO(L)=ORBITAL NUMBER INCLUDED FOR L'TH SYMMETRY
C ALPHA=GAUSSIAN EXPONENTIAL PARAMETERS
C ****
C IMPLICIT REAL *8 (A-F,H,O-Z)
C INTEGER*2 KXX(8184),KKY(8184),KKZ(8184),NB(8184),IX(100),IY(100),
C IZ(100)
C DIMENSION SCoul(125),SEXCH(125),SEXUP(125),SEXDN(125),SOVLP(7,7,7)
C DIMENSION ALP(3,14),CN(3,14),CIJ(8,8)
C DIMENSION FCS1(7,100),FCS2(7,100),FCS3(7,100),FCS(7,100,11)
C DIMENSION SCO(4,14),PCO(3,11),DCO(1,5)
C DIMENSION OV(5,5,5),GC(27),GX(27),GU(27),GD(27)
C DIMENSION GWTSPD(3),IOBNO(3),KSQU(8184),ISQU(100)
C COMMON/GFUC/AKR,W,DELT,W04,DSTEP,MAXK,MAXR
C COMMON/LCS/GCOUL(4801),GEXCH(4801),GEXUP(4801),GEXDN(4801)
C DATA GWTSPD/'S','P','D'
1 FORMAT(A8,F10.5,F7.2,10I5)
READ(5,1) CRYSTL,A,EXPCVG,IDCUB,MXDBNO,MAXA2,IADIM,K2MAXM,
& NORDIM,NKDIM,NRDIM,NKPT,KREAD
PI=3.141592653589793D0
AKR=2.D0*PI/A
AKR2=AKR*AKR
AHALF=A/2.D0
IF (IDCUB.EQ.1) AHALF=A
OMEGA=A**3/DFLOAT(IDCUB)

C OFFINE GAUSSIAN EXPONENTS AND NORMALIZATION CONSTANTS
C
4 FORMAT(9I5)
READ(5,4) (IOBNO(I),I=1,MXDBNO)
DO 10 NOB=1,MXDBNO
ID=IOBNO(NOB)

```

```

DO 10 J=1,1D
READ(5,15) ALPHA
ALP(NOB,J)=ALPHA
A2=ALPHA*2.D0
AAA=(8.D0*ALPHA/P1)**0.25D0/DSQRT(4.D0*PI)
A0=-0.5D0
DO 11 L=1,NOB
A0=A0+1.D0
A1=DFLOAT(2*L-1)
11 AAA=AAA*DSQRT(A1*A2/A0)
CN(NOB,J)=AAA
10 WRITE(6,12) CRYSTL,J,GWTSPD(NOB),ALPHA,AAA
12 FORMAT(1X,A8,I4,A2,'EXPONENT=',F16.8,2X,'NORM=',E16.8)
15 FORMAT(F8.5,4D16.8)

C
C      DEFINE BINOMIAL EXPANSION COEFFICIENTS
C
CIJ(1,1)=1.D0
CIJ(2,1)=1.D0
CIJ(2,2)=1.D0
DO 70 I=3,8
CIJ(I,1)=1.D0
CIJ(I,I)=1.D0
IM1=I-1
DO 70 J=2,IM1
70 CIJ(I,J)=CIJ(IM1,J-1)+CIJ(IM1,J)

C
C      GENERATE INDEPENDENT DIRECT LATTICE VECTORS
C
IDC=1
IF(IDCUB.NE.1) IDC=8/IDCUB
CALL GINDPK(IX,IY,IZ,ISQU,IADIM,IDC,MAXA2,NB,0,1)
DO 60 I=1,IADIM
WRITE(6,4) I,IX(I),IY(I),IZ(I),ISQU(I)
60 CONTINUE

C
C      READ IN FOURIER COEFFICIENTS OF THE COULOMB AND EXCHANGE POTENTIAL
C
DO 23 J=1,KREAD
23 READ(1,END=22) GCOUL(J),GEXCH(J),GEXUP(J),GEXDN(J),K2
22 CONTINUE

C
C      GENERATE INDEPENDENT RECIPROCAL LATTICE VECTORS AND THE PERMUTATION NUMBER
C
CALL GINDPK(KKX,KKY,KKZ,KSQU,NKPT,IDCUB,K2MAXM,NB,1,1)
WRITE(6,2) A,EXPCVG, IDCUB, MXORNO, MAXA2, IADIM, K2MAXM, KREAD,

```

```

&NORDIM,NKDIM,NRDIM,NKPT,(GWTSPD(I),IOBNO(I),I=1,MXORNO)
2 FORMAT(1X,'LATTICE CONST=',F10.5,3X,'CONVERGENT EXPO=',
1F11.4,3X,'ATOMS/LATTICE=',I2,3X,'MAX N=',I5,3X,'MAX A2=',I5,3X,
2'A DIM=',I4,//,1X,'MAX K2=',I6,2X,'V(K) NO=',I6,2X,'DIM FCS(',
3I5,'.',I5,'.',I5,''))'.2X,'NKPT=',I8,//,1X,4(A2,' ORBITAL NO=',I4,
45X),//)

C CALCULATE INTEGERS BETWEEN ORBITALS OF ORDER NORDA AND NORDB WITH DIRECT
C LATTICE VECTORS FROM NRST TO NREND
C NORDA OR NORDB=1 FOR S, 2 FOR P, AND 3 FOR D
C

999 READ(5,4,END=1000) NORDA,NORDB,NRST,NREND
31 FORMAT(1X,//,1X,2A2,3X,'R=(',2I5,')',/,/)
WRITE(6,31) GWTSPD(NORDA),GWTSPD(NORDB),NRST,NREND
NORD=NORDA+NORDB-1
NORD2=NORD+2
NORD3=NORD**3
IAOBNO=IOBNO(NORDA)
IBOBNO=IOBNO(NORDB)
M2MAX=IBOBNO
DO 101 M1=1,IAOBNO
IF (IAOBNO.EQ.IBOPNO) M2MAX=M1
DO 101 M2=1,M2MAX
ALP1=ALP(NORDA,M1)
ALP2=ALP(NORD3,M2)
W=1.0/(ALP1+ALP2)
ALAMDA=ALP1*ALP2*W
DELT=DSQRT(PI*W)
U1=ALP1*W
U2=ALP2*W
DSTEP=U1*AHALF
W04=W/4.00
G=EXPCVG/(AKR2*W04)
IF(G.GT.K2MAXM) G=K2MAXM
MAXK2=G
MAXK=SQRT(G)+2.0
MAXR=DSQRT(EXPCVG/ALAMDA)/AHALF+2.0
MR=SQRT(FLOAT( ISQU(NREND)))+1
IF(MAXR.GT.MR) MAXR=MR
CALL GINTFC(FCS,NORD,NORDIM,NKDIM,NRDIM)
DO 100 NRC=NRST,NREND
AX=AHALF*X(NRC)
AY=AHALF*Y(NRC)
AZ=AHALF*Z(NRC)
RAB2=AX*AX+AY*AY+AZ*AZ
EXPA=ALAMDA*RAB2

```

```

IF(EXPA.GT.EXPCVG) GO TO 101
RAB=DSQRT(RAB2)
AZETA=DEXP(-EXPA)
ADX=-U2*AX
ADY=-U2*AY
ADZ=-U2*AZ
BDX=U1*AX
BDY=U1*AY
BDZ=U1*AZ
CONST=AZETA*CN(NORDA,M1)*CN(NORDB,M2)
DO 124 I=1,NORD3
SCOUL(I)=0.D0
SEXCH(I)=0.D0
SEXUP(I)=0.D0
SEXDN(I)=0.D0
124 CONTINUE
DO 121 I1=1,NORD2
DO 121 I2=1,NORD2
DO 121 I3=1,NORD2
SOVLP(I1,I2,I3)=0.D0
121 CONTINUE
NRX=IX(NRC)+1
NRY=IY(NRC)+1
NRZ=IZ(NRC)+1
DO 127 I=1,NORD2
DO 127 K=1,MAXK
FCS1(I,K)=FCS(I,K,NRX)
FCS2(I,K)=FCS(I,K,NRY)
FCS3(I,K)=FCS(I,K,NRZ)
127 CONTINUE
C
C C
      SUM OVER RECIPROCAL LATTICE VECTORS
      DO 105 K=1,NKPT
KS=KSQU(K)
GK2=(EXPCVG-EXPA)/(AKR2*WD4)
IF(KS.GT.MAXK2.OR.KS.GT.GK2) GO TO 106
K1=KKX(K)+1
K2=KKY(K)+1
K3=KKZ(K)+1
KK=KS+1
N=NB(K)
CO=DFLOAT(N)/6.D0
DO 111 I1=1,NORD
S1=FCS1(I1,K1)
S2=FCS1(I1,K2)

```

```

S3=FCS1(I1,K3)
DO 111 I2=1,NORD
S4=FCS2(I2,K1)
S5=FCS2(I2,K2)
S6=FCS2(I2,K3)
DO 111 I3=1,NORD
IT=I1+I2+I3-3
IF( IT.GE.NORD ) GO TO 111
S7=FCS3(I3,K1)
S8=FCS3(I3,K2)
S9=FCS3(I3,K3)
S=(S1*S5*S9+S4*S8*S3+S2*S6*S7+S3*S5*S7+S2*S4*S9+S1*S6*S3)*CONST*CC
IF( (IT/2)*2.NE.IT ) S=-S
IJ=(I1-1)*NORD+I2-1*NORD+I3
SCOL(IJ)=SCOL(IJ)+S*GCOL(KK)
SEXCH(IJ)=SEXCH(IJ)+S*GEXCH(KK)
SEXUP(IJ)=SEXUP(IJ)+S*GEUP(KK)
SEXDN(IJ)=SEXDN(IJ)+S*GEDN(KK)
111 CONTINUE
105 CONTINUE
106 CONTINUE
KTOL=K
DO 161 I1=1,NORD2
S1=FCS1(I1,1)
DO 161 I2=1,NORD2
S2=FCS2(I2,1)
DO 161 I3=1,NORD2
IT=I1+I2+I3-3
IF( IT.GE.NORD2 ) GO TO 161
S=S1*S2*FCS3(I3,1)*CONST
IF((IT/2)*2.NE.IT) S=-S
SOVLP(I1,I2,I3)=S
161 CONTINUE
C1=2*D0*ALP2
C2=C1*C1
NORDB2=NORDB+2
C
C
SUM OVER BINOMIAL EXPANSIONS IN E0(2.43)
C
C
IJB=0
DO 201 IA3=1,NORDA
DO 201 IA2=1,NORDA
DO 201 IA1=1,NORDA
IA1=IA1+IA2+IA3-2
IF( IA1.NE.NORDA ) GO TO 201
IBIJ=0

```

```

DO 202 IB3=1,NORDB2
DO 202 IB2=1,NORDB2
DO 202 IB1=1,NORDB2
IBT=IB1+IB2+IB3-2
IF( IBT.LT.NORDB2 .OR. IBT.GT.NORDB2 ) GO TO 202
TC=0.00
TX=0.00
TU=0.00
TD=0.00
TO=0.00
CA1=1.00
DO 211 NA1=1,IA1
JA1=IA1-NA1+1
CA2=CIJ(IA1,JA1)
DO 212 NA2=1,IA2
JA2=IA2-NA2+1
CA3=CIJ(IA2,JA2)
DO 213 NA3=1,IA3
JA3=IA3-NA3+1
CB1=CIJ(IA3,JA3)
DO 221 NB1=1,IB1
JB1=IB1-NB1+1
NAB1=JA1+JB1-1
CB2=CIJ(IB1,JB1)
DO 222 NB2=1,IB2
JB2=IB2-NB2+1
NAB2=JA2+JB2-1
CB3=CIJ(IB2,JB2)
DO 223 NB3=1,IB3
JB3=IB3-NB3+1
NAB3=JA3+JB3-1
CO=CIJ(IB3,JB3)*CA1*CA2*CA3*CB1*CB2*CB3
IF( IBT.NE.NORDB1 ) GO TO 225
NIJ=(NAB1-1)*NORD+NAB2-1)*NORD+NAB3
TC=TC+CO*SCOUL(NIJ)
TX=TX+CO*SEXCH(NIJ)
TU=TU+CO*SEXUP(NIJ)
TD=TD+CO*SEXDН(NIJ)
225 TO=TO+CO*SOVLP(NAB1,NAB2,NAB3)
CB3=CB3*BDZ
223 CONTINUE
CB2=CB2*BDY
222 CONTINUE
CB1=CB1*BDX
221 CONTINUE
CA3=CA3*ADZ

```

```

213 CONTINUE
CA2=CA2*ADY
212 CONTINUE
CA1=CA1*ADX
211 CONTINUE
IF(IBT.NE.NORDB) GO TO 226
IBIJ=IBIJ+1
GC(IBIJ)=TC
GX(IBIJ)=TX
GU(IBIJ)=TU
GD(IBIJ)=TD
226 OV(IB1,IB2,IB3)=TO
202 CONTINUE
C
C      CALCULATE KINETIC ENERGY AND MOMENTUM MATRICES Eqs. (2.49A) AND (2.50)
C
IBIJ=0
DO 301 IB3=1,NORDB
IB3M1=IB3-1
IB3M2=IB3-2
DO 301 IB2=1,NORDB
IB2M1=IB2-1
IB2M2=IB2-2
DO 301 IB1=1,NORDB
IBT=IB1+IB2+IB3-2
IF(IBT.NE.NORDB) GO TO 301
IB1M1=IB1-1
IB1M2=IB1-2
PX=-C1*OV(IB1+1,IB2,IB3)
PY=-C1*OV(IB1,IB2+1,IB3)
PZ=-C1*OV(IB1,IB2,IB3+1)
IF(IB1M1.GT.0) PX=PX+DFLOAT(IB1M1)*OV(IB1M1,IB2,IB3)
IF(IB2M1.GT.0) PY=PY+DFLOAT(IB2M1)*OV(IB1,IB2M1,IB3)
IF(IB3M1.GT.0) PZ=PZ+DFLOAT(IB3M1)*OV(IB1,IB2,IB3M1)
AK=C1*DFLOAT(2*IB1-1)*OV(IB1,IB2,IB3)-C2*OV(IB1+2,IB2,IB3)
1 +C1*DFLOAT(2*IB2-1)*OV(IB1,IB2,IB3)-C2*OV(IB1,IB2+2,IB3)
2 +C1*DFLOAT(2*IB3-1)*OV(IB1,IB2,IB3)-C2*OV(IB1,IB2,IB3+2)
IF(IB1M2.GT.0) AK=AK-DFLOAT(IB1M1*IB1M2)*OV(IB1M2,IB2,IB3)
IF(IB2M2.GT.0) AK=AK-DFLOAT(IB2M1*IB2M2)*OV(IB1,IB2M2,IB3)
IF(IB3M2.GT.0) AK=AK-DFLOAT(IB3M1*IB3M2)*OV(IB1,IB2,IB3M2)
IBIJ=IBIJ+1
GO=OV(IB1,IB2,IB3)
GK=AK
GPX=PX
GPY=PY
GPZ=PZ

```

```
      WRITE(2) NRC,M1,M2,IJAB,GC(IBIJ),GX(IRIJ),GU(IRIJ),GD(IBIJ),GK,GQ,
     & GPX,GPY,GPZ
      WRITE(6,300) M1,M2,NRC,KTOL,IJAB,IA1,IA3,IA3,IR1,IR2,IR3,GC(IRIJ),
     1 GX(IBIJ),GU(IRIJ),GD(IRIJ),GK,GQ,GPX,GPY,GPZ
301  CONTINUE
300  FORMAT(3I3,15.13,1X,3I1,3I1,9(1X,E11.5))
201  CONTINUE
100  CONTINUE
101  CONTINUE
      GO TO 999
1000 STOP
      END
```

```

C PROGRAM 3. THE INTEGRALS OF  $\int \cos(\alpha \cdot \mathbf{k} \cdot \mathbf{r})$  WHERE  $\alpha$  GENERATES THE STAR OF K
C
C **** CALCULATE  $\langle G(i, r-a) | \cos(k \cdot r) | G(j, r) \rangle$ 
C A=LATTICE CONSTANT (IN A. U.)
C SCO IDCUB=1, BCC0 IDCUB=2, FCC0 IDCUB=4
C EXPCVG= CONVERGENT CRITERIAL DFXP(-EXPCVG)=0.00
C MXOBNO=NO OF SYMMETRIES CONSIDERED =3 FOR S,P, AND D FUNCTIONS
C MAXK2=THE SQUARE OF THE MAXIMUM MAGNITUDE OF THE RECIPROCAL LATTICE
C VECTORS USED
C MAXA2=THE SQUARE OF THE MAXIMUM MAGNITUDE OF THE DIRECT LATTICE VECTORS
C NKPT=MAXIMUM NO OF RECIPROCAL LATTICE VECTORS.DIMENSION KKX(NKPT)
C DIMENSION FCS1(NRDIM,NRDIM) ECT.
C
C **** IMPLICIT REAL *8 (A-F,H,O-Z)
C INTEGER*2 NRC,M1,M2,IJAB
C INTEGER*2 IX(200),IY(200),IZ(200)
C INTEGER*2 KKX(300),KKY(300),KKZ(300),NB(300)
C DIMENSION SIJ(125)
C DIMENSION ALP(3,14),CN(3,14),CIJ(8,8)
C DIMENSION FCS1(7,20),FCS2(7,20),FCS3(7,20)
C DIMENSION SCO(4,14),PCO(3,11),DCO(1,5)
C DIMENSION GWTSPD(3),IOBNO(3)
C DIMENSION KSOUL(500),ISQU(200)
C COMMON/GSIJF/W,DELT,W04,DSTEP,MAXR
C DATA GWTSPD/'S','P','D'
1 FORMAT(A8,F10.5,F7.2,10I5)
READ(5,1) CRYSTL,A,EXPCVG, IDCUB, MXOBNO, MAXA2, IADIM,K2MAXM,
& NRDIM,NKPT, NRDIM
PI=3.141592653589793D0
AKR=2.D0*PI/A
AKR2=AKR*AKR
AHALF=A/2.D0
IF(IDCUB.EQ.1) AHALF=A
OMEGA=A**3/DFLOAT(IDCUB)
4 FORMAT(9I5)

C DEFINE GAUSSIAN EXPONENTS AND NORMALIZATION CONSTANTS
C
C READ(5,4) (IOBNO(I),I=1,MXOBNO)
DO 10 NOB=1,MXOBNO
ID=IOBNO(NOB)
DO 10 J=1, ID
READ(5,15) ALPHA
ALP(NOB,J)=ALPHA
A2=ALPHA*2.D0

```

```

      AAA=(8.00*ALPHA/PI)**0.2500/DSQRT(4.00*PI)
      A0=-0.500
      DO 11 L=1,NOB
      A0=A0+1.00
      A1=DFLOAT(2*L-1)
11   AAA=AAA*DSQRT(A1*A2/A0)
      CN(NOB,J)=AAA
10   WRITE(6,12) CRYSTL,J,GWTSPD(NOB),ALPHA,AAA
12   FORMAT(1X,A8,I4,A2,'EXPONFNT=',E16.8,2X,'NORM=',E16.8)
15   FORMAT(F8.5,4D16.8)

C
C      DEFINE BINOMIAL EXPANSION COEFFICIENTS
C
      CIJ(1,1)=1.00
      CIJ(2,1)=1.00
      CIJ(2,2)=1.00
      DO 70 I=3,8
      CIJ(I,1)=1.00
      CIJ(I,1)=1.00
      IM1=I-1
      DO 70 J=2,IM1
70   CIJ(I,J)=CIJ(IM1,J-1)+CIJ(IM1,J)

C
C      GENERATE INDEPENDENT DIRECT LATTICE VECTORS
C
      IDC=1
      IF(IDCUB.NE.1) IDC=8/IDCUB
      CALL GINDPK(IX,IY,IZ,ISQU,IADIM,IDC,MAXA2,NB,C,1)
      DO 60 I=1,IADIM
      WRITE(6,4) I,IX(I),IY(I),IZ(I),ISQU(I)
60   CONTINUE

C
C      GENERATE INDEPENDENT RECIPROCAL LATTICE VECTORS AND THE PERMUTATION NUMBER
C
      CALL GINDPK(KKX,KKY,KKZ,KSQU,NKPT,IDCUB,K2MAXM,NB,1,1)
      WRITE(6,2) A,EXPCVG,IDCUB,MX0BNO,MAXA2,IADIM,K2MAXM,
      &NRDIM,NRDIM,NKPT,(GWTSPD(I),IPRNO(I),I=1,MX0BNO)
2   FORMAT(1X,'LATTICE CONSTANT=',F10.5,3X,'EXP CONVERGENT=',F10.5,
      13X,'ATOMS/LATTICE=',I2,3X,'MAX N=',I5,3X,'MAX A2=',I5,3X,
      2'A DIM=',I4,//,1X,'MAX K2=',I6,2X,'DIM FCS',
      3I5,'',I5,''),2X,'NKPT=',I8,//,1X,4(A2,' ORBITAL NO=',I4,5X),//)

C
C      CALCULATE INTEGERS BETWEEN ORBITALS OF ORDER NORDA AND NORDB WITH DIRECT
C      LATTICE VECTORS FROM NRST TO NREND
C      NORDA OR NORDB=1 FOR S, 2 FOR P, AND 3 FOR D
C

```

```

999 READ(5,4,END=1000) NORDA,NORDB,NRST,NREND
31 FORMAT(1X,//,1X,2A2,3X,'R=(',2I5,')',//)
WRITE(6,31) GWTSPD(NORDA),GWTSPD(NORDB),NRST,NRFND
NORD=NORDA+NORDB-1
NORD2=NORD+2
IAOBNO=IOBNO(NORDA)
IBOBNO=IOBNO(NORDB)
M2MAX=IBOBNO
122 CONTINUE
DO 105 K=1,NKPT
KS=KSQ(K)
K1=KKX(K)
K2=KKY(K)
K3=KKZ(K)
RKX=AKR*DFLOAT(K1)
RKY=AKR*DFLOAT(K2)
RKZ=AKR*DFLOAT(K3)
RK2=AKR2*DFLOAT(KS)
KK=KS+1
N=NB(K)
COK=DFLOAT(N)/6.D0
DO 101 M1=1,IAOBNO
IF(IAOBNO.EQ.IBOBNO) M2MAX=M1
DO 101 M2=1,M2MAX
IF(M1.NE.IAOBNO.OR.M2.NE.M2MAX) GO TO 101
ALP1=ALP(NORDA,M1)
ALP2=ALP(NORDB,M2)
W=1.D0/(ALP1+ALP2)
W04=W/4.D0
EXPA=-RK2*W04
IF(DABS(EXPA).GT.EXPCVG) GO TO 101
ALAMDA=ALP1*ALP2*W
DELT=DSQRT(PI*W)
U1=ALP1*W
U2=ALP2*W
DSTEP=U1*AHALF
MAXR=DSQRT(EXPCVG/ALAMDA)/AHALF+2.0
MR=SQRT(DFLOAT(ISQ(NREND)))+1
IF(MAXR.GT.MR) MAXR=MR
CALL GSIJFC(FCS1,RKX,NORD,NORDIM,NRDIM)
CALL GSIJFC(FCS2,RKY,NORD,NORDIM,NRDIM)
CALL GSIJFC(FCS3,RKZ,NORD,NORDIM,NRDIM)
DO 100 NRC=NRST,NREND
AX=AHALF*I(X(NRC))
AY=AHALF*I(Y(NRC))
AZ=AHALF*I(Z(NRC))

```

```

RAB2=AX*AX+AY*AY+AZ*AZ
EXPA=ALAMDA*RAB2
IF(EXPA.GT.EXPCVG) GO TO 101
RAB=DSQRT(RAB2)
AZETA=DEXP(-EXPA)
ADX=-U2*AX
ADY=-U2*AY
ADZ=-U2*AZ
DX=U1*AX
DY=U1*AY
DZ=U1*AZ
CONST=AZETA*CN(NORDA,M1)*CN(NORDB,M2)*COK
NRX=IX(NRC)+1
NRY=IY(NRC)+1
NRZ=IZ(NRC)+1
DO 111 I1=1,NORD
S1=FCS1(I1,NRX)
S2=FCS2(I1,NRX)
S3=FCS3(I1,NRX)
DO 111 I2=1,NORD
S4=FCS1(I2,NRY)
S5=FCS2(I2,NRY)
S6=FCS3(I2,NRY)
DO 111 I3=1,NORD
IT=I1+I2+I3-3
IF(IT.GE.NORD) GO TO 111
S7=FCS1(I3,NRZ)
S8=FCS2(I3,NRZ)
S9=FCS3(I3,NRZ)
S=(S1*S5*S9+S4*S8*S3+S2*S6*S7+S3*S5*S7+S2*S4*S9+S1*S6*S8)*CONST
IF((IT/2)*2.NE.IT) S=-S
IJ=((I1-1)*NORD+I2-1)*NORD+I3
SIJ(IJ)=S
111 CONTNUF
C
C      SUM OVER BINOMIAL EXPANSIONS IN FQ(2.43)
C
IJAB=0.00
DO 201 IA3=1,NORDA
DO 201 IA2=1,NORDA
DO 201 IA1=1,NORDA
IAT=IA1+IA2+IA3-2
IF(IAT.NE.NORDA) GO TO 201
DO 202 IB3=1,NORDB
DO 202 IB2=1,NORDB
DO 202 IB1=1,NORDB

```

```

IBT=IB1+IB2+IB3-2
IF( IBT.NE.NORDB) GO TO 202
TIJ=0.D0
CA1=1.D0
DO 211 NA1=1,IA1
JA1=IA1-NA1+1
CA2=CIJ(IA1,JA1)
DO 212 NA2=1,IA2
JA2=IA2-NA2+1
CA3=CIJ(IA2,JA2)
DO 213 NA3=1,IA3
JA3=IA3-NA3+1
CR1=CIJ(IA3,JA3)
DO 221 NB1=1,IB1
JB1=IB1-NB1+1
NAB1=JA1+JB1-1
CB2=CIJ(IB1,JB1)
DO 222 NB2=1,IB2
JB2=IB2-NB2+1
NAB2=JA2+JB2-1
CB3=CIJ(IB2,JB2)
DO 223 NB3=1,IB3
JB3=IB3-NB3+1
NAB3=JA3+JB3-1
CO=CIJ(IB3,JB3)*CA1*CA2*CA3*CR1*CB2*CB3
NIJ=((NAB1-1)*NORD+NAB2-1)*NORD+NAB3
TIJ=TIJ+CO*SIJ(NIJ)
CB3=CB3*BDZ
223 CONTINUE
CB2=CB2*BDY
222 CONTINUE
CB1=CB1*BDX
221 CONTINUE
CA3=CA3*ADZ
213 CONTINUE
CA2=CA2*ADY
212 CONTINUE
CA1=CA1*ADX
211 CONTINUE
IJAB=IJAB+1
GIJ=TIJ
WRITE(1) NRC,M1,M2,IJAB,GIJ
IF(K.EQ.1)
*WRITE(6,300) NRC,M1,M2,IJAB,IA1,IA2,IA3,IB1,IB2,IB3,TIJ
202 CONTINUE
300 FORMAT(1X,1S,3I4,3X,3I1,'-',3I1,5X,F16.8)

```

```
201 CONTINUE  
100 CONTINUE  
101 CONTINUE  
105 CONTINUE  
      GO TO 999  
1000 STOP  
END
```

```

C PROGRAM 4. SUM OVER DIRECT LATTICE VECTORS FOR H, S, AND P MATRICES
C ****
C PERFORM THE SUM EXP(I K.R) H(R) OVER R
C H IS STORED FOR INDEPENDENT R ONLY. THE GROUP OPERATIONS WHICH GENERATE
C THE STAR OF R IS DONE IN THIS PROGRAM
C A=LATTICE CONSTANT
C ALPHA=THE EXCHANGE PARAMETER
C MXOBNO=NO OF SYMMETRIES CONSIDERED =3 FOR S,P,AND D FUNCTIONS
C MAXA2=THE SQUARE OF THE MAXIMUM MAGNITUDE OF THE DIRECT LATTICE VECTORS
C IBZDIV=DIVISION BETWEEN K=(0,0,0) AND K=(1.0,0)*2*PI/A
C SC IDCUB=1, BCC IDCUB=2, FCC IDCUB=4
C DIMENSION IX(IADIM),SINE(NRDIM,IBZDIV+1),COSN(NRDIM,IBZDIV+1)
C IE0BNO=GTO NUMBER E=S, P, D
C IEATOM=ATOMIC BASIS NO. IEATOM=0 IF INDEPENDENT GTO ARE USED
C IAEE=NO OF DIRECT LATTICE VECTORS USED FOR E-E INTEGRALS
C NKIND=NO OF DIFFERENT TYPE OF MATRICES STORED
C NTOL=NO OF TYPE OF MATRICES TO BE CALCULATED
C NCHO(I) DETERMINES THE TYPE OF MATRICES TO BE CALCULATED
C IF(NDIAG.NE.0.AND.NCHO(1).GT.NKIND) HAMILTONIAN IS DIAGONALIZED
C IPRIT=NO OF K POINTS TO BE PRINTED
C THE WAVE VECTORS ARE ARRANGED IN THE FOLLOWING ORDER OF SYMMETRY
C (XY(I),I=1,LDMAX),(YZ(I),I=1,LDMAX),(ZX(I),I=1,LDMAX),(X2(I),I=1,LDMAX),
C (Z2(I),I=1,LDMAX),(S(I),I=1,LSMAX),(PX(I),PY(I),PZ(I),I=1,LPMAX)
C ****
C IMPLICIT REAL *8 (A-F,H,O-Z)
C REAL*4 SSA,SSB,PSA,PSB,SDA,SDB,PPA,PPB,PDA,PDB,DDA,DDB
C INTEGER*2 IX(100),IY(100),IZ(100),INB(100),KBX(89),KBY(89),KBZ(89)
C INTEGER*2 NPUMPS(3,6),NPUMSD(6,6),NPUMPP(9,6),NPUMPD(18,6),
&NPUMDD(36,6),NTYPS(3),NTYSD(6),NTYPP(9),NTYPD(18),NTYDD(36)
C ,NDUM(3,3,3,3,3)
C DIMENSION SICO(6,8),SINE(12,5),COSN(12,5),H(741),S(741),WT(89)
C DIMENSION X(38,38),GE(741),GX(38,38),GS(741)
C DIMENSION DASIGN(5,6),CS(4,14),CP(3,11),CD(5,5),GIDEN(12)
C DIMENSION ISQU(100)
C DIMENSION ALS(14),ALP(11),ALD(5),COS(14),COP(14),COD(14)
C DIMENSION GTSPD(3)
C COMMON/GTO/CRYSTL,PI,ISATOM,IPATOM,IDATOM
C COMMON/LCA/SSA(40,10),PSA(40,36),SDA(40,120),PPA(40,54),PDA(30,270
C ),DDA(6,540)
C COMMON/LCB/SSB(1,1),PSB(1,1),SDR(1,1),PPB(1,1),PDB(1,1),DDB(1,1)
C COMMON/LCB/SSB(40,10),PSB(40,36),SDB(40,120),PPB(40,54),PDB(30,270
C ),DDB(6,540)
C COMMON/OBNO/ALPHA,NKIND,NTOL,NCHO(5),NSYMP
C DATA GIDEN/'COUL','EXCH','EXUP','EXDN','KINE','OVLP','PX','PY',
&'PZ','H PA','H UP','H DN'/

```

```

1 DATA GWTSPD/'S','P','D'/
1 FORMAT(A8,F12.5,F10.8,10I5)
 READ(5,1) CRYSTL,A,ALPHA, IDCUB,MXOBNO,MAXA2,IADIM,IBZDIV,NRDIM
 PI=3.141592653589793D0
 AKRBZ=2.D0*PI/(A*DFLOAT(IBZDIV))
 KBZPT=IBZDIV+1
 AHALF=A/2.D0
 IF(IDCUB.EQ.1) AHALF=A
 OMEGA=A**3/DFLOAT(IDCUB)
4 FORMAT(16I5)
 READ(5,4) IASS,IAPS,IASD,IAPP,IAPD,IADD
 READ(5,4) NKIND,NTOL,(NCHO(J),J=1,NTOL)
 WRITE(6,3) ALPHA,NKIND,(GIDEN(NCHO(I)),I=1,NTOL)
3 FORMAT(/,IX,'EXCH PARAMETER=',F10.6,10X,'NO READ=',I5,5X,S(3X,A4))
 NSYMP=0
 IF(NCHO(1).GT.NKIND-3.AND.NCHO(1).LT.NKIND) NSYMP=1
C
C READ IN THE EXPANSION COEFFICIENTS IN THE ATOMIC BASIS FUNCTIONS
C
 READ(5,4) ISOBNO,ISATOM,IPORNO,IPATOM,IDOBNO,IDATOM
 LSMAX=ISOBNO
 LDMAX=IDOBNO
 LPMAX=IPORNO
 IF( ISATOM.NE.0) LSMAX=ISATOM
 IF( IDATOM.NE.0) LDMAX=IDATOM
 IF( IPATOM.NE.0) LPMAX=IPATOM
 CALL RDGTO(ALS,ALP,ALD,COS,COP,COD,CS,CP,CD,ISOBNO,LSMAX,IPORNO,
 &LPMAX,DOBNO,LDMAX,0)
 ISSDIM=LSMAX*(LSMAX+1)/2
 IPPDIM=9*LPMAX*(LPMAX+1)/2
 IDDDIM=36*LDMAX*(LDMAX+1)/2
 IPSDIM=3*LSMAX*LPMAX
 ISDDIM=6*LSMAX*LDMAX
 IPDDIM=18*LPMAX*LDMAX
 LDST=1
 LOEND=LDMAX*5
 LSST=LDEND+1
 LSEND=LDEND+LSMAX
 LPST=LSFND+1
 LPEND=LSEND+LPMAX*3
 NB=LPEND
 NBTRI=NB*(NB+1)/2
 WRITE(6,5) IASS,ISSDIM,IAPS,IPSDIM,IASD,ISDDIM,IAPP,IPPDIM,
 1IAPD,IPDDIM,IADD,IDDDIM
5 FORMAT(/,IX,'SS=(',2I5,',')',2X,'PS=(',2I5,',')',2X,'SD=(',2I5,',')',2X,
 1'PP=(',2I5,',')',2X,'PD=(',2I5,',')',2X,'DD=(',2I5,',')',/)


```

```

IDC=1
IF(IDCUB.NE.1) IDC=B/IDCUB

C
C   GENERATE INDEPENDENT DIRECT LATTICE VECTORS
C
      CALL GINDPK(IX,IY,IZ,ISQU,IADIM, IDC,MAXA2,INB,1,1)
5310 FORMAT(6I5)
      DO 60 I=1,IADIM
      WRITE(6,5310) I,IX(I),IY(I),IZ(I),INB(I)
      60 CONTINUE

C
C   GENERATE EQUALLY SPACED POINTS IN THE 1/48TH OF THE INDEPENDENT B. Z.
C
      CALL GBZPT(KBX,KBY,KBZ,WT,NKPT, IDCUB,KBZPT,SUMW)
      WRITE(6,2) CRYSTL,A, IDCUB,MXOBNO,MAXA2,IADIM,NKPT,NRDIM,KBZPT,
1 GWTSPD(1),ISOBNO,ISATOM,GWTSPD(2),IPOBNO,IPATOM,GWTSPD(3),IDOBNO,
2 IDATOM
2 FORMAT(1X,A8,2X,'LATTICE CONST=',F10.5,3X,'ATOMS/LATTICE=',15.3X,
1 'MAX N=',15.3X,'MAX A2=',15.3X,'A DIM=',14.//,1X,'NKPT=',15.3X,
2 'DIMENSION SINE( ',215,')',3X,//,1X,3(A2,
3 'ORBITAL NO=',14.2X,'ATOMIC NO=',14.2X)//)

C
C   DEFINE THE EXPANSION COEFFICIENTS FOR THE D FUNCTION WITH CUBIC SYMETRY
C
      DO 90 I=1,5
      DO 90 J=1,6
90 DASIGN(I,J)=0.0D0
      DASIGN(1,2)=1.0D0
      DASIGN(2,5)=1.0D0
      DASIGN(3,4)=1.0D0
      DASIGN(4,1)=0.5D0
      DASIGN(4,3)=-0.5D0
      C3=0.5D0/DSQRT(3.0D0)
      DASIGN(5,1)=-C3
      DASIGN(5,3)=-C3
      DASIGN(5,6)=2.0D0*C3
      MAXR=SQRT(FLOAT(MAXA2))+2
      RD=0.0D0
      DO 70 NR=1,MAXR
      RKHZ=0.0D0
      DO 71 KB=1,KBZPT
      RK=RK+RKHZ
      SINE(NR,KB)=DSIN(RK)
      COSN(NR,KB)=DCOS(RK)
71 RKBZ=RKBZ+AKRBZ
      RD=RD+AHALF

```

70 CONTINUE

C
C DEFINE THE GROUP OPERATIONS THAT GENERATE THE STAR OF R
C FINDS THE TERM IN THE EXPANSION OF EXP(I K.R) H(R) WHICH IS AN EVEN
C FUNCTION OF RX, RY, AND RZ.
C
CALL GNOPUM(NPUMPS,NTYPS,NDUM,MXORNO,3,2,1,NSYMP)
CALL GNOPUM(NPUMSD,NTYSD,NDUM,MXOBNO,6,1,3,NSYMP)
CALL GNOPUM(NPUMPP,NTYPP,NDUM,MXOBNO,9,2,2,NSYMP)
CALL GNOPUM(NPUMPD,NTYPD,NDUM,MXOBNO,18,2,3,NSYMP)
CALL GNOPUM(NPUMDD,NTYDD,NDUM,MXOBNO,36,3,3,NSYMP)
C
C SUBROUTINE (READ) READS IN THE INTEGRALS GENERATED IN PROGRAM 2 OR 3
C
CALL READ(SSA,PSA,SDA,PPA,PDA,DDA,SSB,PSB,SDB,PPB,PDB,DDB,
1IASS,IAPS,IASD,IAPP,IAPD,IADD,ISSDIM,IPSDIM,ISDDIM,IPPDIM,
2IPDDIM,IDDDIM,CS,CP,CD,LSMAX,ISOBNO,LPMAX,IPOBNO,LDMAX,IDOORNO)
999 READ(5,4,END=10000) KPTST,KPTEND,NDIAG,IPPRINT,IPUNCH
PRINT 915
DO 1000 KPT=KPTST,KPTEND
DO 80 I=1,NBTRI
H(I)=0.00
80 S(I)=0.00
KX=KBX(KPT)
KY=KBY(KPT)
KZ=KBZ(KPT)
K1=KX+1
K2=KY+1
K3=KZ+1
DO 900 NRC=1,IADIM
I1=IX(NRC)+1
I2=IY(NRC)+1
I3=IZ(NRC)+1
CALL GSICO(SICO,SINF,COSN,NRDIM,KBZPT,K1,K2,K3,I1,I2,I3)
N=INB(NRC)
CONST=DFLOAT(N)/6.00
C
C S-S
C
IF(NRC.GT.IASS) GO TO 150
SCSS=(SICO(1,1)+SICO(2,1)+SICO(3,1)+SICO(4,1)+SICO(5,1)+SICO(6,1))
&*CONST
M1=0
DO 100 M1=LSST,LSEND
DO 100 M2=LSST,M1
M1=M1+1

```

I J=M1*(M1-1)/2+M2
H(IJ)=H(IJ)+SSA(NRC,M1)*SCSS
IF(NTOL.GT.1) S(IJ)=S(IJ)+SSB(NRC,M1)*SCSS
100 CONTINUE
150 CONTINUE
C
C P-S
C
IF(NRC.GT.IAPS) GO TO 250
M1=0
DO 200 M1=1,LPMAX
IP=(M1-1)*3+LSEND
DO 200 M2=LSST,LSEND
M1=M1+1
IL=(M1-1)*3
DO 210 NM=1,3
MP=IP+NM
IJ=MP*(MP-1)/2+M2
NT=NTYPS(NM)
DO 211 L=1,6
NL=IL+NPUmps(NM,L)
H(IJ)=H(IJ)+PSA(NRC,NL)*SICO(L,NT)*CONST
IF(NTOL.GT.1) S(IJ)=S(IJ)+PSB(NRC,NL)*SICO(L,NT)*CONST
211 CONTINUE
210 CONTINUE
200 CONTINUE
250 CONTINUE
C
C S-D
C
IF(NRC.GT.IASD) GO TO 350
M1=0
DO 300 M1=LSST,LSEND
DO 300 M2=1,LDMAX
II=M1*(M1-1)/2+M2
M1=M1+1
IL=(M1-1)*6
DO 310 NM=1,6
NT=NTYSD(NM)
CA=0.D0
CB=0.D0
DO 311 L=1,6
NL=IL+NPUmsd(NM,L)
CA=CA+SDA(NRC,NL)*SICO(L,NT)*CONST
IF(NTOL.GT.1) CB=CB+SDB(NRC,NL)*SICO(L,NT)*CONST
311 CONTINUE

```

```

DO 312 I=1,5
IJ=II+(I-1)*LDMAX
H(IJ)=H(IJ)+CA*DASIGN(I,NM)
IF(NTOL.GT.1) S(IJ)=S(IJ)+CB*DASIGN(I,NM)
312 CONTINUE
310 CONTINUE
300 CONTINUE
350 CONTINUE

C
C      P-D
C

IF(NRC.GT.IAPP) GO TO 450
MI=0
DO 400 MI=1,LPMAX
IP1=(MI-1)*3+LSEND
DO 400 M2=1,MI
IP2=(M2-1)*3+LSEND
MI=MI+1
IL=(MI-1)*9
NM=0
DO 410 N1=1,3
MPI=IP1+N1
DO 410 N2=1,3
MP2=IP2+N2
NM=NM+1
IF(MP1.LT.MP2) GO TO 410
IJ=MP1*(MP1-1)/2+MP2
NT=NTYPP(NM)
DO 411 L=1,6
NL=IL+NPUMPP(NM,L)
H(IJ)=H(IJ)+PPA(NRC,NL)*SICO(L,NT)*CONST
IF(NTOL.GT.1) S(IJ)=S(IJ)+PPB(NRC,NL)*SICO(L,NT)*CONST
411 CONTINUE
410 CONTINUE
400 CONTINUE
450 CONTINUE

C
C      P-D
C

IF(NRC.GT.IAPD) GO TO 550
MI=0
DO 500 MI=1,LPMAX
IP=(MI-1)*3+LSEND
DO 500 M2=1,LDMAX
MI=MI+1
IL=(MI-1)*18

```

```

NM=0
DO 510 N1=1,3
NP=IP+N1
II=NP*(NP-1)/2+M2
DO 510 N2=1,6
NM=NM+1
NT=NTYPD(NM)
CA=0.D0
CB=0.D0
DO 511 L=1,6
NL=IL+NPUMPD(NM,L)
CA=CA+PDA(NRC,NL)*SICO(L,NT)*CONST
IF(NTOL.GT.1) CB=CB+PDB(NRC,NL)*SICO(L,NT)*CONST
511 CONTINUE
DO 512 I=1,5
IJ=II+(I-1)*LDMAX
H(IJ)=H(IJ)+CA*DASIGN(I,N2)
IF(NTOL.GT.1) S(IJ)=S(IJ)+CB*DASIGN(I,N2)
512 CONTINUE
510 CONTINUE
500 CONTINUE
550 CONTINUE
C
C      D-D
C
IF(NRC.GT.IADD) GO TO 650
DO 600 M1=1,LDMAX
DO 600 M2=1,LDMAX
IF(M1.GE.M2) MI=M1*(M1-1)/2+M2
IF(M1.LT.M2) MI=M2*(M2-1)/2+M1
IL=(MI-1)*36
DO 610 NI=1,6
DO 610 N2=1,6
IF(M1.GE.M2) NM=(NI-1)*6+N2
IF(M1.LT.M2) NM=(N2-1)*6+NI
NT=NTYDD(NM)
CA=0.D0
CB=0.D0
DO 611 L=1,6
NL=IL+NPUMDD(NM,L)
CA=CA+DDA(NRC,NL)*SICO(L,NT)*CONST
IF(NTOL.GT.1) CB=CB+DDB(NRC,NL)*SICO(L,NT)*CONST
611 CONTINUE
613 CONTINUE
DO 612 II=1,5
NDI=M1+(II-1)*LDMAX

```

```

DO 612 I2=1,5
ND2=M2*(I2-1)*LDMAX
IF(ND1.LT.ND2) GO TO 612
IJ=ND1*(ND1-1)/2+ND2
H(IJ)=H(IJ)+CA*DASIGN(I1,N1)*DASIGN(I2,N2)
IF(NTOL.GT.1) S(IJ)=S(IJ)+CB*DASIGN(I1,N1)*DASIGN(I2,N2)
612 CONTINUE
610 CONTINUE
600 CONTINUE
650 CONTINUE
900 CONTINUE
GT=WT(KPT)
820 FORMAT(20X,I5,'=(',2([4,'.'),[4,'.')',5X,'WT=',F10.5)
WRITE(6,820) KPT,KX,KY,KZ,GT
NOPT=0
810 CONTINUE
NOPT=NOPT+1
DO 950 I=1,NBTRI
GE(I)=H(I)
IF(NTOL.GT.1) GS(I)=S(I)
950 CONTINUE
WRITE(2) KX,KY,KZ,GT,GF
IF(NTOL.GT.1) WRITE(3) KX,KY,KZ,GT,GS
IJ=0
DO 800 I=1,NB
DO 800 J=1,I
IJ=IJ+1
IF(NOPT.EQ.2) GO TO 801
X(I,J)=H(IJ)
X(J,I)=H(IJ)
GO TO 800
801 CONTINUE
X(I,J)=S(IJ)
X(J,I)=S(IJ)
800 CONTINUE
IF(NDIAG.EQ.0) GO TO 1001
IF(NCHO(NOPT).LE.NKIND) GO TO 1002

```

C CALCULATE THE ENERGY EIGENVALUES (GE) AND EIGENVECTORS (GX)

C H X = S X E

C THE OVERLAP MATRIX (S) IS EXPRESSED AS THE PRODUCT OF A UPPER TRIANGULAR
C MATRIX (R) AND ITS TRANSPOSE (R**T)

C H' X' = X' E , WHERE H'=((R**T)**-1) H (R**-1) AND X'= R X

C SUBROUTINES DMTDS AND DMFSO ARE IN IBM SCIENTIFIC SUBROUTINE PACKAGE.
C DIGEN IS THE DOUBLE PRECISION VERSION OF SUBROUTINE EIGEN IN IBM S.S.P.

```

A=10.**(-9)
CALL DMFSD(S,M,A,IE1)
CALL DMTDS(X,NB,NB,S,-1,IF2)
CALL DMTDS(X,NB,NB,S,2,IF3)
DO 7150 I=1,NB
DO 7150 J=1,I
IJ=I*(I-1)/2+J
7150 H(IJ)=X(I,J)
CALL DIGEN(H,X,NB,0)
CALL DMTDS(X,NB,NB,S,1,IF4)
844 FORMAT(1H0,2X,'IER=',4I5)
IF(IF1.NE.0.OR.IF2.NE.0.OR.IF3.NE.0.OR.IF4.NE.0) WRITE(6,844) IE1,
&IE2,IE3,IE4
DO 3561 I=1,NB
IJ=I*(I-1)/2+I
GE(I)=H(IJ)
DO 3561 J=1,NB
3561 GX(I,J)=X(I,J)
918 FORMAT(1X,//,1X,10F13.5,//)
916 FORMAT(1I0,9I13)
WRITE(20) KX,KY,KZ,GT,(GF(I),(GX(J,I),J=1,NB),I=1,NB)
235 FORMAT(1X,10F13.6)
WRITE(6,235) (GE(J),J=1,NB)
PRINT 811
152 FORMAT(6F11.7,3I3,15)
NSPIN=NCHO(1)-NKIND
IF(IPUNCH.NE.0) WRITE(7,152) (GE(I),I=NBS1,NBFND),KX,KY,KZ,NSPIN
GO TO 1001
1002 CONTINUE
CALL DIGEN(H,X,NB,0)
DO 2561 I=1,NB
IJ=I*(I-1)/2+I
GE(I)=H(IJ)
DO 2561 J=1,NB
2561 GX(I,J)=X(I,J)
1001 IF(KPT.GT.(PRINT)) GO TO 1000
PRINT 811
811 FORMAT(1H0)
I2=0
912 CONTINUE
I1=I2+1
I2=I2+10
IF(I2.GT.NB) I2=NB
WRITE(6,916) (I,I=I1,I2)
PRINT 811
IF(NDIAG.NE.0) WRITE(6,918) (GE(I),I=I1,I2)

```

```
PRINT 811
DO 913 I=1,NB
913 WRITE(6,914) (X(I,J),J=I1,I2)
PRINT 915
IF(I2.LT.NB) GO TO 912
IF(NOPT.LE.NTOL.AND.NDIAG.EQ.0) GO TO 810
914 FORMAT(1X,10F13.5)
915 FORMAT(1H1)
1000 CONTINUE
GO TO 999
10000 CONTINUE
STOP
END
```

```

C PROGRAM 5. BLOCH BASIS FUNCTION ALONG THREE PRINCIPLE DIRECTIONS.
C ****
C ACONST=LATTICE CONSTANT (IN A. U.)
C EXPCVG=CONVERGENT CRITERIAL EXP(-EXPCVG)=0.0
C IDCUB=NUMBER OF ATOMS PER LATTICE
C MAXA2=THE SQUARE OF THE MAXIMUM MAGNITUDE OF THE DIRECT LATTICE VECTORS
C DIMENSION IAX(IADIM) ECT.
C IBZDIV=DIVISION BETWEFN K=(0,0,0) AND K=(1,0,0)*2*PI/A
C ISOBNO=GTO NUMBER E=S, P, D
C ISATOM=ATOMIC BASIS NO. ISATOM=0 IF INDEPENDENT GTO ARE USED
C NPGaus=NO OF POINTS USED IN THE GAUSSIAN INTEGRATION OVER THE WIGNER-SEITZ
C SPHERE (CALCULATING THE FOURIER COEFFICIENTS OF THE EXCHANGE POTENTIAL)
C ****
C IMPLICIT REAL *8 (A-F,H,O-Z)
C COMPLEX*16 BASF(38),SC,COSC
C COMPLEX*8 GRASF(38)
C INTEGER*2 IAX(500),IAY(500),IAZ(500),ISQU(500)
C INTEGER*2 KBX(89),KBY(89),KBZ(89)
C DIMENSION WT(89)
C DIMENSION R(96),W(96),Y(100)
C DIMENSION AX(500),AY(500),AZ(500),PRMX(48),PRMY(48),PRMZ(48)
C DIMENSION ALS(14),ALP(11),ALD(5),COS(14),COP(11),COD(5),CS(4,14),
C &CP(3,11),CD(5,5)
C COMMON/GTO/CRYSTL,PI,ISATOM,IPATOM,IDATOM
C PI=3.141592653589793
51 FORMAT(2X,A8,2F10.5,10I5)
READ(5,51) CRYSTL,ACONST,EXPCVG,IDCUB,IBZDIV,IADIM,MAXA2,NPGaus
OMEGA=ACONST**3/DFLOAT(IDCUB)
DIV=DFLOAT(IBZDIV)
WGSZRD=(0.75D0*OMEGA/PI)**0.3333333D0
C
C DEFINE GAUSSIAN EXPONENTS AND EXPANSION COEFFICIENTS
C
4 FORMAT(8I5)
READ(5,4) ISOBNO,ISATOM,IPOBNO,IPATOM,IDOBNO,IDATOM
LSMAX=ISOBNO
LDMAX=IDOBNO
LPMAX=IPOBNO
IF( ISATOM.NE.0) LSMAX=ISATOM
IF( IDATOM.NE.0) LDMAX=IDATOM
IF( IPATOM.NE.0) LPMAX=IPATOM
CALL RGTO(ALS,ALP,ALD,COS,COP,COD,CS,CP,CD,ISOBNO,LSMAX,IPOBNO,
&LPMAX,DOBNO,LDMAX,1)
LDST=1
LDEND=LDMAX*5

```

```

LSST=LDEND+1
LSEND=LDEND+LSMAX
LPST=LSEND+1
LPEND=LSEND+LPMAX*3
PRINT 59
59 FORMAT(1H1)
C
C      GENERATE EQUALLY SPACED POINTS IN THE 1/48TH OF THE INDEPENDENT R. Z.
C
IRZPT=IBZDIV+1
CALL GBZPT(KBX,KBY,KBZ,WT,NKPT, IDCUB,IBZPT,SUMW)
IDC=8/IDCUB
IF(IDCUB.EQ.1) IDC=1
CALL GPERMK(IAX,IAY,IAZ,ISQU,IADIM, IDC,MAXA2,1)
IF(IDCUB.EQ.1) AHALF=ACONST
IF(IDCUB.NE.1) AHALF=ACONST/2.0D
DO 70 I=1,IADIM
AX(I)=AHALF*IAX(I)
AY(I)=AHALF*IAY(I)
AZ(I)=AHALF*IAZ(I)
70 CONTINUE
WRITE(6,52) ACONST, IDCUB, IRZDIV, IADIM, MAXA2, NPGAUS, LSMAX,
& ISOBNO, LPMAX, IPOBNO, LDMAX, IDORNO, EXPCVG
52 FORMAT(1X,'LATTICE CONST=',F10.5,2X,'ATOMS/LATTICE=',
1I5,2X,'B.Z. DIV=',I5,2X,'R NO=',I7,2X,'MAX R**2=',I5,
22X,'GAUS NO=',I5,//,1X,'S=(',2I5,')',2X,'P=(',2I5,')',2X,'D=(',2I5
3,')',5X,'EXP MAX=',F10.2,//)
C
C      DEFINE R AND WEIGHT FACTOR FOR GAUSSIAN INTEGRATION OVER THE WIGNER-SF ITZ
C      SPHERE
C
CALL GWTGAS(NPGAUS,Y,R,W)
DO 54 I=1,NPGAUS
54 R(I)=WGSZRO*(R(I)+1.0D)/2.0D
C
C      READ IN PERMUTED VECTORS ALONG THREE PRINCIPLE DIRECTIONS
C      NPTOL=PERMUTATION NUMBER FOR EACH DIRECTION
C
90 FORMAT(3F10.4)
I=0
91 READ(5,4,END=999) NPTOL
DO 92 J=1,NPTOL
I=I+1
READ(5,90) PRMX(I),PRMY(I),PRMZ(I)
RNORM=DSORT(PRMX(I)**2+PRMY(I)**2+PRMZ(I)**2)
PRMX(I)=PRMX(I)/RNORM

```

```

PRMY(I)=PRMY(I)/RNORM
PRMZ(I)=PRMZ(I)/RNORM
92 CONTINUE
GO TO 91
999 CONTINUE
ITOL=1
62 FORMAT(1S,3F10.1)
CK=2.00*PI/ACONST/DIV
DO 100 KPT=1,NKPT
RKX=CK*KBX(KPT)
RKY=CK*KBY(KPT)
RKZ=CK*KBZ(KPT)
DO 200 IQ=1,NPGAUS
DO 300 NPNO=1,ITOL
RX=R(IQ)*PRMX(NPNO)
RY=R(IQ)*PRMY(NPNO)
RZ=R(IQ)*PRMZ(NPNO)
DO 510 I=1,LPEND
510 BASF(I)=(0.00,0.00)

C
C      SUM OVER PERMUTED DIRECT LATTICE VECTORS
C
DO 500 NRC=1,NRTOL
PX=RX+AX(NRC)
PY=RY+AY(NRC)
PZ=RZ+AZ(NRC)
PP=PX*PX+PY*PY+PZ*PZ
RK=RKX*AX(NRC)+RKY*AY(NRC)+RKZ*AZ(NRC)
SINE=DSIN(RK)
COSINE=DCOS(RK)
SC=DCMPLX(COSINE,SINE)

C
C      S-WAVE FUNCTIONS
C
DO 520 NS=1,ISOBNO
DEL=PP*AL(S(NS))
IF(DEL.GT.EXPCVG) GO TO 520
CONST=DEXP(-DEL)
DO 21 IS=1,LSMAX
II=IS+LDEND
CO=CONST*CS(IS,NS)
BASF(II)=BASF(II)+SC*CO
21 CONTINUE
520 CONTINUE

C
C      P-WAVE FUNCTIONS

```

```

C
DO 530 NP=1,IPOBNO
DEL=PP*ALP(NP)
IF(DEL.GT.EXPCVG) GO TO 530
CONST=DEXP(-DEL)
DO 31 IP=1,LPMAX
II=3*(IP-1)
IX=II+LSEND+1
IY=II+LSEND+2
IZ=II+LSEND+3
CO=CONST*CP(IP,NP)
COSC=CO*SC*(0.D0,-1.D0)
BASF(IX)=BASF(IX)+COSC*PX
BASF(IY)=BASF(IY)+COSC*PY
BASF(IZ)=BASF(IZ)+COSC*PZ
31 CONTINUE
530 CONTINUE

```

```

C
C      D-WAVE FUNCTIONS
C
PXY=PX*PY
PYZ=PY*PZ
PZX=PZ*PX
PX2=(PX*PX-PY*PY)/2.D0
PZ2=(3.D0*PZ*PZ-PP)/(2.00*DSQRT(3.D0))
DO 540 ND=1,IDOBN0
DEL=PP*ALD(ND)
IF(DEL.GT.EXPCVG) GO TO 540
CONST=DEXP(-DEL)
DO 41 ID=1,LDMAX
NDXY=ID
NDYZ=NDXY+LDMAX
NDZX=NDYZ+LDMAX
NDX2=NDZX+LDMAX
NDZ2=NDX2+LDMAX
CO=CONST*CD(ID,ND)
COSC=SC*CO
BASF(NDXY)=BASF(NDXY)+COSC*PXY
BASF(NDYZ)=BASF(NDYZ)+COSC*PYZ
BASF(NDZX)=BASF(NDZX)+COSC*PZX
BASF(NDX2)=BASF(NDX2)+COSC*PX2
BASF(NDZ2)=BASF(NDZ2)+COSC*PZ2
41 CONTINUE
540 CONTINUE
500 CONTINUE
DO 700 I=1,LPEND

```

```
700 GBASF(1)=BASF(1)
      WRITE(1) GBASF
300 CONTINUE
      WRITE(6,750) RX,RY,RZ,(BASF(I),I=1,LPEND)
      PRINT 751
750 FORMAT(9E14.6)
751 FORMAT(1H0)
200 CONTINUE
100 CONTINUE
400 CONTINUE
1000 CONTINUE
      STOP
      END
```

C PROGRAM 6. SELF-CONSISTENCY

```
C*****ACINST=LATTICE CONSTANT (IN A. U.)*****
C*****ALPHA=THE EXCHANGE PARAMETER*****
C*****FACT=PARAMETER USED TO SPEED UP THE SELF-CONSISTENT PROCEDURE*****
C*****ELECT=NUMBER OF ELECTRONS PER ATOM*****
C*****DEN=ENERGY GRIDE SIZE USED IN CALCULATING THE DENSITY OF STATES.*****
C*****IDCUB=NUMBER OF ATOMS PER LATTICE*****
C*****KNMAX=NO. OF RECIPROCAL LATTICE VECTORS CONSIDERED.*****
C*****NEN=NO OF POINTS USED IN CALCULATING THE DENSITY OF STATES*****
C*****IBZDIV=DIVISION BETWEEN K=(0,0,0) AND K=(1,0,0)*2*PI/A*****
C*****N8=NO. OF BASIS FUNCTIONS.*****
C*****NPGaus=NO OF POINTS USED IN THE NUMERICAL GAUSSIAN INTEGRATION OVER*****
C*****THE WIGNER-SEITZ SPHERE. (THE EXCHANGE POTENTIAL)*****
C*****IF(IPUN.NE.0) PUNCH THE CHARGE DENSITY AND THEIR FOURIER COEFFICIENTS*****
C*****COMPLEX*8 BAS(38),SS,TT
REAL*8 XUP,XDN,X1,X2,T,OV,HUP,HDN,TN,QN,AA,BB,CC,S,W,R,AC,DD,WT
&,ROK,SUMW
INTEGER*2 KX(89),KY(89),KZ(89),IX(51),IY(51),IZ(51),NN
DIMENSION W(96),R(96),DUP(96),DDN(96),DENUP(96),DFNDN(96),RK(51)
DIMENSION SIJ(741)
DIMENSION COUP(288),CDN(288),VAUP(288),VADN(288)
DIMENSION VUPR(96),VDNR(96),VMSUP(51),VMSDN(51)
DIMENSION XUP(38),XDN(38),X1(38,38),X2(38,38),T(741),OV(741),
2VMUP(51),VMDN(51),DKUP(51),DKDN(51),EXUP(51),S(741),
3EXDN(51),DK(51),VK(51),VXUP(51),VXDN(51),RKK(51),VK0(51),CDN(51),
4VXOUP(51),VXODN(51),CKUP(51),CKDN(51),VKUP(51),VKDN(51)
DIMENSION WDIR(3),NPUM(3)
DIMENSION HUP(38,38),HDN(38,38)
COMMON/LCS/TSW(3000),EN(3000),SW(3000)
COMMON/LCS/HUP,HDN,T,S
COMMON WT(89)
DATA NPUM/6,12,8/,WDIR/0.28571419,0.45714266,0.25714275/
PI=3.141592653589793
1 FORMAT(6F12.8)
READ(5,1) ACONST,ALPHA,FACT,ELECT,DEN
READ(5,2) IDCUB,KNMAX,NEN,IBZDIV,N8,NPGaus,IPUN
2 FORMAT(20I5)
OMEGA=ACONST**3/DFLOAT(IDCUB)
KBZPT=IBZDIV+1
AKR=2.00*PI/ACONST
AKR2=AKR*AKR
ONETHD=1.00/3.00
SIXPI=-6.0*(3.0/4.0/PI)**.3333333
```

```

R0=(3.0*DMEGA/4.0/PI)**.3333333
COOK1=-16.00*PI*PI/(3.00*DMEGA)
NBST=NB-14
NBEND=NB-9
NCST=NBEND+1
DO 383 IRLV=1,KNMAX
VK(IRLV)=0.0
VXUP(IRLV)=0.0
383 VXDN(IRLV)=0.0
C
C      READ THE FOURIER COEFFICIENTS OF THE COULOMB, AND EXCHANGE POTENTIALS AND
C      THE CHARGE DENSITY.          (OUT PUT OF PROGRAM 1)
C
DO 3712 J=1,KNMAX
READ(8) KS,VKO(J),VX,VX0UP(J),VX0DN(J),VMUP(J),VMDN(J),IX(J),IY(J)
&,IZ(J),NN
CON(J)=NN
AA=AKR2*FLOAT(KS)
RK(J)=DSQRT(AA)
RKK(J)=-AA/8.0/PI
VMSUP(J)=VMUP(J)
VMSDN(J)=VMDN(J)
3712 CONTINUE
C
C      READ THE INITIAL CHARGE DENSITY CALCULATED IN PROGRAM 1.
C
DO 41111 I=1,NPGAUS
41111 RFAD(5,4089) R(I),W(I),DUP(I),DDN(I)
4089 FORMAT(4E14.8)
C
C      GENERATE EQUALLY SPACED POINTS AND THE CORRESPONDING WEIGHT FACTORS IN
C      1/48TH OF THE INDEPENDENT BRILLIOUIN ZONE
C
CALL GBZPT(KX,KY,KZ,WT,NKPT, IDCUB, KBZPT, SUMW)
WRITE(6,3) ACONST,ALPHA,FACT,ELECT,DEN,NKPT,KNMAX, IDCUB,NEN
&,IBZDIV,NB,NPGAUS
3 FORMAT(1X,'LATTICE CONST=',F10.5,2X,'EXCH PARA=',F10.5,2X,
1'FACTOR=',F10.5,2X,'ELECT NO=',F8.2,2X,'DE=',F10.5,/,1X,'B.Z. PT=
2',I5.2X,'R.L.V. NO=',I5.2X,'ATOMS/LATTICEF=',I5.2X,'DE NO=',I5.2X,
3'B.Z. DIV=',I5.2X,'BAND NO=',I5.2X,'GAUS NO=',I5./)
1206 FORMAT(3I5)
C
C      PERFORM ITERATION NUMBER ITFR00D+1 TO ITFRNW.
C      IF(NPART.NE.0) THE FIRST HALF OF THE CALCULATION HAS BEEN DONE.
C
READ(5,1206) ITFR00D,ITFRNW,NPART

```

```

1207 IF(NPART.NE.0) READ(5,1207) FERMIE
1207 FORMAT(F12.8)
1207 IF(ITEROD.EQ.0) GO TO 23510
C
C      READ THE CORECTIONS DUE TO SELF-CONSISTANCY IN THF PREVIOUS ITERATIONS.
C
1207 DO 35610 ITER=1,ITEROD
35610 READ(19) (VK(I),VMSUP(I),VMSDN(I),VXUP(I),VXDN(I),I=1,KNMAX)
23510 CONTINUE
ITERST=ITEROD+1
DO 32323 ITER=ITERST,ITERNW
IF(NPART.NE.0.AND.ITER.EQ.ITERST) GO TO 381
DO 2011 I=1,NEN
SW(I)=0.0
2011 CONTINUE
DO 12000 NM=1,NKPT
WRITE(6,222) KX(NM),KY(NM),KZ(NM),NM,WT(NM)
222 FORMAT(/,30X,3HK=(,3I4,1H),5X,'NM=' ,I5,5X,'WT=' ,F8.5,/ )
9905 FORMAT(5A4)
C
C      READ THE ORIGINAL COULOMB, KINETIC, EXCHANGE, AND OVERLAP MATRICES.
C
1207 DO 370 I=1,NB
1207 DO 370 J=1,I
IJ=J+(I*-I)/2
READ(4,9905) PO,EK,UP,DN,OVLP
HUP(I,J)=PO+EK+UP*ALPHA
HDN(I,J)=PO+EK+DN*ALPHA
OV(IJ)=OVLP
370 CONTINUE
9 FORMAT(A4)
DO 300 IRLV=1,KNMAX
C
C      CALCULATE THE HAMILTONIAN OBTAINED FROM LAST ITERATION BY THF GENRALIZED
C      OVERLAP MATRICES.
C
1207 READ(1) SIJ
AA=VK(IRLV)+VXUP(IRLV)*ALPHA
BB=VK(IRLV)+VXDN(IRLV)*ALPHA
DO 300 I=1,NB
DO 300 J=1,I
IJ=I*(I-1)/2+J
HUP(I,J)=HUP(I,J)+AA*SIJ(IJ)
HDN(I,J)=HDN(I,J)+BB*SIJ(IJ)
HUP(J,I)=HUP(I,J)
HDN(J,I)=HDN(I,J)

```

```

300 CONTINUE
C
C     CALCULATE THE ENERGY EIGENVALUES AND WAVE VECTORS.
C
A=1.D-9
CALL DMFSD(OV,NB,A,IE1)
CALL DMTDS(HUP,NB,NR,OV,-1,IE2)
CALL DMTDS(HUP,NB,NR,OV,2,IE3)
CALL DMTDS(HDN,NB,NB,OV,-1,IE4)
CALL DMTDS(HDN,NB,NB,OV,2,IE5)
DO 7150 I=1,NB
DO 7150 J=1,I
IJ=I*(I-1)/2+J
T(IJ)=HUP(I,J)
7150 S(IJ)=HDN(I,J)
CALL DIGEN(T,X1,NB,0)
CALL DIGEN(S,X2,NB,0)
CALL DMTDS(X1,NB,NB,OV,1,IE6)
CALL DMTDS(X2,NB,NB,OV,1,IE7)
IF(IE1.EQ.0.AND.IE2.EQ.0.AND.IE3.EQ.0.AND.IE4.EQ.0.AND.IE5.EQ.0.
&AND.IE6.EQ.0.AND.IE7.EQ.0) GO TO 5890
WRITE(6,5891) IE1,IE2,IE3,IE4,IE5,IE6,IE7
5891 FORMAT(1X,'IER=' ,7I5)
STOP6
5890 CONTINUE
DO 7151 I=1,NB
IJ=I*(I-1)/2+I
XUP(I)=T(IJ)
7151 XDN(I)=S(IJ)
245 FORMAT(/)
235 FORMAT(12F11.5)
WRITE(6,235) (XUP(J),J=NBST,NB)
PRINT 245
WRITE(6,235) (XDN(J),J=NBST,NB)
DO 357 II=1,NB
WRITE(2) XUP(II),(X1(JJ,II),JJ=1,NB)
357 WRITE(2) XDN(II),(X2(JJ,II),JJ=1,NB)
C
C     CALCULATE THE DENSITY OF STATES.
C
IF(NM.NE.1) GO TO 6532
AA=DMIN1(XUP(NBEND),XDN(NBEND))
XQ=AA-0.001
DO 2010 I=1,NEN
EN(I)=XQ
2010 XQ=XQ+DEN

```

```

6532 CONTINUE
  WZ=WT(NM)/SUMW
  DO 36 KK=NBST,NBEND
  DO 34 J=2,NEN
    M=J-1
    IF(XUP(KK).GT.EN(M).AND.XUP(KK).LE.FN(J)) GO TO 35
34 CONTINUE
35 SW(J)=SW(J)+WZ
36 CONTINUE
  DO 336 KK=NBST,NBEND
  DO 334 J=2,NEN
    M=J-1
    IF(XDN(KK).GT.EN(M).AND.XDN(KK).LE.FN(J)) GO TO 335
334 CONTINUE
335 SW(J)=SW(J)+WZ
336 CONTINUE
12000 CONTINUE
C
C      DETERMINE THE FERMI ENERGY
C
  RHO=ELECT-18.00
  A=0.0
  DO 39 J=1,NEN
    A=A+SW(J)
39 TSW(J)=A
  NENO=NEN-2
  DO 41 J=2,NENO
    K=J-1
    IF(TSW(K).LT.RHO.AND.TSW(J).GE.RHO)GOTO40
41 CONTINUE
  WRITE(6,36741)
36741 FORMAT(1X,'FERMIE IS NOT CORRECT')
C
  GO TO 9999
40 A=RHO-TSW(K)
  B=TSW(J)-RHO
  IF(A.LT.B) FERMIE=EN(K)
  IF(A.GE.B) FERMIE=EN(J)
  K1=K-20
  K2=K+20
  IF(K2.GT.NEN) K2=NEN
  DO 156 IOD=K1,K2
156 WRITE(6,157) EN(IOD),SW(IOD),TSW(IOD)
157 FORMAT(1X,4(10X,F13.7))
  WRITE(6,158) FERMIE
158 FORMAT(1X,'FERMIE ENERGY=',F14.8,/)
  REWIND 1

```

```

REWIND 2
381 DO 382 IRLV=1,KNMAX
      CKUP( IRLV)=0.00
      CKDN( IRLV)=0.00
      VKUP( IRLV)=0.00
382 VKDN( IRLV)=0.00
      NP3=NPGAUSS*3
      DO 45 I=1,NP3
      COUP( I)=0.00
      CODN( I)=0.00
      VAUP( I)=0.00
      VADN( I)=0.00
45 CONTINUE
      DO 89998 NM=1,NKPT
      DO 358 II=1,NB
      READ(2) XUP(II),(X1(JJ,II),JJ=1,NB)
358 READ(2) XDN(II),(X2(JJ,II),JJ=1,NB)

C
C   CALCULATE FOURIER TRANSFORM OF CHARGE DENSITY
C

      DO 121 IRLV=1,KNMAX
      READ(1) SIJ
      AA=0.0
      CC=0.0
      DO 125 IN=NBST,NBEND
      IF(XDN(IN).GT.FERMIE) GO TO 7125
      IJ=0
      DO 7122 I1=1,NB
      DO 7122 I2=1,I1
      IJ=IJ+1
      AC=X2(I1,IN)*SIJ(IJ)*X2(I2,IN)
      IF(I1.NE.I2) AC=AC*2.00
7122 CC=CC+AC
7125 CONTINUE
      IF(XUP(IN).GT.FERMIE) GO TO 125
      IJ=0
      DO 122 I1=1,NB
      DO 122 I2=1,I1
      IJ=IJ+1
      AC=X1(I1,IN)*SIJ(IJ)*X1(I2,IN)
      IF(I1.NE.I2) AC=AC*2.00
122 AA=AA+AC
125 CONTINUE
      VKUP( IRLV)=VKUP( IRLV)+WT(NM)*AA
      VKDN( IRLV)=VKDN( IRLV)+WT(NM)*CC
      AA=0.00

```

```

BB=0.D0
DO 6125 IN=NCST,NB
IJ=0
DO 6122 I1=1,NB
DO 6122 I2=1,I1
IJ=IJ+1
AC=X1(I1,IN)*SIJ(IJ)*X1(I2,IN)
BC=X2(I1,IN)*SIJ(IJ)*X2(I2,IN)
IF(I1.EQ.I2) GO TO 6124
AC=AC*2.D0
BC=BC*2.D0
6124 AA=AA+AC
6122 BB=BB+BC
6125 CONTINUE
CKUP(IRLV)=CKUP(IRLV)+WT(NM)*AA
CKDN(IRLV)=CKDN(IRLV)+WT(NM)*BB
121 CONTINUE
C
C      CALCULATE SPHERICALLY AVERAGED CHARGE DENSITY
C      THE BASIS FUNCTION (BAS) IS CALCULATED IN PROGRAM 5.
C
PCONST=WT(NM)/SUMW
IQ=0
DO 831 IR=1,NPGAUS
DO 832 LDIR=1,3
IQ=IQ+1
SUPCO=0.D0
SDNCO=0.D0
SUPVA=0.D0
SDNVA=0.D0
NPTOL=NPUUM(LDIR)
PCON=PCONST/FLOAT(NPTOL)
DO 833 LP=1,NPTOL
READ(17) BAS
DO 811 I=NCST,NB
SS=(0.D0,0.D0)
TT=(0.D0,0.D0)
DO 812 J=1,NB
SS=SS+X1(J,I)*BAS(J)
TT=TT+X2(J,I)*BAS(J)
812 CONTINUE
SUPCO=SUPCO+CABS(SS)**2
SDNCO=SDNCO+CABS(TT)**2
811 CONTINUE
DO 805 I=NBST,NBEND
IF(XUP(I).GT.FERMIE) GO TO 821

```

```

      SS=(0.00,0.00)
      DO 806 J=1,NB
806  SS=SS+X1(J,I)*BAS(J)
      SUPVA=SUPVA+CABS(SS)**2
821  IF(XDN(I).GT.FERMIE) GO TO 805
      TT=(0.00,0.00)
      DO 807 J=1,NB
807  TT=TT+X2(J,I)*BAS(J)
      SDNVA=SDNVA+CABS(TT)**2
805  CONTINUE
833  CONTINUE
      COUP(IQ)=COUP(IQ)+SUPCO*PCON
      CODN(IQ)=CODN(IQ)+SDNCO*PCON
      VAUP(IQ)=VAUP(IQ)+SUPVA*PCON
      VADN(IQ)=VADN(IQ)+SDNVA*PCON
832  CONTINUE
831  CONTINUE
89998 CONTINUE
      WRITE(6,223)

C
C   THE SPHERICALLY AVERAGED CHARGE DENSITY IS APPROXIMATED AS THE ZEROTH
C   ORDER TERM IN A SIX ORDER KUBIC HARMONIC EXPANSION.
C
      IQ=0
      DO 837 IR=1,NPGAUS
      DENUP(IR)=0.0
      DENDN(IR)=0.0
      DO 838 LDIR=1,3
      IQ=IQ+1
      DENUP(IR)=DENUP(IR)+(COUP(IQ)+VAUP(IQ))*WTDIR(LDIR)
      DENDN(IR)=DENDN(IR)+(CODN(IQ)+VADN(IQ))*WTDIR(LDIR)
834  FORMAT(5E15.8,15)
      IF(IPUN.NE.0) WRITE(7,834) R(IR),COUP(IQ),VAUP(IQ),CODN(IQ),VADN(I
     & Q),LDIR
838  CONTINUE
      II=(IR-1)*3
      WRITE(6,839) R(IR),DENUP(IR),DENDN(IR),(COUP(II+J),CODN(II+J),VAUP
     &(II+J),VADN(II+J),J=1,3)
837  CONTINUE
839  FORMAT(1X,F5.2,14F9.3)
      AA=(CKUP(1)+VKUP(1)-CKDN(1)-VKDN(1))/SUMW
      RHO=(CKUP(1)+VKUP(1)+CKDN(1)+VKDN(1))/SUMW
      WRITE(6,1780) AA,RHO
1780 FORMAT(//,1X,'MAGNETON NUMBER =',F13.7,'RHO=',F16.8,/,1H1)
C
C   MODIFIED THE SELF-CONSISTENT CORRECTIONS TO IMPROVE CONVERGENCE.

```

```

C
DO 378 KN=1,KNMAX
CADS=1.0/CON(KN)/OMEGA/SUMW
CKUP(KN)=CKUP(KN)*CADS
CKDN(KN)=CKDN(KN)*CADS
VKUP(KN)=VKUP(KN)*CADS
VKDN(KN)=VKDN(KN)*CADS
DKUP(KN)=CKUP(KN)+VKUP(KN)
DKDN(KN)=CKDN(KN)+VKDN(KN)
DKUP(KN)=DKUP(KN)*FACT+(1.0-FACT)*VMSUP(KN)
DKDN(KN)=DKDN(KN)*FACT+(1.0-FACT)*VMSDN(KN)
IF(IPUN.NE.0) WRITE(7,5643) IX(KN),IY(KN),IZ(KN),CKUP(KN),CKDN(KN),
& VKUP(KN),VKDN(KN)
5643 FORMAT(3I3,4D15.8)
89437 FORMAT(3I3,4F15.8)
WRITE(6,89437) IX(KN),IY(KN),IZ(KN),CKUP(KN),CKDN(KN),VKUP(KN),
& VKDN(KN)
VMSUP(KN)=DKUP(KN)
VMSDN(KN)=DKDN(KN)
OK(KN)=DKUP(KN)+DKDN(KN)
378 CONTINUE
WRITE(6,223)
WRITE(6,89413) ITER,FACT
89413 FORMAT(IX,'ITERATION=',I3,5X,'FACT=',F6.3,/)
C
C      CALCULATE THE CORRECTION TO THE COULOMB PART OF V(K=0).
C
AA=0.00
R02=R0*R0
R03=R0*R02
DO 451 J=2,KNMAX
RK1=RK(J)
RK2=RK1*RK1
RK3=RK1*RK2
RK4=RK2*RK2
ROK=R0*RK1
AA=AA+(RK(J)-VKUP(J)-VKDN(J))/RK1*((3.00*R02/RK2-6.00/RK4)*DSIN(R0
& K)+(6.00*R0/RK3-R03/RK1)*DCOS(ROK))*CON(J)
451 CONTINUE
DK(1)=COK1*AA
C
C      CALCULATE THE CORRECTION TO THE EXCHANGE POTENTIAL BY NUMERICAL GAUSSIAN
C      INTEGRATION.
C
DO 401 I=1,NPGAUS
VUPR(I)=(DENUP(I)**ONETHD-DUP(I)**ONETHD)*SIXPI

```

```

VDNR(I)=(DENDN(I)**ONETHD-DDN(I)**ONETHD)*SIXPI
401 CONTINUE
EXUP(1)=0.0
EXDN(1)=0.0
CC=2.0*PI*R0/OMEGA
DO 403 I=1,NPGaus
EXUP(1)=EXUP(1)+W(I)*VUPR(I)*R(I)*R(I)
403 EXDN(1)=EXDN(1)+W(I)*VDNR(I)*R(I)*R(I)
EXUP(1)=CC*EXUP(1)
EXDN(1)=CC*EXDN(1)
DO 404 J=2,KNMAX
EXUP(J)=0.0
EXDN(J)=0.0
BB=CC/RK(J)
DO 409 I=1,NPGaus
AA=RK(J)*R(I)
EXUP(J)=EXUP(J)+W(I)*VUPR(I)*R(I)*DSIN(AA)
409 EXDN(J)=EXDN(J)+W(I)*VDNR(I)*R(I)*DSIN(AA)
EXUP(J)=EXUP(J)*BB
EXDN(J)=EXDN(J)*BB
404 CONTINUE
WRITE(6,32211)
32211 FORMAT(6X,'NUCLEAR',5X,'EX UP',6X,'EX DN',5X,'RHOU P',4X,'RHODN',
*6X,'ELE',7X,'VK',10X,'DK',7X,'VXUP',6X,'EXUP',6X,'VXDN',6X,'EXDN')
ANUCLE=0.0
DO 397 J=1,KNMAX
IF(J.EQ.1) GO TO 33397
DK(J)=-DK(J)/RKK(J)-VK0(J)
ANUCLE=ELECT/RKK(J)/OMEGA
33397 WRITE(6,100) IX(J),IY(J),IZ(J),ANUCLE,VXOUP(J),VXODN(J),VMUP(J),
1 VMDN(J),VK0(J),VK(J),DK(J),VXUP(J),EXUP(J),VXDN(J),EXDN(J)
56802 FORMAT(5E14.8)
50100 FORMAT(5A4)
VXUP(J)=EXUP(J)
VXDN(J)=EXDN(J)
VK(J)=DK(J)
397 CONTINUE
100 FORMAT(1X,I2,2I1,12(1X,F9.5))
WRITE(19) (DK(I),DKUP(I),DKDN(I),EXUP(I),EXDN(I),I=1,KNMAX)
WRITE(6,223)
223 FORMAT(1H1)
9998 CONTINUE
REWIND 1
REWIND 2
REWIND 4
REWIND 17

```

32323 CONTINUE
9999 STOP
END

C PROGRAMS 7. THE CENTRAL CELL INTEGRALS OF THE SPIN-ORBIT COUPLING.
(P-P AND D-D BLOCKS)

```
C*****  
C A=LATTICE CONSTANT (IN A. U.)  
C SCO IDCUB=1, BCC0 IDCUB=2, FCC0 IDCUB=4  
C EXPCVG= CONVERGENT CRITERIAL DEXP(-EXPCVG)=0.DC  
C ELECT=NUMBER OF ELECTRONS PER ATOM  
C K2MAX=THE SQUARE OF THE MAXIMUM MAGNITUDE OF THE RECIPROCAL LATTICE  
C VECTORS USED  
C KREAD=NO OF FOURIER COEFFICIENTS READ IN (1)  
C NKPT=DIMENSION OF KXX ECT. MUST BE GREATER THAN NO OF R.L.V. GENERATED  
C ICOBNO=GTO NUMBERS FOR E SYMMETRY  
C IATOM=ATOMIC BASIS NUMBER =0 IF INDEPENDENT GTO IS EMPLOYED  
C*****  
IMPLICIT REAL *8 (A-F,H,O-Z)  
DIMENSION PP(3,3),VCO(1920),RK2(1920),CDC(3,3),GCOUL(4801)  
COMPLEX*16 A0,A1,A2,A3,A4  
DIMENSION R(96),W(96),Y(98)  
DIMENSION SB(25,25,3)  
DIMENSION H(10,10),X1(10,10),T(55),XUP(10),DD(5)  
COMMON/GTO/CRYATL,PI,ISATOM,IPATOM,IDATOM  
COMMON/LCS/KXX,KKY,KKZ,NB,KSQU  
INTEGER*2 KXX(8184),KKY(8184),KKZ(8184),NB(8184)  
DIMENSION ALS(14),ALP(11),ALD(5),CS(14),CP(11),CD(5),SCO(4,14),  
SPCO(3,11),DCO(5,5)  
DIMENSION KSQU(8184)  
1 FORMAT(A8,3F11.5,8I5)  
READ(5,1) CRYSTL,A,ELECT,EXPCVG,IDCUB,NKPT,K2MAX,KREAD  
READ(5,4) ICOBNO,ISATOM,IPOBNO,IPATOM,IDOBN0,IDA  
WRITE(6,3) CRYSTL,A,ELECT,EXPCVG,IDCUB,NKPT,K2MAX,KREAD,ICOBNO,IS  
&ATOM,IPOBNO,IPATOM,IDOBN0,IDA  
3 FORMAT(1X,A8,2X,'LATTICE CONST=',F10.5,2X,'ELECTRON NO=',F10.5,2X,  
1*EXP MAX=',F10.5,2X,'ATOMS/LATTICE=',I5,2X,'NKPT=',I5,2X,'MAX K**2  
E=',I5,/,1X,'K READ=',I5,5X,  
2*SS=(',2I5,')',2X,'PP=',2I5,')',2X,'DD=(',2I5,')',//)  
LSMAX=ICOBNO  
LDMAX=IDOBN0  
LPMAX=IPOBNO  
IF(ISATOM.NE.0) LSMAX=ISATOM  
IF(IDATOM.NE.0) LDMAX=IDA  
IF(IPATOM.NE.0) LPMAX=IPATOM  
4 FORMAT(9I5)  
PI=3.14159265358979300  
AKR=2.D0*PI/A  
AKR2=AKR*AKR
```

```

AHALF=A/2.D0
OMEGA=A**3/DFLOAT(1DCUR)
IDATOM=1
C
C      DEFINES THE GAUSSIAN EXPONENTS, NORMALIZATION CONSTANTS, AND EXPANSION
C      COEFFICIENTS
C
      CALL RDGTO(ALS,ALP,ALD,CS,CP,CD,SCO,PCO,DCO,ISORNO,LSMAX,
     & IPOSNO,LPMAX,1DOBNO,LDMAX,0)
      CALL GINDPK(KKX,KKY,KKZ,KSQU,NKPT,1)CUB,K2MAX,NR,1,1)
      DO 23 J=1,KREAD
23 READ(1,END=22) GCOUL(J),GEX,GFXUP,GFXDN,K2
22 CONTINUE
      GCOUL(1)=-0.16074696D+01
C
C      D-D
C
      CDCD1=1.D0
      CDCD2=CDCD1/2.D0
      CDCD3=CDCD2/DSQRT(3.D0)
      LDEND=5*LDMAX
      DO 534 L=1,3
      DO 534 I=1,LDEND
      DO 534 J=1,LDEND
534 SB(I,J,L)=0.D0
      DO 25 I=1,10
      DO 25 J=1,10
25 H(I,J)=0.D0
      DDA=0.D0
      DDB=0.D0
      DO 45 K1=1,1DOBNO
      DO 45 K2=1,1DOBNO
      U=1.D0/(ALD(K1)+ALD(K2))
      ALAMDA=ALD(K1)*ALD(K2)*U
      DELTA=(PI*U)**1.5
      U1=ALD(K1)*U
      U2=ALD(K2)*U
      CONST=U*DELTA*CD(K1)*CD(K2)/(8.D0*ALD(K1)*ALD(K2))/3.D0
      CONST=CONST/274.074D0**2
      C01=CONST*U1*U2
      C02=-2.D0*ALAMDA*CONST
      C03=C01*U2
      C04=C01*(2.D0*U1-U2)
      C05=2.D0*C02
      UV4=U/4.D0
      A=0.D0

```

```

B=0.00      DO 505 J=1,NKPT
AX=AKR2*KKX(J)**2   AX=AKR2*KKY(J)**2
AY=AKR2*KKY(J)**2   AZ=AKR2*KKZ(J)**2
AZ=AKS0*X+AY+AZ   EXPB=AKS0*UDV4
IF(EXPB.GT.*EXPVCVG) GO TO 405
ADEL=DEXP(-EXPB)
KK=KSQU(J)+1
CO=GCOUL(KK)*NB(J)
AK2=AKS0*CO
AK2K2=(AX*AY+AY*AZ+AZ*AX)*CO
AK4=(AX*AX+AY*AY+AZ*AZ)*CO
A=A+(CO1*AK2K2+CO2*AK2)*ADEL
B=B+(CO3*AK4+CO4*AK2K2+CO5*AK2)*ADEL
505 CONTINUE
405 CONTINUE
SB(K1,15+K2,1)=2.0*B*CDCD2
SB(5+K1,10+K2,1)=A*CDCD1
SB(K1,10+K2,3)=-A*CDCD1
SB(K1,5+K2,2)=A*CDCD1
SB(5+K1,15+K2,3)=-B*CDCD2
SB(5+K1,20+K2,3)=-3.0*B*CDCD3
SB(10+K1,15+K2,2)=-B*CDCD2
SB(10+K1,20+K2,2)=3.0*B*CDCD3
CO=2.0
IF(K1.EQ.K2) CO=1.00
DDA=DDA+A*DCO(I,K1)*DCO(I,K2)*CO
DDB=ddb+B*DCO(I,K1)*DCO(I,K2)*CO
45 CONTINUE
DO 600 I=1,25
DO 600 J=1,1
DO 600 M=1,3
600 SB(I,J,M)=-SB(J,I,M)
8 FORMAT(1X,2A4,3(5X,E14.6))
AA=0.00
DO 4000 I=1,25
DO 4000 J=1,25
WRITE(7,1023) I,J,AA,(SB(I,J,N),N=1,3)
4000 WRITE(6,1023) I,J,AA,(SB(I,J,N),N=1,3)
PRINT 54802
C
C DEFINE THE SPIN-ORBIT INTERACTION MATRICES BETWEEN ATOMIC FUNCTIONS
C AND DIAGONALIZE IT WITH EIGENVALUE (XUP)
C

```

```

H( 1,4)=DDB
H( 1,7)=DDA
H( 1,8)=-DDA
H( 2,3)=DDA
H( 2,6)=-DDA
H( 2,9)=-DDB/2.00
H( 2,10)=-DSQRT(3.00)/2.00*DDB
H( 3,6)=-DDA
H( 3,9)=H(2,9)
H( 3,10)=-H(2,10)
H( 4,7)=H(2,9)
H( 4,8)=-H(2,9)
H( 5,7)=H(2,10)
H( 5,8)=H(2,10)
H( 6,9)=-DDB
H( 7,8)=-DDA
DO 125 I=1,10
DO 125 J=1,I
IJ=I*(I-1)/2+J
125 T(IJ)=H(J,I)
CALL DIGEN(T,X1,10,0)
DO 7151 I=1,10
J=I*(I-1)/2+I
XUP(I)=T(J)
7151 CONTINUE
M=10
85 FORMAT(1H1)
189 FORMAT(1X,I2,9(2X,E12.6))
86 FORMAT(1X,//)
89 FORMAT(3X,9F14.6)
I1=1
71 I2=I1+8
IF(I2.GT.M)I2=M
WRITE(6,85)
WRITE(6,89) (XUP(J),J=I1,I2)
WRITE(6,86)
DO 72 I=1,M
72 WRITE(6,189) I,(X1(I,J),J=I1,I2)
I1=I2+1
IF(I2.LT.M) GO TO 71
C
C      P-P
C
C      FINDS THE ASYMPTOTIC EXPRESSION FOR THE FOURIER COEFFICIENTS OF THE COULOMB
C      POTENTIAL

```

```

VKC0=-8.D0*PI*ELECT/DOMEGA
K1=KSQU(NKPT)
K2=K1-100
K3=K1-50
GK1=FLOAT(K1)*AKR2
GK2=FLOAT(K2)*AKR2
GK3=FLOAT(K3)*AKR2
AA=GK1*GCOUL(K1+1)-VKC0
BR=GK2*GCOUL(K2+1)-VKC0
AA=DSQRT(AA)
BB=DSQRT(BB)
VKC2=AA*(GK1-GK2)/(BB-AA)-GK2
VKC1=(AA*(GK1+VKC2))**2
VTEST=VKC0/GK3+VKC1/(GK3*(GK3+VKC2)**2)
WRITE(6,50) VKC1,VKC2,K3,GCOUL(K3+1),VTEST
50 FORMAT(1X,/,1X,'V(K)=-8*PI*Z/K2/V+',E16.8,2X,'/(K2*(K2+',E16.8,2X,
'')**2)',/,1X,'K2=',I7,2X,'COULDUMB=',E16.8,2X,'TEST=',E16.8,/)
C1=VKC1/AKR2**3
C2=VKC2/AKR2
C3=VKC0/AKR2
WRITE(6,58210) C1,C2,C3
58210 FORMAT(3F20.5)
C
C   DEFINE CONSTANTS TO PERFORM 96 POINTS GAUSSIAN INTEGRATION FOR LARGE VALUE
C   OF THE RECIPROCAL LATTICE VECTORS
C
CALL GWTGAS(96,Y,R,W)
STN=DSQRT(AKR2*DFLOAT(KSQU(NKPT)))
DEN=50.D0*AKR
M=0
DO 901 I=1,20
DO 902 J=1,96
M=M+1
RK=DEN*R(J)/2.D0+(2.D0*STN+DEN)/2.D0
RKS=RK*RK
VCO(M)=VKC0/RKS+VKC1/(RKS*(RKS+VKC2)**2)
VCO(M)=VCO(M)*RK**4*W(J)
RK2(M)=RKS
902 CONTINUE
STN=STN+DEN
901 CONTINUE
DO 533 N=1,LPMAX
DO 533 M=1,LPMAX
533 PP(N,M)=0.D0
DO 40 K1=1,IPOBNO
DO 40 K2=1,IPOBNO

```

```

U=1.D0/(ALP(K1)+ALP(K2))
ALAMDA=ALP(K1)*ALP(K2)*U
DELTA=(PI*U)**1.5
CONST1=U/2.D0*DELTA/(274.074D0**2)*CP(K1)*CP(K2)
CONST2=CONST1*DEN/2.D0*OMEGA/(6.D0*PI*PI)
DO 201 I=1,LPMAX
DO 201 J=1,LPMAX
201 CDC(I,J)=PCO(I,K1)*PCO(J,K2)
UOV4=U/4.D0
CENT1=0.D0
C
C      SUM OVER THE R.L.V. UP TO NKPT
C
DO 500 J=1,NKPT
EXPB=UOV4*AKR2*KSQU(J)
IF(EXPB.GT.EXPCVG) GO TO 400
KK=KSQU(J)+1
ADEL=DEXP(-EXPB)
CENT1=CENT1+ADEL*GCOUL(KK)*AKR2*DFLOAT(KSQU(J))*NB(J)/3.D0
500 CONTINUE
400 CONTINUE
CENT1=CENT1*CONST1
C
C      INTEGRATE FORM NKPT TO CONVERGENT
C
A=0.D0
DO 801 I=1,1920
EXPB=RK2(I)*U/4.D0
IF(EXPB.GT.EXPCVG) GO TO 801
ADEL=DEXP(-EXPB)
A=A+ADEL*VCO(I)
801 CONTINUE
CENT2=CONST2*A
DO 408 I=1,LPMAX
DO 408 J=1,LPMAX
408 PP(I,J)=PP(I,J)+(CENT1+CENT2)*CDC(I,J)
CENT3=CENT1+CENT2
WRITE(6,9) K1,K2,CENT1,CENT2,CENT3
9 FORMAT(1X,2I5,3(2X,E14.8))
40 CONTINUE
PRINT 54802
54802 FORMAT(1H1)
LPST=LDMAX*5+LSMAX
DO 300 I=1,LPMAX
DO 300 J=1,LPMAX
II=LPST+3*(I-1)

```

```
JJ=LPST+3*(J-1)
IX=II+1
IY=II+2
IZ=II+3
JX=JJ+1
JY=JJ+2
JZ=JJ+3
BB=PP(I,J)
A0=(0.00,0.00)
A1=DCMPLX(BB,0.00)
A2=-A1
A3=DCMPLX(0.00,BB)
A4=-A3
WRITE(6,1023) IX,JY,A3,A0
WRITE(7,1023) IX,JY,A3,A0
WRITE(6,1023) IX,JZ,A0,A2
WRITE(7,1023) IX,JZ,A0,A2
WRITE(6,1023) IY,JX,A4,A0
WRITE(7,1023) IY,IX,A4,A0
WRITE(7,1023) IY,IX,A4,A0
WRITE(6,1023) IY,JZ,A0,A3
WRITE(7,1023) IY,JZ,A0,A3
WRITE(6,1023) IZ,JX,A0,A1
WRITE(7,1023) IZ,JX,A0,A1
WRITE(6,1023) IZ,JY,A0,A4
WRITE(7,1023) IZ,JY,A0,A4
300 CONTINUE
1023 FORMAT(2I5,4E15.8)
STOP
END
```

```

C      PROGRAM 8. ENERGY BANDS INCLUDING THE EFFECTS OF SPIN-ORBIT COUPLING
C
C*****CALCULATE THE ENERGY EIGENVALUES (E) AND EIGENVECTORS (X)
C      H X =S X E
C      THE OVERLAP MATRIX (S) IS EXPRESSED AS THE PRODUCT OF A UPPER TRIANGULAR
C      MATRIX (R) AND ITS TRANSPOSE (R**T)
C      H* X* = X* E , WHERE H*=(R**T)**-1 H (R**-1) AND X*= R X
C*****COMPLEX*16 H,X,DCONJG
C*****COMPLEX*8 Y(76,76),GN,CMPLX,CONJG
REAL*8 E(76),FUP(36),W(76),OV,EPS
DIMENSION GUP(741),GDN(741),GOV(741),FIG(76),DUP(36)
DIMENSION INDEX(76)
COMMON/LCS/GN(38,38),GMI(38,38)
COMMON/A/H(76,76)
COMMON/B/X(76,76)
COMMON/C/OV(2926)
EQUIVALENCE(H(1,1),Y(1,1)),(H(1,39),FUP(1))
EQUIVALENCE (X(1,1),GUP(1)),(X(1,26),GDN(1)),(X(1,51),GOV(1))
78210 FORMAT(2I5)
C
C      FIND E AND X FOR K=KST TO KEND
C      IF(IPRINT.NE.0) RESULTS ARE PRINTED
C
      READ(5,78210) KST,KEND,IPRINT
      DO 2 I=1,38
      DO 2 J=1,38
      GMI(I,J)=0.D0
      GN(I,J)=(0.E0,0.E0)
2 CONTINUE
10 FORMAT(2I5,4E15.8)
C
C      READ IN SPIN-ORBIT MATRIX (OUTPUT OF PROGRAM 7)
C
      DO 1 N=1,706
      READ(5,10,END=9) I,J,GA,GB,GC,GD
      GMI(I,J)=GB
      GN(I,J)=CMPLX(GC,GD)
1 CONTINUE
9 CONTINUE
M=76
KK=KST-1
DO 74239 KPT=1,KK
      READ(1) GX,GY,GZ,WEIGT,(EIG(I),I=1,M),(DUP(J),J=1,36)
      DO 74239 I=1,M

```

```

74239 READ(1) (Y(J,I),J=1,M)
C
C      DEFINE THE HAMILTONIAN AND OVERLAP MATRICES
C
DO 56940 KPT=1,KEND
READ(2) GX,GY,GZ,WEIGT,(GUP(I),GDN(I),I=1,741)
READ(3) GX,GY,GZ,WEIGT,(GOV(I),I=1,741)
IF(KPT.LT.KST) GO TO 56940
DO 15 I=1,38
II=I+38
DO 15 J=I,38
JJ=J+38
IJ=J*(J-1)/2+I
H(I,J)=CMPLX(GUP(IJ),GMI(I,J))
G=-GMI(I,J)
H(II,JJ)=CMPLX(GDN(IJ),G)
OV(IJ)=DBLE(GOV(IJ))
15 CONTINUE
C
C      DMFSD REPLACE OV BY AN UPPER TRIANGULAR MATRIX R WHEREF OV=(R**T) R
C      DMFSD IS IN IBM SCIENTIFIC SUBROUTINE PACKAGE
C
CALL DMFSD(OV,38,1,D-7,IER)
IF(IER.NE.0) GO TO 7200
GO TO 300
7200 CONTINUE
C
C      DIGEN DIAGONALIZED MATRIX OV
C      DIGEN IS THE DOUBLE PRECISION VERSION OF SUBROUTINE EIGEN IN IBM S.S.P.
C
CALL DIGEN(OV,GMI,38,0)
DO 55 I=1,38
J=I+(I-1)*I/2
WRITE(6,57) OV(J)
55 CONTINUE
57 FORMAT(1X,11(F10.7,1X))
STOP 5
300 CONTINUE
DO 11 I=1,38
DO 19 J=1,I
IJ=I*(I-1)/2+J
IIJJ=(I+38)*(I+37)/2+J+38
OV(IIJJ)=OV(IJ)
19 CONTINUE
DO 11 J=39,76
IJ=J*(J-1)/2+I

```

```

JJ=J-38
H(I,J)=GN(I,JJ)
OV(IJ)=0.D0
11 CONTINUE
DO 12 I=1,76
DO 12 J=1,I
H(I,J)=DCONJG(H(J,I))
12 CONTINUE
C
C      SUBROUTINE HRIN TRANSFORM H INTO H (R**-1)
C      SUBROUTINE RTINH TRANSFORM H INTO ((R**T)**-1) H
C
C      CALL HRIN(M)
C      CALL RTINH(M)
C
C      CEIGDP DIAGONALIZE A COMPLEX HERMITIAN MATRIX H WITH EIGENVALUE E AND
C      EIGENVECTORS X (NOT INCLUDED IN THIS THESIS)
C
IND=1
EPS=1.D-7
CALL CEIGDP(H,X,E,M,EPS,9000,ITER,IND,W,INDEX,M)
C
C      DEFINE PROJECTION OPERATOR FOR MAJORITY SPIN
C
DO 800 I=1,36
800 FUP(I)=0.0
DO 810 I=1,36
DO 810 K=1,38
810 FUP(I)=FUP(I)+CDABS(X(K,I))**2
DO 820 I=1,36
820 DUP(I)=FUP(I)
C
C      SUBROUTINE FUNCT TRANSFORM EIGENVECTORS X INTO (R**-1) X
C
CALL FUNCT(M)
DO 76581 I=1,M
EIG(I)=E(I)
DO 76581 J=1,M
Y(I,J)=X(I,J)
76581 CONTINUE
56081 CONTINUE
53405 FORMAT(1X,'K='',(3F6.2,'),5X,'ITERATION='',15,5X,'IND='',15,5X,
*'NM='',15,5X,'WEIGHT='',F10.4)
M=76
WRITE(1) GX,GY,GZ,WEIGT,(EIG(I),I=1,M),(DUP(J),J=1,36)
DO 76539 I=1,M

```

```
      WRITE(1) (Y(J,I),J=1,M)
76539  CONTINUE
      WRITE(6,53405) GX,GY,GZ,ITER,IND,KPT,WEIGT
      IF(IPRINT.EQ.0) GO TO 56940
      85 FORMAT(1H1)
      86 FORMAT(1X,//)
      I2=0
      71 CONTINUE
      I1=I2+1
      I2=I2+5
      IF(I2.GT.M) I2=M
      88 FORMAT(5(8X,I10,8X))
      WRITE(6,86)
      WRITE(6,88) (I,I=I1,I2)
      WRITE(6,86)
      WRITE(6,89) (E(I),I=I1,I2)
      WRITE(6,86)
      IF(I2.LE.36) WRITE(6,89) (DUP(I),I=I1,I2)
      WRITE(6,86)
      89 FORMAT(3X,5(6X,F14.7,6X))
      189 FORMAT(1X,I2,10(1X,E12.6))
      DO 72 I=1,M
      72 WRITE(6,189) I,(X(I,J),J=I1,I2)
      WRITE(6,85)
      IF(I2.LT.46) GO TO 71
56940  CONTINUE
      STOP
      END
```

```

C      PROGRAM 9. THE MOMENTUM MATRICES BETWEEN BAND STATES.
C
C*****SUM CONJG(X(I,N,K))*P(I,J,K)*X(J,M,K) OVER ALL STATES I & J.
C      WHERE X IS EIGENVECTOR AT K IN B. Z.
C      P IS THE MOMENTUM MATRIX BETWEEN BASIS BLOCH STATES. (PROGRAMS 2 & 4)
C*****COMPLEX*16 X(76,12),CX(76,12),BX(78),BY(78),BZ(78),A,SX,SY,SZ
C      COMPLEX*8 F(76,76),SBX(78),SBY(78),SBZ(78)
C      DIMENSION E(76),PX(741),PY(741),PZ(741)
C      DIMENSION FUP(36)
C      COMMON/LCS/F
C      4 FORMAT(4I5)
C
C      CALCULATE FOR K FROM NKST TO NKEND
C      RESULTS ARE PRINTED IF (IPRIT.NF.0)
C
C      READ(5,4) NKST,NKEND,IPRIT
C      DO 999 NMK=1,NKEND
C
C      READ IN ENERGY AND WAVE VECTOR. (OUT PUT OF PROGRAM 8)
C
C      READ(1) XK,YK,ZK,WT,(E(I),I=1,76),(FUP(I),I=1,36)
C      DO 10 I=1,76
C      10 READ(1) (F(J,I),J=1,76)
C      199 CONTINUE
C
C      READ IN MOMENTUM MATRIX BETWEEN BASIS BLOCH STATES. (PROGRAMS 2 & 4)
C
C      READ(2) XL,YL,ZL,(PX(I),I=1,741)
C      READ(2) XL,YL,ZL,(PY(I),I=1,741)
C      READ(2) XL,YL,ZL,(PZ(I),I=1,741)
C      IF(XK.NE.XL.OR.YK.NE.YL.OR.ZK.NE.ZL) GO TO 199
C      IF(NMK.LT.NKST)GO TO 999
C      DO 40 I=1,76
C      DO 40 J=1,12
C      X(I,J)=F(I,J+18)
C      40 CX(I,J)=DCONJG(X(I,J))
C      DO 20 I=1,78
C      BX(I)=(0.0D0,0.0D0)
C      BY(I)=(0.0D0,0.0D0)
C      BZ(I)=(0.0D0,0.0D0)
C      20 CONTINUE
C      DO 61 I=2,38
C      II=I+38
C      IMX=I-1

```

```

DO 61 J=1,IMX
IJ=I*(I-1)/2+J
JJ=J+38
SX=CMPLX(PX(IJ),0.E0)
SY=CMPLX PY(IJ),0.E0)
SZ=CMPLX(PZ(IJ),0.E0)
NN=0
DO 60 N=1,12
DO 60 M=1,N
NN=NN+1
A=CX(I,N)*X(J,M)+CX(J,N)*X(I,M)+CX(II,N)*X(JJ,M)*X(II,M)
BX(NN)=BX(NN)+A*SX
BY(NN)=BY(NN)+A*SY
BZ(NN)=BZ(NN)+A*SZ
CONTINUE
60
61 CONTINUE
DO 65 I=1,38
I=I+38
IJ=I*(I+1)/2
SX=CMPLX(PX(IJ),0.E0)
SY=CMPLX PY(IJ),0.E0)
SZ=CMPLX(PZ(IJ),0.E0)
NN=0
DO 66 N=1,12
DO 66 M=1,N
NN=NN+1
A=CX(I,N)*X(I,M)+CX(II,N)*X(II,M)
BX(NN)=BX(NN)+A*SX
BY(NN)=BY(NN)+A*SY
BZ(NN)=BZ(NN)+A*SZ
CONTINUE
66
65 CONTINUE
DO 700 I=1,78
SBX(I)=BX(I)
SBY(I)=BY(I)
SBZ(I)=BZ(I)
700 CONTINUE
WRITE(15) XK,YK,ZK,(SBX(I),SBY(I),SBZ(I),I=1,78)
WRITE(6,59) NMK,XK,YK,ZK,W
59 FORMAT(15.4(F14.5,3X),/)
IF(IPRIT.EQ.0) GO TO 999
DO 151 I=1,12
DO 151 J=1,1
IJ=I*(I-1)/2+J
WRITE(6,152) I,J,SBX(IJ),SBY(IJ),SBZ(IJ)
151 CONTINUE

```

```
152 FORMAT(1X,2I5.8(2X,F13.7))
      PRINT 56194
56194 FORMAT(1H1)
999 CONTINUE
19999 STOP
END
```

```

C PROGRAM 10. THE DENSITY OF STATES
C ****
C CALCULATE THE DENSITY OF STATES BY THE HYBRIDE METHOD
C ENERGY BANDS AND MOMENTUM MATRICES INCLUDING THE FFFECTS OF SPIN-ORBIT
C COUPLING ARE USED
C KL=DIVISION BETWEEN K=(0,0,0) AND K=2*PI/A(1,0,0)
C N8=NUMBER OF STATES CONSIDERED
C A=LATTICE CONSTANT
C EMIN=MINIMUM OF ENERGY
C NEMAX=TOTAL NUMBER OF POINTS WHERE DENSITY OF STATES NEED TO BE CALCULATED
C DE=STEP SIZE IN ENREGY
C VALEL=NUMBER OF BAND ELECTRONS
C DEGCRT=DEGENERATE CRITERIAL USED IN K.P PERTURBATION THEORY
C NKPT=NUMBER OF POINTS IN THE BRILLIQUIN ZONE
C IDCUB=NUMBER OF ATOMS PER LATTICE
C DIMENSION DEKX(NKSUM,NB), ECT.
C ****
COMPLEX*8 PX(12,12),PY(12,12),PZ(12,12),SPLJ,SPNJ,SPJM
COMPLEX*8 HD(5,5),UX(5,5),FX(12)
INTEGER*2 NP(18,18,18)
DIMENSION X(6),DDE(3,3),NPN(6)
DIMENSION EIG(5),WK(5),E(12),IND(5),NABP(9)
DIMENSION SWUP(1003),SWDN(1003),EN(1003),FLECT(1003)
DIMENSION FUP(12),EEW(12)
DIMENSION DEKZ(2083,12)
COMMON/LCS/DEKX(2083,12),DEKY(2083,12)
COMMON/AR/ENG,GDKX,GDKY,GDKZ,GDKM,B2,BDIV,CONUP,CONDN
CALL IDENT('1103 40149 SHI')
10 FORMAT(2I5,5F10.5,4I5)
READ(5,10) KL,NB,A,EMIN,DE,VALEL,DEGCRT,NEMAX,NKPT,NKSUM,IDCUB
Eperc=DFLOAT(IDCUB)
NABPMX=1
MAXBP=2*NABPMX+1
DO 111 N=1,MAXBP
111 NABP(N)=N-NABPMX-1
WRITE(6,11) KL,NB,A,EMIN,DE,VALEL,DEGCRT,NEMAX,NKPT,MAXBP
11 FORMAT(1H , 'KX-LENGTH=',I2.5X,'NO.OF BANDS=',I2.5X,'LATTICE CONSTA
NT=',F6.3,' A',5X,'EMIN=',F8.5,3X,'DE=',F8.5,5X,'NO.OF EL=',F4.1,/
2,.1X,'DEG CRT=',F7.5,5X,'NO OF DE=',I5,5X,'NO OF PT=',I5,5X,'SUB D
3IV=',I5,1//)
PI=3.141592653589793
PIKL=PI/KL
DIVNO=FLOAT(MAXBP)
VNORM=(A/(2.*PI))**3/4.
B=PIKL/A

```

```

BDIV=B/DIVNO
KLDIV=KL*MAXBP
KLD2=KL/2
TWOB=B*2.0
B2=BDIV*BDIV
KLDMAX=KLDIV*3/2
C
C READ MOMENTUM MATRICES AND DEFINE POINTS IN THE R. Z.
C
DO 1 NPT=1,NKPT
READ(1) XK,YK,ZK,((PX(I,J),PY(I,J),PZ(I,J),J=1,I),I=1,NB)
IF(KL.NE.8) GO TO 2351
XK=XK/2.0
YK=YK/2.0
ZK=ZK/2.0
2351 CONTINUE
I=IFIX(XK)+1
J=IFIX(YK)+1
K=IFIX(ZK)+1
NP(J,I,K)=NPT
NP(I,J,K)=NPT
DO 2 L=1,NB
DEKX(NPT,L)=2.0*REAL(PX(L,L))
DEKY(NPT,L)=2.0*REAL(PY(L,L))
DEKZ(NPT,L)=2.0*REAL(PZ(L,L))
2 CONTINUE
1
CONTINUE
REWIND 1
KLP2=KL+2
C
C GENERATE ENERGY DERIVATIVES IN THE NEIGHBORING POINTS OF THE 1/16TH OF THE
C BRILLOUIN ZONE
C
CALL GNBDE(DEKX,DEKY,DEKZ,NKSUM,NB,NP,KLP2,NKPT)
DO 299 NE=1,NEMAX
SWUP(NE)=0.0
SWDN(NE)=0.0
EN(NE)=EMIN+DE*(NE-1)
299 CONTINUE
EMAX=EN(NEMAX)
SUMWT=0.0
NMPT=0
DO 310 NPT=1,NKPT
C
C READ ENERGY AND PROJECTION OPERATOR FOR UP SPIN

```

```

READ(10) XK,YK,ZK,WTT,(E(L),FUP(L),L=1,NB)
KX=IFIX(XK)
KY=IFIX(YK)
KZ=IFIX(ZK)
IF(KL.NE.8) GO TO 319
KX=KX/2
KY=KY/2
KZ=KZ/2
319 CONTINUE
READ(1) XK,YK,ZK,((PX(I,J),PY(I,J),PZ(I,J),J=1,I),I=1,NB)
IF(KZ.NE.0.AND.KX.NE.KY.AND.KZ.NE.KL) GO TO 310
DO 35 I=1,NB
DO 35 J=1,NB
PX(I,J)=CONJG(PX(J,I))
PY(I,J)=CONJG(PY(J,I))
PZ(I,J)=CONJG(PZ(J,I))
35 CONTINUE
CCC
SUBDIVIDE EACH CUBE IN THE B. Z. INTO 27 MINICELLS
NTEST=0
DO 400 IDZ=1,MAXBP
KDZ=MAXBP*KZ+NABP(IDZ)
IF(KDZ.LT.0.OR.KDZ.GT.KLDIV) GO TO 400
KNZ=KZ+NABP(IDZ)+1
SKZ=FLOAT(NABP(IDZ))*BDIV*2.0
DO 401 IDY=1,MAXBP
KDY=MAXBP*KY+NABP(IDY)
IF(KDY.LT.0.OR.KDY.GT.KLDIV) GO TO 401
KNY=KY+NABP(IDY)+1
SKY=FLOAT(NABP(IDY))*BDIV*2.0
DO 402 IDX=1,MAXBP
KDX=MAXBP*KX+NABP(IDX)
IF(KDX.LT.KDY.OR.KDX.GT.KLDIV) GO TO 402
KNX=KX+NABP(IDX)+1
SKX=FLOAT(NABP(IDX))*BDIV*2.0
315 CONTINUE
KTOL=KDX+KDY+KDZ
IF(KTOL.GT.KLDMAX) GO TO 402
NBKPT=NP(KNX,KNY,KNZ)
NMPT=NMPT+1
CALL WFCC16(KDX,KDY,KDZ,KLDIV,WT)
SUMWT=SUMWT+WT
SSQ=SKX*SKX+SKY*SKY+SKZ*SKZ
LST=0
AA=WT*VNORM*16.0

```

```

DO 320 L=1,NB
IF(L.LT.LST) GO TO 320
GDKX=DEKX(NPT,L)
GDKY=DEKY(NPT,L)
GDKZ=DEKZ(NPT,L)
ENG=E(L)
NDEG=1
IF(SSQ.EQ.0.0) GO TO 32
LP1=L+1
DELE=ABS(E(LP1)-E(L))
336 CONTINUE
IF(L.NE.NB.AND.DELE.LT.DEGCRT) GO TO 330
CCC CALCULATE ENERGY BY SECOND ORDER K.P PERTURBATION THEORY
ENG=ENG+SKX*GDKX+SKY*GDKY+SKZ*GDKZ+SSQ
DO 30 J=1,NB
IF(L.EQ.J) GO TO 30
DELE=E(L)-E(J)
SPLJ=SKX*PX(L,J)+SKY*PY(L,J)+SKZ*PZ(L,J)
ENG=ENG+4.0*CABS(SPLJ)**2/DELE
30 CONTINUE
GDKX=DEKX(NPT,L)+(DEKX(NBKPT,L)-DEKX(NPT,L))/DIVNO
GDKY=DEKY(NPT,L)+(DEKY(NBKPT,L)-DEKY(NPT,L))/DIVNO
GDKZ=DEKZ(NPT,L)+(DEKZ(NBKPT,L)-DEKZ(NPT,L))/DIVNO
32 CONTINUE
FEW(L)=ENG
IF(ENG.GT.EMAX) GO TO 320
CONUP=AA*FUP(L)
CONDN=AA-CONUP
93 FORMAT(1H ,3F12.5,2I10,2I5,F14.6,I5,2(2X,F14.8),I5)
GDKX=ABS(GDKX)
GDKY=ABS(GDKY)
GDKZ=ABS(GDKZ)
GDKM=SQRT(GDKX*GDKX+GDKY*GDKY+GDKZ*GDKZ)
IF(GDKM .LT. 1.E-06) GO TO 500
CALL DENSIT(SWUP,SWDN,EN,NEMAX)
GO TO 320
330 CONTINUE
CCC CALCULATE ENERGY BY DEGENERATE SECOND ORDER K.P PERTURBATION THEORY
331 DO 331 N=LP1,NB
IF(ABS(E(L)-E(N)).LT.DEGCRT) NDEG=NDEG+1
DO 332 N=1,NDEG
NN=N+L-1

```

```

DO 332 M=1,N
MM=M+L-1
HD(N,M)=2.0*(SKX*PX(NN,MM)+SKY*PY(NN,MM)+SKZ*PZ(NN,MM))
IF(N.NE.M) GO TO 333
HD(N,M)=HD(N,M)+E(NN)+SSQ
333 CONTINUE
DO 334 J=1,NB
IF(J.GE.L.AND.J.LT.L+NDEG) GO TO 334
DELE=(E(NN)+E(MM))/2.0-E(J)
SPNJ=SKX*PX(NN,J)+SKY*PY(NN,J)+SKZ*PZ(NN,J)
SPJM=SKX*PX(J,MM)+SKY*PY(J,MM)+SKZ*PZ(J,MM)
HD(N,M)=HD(N,M)+4.0*SPNJ*SPJM/DELE
334 CONTINUE
HD(M,N)=CONJG(HD(N,M))
332 CONTINUE
IUD=2
C
C   CEIG DIAGONALIZES A COMPLEX MATRIX (HD) WITH EIGEN VALUE (FIG)
C   SUBROUTINE CEIG IS NOT INCLUDED IN THIS THESIS
C
CALL CEIG(HD,UX,EIG,NDEG,1.E-7,9000,ITER,IUD,WK,IND,5)
LST=L+NDEG
DO 329 N=1,NDEG
ENG=EIG(N)
LN=L+N-1
GDKX=DEKX(NBKPT,LN)+(DEKX(NBKPT,LN)-DEKX(NPT,LN))/DIVNO
GDKY=DEKY(NBKPT,LN)+(DEKY(NBKPT,LN)-DEKY(NPT,LN))/DIVNO
GDKZ=DEKZ(NBKPT,LN)+(DEKZ(NBKPT,LN)-DEKZ(NPT,LN))/DIVNO
EEW(LN)=ENG
IF(ENG.GT.EMAX) GO TO 320
CONUP=AA*FUP(LN)
CONDN=AA-CONUP
GDKX=ABS(GDKX)
GDKY=ABS(GDKY)
GDKZ=ABS(GDKZ)
GDKM=SQRT(GDKX*GDKX+GDKY*GDKY+GDKZ*GDKZ)
IF(GDKM .LT. 1.E-06) GO TO 500
CALL DENSIT(SWUP,SWDN,EN,NEMAX)
329 CONTINUE
GO TO 320
500 CONTINUE
C
C   CONTRIBUTION FROM CRITICAL POINTS ARE NEGLECTED
C
WRITE(6,84) GDKX,GDKY,GDKZ,NPT,KDX,KDY,KDZ,ENG,L,AA,CUP,NDEG
84 FORMAT(1H ,3F12.5,2I10,2I5,F14.6,I5,2(2X,F14.8),I5,2X,1HC)

```

```

IF(NDEG,NE,1,AND,N,NE,NDEG) GO TO 329
320 CONTINUE
88 FORMAT(3I3,F7.4,2X,12F9.5)
WRITE(3) KDX,KDY,KDZ,WT,(EEW(L),L=1,NB)
WRITE(6,88) KDX,KDY,KDZ,WT,(EFW(L),L=1,NB)
402 CONTINUE
401 CONTINUE
400 CONTINUE
IF(KX+KY+KZ,NE,KL*3/2-2,OR,NTEST,NE,0) GO TO 310
NTEST=1
KDZ=KZ*MAXBP+2
IF(KDZ,LT,0,OR,KDZ,GT,KLDIV) GO TO 310
KDY=KY*MAXBP+2
IF(KDY,LT,0,OR,KDY,GT,KLDIV) GO TO 310
KDX=KX*MAXBP+2
IF(KDX,LT,KDY,OR,KDX,GT,KLDIV) GO TO 310
SKZ=2.0*BDIV*2.0
SKX=SKZ
SKY=SKZ
WRITE(6,312) KDX,KDY,KDZ
312 FORMAT(3I10)
GO TO 315
310 CONTINUE
WRITE(6,45) SUMWT,VNORM,B,NMPT
45 FORMAT(1H0,5X,'SUM OF WEIGHT=',E12.5,10X,'VNORM=',F12.3,10X,
      ='B=',F12.5,10X,'NO POINT=',I10)
76 FORMAT(1H1,3X,'ENERGY',5X,'N(E) UP',5X,'ELEC UP',4X,'N(E) DN',
      ,6X,'ELEC DN',4X,'N(E) U+D',4X,'ELEC U+D')
44 FORMAT(1H ,F10.5,11F11.4)
998 WRITE(6,76)
DENHU=0.0
DENHD=0.0
DENC=0.0
DO 296 NE=1,NEMAX
DENHU=DENHU+SWUP(NE)*DE
DENHD=DENHD+SWDN(NE)*DE
SWT=SWUP(NE)+SWDN(NE)
ELECT(NE)=DENHU+DENHD
DMAG=DENHU-DENHD
WRITE(6,44) EN(NE),SWUP(NE),DENHU,SWDN(NF),DENHD,SWT,ELECT(NE),
& DMAG
296 CONTINUE
DO 11000 I=2,NEMAX
K=I-1
IF(ELECT(K),LT,VALEL,AND,ELECT(I),GT,VALEL) FERMIE=EN(I)-
=DE*(ELECT(I)-VALEL)/(ELECT(I)-ELECT(K))

```

```
11000 CONTINUE
      WRITE(6,12351) FERMIE
12351 FORMAT(1X,/,1X,'FERMIE ENERGY=',F10.5)
      NEMAX2=NEMAX+2
      CALL SPLOTE(SWDN,SWUP,FN,NEMAX,EMIN,DE,FERMIE,NEMAX2)
      STOP
      END
```

```

C PROGRAM 11 THE INTERBAND OPTICAL CONDUCTIVITY TENSOR
C ****
C CALCULATE THE INTERBAND OPTICAL CONDUCTIVITY BY THE HYBRIDE METHOD
C KL=DIVISION BETWEEN K=(0,0,0) AND K=2*PI/A(1,0,0)
C NB=NUMBER OF STATES STORED FOR THE MOMENTUM MATRICES
C A=LATTICE CONSTANT
C EMIN=MINIMUM OF ENERGY
C NEMAX=TOTAL NUMBER OF POINTS WHERE DENSITY OF STATES NEED TO BE CALCULATED
C DE=STEP SIZE IN ENERGY
C DEGCRIT=DEGENERATE CRITERIAL USED IN K.P PERTURBATION THEORY
C NKPT=NUMBER OF POINTS IN THE BRILLIOUIN ZONE
C EPERC=NUMBER OF ATOMS PER LATTICE
C DIMENSION PX(PX(78),PY(78),PZ(78))
C ****
COMPLEX*8 PX(78),PY(78),PZ(78)
INTEGER*2 NP(18,18,18),KXX(1357),KYY(1357),KZZ(1357)
DIMENSION SWXX(352),SWXY(352),SWZZ(352),EN(352),SWJON(352)
DIMENSION EE(12),DEX(12),DEY(12),DEZ(12)
DIMENSION NABP(3)
DIMENSION PZPZ(2078,12)
COMMON/LCS/PXPX(2078,12),PXPY(2078,12)
COMMON/AR/FNG,GDKX,GDKY,GDKZ,GDKM,B2,BDIV,CONXX,CONXY,CONZZ,CONST
READ(5,10) KL,NB,A,EMIN,DE,FERMIE,DEGCRIT,NEMAX,NKPT,NKSUM
10 FORMAT(2I5,5F10.5,4I5)
NABPMX=1
MAXBP=2*NABPMX+1
DO 111 N=1,MAXBP
111 NABP(N)=N-NABPMX-1
KLDIV=KL*MAXBP
MAXBP=1
WRITE(6,11) KL,NB,A,EMIN,DE,FERMIE,DEGCRIT,NEMAX,NKPT,MAXBP,NKSUM
11 FORMAT(1H , 'KX-LENGTH=' , I2.5X,'NO.OF BANDS=' , I2.5X,'LATTICE CONSTA
INT=' , F6.3 , ' A' , 5X,'EMIN=' , F8.5,3X,'DE=' , F8.5,5X,'FERMIE=' , F8.5,/
2/.1X,'DEG CRT=' , F7.5,5X,'NO OF DE=' , I5.5X,'NO OF PT=' , I5.5X,'SUB D
3IV=' , I5.5X,'DIM K PTS=' , I5,1//)
PI=3.141592653589793
PIKL=PI/KL
DIVNO=FLOAT(MAXBP)
VNORM=(A/(2.*PI))**3/4.
B=PIKL/A
BDIV=B/DIVNO
KLD2=KL/2
TWO8=B*2.0
B2=BDIV*BDIV
KLDMAX=KLDIV*3/2

```

```

C READ MOMENTUM MATRICES AND ORDER POINTS IN THE B. Z.
C
DO 1 NPT=1,NKPT
READ(1) XK,YK,ZK,(PX(I),PY(I),PZ(I),I=1,78)
IF(KL.NE.8) GO TO 2351
XK=XK/2.0
YK=YK/2.0
ZK=ZK/2.0
2351 CONTINUE
I=IFIX(XK)+1
J=IFIX(YK)+1
K=IFIX(ZK)+1
KXX(NPT)=I-1
KYY(NPT)=J-1
KZZ(NPT)=K-1
NP(1,J,K)=NPT
NP(J,1,K)=NPT
1 CONTINUE
REWIND 1
DO 299 NE=1,NEMAX
SWXX(NE)=0.0
SWXY(NE)=0.0
SWZZ(NE)=0.0
SWJON(NE)=0.0
EN(NE)=EMIN+DE*(NE-1)
299 CONTINUE
EMAX=EN(NEMAX)
MAXBP=3
DO 311 LG=1,NB
DO 30 NPT=1,NKPT
READ(1) XK,YK,ZK,(PX(I),PY(I),PZ(I),I=1,78)
DO 30 LL=1,LG
IJ=LG*(LG-1)/2+LL
PXPX(NPT,LL)=REAL(PX(IJ)*CONJG(PX(IJ))+PY(IJ)*CONJG(PY(IJ)))*8.0
PZPZ(NPT,LL)=REAL(PZ(IJ)*CONJG(PZ(IJ))+PZ(IJ)*CONJG(PZ(IJ)))*8.0
PXPY(NPT,LL)=AIMAG(PX(IJ)*CONJG(PY(IJ)))*16.0
30 CONTINUE
C DEFINE NEIGHBORING POINTS FOR K LIES ON THE SURFACE OF 1/16TH OF THE B. Z.
C
KL2=KL+2
CALL GNRPT(PXPX,PXPY,PZPZ,NKSUM,NB,NP,KL2,NKPT,LG)
SUMWT=0.0
NMPT=0
NCRIT=0

```

```

DO 310 NPT=1,NKPT
KX=KXX(NPT)
KY=KYY(NPT)
KZ=KZZ(NPT)
NTEST=0
C
C SUBDIVIDE EACH CUBE IN THE B. Z. INTO 27 MINICELLS
C
DO 400 IDZ=1,MAXBP
KDZ=MAXBP*KZ+NABP(IDZ)
IF(KDZ.LT.0.OR.KDZ.GT.KLDIV) GO TO 400
KNZ=KZ+NABP(IDZ)+1
SKZ=FLOAT(NABP(IDZ))*BDIV*2.0
DO 401 IDY=1,MAXBP
KDY=MAXBP*KY+NABP(IDY)
IF(KDY.LT.0.OR.KDY.GT.KLDIV) GO TO 401
KNY=KY+NABP(IDY)+1
SKY=FLOAT(NABP(IDY))*BDIV*2.0
DO 402 IDX=1,MAXBP
KDX=MAXBP*KX+NABP(IDX)
IF(KDX.LT.KDY.OR.KDX.GT.KLDIV) GO TO 402
KNX=KX+NABP(IDX)+1
SKX=FLOAT(NABP(IDX))*BDIV*2.0
315 CONTINUE
KTOL=KDX+KDY+KDZ
IF(KTOL.GT.KLDMAX) GO TO 402
NBKPT=NP(KNX,KNY,KNZ)
NMPT=NMPT+1
C
C READ IN ENERGIES AND ENERGY DERIVATIVES CALCULATED IN PROGRAM 10.
C
READ(2) NDX,NDY,NDZ,WT,(EE(I),DEX(I),DEY(I),DEZ(I),I=1,NB)
SUMWT=SUMWT+WT
SSQ=SKX*SKX+SKY*SKY+SKZ*SKZ
CONST=16.0*WT*VNORM
GDKM=SQRT(DEX(1)*DEX(1)+DEY(1)*DEY(1)+DEZ(1)*DEZ(1))
IF(GDKM.LT.1.E-5) NCRT=NCRT+1
IF(SSQ.NE.0.0) GO TO 402
DO 320 LL=1,LG
IF(EE(LG).LT.FERMIE.OR.EE(LL).GT.FERMIE) GO TO 320
ENG=EE(LG)-EE(LL)
IF(ENG.GT.EMAX) GO TO 320
GDKX=ABS(DEX(LG)-DEX(LL))
GDKY=ABS(DEY(LG)-DEY(LL))
GDKZ=ABS(DEZ(LG)-DEZ(LL))
CONXX=PXPX(NPT,LL)*WT

```

```

CONXY=PXPY(NPT,LL)*WT
CONZZ=PZPZ(NPT,LL)*WT
IF(SSQ.EQ.0.0) GO TO 32
CONXX=CONXX+(PXPX(NBKPT,LL)-PXPX(NPT,LL))*WT/DIVNO
CONXY=CONXY+(PXPY(NBKPT,LL)-PXPY(NPT,LL))*WT/DIVNO
CONZZ=CONZZ+(PZPZ(NBKPT,LL)-PZPZ(NPT,LL))*WT/DIVNO
32 CONTINUE
83 FORMAT(1H ,3F12.5,2I10,2I5,F14.6,I5,2(2X,F14.8),I5)
GDKM=SORT(GDKX*GDKX+GDKY*GDKY+GDKZ*GDKZ)
IF(GDKM .LT. 1.E-05) GO TO 500
CALL CONDUC(SWXX,SWXY,SWZZ,SWJDN,EN,NEMAX)
GO TO 320
500 CONTINUE
C
C      CONTRIBUTION FROM CRITICAL POINTS ARE NEGLECTED
C
84 FORMAT(1H ,3F12.5,2I10,2I5,F14.6,2I5,F12.5,2X,'C')
320 CONTINUE
402 CONTINUE
401 CONTINUE
400 CONTINUE
IF(KX+KY+KZ,NE,KL*3/2-2,OR,NTEST.NE.0) GO TO 310
NTEST=1
KDZ=KZ*MAXBP+2
IF(KDZ.LT.0,OR,KDZ.GT.KLDIV) GO TO 310
KDY=KY*MAXBP+2
IF(KDY.LT.0,OR,KDY.GT.KLDIV) GO TO 310
KDX=KX*MAXBP+2
IF(KDX.LT.KDY,OR,KDX.GT.KLDIV) GO TO 310
SKZ=2.0*BDIV*2.0
SKX=SKZ
SKY=SKZ
GO TO 315
310 CONTINUE
REWIND 2
REWIND 1
311 CONTINUE
WRITE(6,45)SUMWT,VNORM,B,NMPT,NCRIT
45 FORMAT(1X,'SUM OF WEIGHT=',E12.5,5X,'VNORM=',F12.3,5X,'B=',F12.5,
      '5X,'NO OF POINT=',I8,5X,'NO OF CRT=',I5,/)
RYTOW=13.6049*I.602191D-19*I2.0*PI/6.626196D-34
CONST=3.D10/(PI*PI*274.074*5.2917D-9)
DO 701 NE=1,NEMAX
CC=CONST/EN(NE)
SWXX(NE)=SWXX(NE)*CC

```

```
SWXY(NE)=SWXY(NE)*CC
SWZZ(NE)=SWZZ(NE)*CC
EA=EN(NE)
EN(NE)=EN(NE)*13.6049
WRITE(6,702) EA,EN(NE),SWXX(NE),SWXY(NE),SWZZ(NE),SWJON(NE)
WRITE(7,703) EN(NE),SWXX(NE),SWXY(NE),SWZZ(NE),SWJON(NE)
701 CONTINUE
702 FORMAT(2F7.3,9(1X,E10.4),2F9.4)
703 FORMAT(5(E14.8,1X))
STOP
END
```

```

C PROGRAM 12. COMPTON PROFILE.
C ****
C ACONST=LATTICE CONSTANT (IN A. U.)
C EXPCVG=CONVERGENT CRITERIAL EXP(-EXPCVG)=0.0
C IDCUB=NUMBER OF ATOMS PER LATTICE
C K2MAX=THE MAXIMUM MAGNITUDE OF THE SQUARE OF THE RECIPROCAL LATTICE VECTOR
C IBZDIV=DIVISION BETWEEN K=(0,0,0) AND K=(1.0,C)*2*PI/A
C IGBTNO=GTO NUMBER &=S, P, D
C IEATOM=ATOMIC BASIS NO. IEATOM=0 IF INDEPENDENT GTO ARE USED
C KSTOL=TOTAL NUMBER OF THE PERMUTED R.L.V. GENERATED
C KSINC=NUMBER OF R.L.V. SUMED IN EACH STEP.
C KSSTEP=NUMBER OF STEP FOR EACH GIVEN VALUE OF Q.
C INCIS=0. THE IS ELECTRONS ARE NOT INCLUDED.
C ****
C IMPLICIT REAL *8 (A-F,H,O-Z)
C REAL*4 EUP(38),EDN(38)
C INTEGER*2 KXX(3000),KKY(3000),KKZ(3000)
C DIMENSION XUP(38,38),XDN(38,38),UP(38),GX(38,38)
C DIMENSION KSQU(3000)
C DIMENSION XK(89),YK(89),ZK(89)
C DIMENSION ALS(14),ALP(11),ALD(5),COS(14),COP(11),COD(5),CS(4,14),
C &CP(3,11),CD(5,5)
C COMMON/GTO/CRYSTL,PI,ISATOM,IPATOM,IDATOM
C COMMON/LCS/KSQU
C COMMON/COMP/PX,PY,PZ,OMEGA,EXPCVG,LSST,LSEND,LPST,LPEND,LDST,LDEND
C PI=3.141592653589793
51 FORMAT(2X,A8,3F10.5,8I5)
READ(5,51) CRYSTL,ACONST,FERMIE,EXPCVG,IDCUB,IBZDIV,NKPT,KSTOL,
&KSINC,KSSSTEP,K2MAX,INCIS
WRITE(6,52) ACONST,FERMIE,IDCUB,IBZDIV,NKPT,K2MAX,KSTOL
OMEGA=ACONST*#3/DFLOAT(IDCUB)
DIV=DFLOAT(IBZDIV)

C DEFINE GAUSSIAN EXPONENTS AND EXPANSION COEFFICIENTS

4 FORMAT(8I5)
READ(5,4) ISOBNO,ISATOM,IPOBNO,IPATOM,IDOBN0,IDATOM
LSMAX=ISOBNO
LDMAX=IDOBN0
LPMAX=IPOBNO
IF(ISATOM.NE.0) LSMAX=ISATOM
IF(IDATOM.NE.0) LDMAX=IDATOM
IF(IPATOM.NE.0) LPMAX=IPATOM
CALL RDGTO(ALS,ALP,ALD,COS,COP,COD,CS,CP,CD,ISOBNO,LSMAX,IPOBNO,
&LPMAX,IDOBN0,LDMAX,1)

```

```

LDST=1
LDEND=LDMAX*5
LSST=LDEND+1
LSEND=LDEND+LSMAX
LPST=LSEND+1
LPEND=LSEND+LPMAX*3
PRINT 59
59 FORMAT(1H1)
C
C
C   GENERATE PERMUTED RECIPROCAL LATTICE VECTORS
C
CALL GPERMK(KKX,KKY,KKZ,KSTRU,KSTOL,1DCUR,K2MAX,1)
NCEND=LPEND
NCST=NCEND-8
NBEND=NCST-1
NBST=NBEND-5
IF(INC1S.EQ.0) NCEND=NCEND-1
NB=LPEND
WRITE(6,52) ACONST,FERMIE,1DCUB,IBZDIV,NKPT,K2MAX,KSTOL,LSMAX
E,ISOBNO,LPMAX,IPOBNO,LDMAX,1DORNO,EXPCVG,NBST,NBEND,NCST,NCEND
2,INC1S
52 FORMAT(1X,'LATTICE CONST=',F10.5,2X,'FERMI E=',F10.5,2X,'ATOMS/LAT
1TICE=',I5.2X,'B.Z. DIV=',I5.2X,'B.Z. PT=',I5.2X,'MAX K**2=',I5.
22X,'RLV NO=',I5,//,1X,'S=(',I5.2I5,')',2X,'P=(',I5.2I5,')',2X,'D=(',I5.
3,')',5X,'EXP MAX=',F10.2,//,1X,'BAND=(',I5.2I5,')',2X,'CORE=',I5.2I5
4.2X,'INCLUDE IS=',I5.//)
62 FORMAT(15.3F10.1)
ID100=100
ID110=110
ID111=111
AKR=2.00*PI/ACONST
CK=AKR/DIV
QROERR=CK*0.001
C
C
C   CONG IS INVERSELY PROPORTIONAL TO THE CROSS SECTIONAL AREA OF EACH CJRF ON
C   THE PLANE PERPENDICULAR TO E DIRECTION. E=X (1,0,0), E=N (1,1,0), E=L (1,1,1)
C
CONX=OMEGA*4.00/(PI*(ACONST*DIV)**2)
CONN=CONX/DSQRT(2.00)
CONL=CONX*0.75D0*DSQRT(3.00)
IF(1DCUB.NE.1) CO=DFLOAT(1DCUB)/8.00
IF(1DCUB.EQ.1) CO=1.00
TW=(2.00*DIV)**3*CO/48.00
90 FORMAT(F10.5,15)
C
C   Q IS A INTEGER MULTIPLE OF THE STEP SEIZE ALLOWED BY THE DIVISION

```

```

C   IN THE BRILLOUIN ZONE.
C   IF(IPUNCH.NE.0) RESULTS ARE PUNCHED.

C   IQ=0
91  CONTINUE
READ(5,90,END=1000) Q,IPUNCH
Q=Q*CK
IQ=IQ+1
COMPXV=0.00
COMPXC=0.00
COMPNC=0.00
COMPNV=0.00
COMPLC=0.00
COMPLV=0.00

C   SUM OVER R.L.V. IN SEVERAL STEPS TO CHECK CONVERGENCE.

KSST=1
DO 900 KSJUM=1,KSSTEP
KSEND=KSST+KSINC
SUMW=0.00
DO 100 KPT=1,NKPT

C   READ K, WEIGHT FACTORS, ENERGIES, AND WAVE FUNCTIONS NEGLECTING THE EFFECT
C   OF SPIN-ORBIT COUPLING.

READ(1) KX,KY,KZ,GT,(EUP(I),GX(JJ,I),JJ=1,NB),I=1,NB)
DO 173 II=1,NB
DO 173 JJ=1,NB
173 XUP(I,J)=GX(I,J)
READ(2) KX,KY,KZ,GT,(EDN(I),GX(JJ,I),JJ=1,NB),I=1,NB)
DO 174 II=1,NB
DO 174 JJ=1,NB
174 XDN(I,J)=GX(I,J)
XK(KPT)=DFLOAT(KX)*CK
YK(KPT)=DFLOAT(KY)*CK
ZK(KPT)=DFLOAT(KZ)*CK
WT=GT
SUMW=SUMW+WT
170 CONTINUE
DO 200 KS=KSST,KSEND
PX=XK(KPT)+AKR*KXX(KS)
PY=YK(KPT)+AKR*KKY(KS)
PZ=ZK(KPT)+AKR*KKZ(KS)

C   SELECT K POINTS THAT SATISFY THE MOMENTUM CONSERVATION RELATION.

```

```

C
IPX=0
IF(DABS(PX-Q).LT.QROERR) IPX=IPX+1
IF(DABS(PY-Q).LT.QROERR) IPX=IPX+1
IF(DABS(PZ-Q).LT.QROERR) IPX=IPX+1
IF(DABS(PX+Q).LT.QROERR) IPX=IPX+1
IF(DABS(PY+Q).LT.QROERR) IPX=IPX+1
IF(DABS(PZ+Q).LT.QROERR) IPX=IPX+1
IPN=0
IF(DABS(Q-PX-PY).LT.QROERR) IPN=IPN+1
IF(DABS(Q-PX+PY).LT.QROERR) IPN=IPN+1
IF(DABS(Q+PX-PY).LT.QROERR) IPN=IPN+1
IF(DABS(Q+PX+PY).LT.QROERR) IPN=IPN+1
IF(DABS(Q-PY-PZ).LT.QROERR) IPN=IPN+1
IF(DABS(Q-PY+PZ).LT.QROERR) IPN=IPN+1
IF(DABS(Q+PY-PZ).LT.QROERR) IPN=IPN+1
IF(DABS(Q+PY+PZ).LT.QROERR) IPN=IPN+1
IF(DABS(Q-PZ-PX).LT.QROERR) IPN=IPN+1
IF(DABS(Q-PZ+PX).LT.QROERR) IPN=IPN+1
IF(DABS(Q+PZ-PX).LT.QROERR) IPN=IPN+1
IF(DABS(Q+PZ+PX).LT.QROERR) IPN=IPN+1
IPL=0
IF(DABS(Q-PX-PY-PZ).LT.QROERR) IPL=IPL+1
IF(DABS(Q+PX-PY-PZ).LT.QROERR) IPL=IPL+1
IF(DABS(Q-PX+PY-PZ).LT.QROERR) IPL=IPL+1
IF(DABS(Q+PX+PY-PZ).LT.QROERR) IPL=IPL+1
IF(DABS(Q-PY+PY+PZ).LT.QROERR) IPL=IPL+1
IF(DABS(Q+PY+PY+PZ).LT.QROERR) IPL=IPL+1
IF(DABS(Q-PX+PY+PZ).LT.QROERR) IPL=IPL+1
IF(DABS(Q+PX+PY+PZ).LT.QROERR) IPL=IPL+1
IF(DABS(Q+PY-PY-PZ).LT.QROERR) IPL=IPL+1
IF(DABS(Q+PY+PY-PZ).LT.QROERR) IPL=IPL+1
IF(DABS(Q-PY+PY+PZ).LT.QROERR) IPL=IPL+1
IF(DABS(Q+PY+PY+PZ).LT.QROERR) IPL=IPL+1
IF(IPX.EQ.0.AND.IPN.EQ.0.AND.IPL.EQ.0) GO TO 200
C
C CALCULATE THE FOURIER TRANSFORM OF THE LOCALIZED BASIS FUNCTION.
C
CALL FOURFC(UP,ALS,ALD,CS,CP,CD,ISOBNO,LSMAX,IPORNO,
1LPMAX,LDENO,LDMAX)
SUMCO=0.D0
DO 103 I=NCST,NCEND
SS=0.D0
TT=0.D0
DO 202 JJ=1,NB
SS=SS+XUP(JJ,II)*UP(JJ)
TT=TT+XDN(JJ,II)*UP(JJ)
103 CONTINUE
SUMCO=SUMCO+TT*TT+SS*SS
202 CONTINUE
103 CONTINUE

```

```

EVA=0. DO
SUMVA=0. DO
DO 102 I=NBST*NBEND
IF(FUP(I11).GT.*FERMIE) GO TO 104
TT=0. DO
DO 201 JJ=1,NB
TT=TT+XUP(JJ,I11)*UP(JJ)
201 CONTINUE
SUMVA=SUMVA+TT*TT
104 CONTINUE
IF(EDN(I11).GT.*FERMIE) GO TO 105
TT=0. DO
DO 204 JJ=1,NB
TT=TT+XDN(JJ,I11)*UP(JJ)
204 CONTINUE
SUMVA=SUMVA+TT*TT
105 CONTINUE
102 CONTINUE
COMPC=COMPXC+SUMCO*WT*DFLOAT(IPX)
COMPXV=COMPXV+SUMVA*WT*DFLOAT(IPX)
COMPNV=COMPNV+SUMVA*WT*DFLOAT(IPN)
COMPNC=COMPNC+SUMCO*WT*DFLOAT(IPN)
COMPLC=COMPLC+SUMCO*WT*DFLOAT(IPL)
COMPLV=COMPLV+SUMVA*WT*DFLOAT(IPL)
200 CONTINUE
100 CONTINUE
PROFXC=COMPXC*CONX
PROFNC=COMPNC*CONN
PROFNV=COMPNV*CONN
PROFLC=COMPLC*CONN
PROFLV=COMPLV*CONN
PFX=PROFXC+PROFXV
PFN=PROFNC+PROFNV
PFL=PROFLC+PROFLV
Q110=Q/DSORT(2.0D0)
Q111=0/DSORT(3.0D0)
WRITER(6,111) I0,Q,PFX,PROFXC,PROFXV,Q110,PFN,PROFNC,PROFNV,
Q111,PFL,PROFLC,PROFLV,KSEND
111 FORMAT(13,1X,'O=','F6.3',1X,'J(100)=','F6.3',2X,'( ','2F6.3',0,0,2X,
      'O=','F6.3',1X,'J(110)=','F6.3',2X,'( ','2F6.3',0,1,2X,'K5=','I4)
REWIND 1
REWIND 2
KSST=KSEND+1
900 CONTINUE

```

```
901 CONTINUE
IF(IPUNCH.EQ.0) GO TO 999
WRITE(7,911) Q,PFX,PROFXC,PROFXV,IDL0C
WRITE(7,911) Q110,PFN,PROFNC,PROFNV,IDL110
WRITE(7,911) Q111,PFL,PROFLC,PROFLV,IDL111
911 FORMAT(4E16.8,10X,16)
999 CONTINUE
GO TO 91
1000 CONTINUE
IF(DABS(TW-SUMW).GT.0.1D-5) WRITE(6,5314) TW,SUMW
5314 FORMAT(//,1X,'SUMW=',2F10.6)
STOP
END
```

```

SUBROUTINE CONDUC(SWXX,SWXY,SWZZ,SWJON,EN,NEMAX)
C***** **** * ***** * ***** * ***** * ***** * ***** * ***** * ***** * ***** *
C THE CONTRIBUTION OF EACH MINICELL TO THE CONDUCTIVITY TENSOR
C***** **** * ***** * ***** * ***** * ***** * ***** * ***** * ***** * ***** *
DIMENSION SWXX(NEMAX),SWXY(NEMAX),SWZZ(NEMAX),EN(NEMAX),
1 SWJON(NEMAX)
COMMON/AR/ENG,GDKX,GDKY,GDKZ,GDKM,B2,B,CONXX,CONXY,CONZZ,CONST
ALX=GDKX/GDKM
ALY=GDKY/GDKM
ALZ=GDKZ/GDKM

C
C NOW ARRANGE SUCH THAT ALX .GE. ALY .GE. ALZ
C
IF(ALY .GE. ALZ) GO TO 351
353 ADD=ALY
ALY=ALZ
ALZ=ADD
351 IF(ALX .GE. ALY) GO TO 352
ADD=ALX
ALX=ALY
ALY=ADD
IF(ALY .LT. ALZ) GO TO 353
352 CONTINUE
W1=B*ABS(ALX-ALY-ALZ)
W2=B*(ALX-ALY+ALZ)
W3=B*(ALX+ALY-ALZ)
W4=B*(ALX+ALY+ALZ)
AAXX=CONXX/GDKM
AAXY=CONXY/GDKM
AAZZ=CONZZ/GDKM
AAJON=CONST/GDKM
SMAX=6.5*B2
DEMAX=(ALX+ALY+ALZ)*B*GDKM
DO 300 NE=1,NEMAX
EE=EN(NE)

C CALCULATES AREA OF PLANE OF ENERGY 'E' IN A GIVEN CUBE.
C MAX VALUE OF AREA CAN BE SQRT(3.)*4.*B*B=6.5*B*B, IF S,SMAX,ERROR POINTED
C
DEW=ABS(EE-ENG)
IF(DEW .GT. DEMAX) GO TO 300
W=DEW/GDKM
IF(W .GT. W4) GO TO 300
IF(W .GT. W1) GO TO 360
IF(ALX .LT. ALY+ALZ) GO TO 365
S=4.*B2/ALX

```

```

GO TO 395
365 S=((2.*ALX*(ALY+ALZ)+ALY*ALZ)-1.)*B2-W*W)/(ALX*ALY*ALZ)
GO TO 395
360 CONTINUE
IF(W .GT. W2) GO TO 370
S=(B2*(ALX*(ALY+ALZ)+3.*ALY*ALZ)-8.*W*(ALY+ALZ-ALX)-(W*W+B2)/2.)/
/(ALX*ALY*ALZ)
GO TO 395
370 CONTINUE
IF(W .GT. W3) GO TO 375
S=2.*(B2*(ALX+ALY)-B*W)/(ALX*ALY)
GO TO 395
375 CONTINUE
S=((W4-W)**2)/(2.*ALX*ALY*ALZ)
395 CONTINUE
IF(S .LT. SMAX) GO TO 899
WRITE(6,750)ALX,ALY,ALZ,W1,W2,W3,W4,W,S,NF,NPT
750 FORMAT(1H ,9E12.3,2I5)
899 CONTINUE
SWXX(NE)=SWXX(NE)+S*AAXX
SWXY(NE)=SWXY(NE)+S*AAXY
SWZZ(NE)=SWZZ(NE)+S*AAZZ
SWJON(NE)=SWJON(NE)+S*AAJON
300 CONTINUE
RETURN
END

```

```

SUBROUTINE CNULOM(CHARGE,SUM,RS,FACT)
C **** CALCULATE THE FOURIER COEFFICIENTS OF THE CHARGE DENSITY
C **** IMPLICIT REAL*8(A-F,H,O-Z)
DIMENSION CHARGE(1)
COMMON/CONST/A,RO,PI,ONFTHD
COMMON/VKO/C(7,11),EX(7,11),FACTO(10),IB(7,11),NORR(7),NSTA
RS2=RS*RS2
RS3=RS*RS2
CON=1.00
DO 79 I=1,NSTA
CO2=FACT*CHARGE(I)
NN=NDRB(I)
DO 79 J=1,NN
DO 78 K=J,NN
CO=C(I,J)*C(I,K)*CO2*CON
IAB=IB(I,J)+IB(I,K)-1
E=EX(I,J)*EX(I,K)
EE=E*E
T=E+E+RS
T2=T*T
GO TO (71,72,73,74,75,76,77),IAB
71 SUM=SUM+2.D0*E*CO/T2
70 TO 78
72 SUM=SUM+2.D0*CO*(3.D0*EE-RS)/(T2*T)
73 GO TO 78
74 SUM=SUM+24.D0*E*CO*(EE-RS)/(T2*T2)
75 GO TO 78
76 SUM=SUM+240.D0*CO*E*(3.D0*EE*EE-10.D0*EE*RS+3.D0*RS2)/(T**6)
77 E4=EE*EE
78 SUM=SUM+4.0320.D0*E*CO*(E4*EE-7.D0*E4*RS+21.D0*EE*RS2-RS3)/(T**8)
79 CON=2.D0
CON=1.D0
RETURN
END

```

```

SUBROUTINE DENSIT(SWUP, SWDN, EN, NEMAX)
C*****CALCULATE THE CONTRIBUTION TO THE DENSITY OF STATES*****
C*****DIMENSION SWUP(NEMAX), SWDN(NEMAX), EN(NEMAX)
COMMON/AR/ENG, GDX, GDY, GDZ, GDM, B2, B, CONUP, CONDN
ALX=GDX/GDM
ALY=GDY/GDM
ALZ=GDZ/GDM
C NOW ARRANGE SUCH THAT ALX .GE. ALY .GE. ALZ
IF(ALY .GE. ALZ) GO TO 351
353 ADD=ALY
ALY=ALZ
ALZ=ADD
351 IF(ALX .GE. ALY) GO TO 352
ADD=ALX
ALX=ALY
ALY=ADD
IF(ALY .LT. ALZ) GO TO 353
352 CONTINUE
W1=B*ABS(ALX-ALY-ALZ)
W2=B*(ALX-ALY+ALZ)
W3=B*(ALX+ALY-ALZ)
W4=B*(ALX+ALY+ALZ)
AAUP=CONUP/GDM
AADN=CONDN/GDM
SMAX=6.5*B2
DEMAX=(ALX+ALY+ALZ)*B*GDM
C CALCULATES AREA OF PLANE OF ENERGY 'E' IN A GIVEN CUBE.
MAX VALUE OF AREA CAN BE SQRT(3.)*4.*B*B=6.5*B*B, IF S>SMAX, ERROR PRINTED
DO 300 NE=1,NEMAX
EE=EN(NE)
DEW=ABS(EE-ENG)
IF(DEW .GT. DEMAX) GO TO 300
W=DEW/GDM
IF(W .GT. W4) GO TO 300
IF(W .GT. W1) GO TO 360
IF(ALX .LT. ALY+ALZ) GO TO 365
S=4.*B2/ALX
GO TO 395
365 S=((2.*(ALX*(ALY+ALZ)+ALY*ALZ)-1.)*B2-W*W)/(ALX*ALY*ALZ)
GO TO 395
360 CONTINUE
IF(W .GT. W2) GO TO 370

```

```

S=(B2*(ALX*(ALY+ALZ)+3.*ALY*ALZ)-B*w*(ALY+ALZ-ALX)-(W*w+B2)/2.)
1/(ALX*ALY*ALZ)
GO TO 395
370 CONTINUE
IF(W .GT. W3) GO TO 375
S=2.*(B2*(ALX+ALY)-B*w)/(ALX*ALY)
GO TO 395
375 CONTINUE
S=((W4-W)**2)/(2.*ALX*ALY*ALZ)
395 CONTINUE
IF(S .LT. SMAX) GO TO 899
WRITE(6,750)ALX,ALY,ALZ,W1,W2,W3,W4,W,S,NF,NPT
750 FORMAT(1H ,9E12.3,2I5)
899 CONTINUE
SWUP(NE)=SWUP(NE)+S*AAUP
SWDN(NE)=SWDN(NE)+S*AADN
300 CONTINUE
RETURN
END

```

```

SUBROUTINE FOURFC(UP,ALS,ALP,ALD,CS,CP,CD,ISOBNO,LSMAX,IPOBNO,
ILPMAX,IDOBN0,LDMAX)
C*****CALCULATE THE FOURIER TRANSFORM OF THE LOCALIZED BASIS FUNCTION.
C*****IMPLICIT REAL *8 (A-F,H,O-Z)
DIMENSION UP(1),ALS(1),ALP(1),ALD(1),
&CS(LSMAX,ISOBNO),CP(ILPMAX,IPOBNO),CD(LDMAX,IDOBN0)
COMMON/COMP/PX,PY,PZ,OMEGA,EXPCVG,LSST,LSEND,LPST,LPFND,LDST,LDEND
PI=3.141592653589793
DO 10 I=1,LPEND
10 UP(I)=0.0D0
CC=1.0D0/DSQRT(OMEGA)
PP=PX*PX+PY*PY+PZ*PZ
C
C      S-FUNCTIONS
C
DO 20 NS=1,ISOBNO
DEL=PP/(4.0D0*ALS(NS))
IF(DEL.GT.EXPCVG) GO TO 20
DEL=DEXP(-DEL)
SLAM=PI/ALS(NS)
CONST=CC*SLAM*DSQRT(SLAM)*DEL
DO 21 IS=1,LSMAX
II=IS+LDEND
21 UP(II)=UP(II)+CONST*CS(IS,NS)
20 CONTINUE
C
C      P-FUNCTIONS
C
DO 30 NP=1,IPOBNO
DEL=PP/(4.0D0*ALP(NP))
IF(DEL.GT.EXPCVG) GO TO 30
DEL=DEXP(-DEL)
SLAM=PI/ALP(NP)
CONST=-CC*SLAM*DSQRT(SLAM)*DEL/(2.0*ALP(NP))
DO 31 IP=1,ILPMAX
PCO=CONST*CP(IP,NP)
II=3*(IP-1)
IX=II+LSEND+1
IY=II+LSEND+2
IZ=II+LSEND+3
UP(IX)=UP(IX)+PCO*PX
UP(IY)=UP(IY)+PCO*PY
UP(IZ)=UP(IZ)+PCO*PZ
31 CONTINUE

```

```

30 CONTINUE
C
C      D-FUNCTIONS
C
      PXY=PX*PY
      PYZ=PY*PZ
      PZX=PZ*PX
      PX2=(PX*PX-PY*PY)/2.00
      PZ2=(3.00*PZ*PZ-PP)/(2.00*DSQRT(3.00))
      DO 40 ND=1,100
      DEL=PP/(4.00*ALD(ND))
      IF(DEL.GT.EXPCVG) GO TO 40
      DEL=DEXP(-DEL)
      SLAM=PI/ALD(ND)
      CONST=-CC*SLAM*DSQRT(SLAM)*DEL/(4.00*ALD(ND)*ALD(ND))
      DO 41 ID=1,LDMAX
      DCO=CONST*CD(ID,ND)
      NDXY=ID
      NDYZ=NDXY+LDMAX
      NDZX=NDYZ+LDMAX
      NDX2=NDZX+LDMAX
      NDZ2=NDX2+LDMAX
      UP(NDXY)=UP(NDXY)+DCO*PXY
      UP(NDYZ)=UP(NDYZ)+DCO*PYZ
      UP(NDZX)=UP(NDZX)+DCO*PZX
      UP(NDX2)=UP(NDX2)+DCO*PX2
      UP(NDZ2)=UP(NDZ2)+DCO*PZ2
41  CONTINUE
40  CONTINUE
      RETURN
      END

```

```

SUBROUTINE FUNCT(M)
C *****
C Y IS REPLACED BY (OV**-1) Y
C (KK,I,J)=2*M*(J-1)+2*(I-1)+KK
C (KK,N,J)=2*M*(J-1)+2*(N-1)+KK
C *****
REAL*8 Y,OV
COMMON/B/Y(11552)
COMMON/C/OV(2926)
M2=M*2
DO 100 I=1,M
II=M+1-I
LL=II*(II+1)/2
II2=2*(II-1)
DO 100 J=1,M
DO 100 KK=1,2
JKK=M2*(J-1)+KK
KKIJ=JKK+II2
IF(II.EQ.M) GO TO 102
I1=II+1
DO 101 N=I1,M
IN=N*(N-1)/2+II
KKNJ=JKK+2*(N-1)
Y(KKIJ)=Y(KKIJ)-OV(IN)*Y(KKNJ)
101 CONTINUE
102 CONTINUE
Y(KKIJ)=Y(KKIJ)/OV(LL)
100 CONTINUE
RETURN
END

```

```

SUBROUTINE GBZPT(KBX,KBY,KBZ,WT,KPT,IDCUB,KBZPT,TW)
C*****SC IDCUB=1, RCC IDCUB=2, FCC IDCUB=4
C*****WT=THE FRACTION OF EACH CURE CENTERED AT EACH (KBX,KBY,KBZ) THAT LIES
C*****WITHIN THE INDEPENDENT 1/48TH OF THE B. Z.
C*****TW=SUMW=THE SUM OF WT IN THE 1/48TH OF THE ZONE
C*****KPT=TOTAL NO OF POINTS GENERATED
C*****
REAL*8 W,SUMW,WT(1),TW
INTEGER*2 KBX(1),KBY(1),KBZ(1)
KPT=0
KL=KBZPT-1
SUMW=0.D0
IF(IDCUB.NE.4) GO TO 110
DO 100 II=1,KBZPT
DO 100 JJ=1,II
DO 100 KK=1,JJ
KX=II-1
KY=JJ-1
KZ=KK-1
KT=KX+KY+KZ
KM=KL*3/2
IF(KT.GT.KM) GO TO 100
KPT=KPT+1
W=1.D0
IF(KT.EQ.KM) W=W*0.5D0
IF(KX.EQ.KL) W=W*0.5D0
IF(KX.EQ.0) W=W*0.5D0
IF(KY.EQ.0) W=W*0.5D0
IF(KZ.EQ.0) W=W*0.5D0
IF(KX.EQ.KY.OR.KY.EQ.KZ) W=W*0.5D0
IF(KX.EQ.KZ) W=W/3.D0
KBX(KPT)=KX
KBY(KPT)=KY
KBZ(KPT)=KZ
WT(KPT)=W
6 FORMAT(4I5,F10.5)
WRITE(6,6) KPT,KX,KY,KZ,W
SUMW=SUMW+W
100 CONTINUE
GO TO 310
110 IF(IDCUB.NE.2) GO TO 210
KPT=0
DO 200 II=1,KBZPT
DO 200 JJ=1,II
DO 200 KK=1,JJ

```

```

KX=II-1
KY=JJ-1
KZ=KK-1
KT=KX+KY+KZ
KM=KL*3/2
IF(KT.GT.KM) GO TO 200
KXY=KX+KY
IF(KXY.GT.KL) GO TO 200
KPT=KPT+1
W=1.0D0
IF(KX.EQ.KL) W=W*0.500
IF(KX.EQ.0) W=W*0.500
IF(KY.EQ.0) W=W*0.500
IF(KZ.EQ.0) W=W*0.500
IF(KX.EQ.KY.OR.KY.EQ.KZ) W=W*0.500
IF(KX.EQ.KZ) W=W/3.0D0
KYZ=KY+KZ
IF(KXY.EQ.KL.AND.KYZ.EQ.KL.AND.KY.NE.KL/2) W=W/3.0D0
KBX(KPT)=KX
KBY(KPT)=KY
KBZ(KPT)=KZ
WT(KPT)=W
SUMW=SUMW+W
200 CONTINUE
GO TO 310
210 IF(IDCUB.NE.1) STOP 3
KPT=0
DO 300 II=1,KBZPT
DO 300 JJ=1,II
DO 300 KK=1,JJ
KX=II-1
KY=JJ-1
KZ=KK-1
KPT=KPT+1
W=1.0D0
IF(KX.EQ.KL) W=W*0.500
IF(KY.EQ.KL) W=W*0.500
IF(KZ.EQ.KL) W=W*0.500
IF(KX.EQ.0) W=W*0.500
IF(KY.EQ.0) W=W*0.500
IF(KZ.EQ.0) W=W*0.500
IF(KX.EQ.KY.OR.KY.EQ.KZ) W=W*0.500
IF(KX.EQ.KZ) W=W/3.0D0
KBX(KPT)=KX
KBY(KPT)=KY
KBZ(KPT)=KZ

```

```
WT(KPT)=W
SUMW=SUMW+W
300 CONTINUE
310 CONTINUE
IF(IDCUB.NE.1) CO=DFLOAT(IDCUB)/8.00
IF(IDCUB.EQ.1) CO=1.00
TW=(2.00*DFLOAT(KL))**3*CO/48.00
IF(TW.EQ.SUMW) RETURN
400 FORMAT(1X,'ATOMS/LATTICE=',I3.5X,'SUM OF WT=',2F12.6,/)
WRITE(6,400) IDCUB,SUMW,TW
RETURN
END
```

```

SUBROUTINE GINDPK(KKX,KKY,KKZ,KSQ,NKPT, IDCUB, K2MAX, NB, NBCAL, ISORT)
C***** ****
C GENERATE INDEPENDENT RECIPROCAL LATTICE VECTORS WITH MAGNITUDE SQUARE LESS
C THAN K2MAX
C IF( ISORT.NE.0) THE RECIPROCAL LATTICE VECTORS ARE SORTED IN ORDER OF
C INCREASING MAGNITUDE
C IF(NBCAL.NE.0) NO OF PERMUTATION FOR EACH VECTOR (NB) ARE GENERATED
C   SC IDCUB=1, BCC IDCUB=2, FCC IDCUB=4
C*****
INTEGER*2 KKX(1),KKY(1),KKZ(1),NB(1),N
DIMENSION KSQ(1)
G=K2MAX
MAXKX=SQRT(G)+2
KPT=0
IF(IDCUB.NE.4) GO TO 200
DO 100 III=1,MAXKX,2
DO 100 JJJ=1,III,2
DO 100 KKK=1,JJJ,2
KX=III-1
KY=JJJ-1
KZ=KKK-1
DO 100 MMM=1,2
K2=KX*KX+KY*KY+KZ*KZ
IF(K2.GT.K2MAX) GO TO 101
KPT=KPT+1
IF(KPT.GT.NKPT) STOP 1
IPT=KPT
IF(KPT.EQ.1.OR.ISORT.EQ.0) GO TO 103
IM=KPT-1
IF(K2.GE.KSQ(IM)) GO TO 103
III=KPT
102 KKX(II)=KKX(IM)
KKY(II)=KKY(IM)
KKZ(II)=KKZ(IM)
KSQ(II)=KSQ(IM)
II=II-1
IM=II-1
IF(K2.LT.KSQ(IM)) GO TO 102
IPT=II
103 KKX(IPT)=KX
KKY(IPT)=KY
KKZ(IPT)=KZ
KSQ(IPT)=K2
101 CONTINUE
KX=KX+1
KY=KY+1

```

```

      KZ=KZ+1
100  CONTINUE
      GO TO 300
200  CONTINUE
      DO 201 III=1,MAXXX
      DO 201 JJJ=1,III
      DO 201 KKK=1,JJJ
      ITOL=III+JJJ+KKK-3
      IF (ITOL.NE.(ITOL/2)*2.AND.IDCUB.EQ.2) GO TO 201
      KX=III-1
      KY=JJJ-1
      KZ=KKK-1
      K2=KX*KX+KY*KY+KZ*KZ
      IF(K2.GT.K2MAX) GO TO 201
      KPT=KPT+1
      IF(KPT.GT.NKPT) STOP 1
      IPT=KPT
      IF(KPT.EQ.1.OR.ISORT.EQ.0) GO TO 203
      IM=KPT-1
      IF(K2.GE.KSQ(IM)) GO TO 203
      II=KPT
202  KKX(II)=KKX(IM)
      KKY(II)=KKY(IM)
      KKZ(II)=KKZ(IM)
      KSQ(II)=KSQ(IM)
      II=II-1
      IM=II-1
      IF(K2.LT.KSQ(IM)) GO TO 202
      IPT=II
203  KKX(IPT)=KX
      KKY(IPT)=KY
      KKZ(IPT)=KZ
      KSQ(IPT)=K2
201  CONTINUE
300  CONTINUE
      NKPT=KPT
      IF(NBCAL.EQ.0) RETURN
      DO 500 I=1,NKPT
      KX=KKX(I)
      KY=KKY(I)
      KZ=KKZ(I)
      N=48
      IF(KX.EQ.0) N=N/2
      IF(KY.EQ.0) N=N/2
      IF(KZ.EQ.0) N=N/2
      IF(KX.EQ.KY.OR.KY.EQ.KZ) N=N/2

```

```
IF(KX.EQ.KZ) N=N/3  
NB(I)=N  
500 CONTINUE  
RETURN  
END
```

```

SUBROUTINE GINTFC(FCS,NORD,NORDIM,NKDIM,NRDIM)
C***** **** * **** * **** * **** * **** * **** * **** * **** * **** * **** *
C   GENERATE FUNCTION G(N,K,R) DEFINED IN EQ. (2.44)
C***** **** * **** * **** * **** * **** * **** * **** * **** * **** * **** *
      IMPLICIT REAL *8 (A-F,H,O-Z)
      DIMENSION FCS(NORDIM,NKDIM,NRDIM)
      DIMENSION H(10),F(10)
      COMMON/GFUC/AKR,W,DELT,W04,DSTEP,MAXK,MAXR
      NOOD=(NORD/2)*2
      IF(NOOD.EQ.NORD) NEVEN=NORD-1
      IF(NOOD.NE.NORD) NEVEN=NORD
      NODDM1=NOOD-1
      H(1)=1.0D0
      RK=0.0D0
      DO 200 K=1,MAXK
      EXPA=-RK*RK*W04
      ADEL=DEXP(EXPA)
      CONST=DELT*ADEL
      IF(NEVEN.LT.3) GO TO 101
      H(2)=RK*W
      DO 100 N=3,NEVEN
      NM1=N-1
      NM2=N-2
      H(N)=RK*W*H(NM1)-2.0D0*W*DFLOAT(NM2)*H(NM2)
100   CONTINUE
101   CONTINUE
      RD=0.0D0
      DO 205 NR=1,MAXR
      COOK=RD*RK
      CO=1.0D0
      DO 201 L=1,NEVEN,2
      FCS(L,K,NR)=CONST*H(L)*CO*DCOS(COOK)
      CO=-CO*0.25D0
201   CONTINUE
      RD=RD+DSTEP
205   CONTINUE
      IF(NORD.EQ.1) GO TO 220
      F(1)=ADEL
      F(3)=(1.0D0+2.0D0/3.0D0*EXPA)*ADEL
      IF(NOOD.LT.6) GO TO 202
      DO 203 N=5,NODDM1+2
      AN=DFLOAT(N)
      F(N)=2.0D0*(AN+EXPA-1.500)*F(N-2)/AN-(1.0D0-3.0D0/AN)*F(N-4)
203   CONTINUE
202   CONTINUE
      RD=0.0D0

```

```
DO 211 NR=1,MAXR
COK=RK*RK
CO=1.D0
DO 210 L=2,N0OD+2
N=L-1
CO=CO*W*DFLOAT(N)*0.5D0
FCS(L,K,NR)=RK*F(N)*DELT*CO*DSIN(COK)
210 CONTINUE
RD=RD+DSTEP
211 CONTINUE
220 RK=RK+AKR
200 CONTINUE
N1=N0OD+2
N2=NEVEN+2
FINT=DELT
DO 300 L=3,N2,2
300 FINT=FINT*W*DFLOAT(L-2)/2.D0
DO 311 NR=1,MAXR
FCS(N1,1,NR)=0.D0
311 FCS(N2,1,NR)=FINT
RETURN
END
```

```

SUBROUTINE GNBDE(DEKX,DEKY,DEKZ,NKSUM,NB,NP,KLD,NKPT)
C***** **** * **** * **** * **** * **** * **** * **** * **** * **** * **** *
C GENERATE ENERGY DERIVATIVES IN THE NEIGHBORING POINTS OF THE 1/16TH OF THE
C BRILLOUIN ZONE
C FOR F. C. C. LATTICE ONLY
C***** **** * **** * **** * **** * **** * **** * **** * **** * **** * **** *
INTEGER*2 NP(KLD,KLD,KLD)
DIMENSION DEKX(NKSUM,NB),DEKY(NKSUM,NB),DEKZ(NKSUM,NB)
NPT=NKPT
KL=KLD-2
KA=KL+1
KM=3*KL/2
DO 5 K=1,KA
DO 5 I=1,KA
DO 5 J=1,I
KT=I+J+K-3
IF(KT .NE. KM) GO TO 5
KXP=IABS(I-KL)
KYP=IABS(J-KL)
KZP=IABS(K-KL)
I1=I+1
J1=J+1
K1=K+1
KXP1=KXP+1
KYP1=KYP+1
KZP1=KZP+1
KXP2=KXP+2
KYP2=KYP+2
KZP2=KZP+2
IF(I .GT. KL) GO TO 4
IF(K.GT.KL) GO TO 14
DO 20 NM=1,6
NPT=NPT+1
GO TO (21,22,23,24,25,26),NM
21 NP(I1, J, K)=NPT
NOD=NP(KXP1,KYP2,KZP2)
IF(KXP1.GE.KYP2) GO TO 28
GO TO 29
22 NP( I,J1, K)=NPT
NOD=NP(KXP2,KYP1,KZP2)
IF(KXP2.GE.KYP1) GO TO 28
GO TO 29
23 NP( I, J,K1)=NPT
NOD=NP(KXP2,KYP2,KZP1)
IF(KXP2.GE.KYP2) GO TO 28
GO TO 29

```

```

24 NP(I1,J1,K)=NPT
NOD=NP(KXP1,KYP1,KZP2)
IF(KXP1.GE.KYP1) GO TO 28
GO TO 29
25 NP(I1,J,K1)=NPT
NOD=NP(KXP1,KYP2,KZP1)
IF(KXP1.GE.KYP2) GO TO 28
GO TO 29
26 NP(I,J1,K1)=NPT
NOD=NP(KXP2,KYP1,KZP1)
IF(KXP2.GE.KYP1) GO TO 28
29 DO 30 L=1,NB
DEKX(NPT,L)=-DEKY(NOD,L)
DEKY(NPT,L)=-DEKX(NOD,L)
DEKZ(NPT,L)=-DEKZ(NOD,L)
30 CONTINUE
GO TO 20
28 DO 31 L=1,NB
DEKX(NPT,L)=-DEKX(NOD,L)
DEKY(NPT,L)=-DEKY(NOD,L)
DEKZ(NPT,L)=-DEKZ(NOD,L)
31 CONTINUE
20 CONTINUE
GO TO 5
4 CONTINUE
DO 40 NM=1,3
NPT=NPT+1
GO TO (41,42,43),NM
41 NP(I,J1,K)=NPT
NOD=NP(KXP,KYP1,KZP2)
IF(KXP .GE.KYP1) GO TO 48
GO TO 49
42 NP(I,J,K1)=NPT
NOD=NP(KXP,KYP2,KZP1)
IF(KXP .GE.KYP2) GO TO 48
GO TO 49
43 NP(I,J1,K1)=NPT
NOD=NP(KXP,KYP1,KZP1)
IF(KXP .GE.KYP1) GO TO 48
49 DO 45 L=1,NB
DEKX(NPT,L)=-DEKY(NOD,L)
DEKY(NPT,L)=-DEKX(NOD,L)
DEKZ(NPT,L)=-DEKZ(NOD,L)
45 CONTINUE
GO TO 40
48 DO 46 L=1,NB

```

```

DEKX(NPT,L)=-DEKX(NOD,L)
DEKY(NPT,L)=-DEKY(NOD,L)
DEKZ(NPT,L)=-DEKZ(NOD,L)
46 CONTINUE
40 CONTINUE
40 GO TO 5
14 CONTINUE
DO 50 NM=1,3
NP T=NPT+1
GO TO (51,52,53),NM
51 NP(I,J,K)=NPT
NOD=NP(KXP2,KYP1,KZP)
IF(KXP2,GE,KYP1) GO TO 58
GO TO 59
52 NP(I,I,J,K)=NPT
NOD=NP(KXP1,KYP2,KZP)
IF(KXP1,GE,KYP2) GO TO 58
GO TO 59
53 NP(I,I,J,K)=NPT
NOD=NP(KXP1,KYP1,KZP)
IF(KXP1,GE,KYP1) GO TO 58
59 DO 55 L=1,NB
DEKX(NPT,L)=-DEKY(NOD,L)
DEKY(NPT,L)=-DEKX(NOD,L)
DEKZ(NPT,L)=-DEKZ(NOD,L)
55 CONTINUE
GO TO 50
58 DO 56 L=1,NB
DEKX(NPT,L)=-DEKX(NOD,L)
DEKY(NPT,L)=-DEKY(NOD,L)
DEKZ(NPT,L)=-DEKZ(NOD,L)
56 CONTINUE
50 CONTINUE
CONTINUE
DO 10 I=1,KL
DO 10 K=1,KA
KT=I+I+J-3
IF(KT,GT,KM) GO TO 10
NP T=NPT+1
NP(I,I+1,K)=NPT
NOD=NP(I+1,I,K)
DO 11 L=1,NB
DEKX(NPT,L)=DEKY(NOD,L)
DEKY(NPT,L)=DEKX(NOD,L)
DEKZ(NPT,L)=DEKZ(NOD,L)
11 CONTINUE

```

```
10 CONTINUE
  WRITE(6,99) NPT
99 FORMAT(I10)
RETURN
END
```

```

SUBROUTINE GNBPT(PXPX,PXPY,PZPZ,NKSUM,NB,NP,KLD,NKPT,LG)
C***** *****
C      GENERATES THE PRODUCT OF MOMENTUM MATRICES IN THE NEIGHBORING POINTS OF
C      1/16TH OF THE INDEPENDENT B. Z.
C***** *****
INTEGER*2 NP(KLD,KLD,KLD)
DIMENSION PXPX(NKSUM,NB),PXPY(NKSUM,NB),PZPZ(NKSUM,NB)
NPT=NKPT+1
KL=KLD-2
KA=KL+1
KM=3*KL/2
DO 5 K=1,KA
DO 5 I=1,KA
DO 5 J=1,I
KT=I+J+K-3
IF(KT .NE. KM) GO TO 5
KXP=IAbs(I-KL)
KYP=IAbs(J-KL)
KZP=IAbs(K-KL)
I1=I+1
J1=J+1
K1=K+1
KXP1=KXP+1
KYP1=KYP+1
KZP1=KZP+1
KXP2=KXP+2
KYP2=KYP+2
KZP2=KZP+2
IF(I .GT. KL) GO TO 4
IF(K .GT. KL) GO TO 14
NP(I1, J, K)=NP(KXP1,KYP2,KZP2)
NP( I, J1, K)=NP(KXP2,KYP1,KZP2)
NP( I, J,K1)=NP(KXP2,KYP2,KZP1)
NP(I1, J1, K)=NP(KXP1,KYP1,KZP2)
NP(I1, J,K1)=NP(KXP1,KYP2,KZP1)
NP( I,J1,K1)=NP(KXP2,KYP1,KZP1)
DO 28 NM=1,6
GO TO (21,22,23,24,25,26),NM
21 CONTINUE
IF(KXP1.GE.KYP2) GO TO 28
NP(I1, J, K)=NPT
NOD=NP(KXP1,KYP2,KZP2)
GO TO 29
22 CONTINUE
IF(KXP2.GE.KYP1) GO TO 28
NP( I,J1, K)=NPT

```

```

NOD=NP(KXP2,KYP1,KZP2)
GO TO 29
23 CONTINUE
IF(KXP2.GE.KYP2) GO TO 28
NP(I,J,K1)=NPT
NOD=NP(KXP2,KYP2,KZP1)
GO TO 29
24 CONTINUE
IF(KXP1.GE.KYP1) GO TO 28
NP(I1,J1,K)=NPT
NOD=NP(KXP1,KYP1,KZP2)
GO TO 29
25 CONTINUE
IF(KXP1.GE.KYP2) GO TO 28
NP(I1,J,K1)=NPT
NOD=NP(KXP1,KYP2,KZP1)
GO TO 29
26 CONTINUE
IF(KXP2.GE.KYP1) GO TO 28
NP(I,J1,K1)=NPT
NOD=NP(KXP2,KYP1,KZP1)
29 DO 30 L=1,LG
PXPX(NPT,L)=PXPX(NOD,L)
PXPY(NPT,L)=-PXPY(NOD,L)
PZPZ(NPT,L)=PZPZ(NOD,L)
30 CONTINUE
NPT=NPT+1
28 CONTINUE
GO TO 5
4 CONTINUE
NP(I,J1,K)=NP(KXP,KYP1,KZP2)
NP(I,J,K1)=NP(KXP,KYP2,KZP1)
NP(I,J1,K1)=NP(KXP,KYP1,KZP1)
DO 48 NM=1,3
GO TO (41,42,43),NM
41 CONTINUE
IF(KXP.GE.KYP1) GO TO 48
NP(I,J1,K)=NPT
NOD=NP(KXP,KYP1,KZP2)
GO TO 49
42 CONTINUE
IF(KXP.GE.KYP2) GO TO 48
NP(I,J,K1)=NPT
NOD=NP(KXP,KYP2,KZP1)
GO TO 49
43 CONTINUE

```

```

IF(KXP .GE .KYP1) GO TO 48
NP(I,J1,K1)=NPT
NOD=NP(KXP,KYP1,KZP1)
49 DO 45 L=1,LG
PXPX(NPT,L)=PXPX(NOD,L)
PXPY(NPT,L)=-PXPY(NOD,L)
PZPZ(NPT,L)=PZPZ(NOD,L)
45 CONTINUE
NPT=NPT+1
48 CONTINUE
GO TO 5
14 CONTINUE
NP(I,J1,K)=NP(KXP2,KYP1,KZP)
NP(I1,J,K)=NP(KXP1,KYP2,KZP)
NP(I1,J1,K)=NP(KXP1,KYP1,KZP)
DO 58 NM=1,3
GO TO (51,52,53),NM
51 CONTINUE
IF(KXP2.GE.KYP1) GO TO 58
NP(I,J1,K)=NPT
NOD=NP(KXP2,KYP1,KZP)
GO TO 59
52 CONTINUE
IF(KXP1.GE.KYP2) GO TO 58
NP(I1,J,K)=NPT
NOD=NP(KXP1,KYP2,KZP)
GO TO 59
53 CONTINUE
IF(KXP1.GE.KYP1) GO TO 58
NP(I1,J1,K)=NPT
NOD=NP(KXP1,KYP1,KZP)
59 DO 55 L=1,LG
PXPX(NPT,L)=PXPX(NOD,L)
PXPY(NPT,L)=-PXPY(NOD,L)
PZPZ(NPT,L)=PZPZ(NOD,L)
55 CONTINUE
NPT=NPT+1
58 CONTINUE
CONTINUE
DO 10 I=1,KL
DO 10 K=1,KA
KT=I+I+J-3
IF(KT.GT.KM) GO TO 10
NP(I,I+1,K)=NPT
NOD=NP(I+1,I,K)
DO 11 L=1,LG

```

```
PXPX(NPT,L)=PXPX(NOD,L)
PXPY(NPT,L)=-PXPY(NOD,L)
PZPZ(NPT,L)=PZPZ(NOD,L)
11 CONTINUE
NPT=NPT+1
10 CONTINUE
WRITE(6,99) NPT
99 FORMAT(I10)
RETURN
END
```

```

SUBROUTINE GNOPUM(NPUM,NTYP,N,ND,NABTOL,NORDA,NORDB,NSYMP)
C*****NPUM DEFINES THE GROUP OPERATIONS THAT GENERATES THE STAR OF R*****
C*****NTYP DEFINES THE TERM IN THE EXPANSION OF EXP(I K.R) H(R) WHICH IS AN EVEN*****
C*****FUNCTION OF RX, RY, AND RZ.
C*****INTFGER*2 N(ND,ND,ND,ND,ND,ND),NPUM(NABTOL,6),NTYP(NARTOL)
NM=0
DO 201 IA3=1,NORDA
DO 201 IA2=1,NORDA
DO 201 IA1=1,NORDA
IAT=IA1+IA2+IA3-2
IF( IAT.NE.NORDA) GO TO 201
DO 202 IB3=1,NORDB
DO 202 IB2=1,NORDB
DO 202 IB1=1,NORDB
IBT=IB1+IB2+IB3-2
IF( IBT.NE.NORDB) GO TO 202
NM=NM+1
N(IA1,IA2,IA3,IB1,IB2,IB3)=NM
202 CONTINUE
201 CONTINUE
NM=0
DO 101 IA3=1,NORDA
DO 101 IA2=1,NORDA
DO 101 IA1=1,NORDA
IAT=IA1+IA2+IA3-2
IF( IAT.NE.NORDA) GO TO 101
DO 102 IB3=1,NORDB
DO 102 IB2=1,NORDB
DO 102 IB1=1,NORDB
IBT=IB1+IB2+IB3-2
IF( IBT.NE.NORDB) GO TO 102
NM=NM+1
NPUM(NM,1)=N(IA1,IA2,IA3,IB1,IB2,IB3)
NPUM(NM,2)=N(IA3,IA1,IA2,IB3,IB1,IB2)
NPUM(NM,3)=N(IA2,IA3,IA1,IB2,IB3,IB1)
NPUM(NM,4)=N(IA1,IA3,IA2,IB1,IB3,IB2)
NPUM(NM,5)=N(IA3,IA2,IA1,IB3,IB2,IB1)
NPUM(NM,6)=N(IA2,IA1,IA3,IB2,IB1,IB3)
IA81=IA1+IB1
IA82=IA2+IB2
IA83=IA3+IB3
IF( NSYMP.EQ.0) GO TO 103
IA81=IA81+1
IA82=IA82+1

```

```
IAB3=IAB3+1
103 CONTINUE
NT=1
IF((IAB1/2)*2.NE.IAB1) NT=NT+1
IF((IAB2/2)*2.NE.IAB2) NT=NT+2
IF((IAB3/2)*2.NE.IAB3) NT=NT+4
NTYP(NM)=NT
99 FORMAT(15, '=(0,1X,3I1,''-',3I1,1X,')', 3X, 'NTYP=', 15, 3X, 'PERMUTATION
1=(0,5(I3, ','), I3, ')')
WRITE(6,99) NM,IA1,IA2,IA3,IB1,IB2,IB3,NTYP(NM),(NPUM(NM,I),I=1,6)
102 CONTINUE
101 CONTINUE
RETURN
END
```

```

SUBROUTINE GPERMK(KKX,KKY,KKZ,KSQ,NKPT, IDCUB,K2MAX,ISORT)
C***** *****
C GENERATE PERMUTED RECIPROCAL LATTICE VECTORS WITH MAGNITUDE SQUARE LESS
C THAN K2MAX
C IF (ISORT.NE.0) THE RECIPROCAL LATTICE VECTORS ARE SORTED IN ORDER OF
C INCREASING MAGNITUDE
C SC IDCUB=1, BCC IDCUB=2, FCC IDCUB=4
C*****
INTEGER*2 KKX(NKPT),KKY(NKPT),KKZ(NKPT)
DIMENSION KSQ(NKPT)
G=K2MAX
MAX=SQRT(G)+1
MAXXX=2*MAX+1
KPT=0
IF (IDCUB.NE.4) GO TO 200
DO 100 III=1,MAXXX,2
DO 100 JJJ=1,MAXXX,2
DO 100 KKK=1,MAXXX,2
KX=III-1-MAX
KY=JJJ-1-MAX
KZ=KKK-1-MAX
DO 100 MMM=1,2
K2=KX*KX+KY*KY+KZ*KZ
IF (K2.GT.K2MAX) GO TO 101
KPT=KPT+1
IF (KPT.GT.NKPT) STOP 2
IPT=KPT
IF (KPT.EQ.1.OR.ISORT.EQ.0) GO TO 103
IM=KPT-1
IF (K2.GE.KSQ(IM)) GO TO 103
II=KPT
102 KKX(II)=KKX(IM)
KKY(II)=KKY(IM)
KKZ(II)=KKZ(IM)
KSQ(II)=KSQ(IM)
II=II-1
IM=II-1
IF (II.GT.1.AND.K2.LT.KSQ(IM)) GO TO 102
IPT=II
103 KKX(IPT)=KX
KKY(IPT)=KY
KKZ(IPT)=KZ
KSQ(IPT)=K2
101 CONTINUE
KX=KX+1
KY=KY+1

```

```

KZ=KZ+1
100 CONTINUE
      GO TO 300
200 CONTINUE
      DO 201 III=1,MAXXX
      DO 201 JJJ=1,MAXXX
      DO 201 KKK=1,MAXXX
      KX=III-1-MAX
      KY=JJJ-1-MAX
      KZ=KKK-1-MAX
      ITOL=KX+KY+KZ
      IF (ITOL.NE.(ITOL/2)*2.AND.IDCUB.EQ.2) GO TO 201
      K2=KX*KX+KY*KY+KZ*KZ
      IF (K2.GT.K2MAX) GO TO 201
      KPT=KPT+1
      IF (KPT.GT.NKPT) STOP 2
      IPT=KPT
      IF (KPT.EQ.1.OR.ISORT.EQ.0) GO TO 203
      IM=KPT-1
      IF (K2.GE.KSQ(IM)) GO TO 203
      II=KPT
202  KKX(II)=KKX(IM)
      KKY(II)=KKY(IM)
      KKZ(II)=KKZ(IM)
      KSQ(II)=KSQ(IM)
      II=II-1
      IM=II-1
      IF (K2.LT.KSQ(IM).AND.II.GT.1) GO TO 202
      IPT=II
203  KKX(IPT)=KX
      KKY(IPT)=KY
      KKZ(IPT)=KZ
      KSQ(IPT)=K2
201  CONTINUE
300  CONTINUE
      NKPT=KPT
      RETURN
      END

```

```

SUBROUTINE GWTGAS(N, Y, XR, WR)
C*****FINDS ZEROES OF LEGENDRE POLYNOMIAL OF ORDER N AND THE CORRESP.
C WEIGHT FACTORS FOR THE GAUSSIAN INTEGRATION USING THE DEFINITION
C W(I)=2/((DP(N,X)/DX)**2 * (1-X**2)) AT X=X(I) WHERE P(N,X)=0 AND
C DP(N,X)/DX = N*P(N-1,X)/(1-X*X).
C Y IS AN WORKING FUNCTION DIMENSIONED N+1
C*****IMPLICIT REAL*8 (A-H,O-Z)
DIMENSION Y(1),XR(1),WR(1)
NHAF=N/2
WC=2.D0/DFLOAT(N*N)
NR=0
DX=2.D0/DFLOAT(N)
IF(N .EQ. 2*(N/2)) GO TO 100
C
C IF ORDER IS ODD, ONE OF THE ZEROES IS X=0
C
C XR(1)=0.D0
CALL DLEP(Y,0.D0,N)
WR(1)=WC/(Y(N)**2)
NR=1
100 CONTINUE
XOLD=0.1D-5
DO 200 I=1,NHAF
C
C SUBROUTINE DLEP COMPUTES THE LEGENDRE POLYNOMIALS FOR ARGUMENT VALUE XOLD
C AND ORDERS 0 UP TO N (IN IBM SCIENTIFIC SUBROUTINE PACKAGE)
C
CALL DLEP(Y,XOLD,N)
YOLD=Y(N+1)
NR=NR+1
XNEW=XOLD+DX
CALL DLEP(Y,XNEW,N)
YNEW=Y(N+1)
IF(DX .LT. 1.D-16 .OR. DABS(YNEW) .LT. 1.D-16) GO TO 130
YSGN=YNEW/YOLD
IF (YSGN .GT. 0.) GO TO 120
C
C CLOSE-IN ON THE ZERO -- SIGN OF THE POLYNOMIAL HAS CHANGED.
C
DX=DX/2.D0
GO TO 110
120 XOLD=XNEW
YOLD=YNEW
GO TO 110

```

```

130  XR(NR)=XNEW
      WR(NR)=WC*(1.00-XNEW**2)/(Y(N)**2)
      XOLD=0.1D-5+XNEW
      DX=2.00/DFLOAT(N)
C
C      SINCE THE ZEROES ARE MORE CROWDED NEAR X=1, DECREASE THE STEP
C      SIZE AS WE GET CLOSER TO THIS END.
C
200  IF(NR .GT. 1) DX=(XR(NR)-XR(NR-1))/2.00
      CONTINUE
      DO 249 I=1,NR
          II=NR+1
          XR(II)=XR(I)
          WR(II)=WR(I)
249  CONTINUE
      DO 250 I=1,NR
          II=2*NR-I+1
          XR(I)=-XR(II)
          WR(I)=WR(II)
250  CONTINUE
999  RETURN
      END

```

```

SUBROUTINE GSICO(SICO,SINE,COSN,NRDIM,KBZPT,K1,K2,K3,I1,I2,I3)
C **** GENERATE THE EXPANSION TERMS IN EXP(I K.R) ACCORDING TO THE PROPER
C PERMUTATION
C ****
IMPLICIT REAL *8 (A-F,H,O-Z)
DIMENSION SINE(NRDIM,KBZPT),COSN(NRDIM,KBZPT),SICO(6,8)
SICO(1,1)=COSN(I1,K1)*COSN(I2,K2)*COSN(I3,K3)
SICO(2,1)=COSN(I2,K1)*COSN(I3,K2)*COSN(I1,K3)
SICO(3,1)=COSN(I3,K1)*COSN(I1,K2)*COSN(I2,K3)
SICO(4,1)=COSN(I1,K1)*COSN(I3,K2)*COSN(I2,K3)
SICO(5,1)=COSN(I3,K1)*COSN(I2,K2)*COSN(I1,K3)
SICO(6,1)=COSN(I2,K1)*COSN(I1,K2)*COSN(I3,K3)
SICO(1,2)=SINE(I1,K1)*COSN(I2,K2)*COSN(I3,K3)
SICO(2,2)=SINE(I2,K1)*COSN(I3,K2)*COSN(I1,K3)
SICO(3,2)=SINE(I3,K1)*COSN(I1,K2)*COSN(I2,K3)
SICO(4,2)=SINE(I1,K1)*COSN(I3,K2)*COSN(I2,K3)
SICO(5,2)=SINE(I3,K1)*COSN(I2,K2)*COSN(I1,K3)
SICO(6,2)=SINE(I2,K1)*COSN(I1,K2)*COSN(I3,K3)
SICO(1,3)=COSN(I1,K1)*SINE(I2,K2)*COSN(I3,K3)
SICO(2,3)=COSN(I2,K1)*SINE(I3,K2)*COSN(I1,K3)
SICO(3,3)=COSN(I3,K1)*SINE(I1,K2)*COSN(I2,K3)
SICO(4,3)=COSN(I1,K1)*SINE(I3,K2)*COSN(I2,K3)
SICO(5,3)=COSN(I3,K1)*SINE(I2,K2)*COSN(I1,K3)
SICO(6,3)=COSN(I2,K1)*SINE(I1,K2)*COSN(I3,K3)
SICO(1,4)=SINE(I1,K1)*SINE(I2,K2)*COSN(I3,K3)
SICO(2,4)=SINE(I2,K1)*SINE(I3,K2)*COSN(I1,K3)
SICO(3,4)=SINE(I3,K1)*SINE(I1,K2)*COSN(I2,K3)
SICO(4,4)=SINE(I1,K1)*SINE(I3,K2)*COSN(I2,K3)
SICO(5,4)=SINE(I3,K1)*SINE(I2,K2)*COSN(I1,K3)
SICO(6,4)=SINE(I2,K1)*SINE(I1,K2)*COSN(I3,K3)
SICO(1,5)=COSN(I1,K1)*COSN(I2,K2)*SINE(I3,K3)
SICO(2,5)=COSN(I2,K1)*COSN(I3,K2)*SINE(I1,K3)
SICO(3,5)=COSN(I3,K1)*COSN(I1,K2)*SINE(I2,K3)
SICO(4,5)=COSN(I1,K1)*COSN(I3,K2)*SINE(I2,K3)
SICO(5,5)=COSN(I1,K1)*COSN(I2,K2)*SINE(I1,K3)
SICO(6,5)=COSN(I2,K1)*COSN(I1,K2)*SINE(I3,K3)
SICO(1,6)=SINE(I1,K1)*COSN(I2,K2)*SINE(I3,K3)
SICO(2,6)=SINE(I2,K1)*COSN(I1,K2)*SINE(I3,K3)
SICO(3,6)=SINE(I3,K1)*COSN(I1,K2)*SINE(I2,K3)
SICO(4,6)=SINE(I1,K1)*COSN(I3,K2)*SINE(I2,K3)
SICO(5,6)=SINE(I3,K1)*COSN(I2,K2)*SINE(I1,K3)
SICO(6,6)=SINE(I2,K1)*COSN(I1,K2)*SINE(I3,K3)
SICO(1,7)=COSN(I1,K1)*SINE(I2,K2)*SINE(I3,K3)
SICO(2,7)=COSN(I2,K1)*SINE(I3,K2)*SINE(I1,K3)
SICO(3,7)=COSN(I3,K1)*SINE(I1,K2)*SINE(I2,K3)

```

```

SICO(4,7)=-COSN(11•K1)*SINE(13•K2)*SINE(12•K3)
SICO(5,7)=-COSN(13•K1)*SINE(12•K2)*SINE(11•K3)
SICO(6,7)=-COSN(12•K1)*SINE(11•K2)*SINE(13•K3)
SICO(1,8)=-SINE(11•K1)*SINE(12•K2)*SINE(13•K3)
SICO(2,8)=-SINE(12•K1)*SINE(13•K2)*SINE(11•K3)
SICO(3,8)=-SINE(13•K1)*SINE(11•K2)*SINE(12•K3)
SICO(4,8)=-SINE(11•K1)*SINE(13•K2)*SINE(12•K3)
SICO(5,8)=-SINE(13•K1)*SINE(12•K2)*SINE(11•K3)
SICO(6,8)=-SINE(12•K1)*SINE(11•K2)*SINE(13•K3,
RETURN
END

```

```

SUBROUTINE GS1JFC(FCS,RK,NORD,NORDIM,NRDIM)
C***** *****
C GENERATE FUNCTION G(N,RK,R) IN EQ(8.44) FOR A GIVEN VALUE OF RK
C***** *****
IMPLICIT REAL *8 (A-F,H,O-Z)
DIMENSION FCS(NORDIM,NRDIM)
DIMENSION H(10),F(10)
COMMON/GS1JF/W,DELT,W04,DSTEP,MAXR
NOOD=(NORD/2)*2
IF(NOOD.EQ.NORD) NEVEN=NORD-1
IF(NOOD.NE.NORD) NEVEN=NORD
NOODM1=NOOD-1
H(1)=1.0D0
EXPX=-RK*RK*W04
ADEL=DEXP(EXPX)
CONST=DELT*ADEL
IF(NEVEN.LT.3) GO TO 101
H(2)=RK*W
DO 100 N=3,NEVEN
NM1=N-1
NM2=N-2
H(N)=RK*W*H(NM1)-2.D0*W*DFLOAT(NM2)*H(NM2)
100 CONTINUE
101 CONTINUE
RD=0.D0
DO 205 NR=1,MAXR
COOK=RD*RK
CO=1.D0
DO 201 L=1,NEVEN,2
FCS(L,NR)=CONST*H(L)*CO*DCOS(COOK)
CO=-CO*0.25D0
201 CONTINUE
RD=RD+DSTEP
205 CONTINUE
IF(NORD.EQ.1) RETURN
F(1)=ADEL
F(3)=(1.D0+2.D0/3.D0*EXPX)*ADEL
IF(NOOD.LT.6) GO TO 202
DO 203 N=5,NOODM1,2
AN=DFLOAT(N)
F(N)=2.D0*(AN+EXPX-1.5D0)*F(N-2)/AN-(1.D0-3.D0/AN)*F(N-4)
203 CONTINUE
202 CONTINUE
RD=0.D0
DO 211 NR=1,MAXR
COOK=RD*RK

```

```
CO=1.00
DO 210 L=2,NODD,2
N=L-1
CO=CO*W*DFLOAT(N)*0.5D0
FCS(L,NR)=RK*F(N)*DELT*CO*DSIN(COK)
210 CONTINUE
RD=RD+DSTEP
211 CONTINUE
RETURN
END
```

```

SUBROUTINE HRIN(M)
C **** T IS REPLACED BY T (OV**-1)
C   (KK,I,J)=2*M*(J-1)+2*(I-1)+KK
C   (KK,I,N)=2*M*(N-1)+2*(I-1)+KK
C ****
REAL*8 T,OV
COMMON/A/T(11552)
COMMON/C/OV(2926)
M2=M*2
DO 100 J=1,M
JJ=J*(J+1)/2
MJ=M2*(J-1)
DO 100 KK=1,2
DO 100 I=1,M
IKK=2*(I-1)+KK
KKIJ=MJ+IKK
IF(J.EQ.1) GO TO 102
JK=J-1
DO 101 N=1,JK
NJ=J*(J-1)/2+N
KKIN=M2*(N-1)+IKK
T(KKIJ)=T(KKIJ)-T(KKIN)*OV(NJ)
101 CONTINUE
102 CONTINUE
T(KKIJ)=T(KKIJ)/OV(JJ)
100 CONTINUE
RETURN
END

```

```

SUBROUTINE READ(SSA,PSA,SDA,PPA,PDA,SSB,PSB,SDB,PPB,PDR,DDR,
1IASS,IAPS,IASD,IAPP,IAPD,IADD,ISSDIM,IPSDIM,ISDDIM,IPPDIM,
2IPDDIM,IDDDIM,CS,CP,CD,LSMAX,ISOBNO,LPMAX,IPOBNO,LDMAX,IDOBNO)
C***** READ IN THE INTEGRALS GENERATED IN PROGRAM 2 OR 3.
C NCHO(I)=1 COULOMB, 2 PARAMAGNETIC EXCH, 3 UP EXCH, 4 DOWN EXCH, 5 KINETIC,
C 6 OVERLAP, 7 PX, 8 PY, 9 PZ, 10H PARAMAGNETIC, 11H UP, 12 H DOWN.
C***** REAL*8 ALPHA,CS(LSMAX,ISOBNO),CP(LPMAX,IPOBNO),CD(LDMAX,IDOBNO),
&BX(360),CO,CM
INTEGER*2 NRC,M1,M2,NSYM
DIMENSION SSA(IASS,ISSDIM),SSB(IASS,ISSDIM),PSA(IAPS,IPSDIM),
1PSB(IAPS,IPSDIM),SDA(IASD,ISDDIM),SDB(IASD,ISDDIM),
2PPA(IAPP,IPPDIM),PPB(IAPP,IPPDIM),PDA(IAPD,IPDDIM),
3PD(B(IAPD,IPDDIM),DDA(IADD,IPDDIM),DDB(IADD,IPDDIM))
DIMENSION AX(10)
COMMON/DBNO/ALPHA,NKIND,NTOL,NCHO(5),ISYMP
DO 111 NRC=1,IASS
DO 111 IJ=1,ISSDIM
SSA(NRC,IJ)=0.00
IF(NTOL.GT.1) SSB(NRC,IJ)=0.00
111 CONTINUE
110 READ(11,END=200) NRC,M1,M2,NSYM,(AX(NM),NM=1,NKIND)
IF(NRC.GT.IASS) GO TO 110
DO 103 N=1,NTOL
NTYP=NCHO(N)
IF(NTYP.LE.NKIND) BX(N)=AX(NTYP)
IF(NTYP.EQ.NKIND+1) BX(N)=AX(1)+ALPHA*AX(2)+AX(5)
IF(NTYP.EQ.NKIND+2) BX(N)=AX(1)+ALPHA*AX(3)+AX(5)
IF(NTYP.EQ.NKIND+3) BX(N)=AX(1)+ALPHA*AX(4)+AX(5)
103 CONTINUE
IJ=0
DO 104 I1=1,LSMAX
DO 104 I2=1,I1
IJ=IJ+1
CO=CS(I1,M1)*CS(I2,M2)
IF(M1.NE.M2) CO=CO+CS(I1,M2)*CS(I2,M1)
SSA(NRC,IJ)=SSA(NRC,IJ)+BX(1)*CO
IF(NTOL.GT.1) SSB(NRC,IJ)=SSB(NRC,IJ)+BX(2)*CO
104 CONTINUE
GO TO 110
200 CONTINUE
DO 211 NRC=1,IAPS
DO 211 IJ=1,IPSDIM
PSA(NRC,IJ)=0.00
IF(NTOL.GT.1) PSB(NRC,IJ)=0.00

```

```

211 CONTINUE
210 READ(12,END=300) NRC,M1,M2,NSYM,(AX(NM),NM=1,NKIND)
  IF(NRC.GT.IAPS) GO TO 210
  DO 203 N=1,NTOL
  NN=(N-1)*3+NSYM
  NTYP=NCHO(N)
  IF(NTYP.LE.NKIND) BX(NN)=AX(NTYP)
  IF(NTYP.EQ.NKIND+1) BX(NN)=AX(1)+ALPHA*AX(2)+AX(5)
  IF(NTYP.EQ.NKIND+2) BX(NN)=AX(1)+ALPHA*AX(3)+AX(5)
  IF(NTYP.EQ.NKIND+3) BX(NN)=AX(1)+ALPHA*AX(4)+AX(5)
  IF(ISYMP.NE.0) BX(NN)=-BX(NN)
203 CONTINUE
  IF(NSYM.LT.3) GO TO 210
  IJ=0
  DO 204 I1=1,LPMAX
  DO 204 I2=1,LSMAX
  CO=CP(I1,M1)*CS(I2,M2)
  DO 204 NM=1,3
  IJ=IJ+1
  PSA(NRC,IJ)=PSA(NRC,IJ)+BX(NM)*CO
  IF(NTOL.GT.1) PSB(NRC,IJ)=PSB(NRC,IJ)+BX(NM+3)*CO
204 CONTINUE
  GO TO 210
300 CONTINUE
  DO 311 NRC=1,IASD
  DO 311 IJ=1,ISDDIM
  SDA(NRC,IJ)=0.D0
  IF(NTOL.GT.1) SDB(NRC,IJ)=0.D0
311 CONTINUE
310 READ(13,END=400) NRC,M1,M2,NSYM,(AX(NM),NM=1,NKIND)
  IF(NRC.GT.IASD) GO TO 310
  DO 303 N=1,NTOL
  NN=(N-1)*6+NSYM
  NTYP=NCHO(N)
  IF(NTYP.LE.NKIND) BX(NN)=AX(NTYP)
  IF(NTYP.EQ.NKIND+1) BX(NN)=AX(1)+ALPHA*AX(2)+AX(5)
  IF(NTYP.EQ.NKIND+2) BX(NN)=AX(1)+ALPHA*AX(3)+AX(5)
  IF(NTYP.EQ.NKIND+3) BX(NN)=AX(1)+ALPHA*AX(4)+AX(5)
303 CONTINUE
  IF(NSYM.LT.6) GO TO 310
  IJ=0
  DO 304 I1=1,LSMAX
  DO 304 I2=1,LDMAX
  CO=CS(I1,M1)*CD(I2,M2)
  DO 304 NM=1,6
  IJ=IJ+1

```

```

      SDA(NRC,IJ)=SDA(NRC,IJ)+BX(NM)*CO
      IF(NTOL.GT.1) SDB(NRC,IJ)=SDB(NRC,IJ)+BX(NM+6)*CO
304  CONTINUE
      GO TO 310
400  CONTINUE
      DO 411 NRC=1,IAPP
      DO 411 IJ=1,IPPDIM
      PPA(NRC,IJ)=0.D0
      IF(NTOL.GT.1) PPB(NRC,IJ)=0.DC
411  CONTINUE
410  READ(14,END=500) NRC,M1,M2,NSYM,(AX(NM),NM=1,NKIND)
      IF(NRC.GT.IAPP) GO TO 410
      DO 403 N=1,NTOL
      NN=(N-1)*9+NSYM
      NTYP=NCHO(N)
      IF(NTYP.LE.NKIND) BX(NN)=AX(NTYP)
      IF(NTYP.EQ.NKIND+1) BX(NN)=AX(1)+ALPHA*AX(2)+AX(5)
      IF(NTYP.EQ.NKIND+2) BX(NN)=AX(1)+ALPHA*AX(3)+AX(5)
      IF(NTYP.EQ.NKIND+3) BX(NN)=AX(1)+ALPHA*AX(4)+AX(5)
403  CONTINUE
      IF(NSYM.LT.9) GO TO 410
      IJ=0
      DO 404 I1=1,LPMAX
      DO 404 I2=1,I1
      CO=CP(I1,M1)*CP(I2,M2)
      CM=CP(I2,M1)*CP(I1,M2)
      DO 405 L1=1,3
      DO 405 L2=1,3
      NM=(L1-1)*3+L2
      IJ=IJ+1
      PPA(NRC,IJ)=PPA(NRC,IJ)+BX(NM)*CO
      IF(NTOL.GT.1) PPB(NRC,IJ)=PPB(NRC,IJ)+BX(NM+9)*CO
      IF(M1.EQ.M2) GO TO 405
      NM=(L2-1)*3+L1
      PPA(NRC,IJ)=PPA(NRC,IJ)+BX(NM)*CM
      IF(NTOL.GT.1) PPB(NRC,IJ)=PPB(NRC,IJ)+BX(NM+9)*CM
405  CONTINUE
404  CONTINUE
      GO TO 410
500  CONTINUE
      DO 511 NRC=1,IAPD
      DO 511 IJ=1,IPDDIM
      PDA(NRC,IJ)=0.D0
      IF(NTOL.GT.1) PDB(NRC,IJ)=0.D0
511  CONTINUE
510  READ(15,END=600) NRC,M1,M2,NSYM,(AX(NM),NM=1,NKIND)

```

```

IF (NRC.GT.IAPD) GO TO 510
DO 503 N=1,NTOL
NN=(N-1)*18+NSYM
NTYP=NCHO(N)
IF (NTYP.LE.NKIND) BX(NN)=AX(NTYP)
IF (NTYP.EQ.NKIND+1) BX(NN)=AX(1)+ALPHA*AX(2)+AX(5)
IF (NTYP.EQ.NKIND+2) BX(NN)=AX(1)+ALPHA*AX(3)+AX(5)
IF (NTYP.EQ.NKIND+3) BX(NN)=AX(1)+ALPHA*AX(4)+AX(5)
IF (ISYMP.EQ.0) BX(NN)=-BX(NN)
503 CONTINUE
IF (NSYM.LT.18) GO TO 510
IJ=0
DO 504 I1=1,LPMAX
DO 504 I2=1,LDMAX
CO=CP(I1,M1)*CD(I2,M2)
DO 504 NM=1,18
IJ=IJ+1
PDA(NRC,IJ)=PDA(NRC,IJ)+BX(NM)*CO
IF (NTOL.GT.1) PDB(NRC,IJ)=PDB(NRC,IJ)+RX(NM+18)*CN
504 CONTINUE
GO TO 510
600 CONTINUE
DO 611 NRC=1,IADD
DO 611 IJ=1,IDDIM
DDA(NRC,IJ)=0.D0
IF (NTOL.GT.1) DDB(NRC,IJ)=0.D0
611 CONTINUE
610 READ(16,END=700) NRC,M1,M2,NSYM,(AX(NM),NM=1,NKIND)
IF (NRC.GT.IADD) GO TO 610
DO 603 N=1,NTOL
NN=(N-1)*36+NSYM
NTYP=NCHO(N)
IF (NTYP.LE.NKIND) BX(NN)=AX(NTYP)
IF (NTYP.EQ.NKIND+1) BX(NN)=AX(1)+ALPHA*AX(2)+AX(5)
IF (NTYP.EQ.NKIND+2) BX(NN)=AX(1)+ALPHA*AX(3)+AX(5)
IF (NTYP.EQ.NKIND+3) BX(NN)=AX(1)+ALPHA*AX(4)+AX(5)
603 CONTINUE
IF (NSYM.LT.36) GO TO 610
IJ=0
DO 604 I1=1,LPMAX
DO 604 I2=1,T1
CO=CD(I1,M1)*CD(I2,M2)
DO 605 L1=1,6
DO 605 L2=1,6
NM=(L1-1)*6+L2

```

```
IJ=IJ+1
DDA(NRC,IJ)=DDA(NRC,IJ)+BX(NM)*CO
IF(NTOL.GT.1) DDB(NRC,IJ)=DDB(NRC,IJ)+BX(NM+36)*CO
IF(M1.EQ.M2) GO TO 605
NM=(L2-1)*6+L1
DDA(NRC,IJ)=DDA(NRC,IJ)+RX(NM)*CM
IF(NTOL.GT.1) DDB(NRC,IJ)=DDB(NRC,IJ)+RX(NM+36)*CM
605 CONTINUE
604 CONTINUE
GO TO 610
700 CONTINUE
RETURN
END
```

```

SUBROUTINE RDGTO(ALS,ALP,ALD,CS,CP,CD,SCO,PCO,DCO,ISOBNO,LSMAX,
& IPOBNO,LPMAX,IDOBN0,LDMAX,ICOMB)
C*****DEFINE GTO E=S, P, AND D.
C  IDOBNO=GTO NUMBERS FOR E SYMMETRY
C  IEATOM=ATOMIC BASIS NUMBER =0 IF INDEPENDENT GTO IS EMPLOYED
C  CE=NORMALIZATION CONSTANTS. ADDITIONAL ANGULAR FACTOR IS NECESSARY
C  FOR X**2-Y**2 (0.5), AND 3*Z**2-R**2 (0.5/SQRT(3.0)).
C  ALG=GAUSSIAN EXPONENTIAL PARAMETERS FOR E SYMMETRY
C  ECO=EXPANSION COEFFICIENTS FOR THE ATOMIC E-GTO=DELTA FUNCTION IF IEATOM=0
C  IF(ICOMB.NE.0) ECO=ECO*CE
C*****IMPLICIT REAL *8 (A-F,H,O-Z)
DIMENSION ALS(1),ALP(1),ALD(1),CS(1),CP(1),CD(1),SCO(LSMAX,ISOBNO)
&,PCO(LPMAX,IPOBNO),DCO(LDMAX,IDOBN0)
COMMON/GTO/CRYSTL,PI,ISATOM,IPATOM,IDATOM
DATA GWTS,GWTP,GWTD/'S','P','D'/
DO 10 J=1,ISOBNO
READ(5,11) ALS(J),(SCO(L,J),L=1,ISATOM)
AAA=2.00*(8.00*ALS(J)**3/PI)**.25DC
CS(J)=AAA/DSQRT(4.00*PI)
10 WRITE(6,15) CRYSTL,J,ALS(J),CS(J),(L,GWTS,SCO(L,J),L=1,ISATOM)
IF(ISATOM.GT.0) GO TO 24
DO 22 N=1,ISOBNO
DO 23 J=1,ISOBNO
23 SCO(N,J)=0.00
22 SCO(N,N)=1.00
24 IF(ICOMB.EQ.0) GO TO 21
DO 25 N=1,LSMAX
DO 25 J=1,ISOBNO
25 SCO(N,J)=SCO(N,J)*CS(J)
21 CONTINUE
DO 12 J=1,IPOBNO
READ(5,11) ALP(J),(PCO(L,J),L=1,IPATOM)
AAA=DSQRT(8.00/3.00)*(32.00*ALP(J)**5/PI)**.25DC
CP(J)=AAA/DSQRT(3.00/(4.00*PI))
12 WRITE(6,15) CRYSTL,J,ALP(J),CP(J),(L,GWTP,PCO(L,J),L=1,IPATOM)
IF(IPATOM.GT.0) GO TO 34
DO 32 N=1,IPOBNO
DO 33 J=1,IPOBNO
33 PCO(N,J)=0.00
32 PCO(N,N)=1.00
34 IF(ICOMB.EQ.0) GO TO 31
DO 35 N=1,LPMAX
DO 35 J=1,IPOBNO
35 PCO(N,J)=PCO(N,J)*CP(J)

```

```

31 CONTINUE
DO 13 J=1,IDOBN0
READ(5,11) ALD(J),(DCO(L,J),L=1,IDATOM)
AAA=16.00/DSQRT(15.00)*(ALD(J)**7/(2.00*p1))**0.2500
CD(J)=AAA*DSQRT(15.00/4.00/p1)
13 WRITE(6,15) CRYSTL,J,ALD(J),CD(J),(L,GWTD,DCO(L,J),L=1,IDATOM)
IF(IDATOM.GT.0) GO TO 44
DO 42 N=1,IDOBN0
DO 43 J=1,IDOBN0
43 DCO(N,J)=0.00
42 DCO(N,N)=1.00
44 IF(ICOMB.EQ.0) GO TO 41
DO 45 N=1,LDMAX
DO 45 J=1,IDOBN0
45 DCO(N,J)=DCO(N,J)*CD(J)
41 CONTINUE
11 FORMAT(F8.5,4016.8)
15 FORMAT(1X,A8,I2,2X,'EXPO=',F13.6,2X,'NORM=',E16.8,4(13,A1,'=',E14.
     *8))
      RETURN
END

```

```

SUBROUTINE RTINH(M)
C **** T IS REPLACED BY ((OV*T)**-1) T
C   (KK,I,J)=2*M*(J-1)+2*(I-1)+KK
C   (KK,N,J)=2*M*(J-1)+2*(N-1)+KK
C **** REAL*8 T,OV
C COMMON/A/T(11552)
C COMMON/C/OV(2926)
M2=M*2
DO 100 I=1,M
I2=2*(I-1)
II=I*(I+1)/2
DO 100 KK=1,2
DO 100 J=1,M
JKK=M2*(J-1)+KK
KKIJ=JKK+I2
IF (I.EQ.1) GO TO 102
IK=I-1
DO 101 N=1,IK
NI=I*(I-1)/2+N
KKNJ=JKK+2*(N-1)
T(KKIJ)=T(KKIJ)-OV(NI)*T(KKNJ)
101 CONTINUE
102 CONTINUE
T(KKIJ)=T(KKIJ)/OV(II)
100 CONTINUE
RETURN
END

```

```

SUBROUTINE SEXCH(AX,AY,AZ,IDIM)
C ****
C THIS SUBROUTINE CALCULATES THE ZEROTH ORDER TERM IN THE KUBIC HARMONIC
C EXPANSION OF DENSITY
C (RX(I),RY(I),RZ(I)) ARE FOUR DIRECTIONS CHOSEN TO CALCULATE THE ANGULAR
C AVERAGE OF DENSITY
C C41(I), C61(I), AND C81(I) ARE KUBIC HARMONICS WITH L=4, 6, AND 8
C ****
C IMPLICIT REAL*8(A-F,H,O-Z)
C DIMENSION AX(IDIM),AY(IDIM),AZ(IDIM)
C DIMENSION RX(4),RY(4),RZ(4),WT(4),C41(4),C61(4),C81(4)
C COMMON/VKO/C(7,11),EX(7,11),FACTO(10),IB(7,11),NORB(7),NSTA
C COMMON/EXCH/R(96),W(96),EXCH(96),EXUP(96),EXDN(96)
C COMMON/CHARGE/CHARGE(7),CHARUP(7),CHARDN(7)
C COMMON/CONST/A,RO,PI,ONETHD
2 FORMAT(12F6.3)
READ(5,2) (RX(I),RY(I),RZ(I),I=1,4)

C
C CALCULATE THE WEIGHT FACTOR ALONG EXCH DIRECTION

CONST=1.00/(4.00*PI)
SD4PI=DSQRT(CONST)
DO 3 I=1,4
RR=RX(I)*RX(I)+RY(I)*RY(I)+RZ(I)*RZ(I)
RA=DSQRT(RR)
RX(I)=RX(I)/RA
RY(I)=RY(I)/RA
RZ(I)=RZ(I)/RA
X2=RX(I)*RX(I)
Y2=RY(I)*RY(I)
Z2=RZ(I)*RZ(I)
X4=X2*X2
Y4=Y2*Y2
Z4=Z2*Z2
C41(I)=1.25D0*DSQRT(21.00)*(X4+Y4+Z4-0.6D0)
C61(I)=231.00*DSQRT(26.00)/8.00*(X2*Y2*Z2+C41(I)/22.00-1.00/105.00
      E)
      C81(I)=65.00*DSQRT(561.00)/16.00*(X4*X4+Y4*Y4+Z4*Z4-28.00*C61(I)/
      E5.00-210.00*C41(I)/143.00-1.00/6.00)
      C41(I)=C41(I)*SD4PI
      C61(I)=C61(I)*SD4PI
      C81(I)=C81(I)*SD4PI
3 CONTINUE
      W1=(C41(2)*C61(3)-C41(3)*C61(2))*C81(4)+(C41(4)*C61(2)-
      E   C41(2)*C61(4))*C81(3)+(C41(3)*C61(4)-C41(4)*C61(3))*C81(2)           W1
      W2=(C41(3)*C61(4)-C41(4)*C61(3))*C81(1)+(C41(4)*C61(1)-

```

```

      E   C41(1)*C61(4))*C81(3)+(C41(1)*C61(3)-C41(3)*C61(1))*C81(4)      W2
      E   W3=(C41(2)*C61(4)-C41(4)*C61(2))*C81(1)+(C41(4)*C61(1)-
      E   C41(1)*C61(4))*C81(2)+(C41(1)*C61(2)-C41(2)*C61(1))*C81(4)      W3
      E   W4=(C41(2)*C61(3)-C41(3)*C61(2))*C81(1)+(C41(3)*C61(1)-
      E   C41(1)*C61(3))*C81(2)+(C41(1)*C61(2)-C41(2)*C61(1))*C81(3)      W4
      E   WW=W1+W2+W3+W4
      E   WT(1)=W1/WW
      E   WT(2)=W2/WW
      E   WT(3)=W3/WW
      E   WT(4)=W4/WW
      DO 4 I=1,4
4  WRITE(6,5) RX(I),RY(I),RZ(I),WT(I),C41(I),C61(I),C81(I)
      PRINT 6
5  FORMAT(1X,'A=(',3F10.5,',')',5X,'WT=',F10.5,5X,'K41=',F10.5,3X,'K61
      E=',F10.5,3X,'K81=',F15.5)
6  FORMAT(1H )
C
      CALCULATE THE DFNSITY ALONG FOUR DIRECTIONS (RX(I),RY(I),RZ(I)) AND TAKE
      THE AVERAGE
C
      PRINT 233
233 FORMAT(1X,//,14X,'R',9X,'WT',9X,'DENSITY',10X,'DENSITY JP',7X,
      E'DENSITY DOWN',//)
      DO 200 KR=1,96
      DENS=0.D0
      DENSUP=0.D0
      DENSDN=0.D0
      DO 201 ND=1,4
      X=R(KR)*RX(ND)
      Y=R(KR)*RY(ND)
      Z=R(KR)*RZ(ND)
      DO 72 I=1,NSTA
      SUM=0.D0
      N=NORB(I)
      DO 10 JJ=1,1DIM
      PSI=0.D0
      RA=DSQRT((AX(JJ)-X)**2+(AY(JJ)-Y)**2+(AZ(JJ)-Z)**2)
      DO 20 J=1,N
      EAX=RA*EX(I,J)
      IF(EAX.GT.40.D0)GO TO 101
      IBB=IB(I,J)-1
      RFX=C(I,J)*RA**IBR*DEXP(-EAX)
      GO TO 20
101 REX=0.0
20 PSI=PSI+REX
10 SUM=SUM+PSI*PSI

```

```
65 DENS=DENS+SUM*CHARGE(I)*CONST*WT(ND)
DENSUP=DENSUP+SUM*CHARUP(I)*CONST*WT(ND)
DENSDN=DENSDN+SUM*CHARDN(I)*CONST*WT(ND)
72 CONTINUE
201 CONTINUE
      WRITE(6,231) KR,R(KR),W(KR),DENS,DFNSUP,DENSDN
231 FORMAT(1X,I5,2F11.5,6E18.8)
EXCH(KR)=DENS
EXUP(KR)=DENSUP
EXDN(KR)=DENSDN
200 CONTINUE
RETURN
END
```

```

SUBROUTINE SPLOTE(S,F,E,NEPTS,EMIN,DE,FERMIE,NMAX)
C*****PLOT THE DENSITY OF STATES
C*****DIMENSION S(NMAX),F(NMAX),E(NMAX)
I=NEPTS
J=I+1
K=I+2
CALL PLOT(05.,-11.,-3)
CALL PLOT(0.,2.,-3)
F( J )=EMIN
E( K )=DE*(I-1)/10.
FERM=(FFERMIE-E( J ))/E(K)
WRT=FERM-0.32
CALL PLOT(FERM,0.0,3)
CALL PLOT(FERM,7.0,2)
CALL SYMBOL(WRT,7.5,0.21,4HF.E.,0.,4)
CALL SCALE(F,8.,I,1)
CALL AXIS(0..0.,11HENFRGY (RY),-11,10.,0.,E( J ),F( K ))
CALL AXIS(0..0.,37HDENSITY OF STATES (ELECTRONS/ATOM-RY),37.8..
S90.,F( J ),F( K ))
CALL SYMBOL(1.0,7.5,0.21,13HMAJORITY SPIN,0..13)
CALL LINE(E,F,I,1,0,0)
CALL PLOT(15.,-11.,-3)
CALL PLOT(0.,2.,-3)
150 CONTINUE
CALL PLOT(FERM,0.0,3)
CALL PLOT(FERM,7.0,2)
CALL SYMBOL(WRT,7.5,0.21,4HF.E.,0.,4)
CALL SCALE(S,8.,I,1)
CALL AXIS(0..0.,11HENERGY (RY),-11,10.,0.,E( J ),E( K ))
CALL AXIS(0..0.,37HDENSITY OF STATES (ELECTRONS/ATOM-RY),37.8..
S90.,S( J ),S( K ))
CALL SYMBOL(1.0,7.5,0.21,13HMINORITY SPIN,0..13)
CALL LINE(E,S,I,1,0,0)
CALL PLOT(15.,-11.,-3)
CALL PLOT(0.,2.,-3)
IF(NSPINO .EQ. 2) GO TO 152
CALL PLOT(FERM,0.0,3)
CALL PLOT(FERM,7.0,2)
CALL SYMBOL(WRT,7.5,0.21,4HF.E.,0.,4)
DO 153 II=1,I
S(II)=S(II)+F(II)
CALL SCALE(S,8.,I,1)
CALL AXIS(0..0.,11HENERGY (RY),-11,10.,0.,E( J ),F( K ))
CALL AXIS(0..0.,37HDENSITY OF STATES (ELECTRONS/ATOM-RY),37.8..

```

```
E90.,S(J),S(K))
CALL SYMBOL(1.0,7.5,0.21,9HBOTH SPIN,0..9)
CALL LINE(E,S,I,1,0,0)
CALL PLOT(15..-11.,-3)
152 CONTINUE
CALL PLOT(0..0.,999)
RETURN
END
```

```

SUBROUTINE SVKO(VKO)
C*****CALCULATION OF THE COULOMB POTENTIAL AT K=(0,0,0)*****
C*****IMPLICIT REAL*8(A-F,H,O-Z)*****
COMMON/VKO/C(7,11),FX(7,11),FACTO(10),IB(7,11),NORB(7),NSTA
COMMON/CHARGE/CHARGE(7),CHARUP(7),CHARDN(7)
VKO=0.D0
DO 23 L=1,NSTA
SUM=0.D0
CON=1.D0
N=NORB(L)
DO 20 J=1,N
DO 21 K=J,N
COL=C(L,J)*C(L,K)*CON
JA=IB(L,J)+IB(L,K)+2
EAX=EX(L,J)+EX(L,K)
IR=JA+1
SUM=SUM+FACTO(JA)*COL/(EAX**IR)
21 CON=2.0
20 CON=1.D0
23 VKO=VKO+SUM*CHARGE(L)
RETURN
END

```

```
SUBROUTINE WFCC16(KX,KY,KZ,KL,WT)
C*****FOR EACH(KX,KY,KZ) CALCULATE THE PORTION OF THE CUBE THAT LIES INSIDE THE
C 1/16TH OF THE INDEPENDENT B. Z. (F. C. C.)
C*****KM=3*KL/2
C*****WT=1.0
C*****KT=KX+KY+KZ
C*****IF(KT .EQ. KM) WT=WT*0.5
C*****IF(KX .EQ. KL) WT=WT*0.5
C*****IF(KY .EQ. KL) WT=WT*0.5
C*****IF(KZ .EQ. KL) WT=WT*0.5
C*****IF( KZ .EQ. 0) WT=WT*0.5
C*****IF( KY .EQ. 0) WT=WT*0.5
C*****IF( KX .EQ. 0) WT=WT*0.5
C*****IF(KX .EQ. KY ) WT=WT*0.5
C*****RETURN
C*****END
```

VITA

Ching-ping Shih Wang was born on February 16, 1947 in Shang-hai, China. In 1949 she and her family moved to Taiwan, Republic of China. She graduated from Taipei First Girls' High School in 1965. She received the degree of Bachelor of Science in Physics from Tunghai University, Taichung, Taiwan, in 1969. In September 1969, she came to the United States for post-graduate studies and received the degree of Master of Science from Louisiana State University, Baton Rouge, Louisiana, in January 1971. She is now a candidate for the degree of Doctor of Philosophy in the Department of Physics and Astronomy at Louisiana State University.

She is a member of the American Physical Society and of the National Honor Society Phi-Kappa-Phi.

EXAMINATION AND THESIS REPORT

Candidate: WANG, Ching-Ping Shih

Major Field: Physics

Title of Thesis: Band Structure of Nickel: Spin Orbit Coupling, the Fermi Surface, and the Optical Conductivity

Approved:

Joseph Callaway
Major Professor and Chairman

Donald J. Raynham
Dean of the Graduate School

EXAMINING COMMITTEE:

R. L. W. Haynes
Paula G. King
John Kindt
Herbert Hilles

Date of Examination:

June 24, 1974